Experimental and computational studies into the effect of salinisation on Zn in solid-solution interactions relevant to tropical soils

By Md Hanif

Thesis Submitted for

the Degree of Doctor of Philosophy

Department of Earth Science and Engineering

Imperial College London

2021

I declare that the research presented in this thesis is my own work and that all other sources have been appropriately referenced.

The copyright of this thesis rests with the author. Unless otherwise indicated, its contents are licensed under a Creative Commons Attribution-Non Commercial 4.0 International Licence (CC BY-NC). Under this licence, you may copy and redistribute the material in any medium or format. You may also create and distribute modified versions of the work. This is on the condition that: you credit the author and do not use it, or any derivative works, for a commercial purpose. When reusing or sharing this work, ensure you make the licence terms clear to others by naming the licence and linking to the licence text. Where a work has been adapted, you should indicate that the work has been changed and describe those changes. Please seek permission from the copyright holder for uses of this work that are not included in this licence or permitted under UK Copyright Law.

Abstract

Salinization of soils and aquifers in coastal areas worldwide increases due to seawater level rise. Increasing concentrations of Na^+ and Cl^- associated with the salinity increase change the geochemical cycles of heavy metals like Zn and hence have a fundamental impact on the adsorption of Zn in soils. Zinc is a critical pollutant metal in soils due to industrial activities and solid-solution interface processes arguably exercise the most important control of the Zn cycle in soils and sediments. To this end, surface complexation models (SCMs) are a promising technique to define the adsorption of Zn at solid-solution interfaces in different environmental conditions. These models are based on experimental data, and whilst SCM has been successfully used and parametrised for Zn and other metals in saline solutions < 0.1 mol L^{-1} NaCl, this has not been achieved for solutions with higher salinity.

This thesis aim was to better understand Zn adsorption on soils and goethite in NaCl saline solutions and evaluate surface complexation models (SCMs) performance to predict the effect of salinisation on zinc (Zn) interface processes in tropical soils. This work found that the Davies equation successfully corrects for changes in activities up to 0.7 mol L^{-1} ion strength. Zn species in the aqueous solution are largely controlled by complexation with inorganic ions (Cl, HCO_3) and dissolved organic carbon (DOC), especially at pH between 4 and 8. Zn complexation with Cl ions increases with increasing NaCl concentration from 0.1 to 0.3 and 0.7 mol L^{-1}, therefore, decreasing Zn adsorption on soils at pH 3 to 6. The addition of carbonate ion (HCO_3) in NaCl solutions does not change Zn adsorption in soils at $[Zn]_{init}$ = 0.08 mmol L^{-1}, however, an increased (30 - 35%) of Zn adsorption is observed at pH 6 to 7.5 at $[Zn]_{init}$ = 0.8 mmol L^{-1}. Multi-surface models (MSMs) with experimentally determined model parameters and generic surface complexation databases predict well Zn adsorption on soils in NaCl concentrations in the presence of carbonate. Model underprediction is generally observed at a low pH range (3 – 5) in 0.3 and 0.7 mol L^{-1} NaCl solution which might be primarily due to the absence of ternary surface complexation constants (≡FeO-ZnCl and ≡FeO-$ZnHCO_3$) in the database of iron (hydr)oxides. To explore ternary surface complexes of Zn on goethite in 0.3 and 0.7 mol L^{-1} NaCl solution at low pH, a constant capacitance model protocol is established and successfully determines the stability constants of ternary surface complexes at $[Zn]_{init}$ = 0.08 mmol L^{-1}. At $[Zn]_{init}$ = 0.8 mmol L^{-1}, ternary surface complexes are not reported by model estimation. The results of this thesis highlighted that existing surface complexation databases well predict Zn adsorption in low concentrations of NaCl, but at higher concentrations (> 0.1 mol L^{-1} NaCl), the model databases need to incorporate ternary surface complexes.

Acknowledgments

First and foremost, I would like to thank my supervisor, Prof. Dominik Weiss for his continuous guidance, supervision, and teaching me a great deal about science during my PhD studies. I am grateful to him to give me the opportunity to have worked on such an interesting topic. I would like to thank my co-supervisors, Prof. Guy Kirk from Cranfield University and Dr Yves Plancherel from Imperial College London, UK for providing direction and invaluable feedback on this work. I would like to thank all members of the Environmental Geochemistry group for their feedback and advice about my topic during numerous group meetings and continuous support during lab work. In particular, thanks to Dr Matthew Edward Kirby and Dr Jay Bullen for teaching me how to do lab work and use the CO_2 and pH electrodes. I would like to thank my UROP and In2 Science summer students who tested out some of my experimental procedures.

This work used different experimental techniques and I was very fortunate to receive training. Therefore, I would like to thank Dr Jens Najorka from the Natural History Museum for helping me conduct the XRD analysis of soil samples and offering expert knowledge in minerals identification. Thanks to Dr Jon Watson for his help teaching and running the ICP-MS. Thanks to Dr Jay Bullen for helping me with the characterization of goethite minerals and teaching me about potentiometric titration and surface complexation models.

I am very grateful to the Islamic Development Bank for providing tuition fees and living allowance during my PhD studies. Thanks to the Imperial Hardship fund for providing financial support during the COVID 19 pandemic.

Last but not least, thanks to my parents, my wife – Ismet and my two daughter's - Rehenuma and Rameen for supporting me during my PhD. Without their unending support, I could not have reached this stage.

Publications

Submitted – PhD Related

1. Hanif, Md., Bullen, Jay., Plancherel, Y., Kirby, M., Kirk, G., Weiss, D.J. The effect of salinisation on Zn adsorption by coastal soils of Bangladesh, European Journal of Soil Science.

In Preparation – PhD Related

2. Hanif, Md., Bullen, Jay., Plancherel, Y., Kirk, G., Weiss, D.J. Geochemical multi-surface modelling approach to predict Zn adsorption in tropical soils in NaCl saline solutions, Geoderma.
3. Hanif, Md., Bullen, Jay., Plancherel, Y., Kirk, G., Weiss, D.J. Interface processes of Zn and goethite in saline solutions: effect of bicarbonate and parameterisation of accurate surface complexation model, Geochimica et Cosmochimica Acta

Published – Group Work

4. Weiss, D., Northover, G., Hanif, MD., and others. 2021. Isotope fractionation of zinc in the paddy rice soil-water environment and the possible role of 2'deoxymugenic acid (DMA) as zincophore under Zn limiting conditions. *Chemical Geology*, 577(5): 120271.

Education Paper – Teaching During PhD

5. Kirby, M., Bullen, Jay., Hanif, MD., Weiss, D,. 2020. Determining the Effect of pH on Iron Oxidation Kinetics in Aquatic Environments: Exploring a Fundamental Chemical Reaction To Grasp the Significant Ecosystem Implications of Iron Bioavailability, *Journal of Chemical Education,* 97(1), 215-220.

List of Contents

Abstract **3**

List of Tables **12**

List of Figures **13**

1. Introduction **16**

2. Literature Review **21**

2.1 Zinc: micronutrient and contaminant metal 21

2.2 Climate change and soil salinity 21

2.3 Impact of soil salinization 23

2.4 Zinc in soils 23

2.4.1 Zinc concentrations in soil solution 24

2.4.2 Zinc in the soil solid phase 25

2.5 Zinc adsorption in soils: The role of solution and solid phases 26

2.5.1 Effect of soil solution parameters 26

2.5.2 Effect of solid phases (carbonates, organic matter, Fe-oxides and clay minerals). 26

2.6 Zn adsorption in soils: Adsorption mechanisms and surface complexes 28

2.7 Surface complexation models 30

2.7.1 CCM, DLM, and TLM model 30

2.7.2 Introducing the concept of multi-surface models 31

2.7.2.1 Binding to Iron/Aluminium (hydr)oxides 33

2.7.2.2 Binding to organic matter 33

2.7.2.3 Binding to clay 35

2.8 Effect of NaCl and HCO_3 concentrations on the adsorption of Zn on goethite and soils 35

2.8.1 Effect of NaCl concentrations on the adsorption of Zn onto goethite 35

2.8.2 Effect of NaCl concentrations on the adsorption of Zn on soils 36

2.8.3 Effect of carbonate on the adsorption of Zn on soils and goethite in NaCl solutions 37

2.9 Application of surface complexation models on the adsorption of Zn and carbonate onto goethite and on soils in different NaCl concentrations. 38

2.9.1 Application of CCM, DLM, and TLM on adsorption of Zn and carbonate onto goethite 38

2.9.2 Application of multi-surface models (MSMs) for soils 39

2.10 Activity correction 40

2.11 Research aim and objectives 40

2.11.1 What is the role of changing speciation due to increased NaCl concentrations on Zn adsorption on tropical soil? 41

2.11.2 Can multi-surface adsorption models accurately predict Zn adsorption on tropical soils? 41

2.11.3 What is the role of ternary surface complexes in predicting accurately Zn adosprion on goethite? 42

3. Materials and Methods 43

3.1 Chemicals and Solutions 43

3.2 Instrumentation and Methods 44

3.2.1 Measurement of pH 44

3.2.2 Determination of Zn 44

3.3 Model calculation of Zn aqueous speciation in NaCl concentrations and examine the applicability of surface complexation models in seawater ionic concentration (0.7 mol L^{-1} NaCl) 45

3.3.1 Estimation of the suitability of the Davis equation for activity correction at seawater ionic strength (0.7 mol L^{-1} NaCl) 46

3.3.2 The aqueous speciation of Zn 46

3.3.2.1 Solution compositions for speciation analysis 46

3.3.2.2 Speciation model used 47

3.3.3 Examination of the effect of increasing NaCl concentrations and HCO_3 on the adsorption of Zn on tropical soils 48

3.3.3.1 Soils Characteristics 48

3.3.3.2 Mineralogical and Elemental Features of Soils 49

3.3.3.3 Batch adsorption experiments 52

3.3.4 Examination of multi-surface models (MSMs) performance for predicting Zn adsorption on soils 53

3.3.4.1 Binding to phyllosilicate clay minerals 53

3.3.4.2 Binding to iron (hydr)oxide 53

3.3.4.3 Binding to soil organic matter 53

3.4 Development of surface complexation model parameters for the accurate quantification of Zn on goethite 55

3.4.1 Surface properties of goethite 55

3.4.1.1 Synthesis of goethite 55

3.4.1.2 Mineralogical and elemental features of goethite 55

3.4.1.3 Surface area of Goethite 56

3.4.1.4 Determination of Surface Charge 56

3.4.2 Development of surface complexation model parameters for accurate predicting Zn in the highly saline environment 57

3.4.2.1 Batch adsorption experiments 57

3.4.2.2 Surface complexation model for goethite 57

3.5 Statistical analysis 59

Chapter 4: Estimating and Predicting Zn adsorption in a tropical soil under NaCl salinization using Multi-Surface Thermodynamic Models (MSMs) 60

4.1 Introduction 60

4.2 Results 63

4.2.1 Comparison of Zn speciation computations at 0.67 mol L^{-1} NaCl solution using Davies and SIT activity correction models 63

4.2.2 Zn speciation model for NaCl solutions in the presence of dissolved organic carbon (DOC) and bicarbonate (HCO_3) 64

4.2.2.1 Speciation of Zn in NaCl solutions in the presence of DOC 64

4.2.2.2 Speciation of Zn in NaCl solutions in the presence of DOC and HCO_3 65

4.2.3 Adsorption of Zn on Tropical Bay soil in NaCl solutions: Applicability of MSMs 68

4.2.3.1 pH adsorption edge in different NaCl concentration: 68

4.2.3.2 Comparison of multi surface model and experimental data 69

4.2.3.3 Relative importance of soil reactive sites for Zn adsorption: 69

4.2.4 Application of multi surface model to predict the effect of NaCl salinity increase on Zn speciation and adsorption on coastal soils of Bangladesh 71

4.2.4.1 Effect of NaCl salinisation on Zn speciation 71

4.2.4.2 Effect of NaCl salinity on Zn adsorption in soil 72

4.3 Discussion: 73

4.3.1 Suitability of the Davies equation at seawater ionic strength 73

4.3.2 Effect of NaCl, HCO_3 and DOC on the speciation of Zn in aqueous solution 74

4.3.3 Zn adsorption in NaCl concentrations 75

4.3.4 MSMs prediction and validation in different NaCl concentrations 76

4.4. Conclusion 77

Chapter 5: Geochemical multi-surface modelling approach to predict Zn adsorption in tropical soils in NaCl saline solutions. 79

5.1 Introduction 79

5.2 Results: 82

5.2.1 Soils Properties 82

5.2.2 Batch Adsorption Results 85

5.2.2.1 Effect of NaCl solutions on Zn adsorption 85

5.2.2.2 Effect of NaCl and HCO_3 on Zn adsorption 87

5.2.3 Testing the validity of multi-surface models to predict Zn adsorption on Bay and Tiaong soil 90

5.2.3.1 Application of MSMs to predict Zn adsorption in NaCl concentrations 90

5.2.3.2 Application of MSMs to predict Zn adsorption in NaCl – HCO_3 system..... 91

5.2.4 Contribution of soil components on Zn adsorption based on model..... 92

5.3 Discussion 98

5.3.1 How does NaCl salinity affect Zn adsorption in soils? 98

5.3.2 Effect of carbonate on Zn adsorption in NaCl solutions..... 99

5.3.3 Model performance and the reasons for model underestimation 101

5.4 Conclusions 103

Chapter 6: Interface processes of Zn and goethite in saline solutions: parameterisation of accurate surface complexation model 105

6.1 Introduction: 105

6.2 Results..... 107

6.2.1 Goethite Characterization..... 107

6.2.2 Acid-Base Properties of Goethite..... 108

6.2.2.1 Potentiometric titration of goethite in 0.1, 0.3 and 0.7 mol L^{-1} NaCl solutions 108

6.2.2.2 Acid-base properties of goethite: surface complexation modelling using CCM 109

6.2.3 Zn Adsorption onto Goethite and Development of Surface Complexation Constants 111

6.2.3.1 Effect of Increasing NaCl concentration on Zn adsorption onto goethite..... 111

6.2.3.2 Surface Complexations Constants of Zn in 0.1, 0.3, and 0.7 mol L^{-1} NaCl Solutions 112

6.2.3.2.1 Equilibria in solution..... 112

6.2.3.2.2 Modelling Zn adsorption in NaCl solutions 113

6.2.4 Models Improvement by Introducing Ternary Surface Species and their Validation 116

6.2.4.1 Ternary Surface Species 116

6.2.4.2 Model Validation 117

6.2.4.3 Modelling Zn Adsorption at Higher Initial Concentration 118

6.3 Discussion 119

6.3.1 Zn adsorption on goethite 119

6.3.2 Modelling approach and its development 120

6.4 Conclusions 122

Chapter 7: Conclusion and Future Research 124

7.1 Summary and Conclusions 124

7.2 New Concepts Emerging from this Work 126

7.3 Future Research 126

References 129

Appendices 144

List of Tables

Table 3.1 Chemical reagents used in this work 43
Table 3.2 Zn species and their equilibrium constants in IUPAC technical report (Powell et al., 2013) and Visual Minteq database at I = 0 M. 46
Table 3.3 Parameter values for cation complexation to soil organic matter in the NICA-Donnan models 48
Table 3.4 Experimental soil properties 48
Table 3.5 Selected soil properties of investigated and modelled soil samples 51
Table 3.6 DDL model parameters of HFO in two surface sites (strong site and weak site). . 55
Table 3.7 List of experimental setup, model works and the relevant methods used in this thesis……58
Table 5.1 Quantification of soil minerals by the Rietveld method 84
Table 5.2 Elemental analysis of soil samples by XRF 85
Table 5.3 Saturation index values of various Zn mineral phases in Bay and Tiaong soil at $[Zn]_{initial}$ = 0.8 mM by model analysis..... 94
Table 5.4 Saturation index values of various Zn mineral phases in Bay and Tiaong soil at $[Zn]_{initial}$ = 0.8 mM in the presence of 8 mmol L^{-1} HCO_3 by model analysis..... 97
Table 6.1 Acid-base properties of goethite in different NaCl concentration (0.1 mol L^{-1}, 0.3 mol L^{-1}, and 0.7 mol L^{-1}, respectively) using CCM and DLM 111
Table 6.2 Aqueous complexation constants of Zn and carbonate used to model Zn and carbonate adsorption on goethite in 0.1, 0.3 and 0.7 mol L^{-1} NaCl solution..... 113
Table 6.3 Surface complexation reactions and constants describing Zn adsorption onto goethite in 0.1, 0.3, and 0.7 mol L^{-1} NaCl solutions. 115
Table 6.4 Surface complexation reactions and constants describing Zn adsorption onto goethite in 0.1, 0.3, and 0.7 mol L^{-1} NaCl solutions at $[Zn]_{init}$ = 0.8 mmol L^{-1}. 119

List of Figures

Figure 1.1 Soil salinity and pollution hotspots map in the South-Western region of Bangladesh……...16
Figure 2.1 Effect of sea level rise in Bangladesh. 22
Figure 2.2 Key processes controlling the cycles of Zn in soils. 24
Figure 2.3 Schematic illustration of the constant capacitance model (A), double layer model (B), and triple layer model (C) adapted from (Bradl, 2004). 31
Figure 2.4 Multi-surface models to predict metals adsorption in soils 32
Figure 2.5 Effect of NaCl concentration and HCO_3^- ion on the adsorption of Zn on soil. ... 37
Figure 3.1 Calibration curves of pH meter at pH of 4.00, 7.00 and 10.00 in standard buffer solutions (red line) and in concentrated electrolytes..... 44
Figure 3.2 Calibration curve of Zn standard. 45
Figure 4.1 A comparison of Zn speciation model results at 0.67 mol L^{-1} NaCl ionic strength obtained with the Davies equation in Visual MINTEQ and those yielded by SIT method . .. 64
Figure 4.2 Visual MINTEQ Model results of Zn species in different NaCl concentrations.. 65
Figure 4.3 Visual MINTEQ model results of speciation diagram of Zn in NaCl-HCO_3- DOC system (calcareous solution) 67
Figure 4.4 Percent adsorption of Zn on Bay soil (10 g/L) as a function of pH in 0.1 (□), 0.3 (Δ) and 0.7 (◊) mol L^{-1} NaCl concentration at Zn initial concentration = 0.08 mmol L^{-1}. 68
Figure 4.5 Contribution of soil components (clay, hydrous ferric oxides (HFO) and SOM) to Zn adsorption in the studied soils in 0.1, 0.3 and 0.7 mol L^{-1} NaCl concentration, as predicted by the MSMs with $[Zn]_{init}$ = 0.08 mmol L^{-1}. 70
Figure 4.6 MSMs prediction of Zn adsorption and its distribution within soil components (clay, hydrous ferric oxides (HFO) and SOM) in some soils of the Ganges Tidal Floodplain in Bangladesh in different NaCl concentrations (0.1, 0.3 and 0.7 mol L^{-1}) at $[Zn]_{init}$ = 0.08 mmol L^{-1}. 72
Figure 5.1 XRD spectrum of minerals in the bulk soils. 83
Figure 5.2 XRD spectrum of minerals in the clay fraction (< 2 μm). 84
Figure 5.3 Percent adsorption of Zn on Bay and Tiaong soil (10 g L^{-1}) as a function of pH in 0.1 (□), 0.3 (Δ) and 0.7 (◊) mol L^{-1} NaCl solution at two different initial concentration: 0.08 mmol L^{-1} and 0.8 mmol L^{-1}. 86

Figure 5.4 Percent adsorption of Zn on Bay soil as a function of pH in 0.1 (A), 0.3 (B) and 0.7 (C) mol L^{-1} NaCl concentration, respectively at $[Zn]_{init}$ = 0.08 mmol L^{-1} in the presence of carbonate: ○: 8 mmol L^{-1}. 88
Figure 5.5 Percent adsorption of Zn on Tiaong soil as a function of pH in 0.1, 0.3 and 0.7 mol L^{-1} NaCl concentration, respectively at $[Zn]_{init}$ = 0.08 mmol L^{-1} in the presence of carbonate: ○: 8 mmol L^{-1}. 88
Figure 5.6 Percent adsorption of Zn on Bay soil as a function of pH in 0.1, 0.3 and 0.7 mol L^{-1} NaCl concentration, respectively at $[Zn]_{init}$ = 0.8 mmol L^{-1} in the presence of carbonate: ○: 8 mmol L^{-1}. 89
Figure 5.7 Adsorption of Zn on Tiaong soil (in percentage) as a function of pH in 0.1, 0.3 and 0.7 mol L^{-1} NaCl concentration, respectively at $[Zn]_{init}$ = 0.8 mmol L^{-1} in the presence of carbonate: ○: 8 mmol L^{-1} 90
Figure 5.8 Contribution of soil components (clay, hydrous ferric oxides (HFO) and SOM) to Zn adsorption in the studied soils in different NaCl concentrations, as predicted by the MSMs: A) $[Zn]_{initial}$ = 0.08 mmol L^{-1}; B) $[Zn]_{initial}$ = 0.8 mmol L^{-1} 93
Figure 5.9 Contribution of soil components (clay, hydrous ferric oxides (HFO) and SOM) to Zn adsorption in the studied soils in different NaCl concentration at $[Zn]_{initial}$ = 0.08 mmol L^{-1} in the presence of 8 mmol L^{-1} HCO_3, as predicted by the MSMs: A) Bay soil; B) Tiaong soil. 95
Figure 5.10 Contribution of soil components (clay, hydrous ferric oxides (HFO) and SOM) to Zn adsorption in the studied soils in different NaCl concentration at $[Zn]_{initial}$ = 0.8 mmol L^{-1} in the presence of 8 mmol L^{-1} HCO_3, as predicted by the MSMs: A) Bay soil; B) Tiaong soil. 96
Figure 6.1 X-ray diffraction analysis of synthesis goethite. 108
Figure 6.2 Potentiometric titration of goethite (40 ml of 8 g L^{-}) at 0.1 (○), 0.3 (Δ), and 0.7 (□) mol L^{-1} NaCl concentration and 25°C, shown as surface charge (Q) in Coul m^{-2}. 109
Figure 6.3 Zn adsorption on goethite (1.6 g L^{-1}) as a function of pH in 0.1 (□), 0.3 (Δ) and 0.7 (◊) mol L^{-1} NaCl solution at two different initial concentration: 0.08 mmol L^{-1} (A) and 0.8 mmol L^{-1} (B). 111
Figure 6.4 Model predicted Zn Adsorption onto goethite as a function of pH in 0.1, 0.3 and 0.7 mol L^{-1} NaCl solutions. 114
Figure 6.5 Model fit of Zn Adsorption onto goethite in 0.3 and 0.7 mol L^{-1} NaCl solution in the presence of the ternary surface complex. A: model fit in 0.3 mol L^{-1} NaCl solution; B:

model fit in 0.7 mol L^{-1} NaCl solution with one ternary surface complex, C: model fit in 0.7 mol L^{-1} NaCl solution with two ternary surface complexes. 116
Figure 6.6 Model prediction of Zn adsorption at $[Zn]_{init}$ = 0.8 mmol L^{-1} in 0.1 (A), 0.3 (B), and 0.7 (C) mol L^{-1} NaCl solutions using surface complexation reactions and constants in Table 6.3. 117
Figure 6.7 Model prediction of Zn adsorption at $[Zn]_{init}$ = 0.8 mmol L^{-1} in 0.7 mol L^{-1} NaCl solution with the complex of surface precipitation. Model is predicted with surface species 1 and 2 and their corresponding equilibrium constants in 0.7 mol L^{-1} NaCl solution in Table 6.3. The equilibrium constant of the surface precipitate complex ($\equiv FeOZn(OH)_2^-$ = -13.98) is added to the model to improve model fit. 118
Figure 6.8 Modelling approach of Zn adsorption at $[Zn]_{init}$ = 0.8 mmol L^{-1}. Model prediction at $[Zn]_{init}$ = 0.8 mmol L^{-1} in 0.1 (A), 0.3 (B), and 0.7 (C) mol L^{-1} NaCl solutions is done using surface complexation reactions and constants in Table 6.4. 119

1. Introduction

Worldwide 20% of total cultivated and 33% of irrigated agricultural lands are afflicted by several types of salinities (Shahid et al., 2018). The extent of salinity is increased in coastal areas due to climate change and around 50 % of arable land will be affected worldwide by varying degrees of salinity by 2050 (Zaman et al., 2018). The outlook is particular bad in low lying countries like Bangladesh where about 30% of the cultivable land is in coastal areas (Fig. 1.1) (Dasgupta et al., 2015; Haque, 2006). As salinity increases, land use patterns of coastal areas change and many agricultural lands convert to industrial lands (Ahmed et al., 2010). As a result of these transformations, by-products of industrial processes which contain high concentrations of Zn and other trace metals are discharged directly to soils in toxic concentrations. The ascending concentration of Zn and trace metals can be environmentally dangerous if not cared for correctly (Fisher-Power et al., 2016).

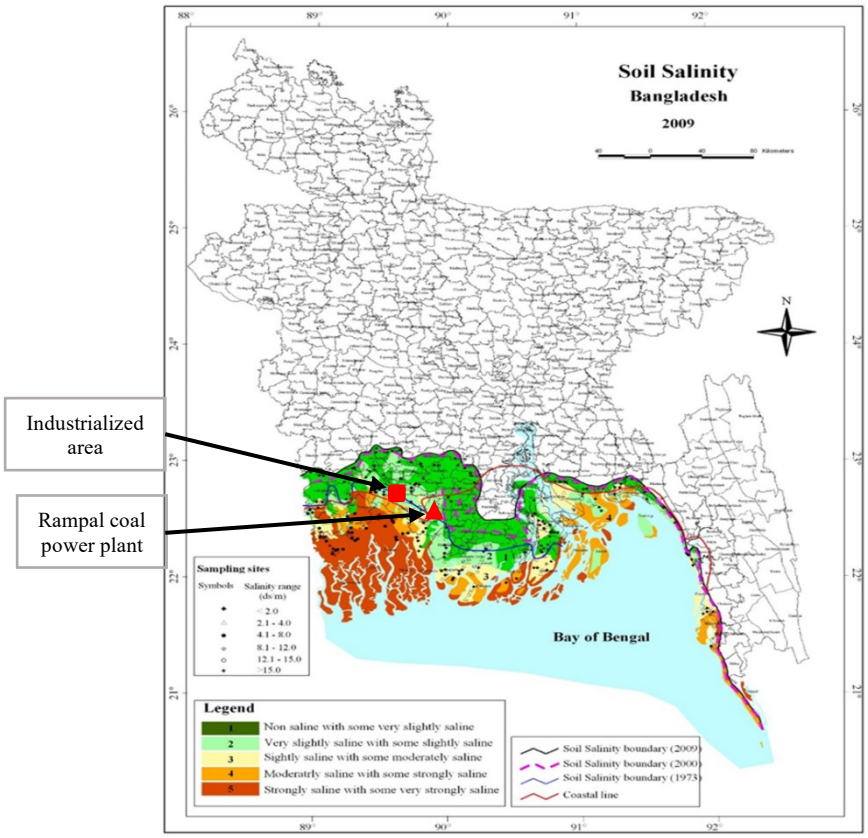


Figure 1.1 Soil salinity and pollution hotspots map in the South-Western region of Bangladesh (SRDI, 2010 and Islam et al., 2018). Soil salinity increases due to the inundation of seawater, and it is estimated that the salinity affected area has increased to about 1.06 million hectares from 0.83 million hectares from 1973 to 2009 (SRDI, 2010). High concentrations of heavy metals in soils and water samples are estimated in industrialized areas (red marked areas). High concentration of heavy metals in soils of coastal areas are also expected as many agricultural lands convert to industrial lands. The Rampal coal power plant is one of the examples of agricultural land conversion to industrial land.

Zinc (Zn) plays a dual role in the environment. It acts as a micronutrient and as a toxic trace metal depending on its concentration. As a micronutrient, it plays an important role in plants and human biological systems (Brown et al., 2002; Impa and Johnson-Beebout, 2012) and its deficiency limits plant growth (Alloway, 2008) and reduces as much as 20% of plant yield. As a toxic trace metal, Zn reduces plant growth and yield and for humans excess Zn causes apoptosis and necrosis of cells (Briffa et al., 2020).

Adsorption is probably the most important chemical process affecting Zn movement in soils and sediments. Zn adsorption on soils and sediments is influenced by ionic strength, dissolved organic matter (DOM), pH of soil solution, ions in soil solution (Cl^-, NO_3^-, SO_4^{2-}, etc.) and reactive major cations pool (Ca^{2+}, Mg^{2+}, K^+, Al^{3+}, etc.) of soil and sediments (Fisher-Power et al., 2016; Sauve et al., 2000; Weng et al., 2002). In coastal areas, the distinctive features of soil and aquifer solutions are the presence of higher concentrations of ions like Na^+, Ca^{2+}, Cl^-, HCO_3^-, and SO_4^{2-} (Akter et al., 2020). Zinc forms complexes with Cl^- and HCO_3^- ions (Powell et al., 2013) and the formation of these complexes influences the adsorption processes of Zn on soils and sediments (Bonten et al., 2008). Therefore, an understanding of the dependence of Zn adsorption on NaCl and carbonate solution is critical to unravelling mobility and plant availability in calcareous high saline regions. However, our understanding of Zn speciation and Zn adsorption in higher concentration of NaCl (> 0.1 mol L^{-1}) and combined NaCl-HCO_3 rich solutions is very limited, with very few studies reported in the literature (Villalobos et al., 2001; Villalobos et al., 2003).

The adsorption capacity of Zn on soils and sediments is widely described using adsorption isotherms with empirical models developed by Langmuir and Freundlich (Bradl, 2004; Gupta et al., 2021); however, these adsorption isotherms are of limited use in describing adsorption systems with changing solution and mineral chemistry (Bradl, 2004). The adsorption isotherm do not contain any mineral structural information regarding adsorbed species (Koretsky, 2000). To overcome the limitations of these models, surface complexation models (SCMs) were developed as they represent adsorption process on minerals (Koretsky, 2000). SCMs are a powerful approach to surface reaction modelling based on thermodynamics and are analogous to aqueous speciation models (Koretsky, 2000; Sun and Li, 2021).

Over the last two decades, the development of surface complexation model parameters has made considerable progress in describing metal's behaviour in solid-solution interaction (Groenenberg and Lofts, 2014). Surface complexation thermodynamic models for metals binding onto the soil organic matter (Gustafsson, 2001; Van Riemsdijk et al., 2006), oxide

minerals (Dzombak and Morel, 1990; Hiemstra and VanRiemsdijk, 1996; Tonkin et al., 2004) and clay minerals (Gu and Evans, 2007; Spathariotis and Kallianou, 2001) are well reported in the literature. The combination of these surface complexation models is called multi-surface models (MSMs), which now predict metals adsorption in a complex soil system (Groenenberg and Lofts, 2014; Weng et al., 2001). MSMs are capable of describing metal (Zn, Cu, Ni, Cd, Cr, Pb) mobility in a wide range of soils (Bonten et al., 2008; Duffner et al., 2014; Groenenberg and Lofts, 2014; Khai et al., 2008; Ren et al., 2017; Weng et al., 2001). Despite numerous recent studies investigating the speciation of Zn in soils using MSMs, MSMs have not been used before to predict Zn adsorption on soils in high concentration of NaCl. The model parameters in aqueous speciation and multi-surface models have generally been adjusted/calibrated at a low ionic strength (Duffner et al., 2014; Gustafsson and Kleja, 2005; Gustafsson et al., 2003). In addition, the activity correction of equilibrium models is mostly done by extended Debye-Huckel equation and/or Davies equation which works very well to ionic strength = 0.5 mol L^{-1}. Therefore, it is uncertain if, under high ionic strength (≈ 0.7 mol L^{-1}), Zn aqueous speciation and adsorption can still be projected precisely with calibrated MSMs and speciation models. This thesis tests the applicability of aqueous speciation and MSMs to predict Zn speciation in soil solution and adsorption on soils in different NaCl concentration and reported the findings in chapter 4.

Model parameters used in MSMs have usually been estimated by different methods (Groenenberg and Lofts, 2014). Model parameters of oxide minerals are defined by the concentration of amorphous and crystalline iron (hydr)oxides and determined experimentally. Model parameters of clay is defined by the charge of clay and is assumed to be similar to the cation exchange capacity (CEC) of illite which is in the range of 0.1 to 0.4 mol kg^{-1} (Weng et al., 2001). The charge of clay can also be estimated from the equation given by van Reeuwijk (Khai et al., 2008; van Reeuwijk, 1993). Model parameters of soil organic matter (SOM) are defined by the site density of active SOM and can be estimated by measuring the concentration of the humic substance and then optimizing with cation exchange capacity of organic matter (Khai et al., 2008; Weng et al., 2001). The site density of active SOM varies between 31% to 87% of humic acid due to the heterogeneous molecules of organic matter (Groenenberg and Lofts, 2014). In most of the literature, the concentration of clay and SOM used in MSMs were adjusted in a way so that the root mean square error (RMSE) between experimentally measured and model simulated was minimum. However, it is uncertain if, under a real soil environment where soil solution contains a high concentration of competitive and complexing ions due to

saline water intrusion, groundwater irrigation and fertilization, Zn adsorption can still be predicted with the density of clay, amorphous and crystalline iron (hydr)oxides and SOM that used and adjusted in a low concentration of Zn adsorption system. This thesis tests the validity of MSMs parameter obtained from adsorption experiments in chapter 4 to predict adsorption processes of Zn at higher initial Zn concentration in varying NaCl concentrations and in the presence of carbonate. The findings are reported in chapter 5.

In coastal aqueous system where Cl^- ions tend to form strong complexes with Zn, it is expected that Zn can adsorb on the surface of goethite as ternary surface complexes. The adsorption of Zn as a ternary surface complex is mostly reported on the surface of iron (hydr)oxides (Chesne and Kim, 2014). The model parameters derived from single metal sorbate system at low concentration of NaCl led to inaccurate prediction of metal adsorption onto goethite at high concentration of NaCl (> 0.1 mol L^{-1}) as observed for Cu, Zn, Cd, and Pb (Duff and Amrhein, 1996; Gao and Mucci, 2003; Villalobos et al., 2001). The error has been attributed to absence ternary surface complexation in the model parameters. Similar observations are expected during the model prediction of Zn adsorption on soils by MSMs at high concentration of NaCl and HCO_3. Therefore, the challenge is to develop a surface complexation model of Zn on goethite in high concentration of NaCl such as those in the coastal areas. This thesis fills the gap by introducing ternary surface complexes of Zn in the surface complexation model for a more accurate description of Zn adsorption in high NaCl concentration, developing model parameters of ternary surface complexes and evaluating its performance in different initial concentrations of Zn.

The thesis aims to improve our understanding of the speciation and adsorption of Zn on soils and gothite in saline and alkaline solutions using surface complexation and multi-surface models. The objectives are:

1. To assess the accuracy of geochemical speciation codes (Visual Minteq) and multi-surface models (MSMs) with predefined databases to predict Zn speciation and surface processes on tropical soils in NaCl solutions and to probe possible application to predict the effect of salinisation on Zn geochemistry in coastal soils in Bangladesh.
2. To evaluate the validity of MSMs parameter obtained from adsorption experiments with two tropical soils during objective 1 to predict surface processes of Zn at higher initial Zn concentration ($[Zn_{init}]$ = 0.8 mmol L^{-1}) in varying NaCl solutions (0.1, 0.3, and 0.7 mol L^{-1}) and in the presence of carbonate (8 mmol L^{-1}).

3. To develop a geochemical model and determine intrinsic equilibrium constants for Zn surface complexation with goethite in NaCl solutions.

The thesis structured is as follows:

- Chapter 2 presents a background information of Zn adsorption on soils and sediments in different NaCl concentration, the limitation in adsorption experiments, review of surface complexation and multi-surface models, and current interest in using these models.
- Chapter 3 outline the methods and materials used.
- Chapter 4 reveals the performance of aqueous speciation model and MSMs to predict Zn aqueous speciation in high concentration of NaCl, prevalent in carbonate concentration and the adsorption of Zn on soil in different NaCl concentration.
- Chapter 5 validates the application of previously optimized MSMs parameters to predict Zn adsorption on soils in different experiment system, identifies by model analysis the relative importance of soil components (clay, SOM, and iron oxides) on Zn adsorption and the major mechanisms in which the different concentration of NaCl-HCO_3 solution affect the adsorption of Zn on soils, explaining the limitations of MSMs.
- Chapter 6 demonstrates the application of the surface complexation model for predicting Zn adsorption onto goethite in a high concentration of NaCl within constant capacitance model (CCM), identifies model limitations, developing an improved model in a high concentration of NaCl (> 0.1 mol L^{-1}) by introducing ternary surface complexes of Zn.
- Chapter 7 summarises the key findings of this thesis and highlights the area of future research.
- The input files for FITEQL program and several appendices are available at the end of the thesis.

2. Literature Review

2.1 Zinc: micronutrient and contaminant metal

Zinc (Zn) is essential for plants and animals (Alloway, 2008). As it requires only low concentrations for the functional integrity of many organ systems, as well as for growth, development and tissue repair, Zn is considered as an essential micronutrient (Gu and Lin, 2010). In plants, Zn acts as a regulatory, catalytical and structural cofactor of many enzymatic reactions. It is essential for protein synthesis, plants growth hormones, maintenance of cell membrane and the metabolism of carbohydrate (Broadley et al., 2012), therefore, plant growth and crop yield are reduced with Zn deficiency (Alloway, 2009).

Zinc generates toxic concentrations as a by-product of industrial processes (Fisher-Power et al., 2016). As a result, Zn becomes toxic to plants and animals, and, in this case, Zn refers to a contaminant metal (Rengel, 1999). As a contaminant metal, Zn leads to chlorosis and low biomass production, changed water balance and nutrient adsorption, reduced photosynthesis and growth (Singh et al., 2016). In addition, a higher amount of Zn is accumulated by plants growing in contaminated/polluted sites (Yoon et al., 2006). When the yields of those plants enter the route of the food chain, heavy metals like Zn will enter human and animal tissues (Mishra et al., 2020). The high concentration of Zn in the human system will make them vulnerable to several diseases, e.g., nausea, cholesterol balance and infertility (Zhang et al., 2012).

2.2 Climate change and soil salinity

The concentration of atmospheric global warming gases (CO_2, CH_4, etc.) has increased rapidly in the last 150-200 years due to industrialization, urban and rural development, human activities, and intensive agricultural activities (Oppenheimer et al., 2019). As a result, global temperature is increasing and the Earth's climate is changing with several noticeable effects (Ramanathan and Feng, 2009). For example, precipitation patterns have altered and more droughts, heat waves and stronger cyclones are observed in coastal areas (Fang et al., 2019) where around 600 million people live (Wheeler, 2011). Research suggests that this number will increase to about one billion by 2050 as the mean global sea level rises by > 1 m (Brecht et al., 2012). In Bangladesh, about 15 million people in the coastal area will be affected if the sea level rises by 1 metre (Fig. 2.1).

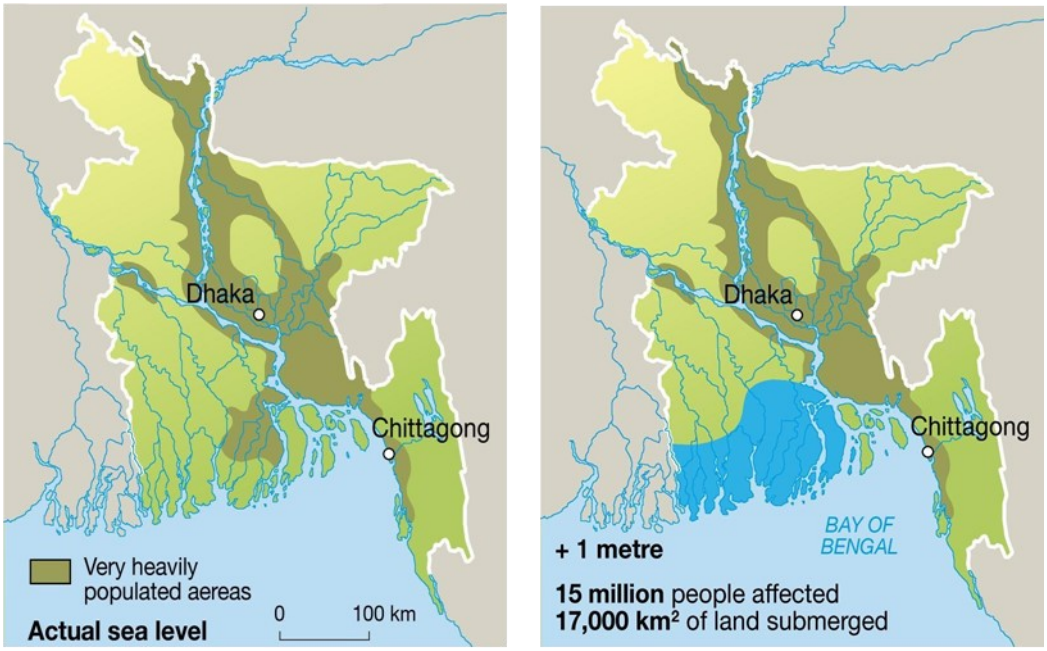


Figure 2.1 Effect of sea level rise in Bangladesh. Model results predict that 15 million people in the coastal area of Bangladesh will be affected if the sea level rises by 1 metre (GRID-Arendal, 2009).

Climate change has a direct impact on coastal soils and agriculture development through saltwater intrusion; saltwater intrusion leads to the salinization of soils and groundwater aquifers in coastal areas (Corwin, 2021). It has been estimated that worldwide around 20% of arable lands are affected by salinity. The extent of soil and groundwater salinity is increasing and as a result, around 50% of arable land will be affected worldwide by varying degree of salinity by the year 2050 (Shahid et al., 2018). The scenario is particularly worrying for low lying coastal areas of tropical countries, e.g., Bangladesh, Phillipines, Nigeria, Sierra Leone, Haiti and Eritrea (Martin, 2015). In Bangladesh, coastal area occupies around 30% of the cultivable land (Dasgupta et al., 2015; Dasgupta et al., 2014; Haque, 2006). These areas of Bangladesh are suitable for agricultural practices, and the fertility status and organic matter content of soils are classified medium to high (SRDI, 2010). Apart from the medium to high fertility status, the agricultural productivity in these areas is relatively low compared with other areas of Bangladesh. From 1973 to 2009, salt affected land increased to 26.7% and around 105.6 million hectares coastal land were affected by various degree of soil salinity in 2009 (SRDI, 2010). By 2050, model results show that 39% of the coastal agricultural land in Bangladesh will be affected by various degree of soil salinity (Dasgupta et al., 2015). Therefore, salinization of soils and groundwater aquifers in the coastal area of Bangladesh are posing a greatest threat to livelihoods and public health (Dasgupta et al., 2015). Similar threats are also expected in other low lying tropical countries.

2.3 Impact of soil salinization

High soil salinity levels are one of the dominant factors that reduce crop productivity in coastal areas; salts appear as NaCl (Sparks, 2003). Besides NaCl soil salinity, coastal soil solutions contain high concentrations of ions such as Ca^{2+}, Mg^{2+}, K^{+}, HCO_3^{-}, SO_4^{2-}, and NO_3^{-}. High concentrations of these inorganic ligands create ion imbalance in the soil solution, thereby inhibiting the uptake of Zn by plants (Corwin, 2021). One proposed mechanism for Zn mobility is that the presence of cations (Ca^{2+}, Mg^{2+}, Na^{+}, K^{+}) in soil solution leads to competition for sorption sites (SOM and clay), increasing Zn availability and mobility (Acosta et al., 2011; Wang and Harrell, 2005). Among the cations, Ca^{2+} and Mg^{2+} ions are much more effective competitors than Na^{+} and K^{+} ions; compared with Na^{+} and K^{+} ions, K is a more effective competitor for the Zn adsorption sites in soils (Acosta et al., 2011). Na forms an outer-sphere complex and K forms an inner-sphere complex with mineral surfaces. As Zn adsorption to mineral surfaces is reported as inner-sphere complexes, K is more competitive (Jalali and Zinli, 2012; Sposito, 1984; Wang and Harrell, 2005).

A second mechanism for Zn mobility involves inorganic anions (Cl^{-}, SO_4^{2-}, HCO_3^{-}) forming complexes with Zn (Powell et al., 2013) which decreases Zn availability as plants only uptake Zn in the form of Zn^{2+}, Zn-DOM complexes and $ZnOH^{+}$ (Alloway, 2009). In soils with high concentration of organic matter, complexes of Zn with inorganic ions decrease Zn adsorption as the adsorption sites of SOM cannot adsorb Zn at a ternary surface complex. Therefore, Zn mobility is increased with the presence of anions in soils with high SOM content (Lumsdon et al., 1995). In soils with high concentration of iron (hydr)oxides, the complexation of Zn with anions increases Zn adsorption by ternary surface complexation, reducing Zn mobility (Chesne and Kim, 2014). Precipitation of Zn depends on the concentration of anions in soil solution. For example, Zn precipitates as $ZnCO_3$ (smithsonite) and ZnO (zincite) in soil solution with high concentration of free Zn^{2+} ion and HCO_3^{-} ion (Johnson-Beebout et al., 2009; Lindsay, 1979).

2.4 Zinc in soils

Zinc enters soils by weathering of rocks and minerals. High Zn concentration is generally found in basaltic igneous rocks (48 – 240 mg kg^{-1}), whereas low Zn concentration (5 – 140 mg kg^{-1}) is found in silica-rich igneous rocks like granite and gneiss. In sedimentary rocks, Zn is higher in black shales (34 – 1500 mg kg^{-1}), medium in shales and clays (18 – 180 mg kg^{-1}) and lower in sandstone (2 – 41 mg kg^{-1}) (Montalvo et al., 2016; Nagajyoti et al., 2010). Due these

variations in parent rocks and minerals, the concentration of Zn is variable in soils ranging from 10 – 100 mg kg^{-1} and Zn is often found in higher concentrations that 100 mg kg^{-1} in uncontaminated soils (Alloway, 2008; Montalvo et al., 2016). A simplified figure of Zn cycles in soils and the key processes controlling the cycles of Zn between the solid and solution phases of soils are presented in Fig. 2.2.

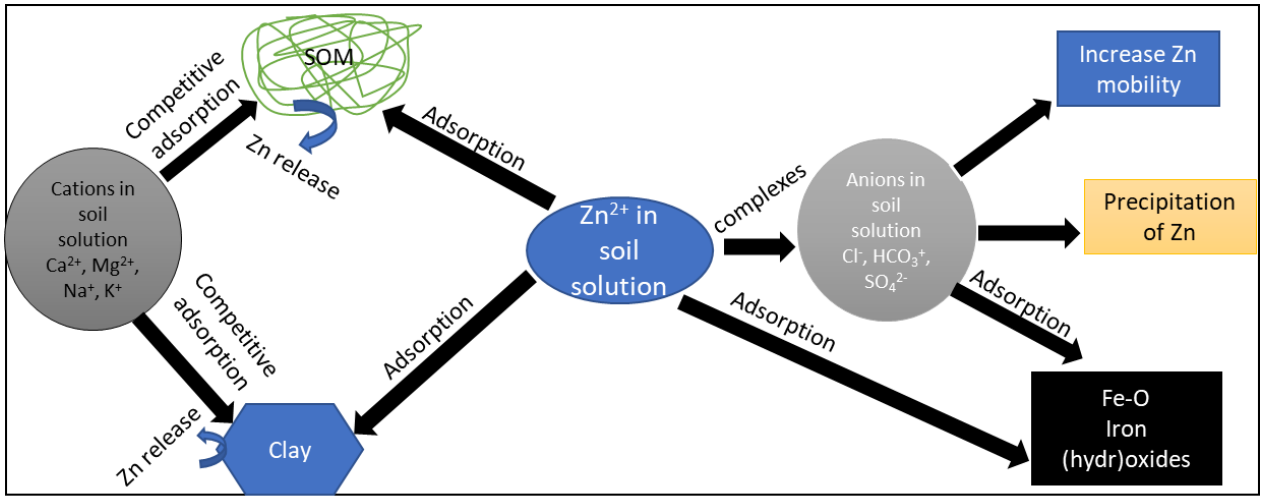


Figure 2.2 Key processes controlling the cycles of Zn in soils. Zinc is adsorbed by soil organic matter (SOM), iron (hydr)oxides, and clay. The presence of cations in soil solution leads to competition for adsorption sites (SOM, iron (hydr)oxides and clay) increasing Zn availability and mobility. Cations also cause competitive adsorption with anions. Inorganic anions form complexes with Zn which increases Zn mobility. Precipitation of Zn depends on the concentration of anions and Zn in soil solution.

2.4.1 Zinc concentrations in soil solution

Generally, Zn concentrations in soil solutions are low and ranges from 4×10^{-10} to 4×10^{-6} mol L^{-1} (Montalvo et al., 2016). The forms of Zn in soil solution and its bioavailability as well as mobility, depends on soil pH and the presence of other ions (Degryse et al., 2009). Soil pH is negatively correlated with Zn in soil solutions which indicate that Zn in soil solution is very low at high pH due to strong adsorption (Jeffery and Uren, 1983). Zn speciation is dominated by the presence of free Zn ion (Zn^{2+}) in acidic and weakly alkaline soil solutions (pH < 8) in the absence of inorganic and organic ligands; inorganic and organic ligands like chloride, carbonate and humic substances in acidic and weakly alkaline soil solutions form complexes with free Zn^{2+} ion. These complexations reduce free Zn bioavailability, change Zn mobility and adsorption behaviour in soils (Bonten et al., 2008; Weng et al., 2002). In alkaline soil solutions, Zn speciation is dominated by free Zn^{2+} ion and other species like $Zn(OH)_2$, $ZnCO_3$ and $Zn(CO_3)_2^{2-}$ (Lindsay, 1979; Powell et al., 2013).

2.4.2 Zinc in the soil solid phase

Zn in the soil solid phase is adsorbed by soild surfaces or present as precipitates (Montalvo et al., 2016). When the mechanism of Zn transfer from the soil solution to the soil solid phase is unknown, the term sorption is used to describe this transformation (Bradl, 2004).

Organic matter, clays and metal oxides are the most important solid surfaces involved in the adsorption of Zn on soils (Fisher-Power et al., 2016); the role of solid surfaces for Zn adsorption depends on soils type (Duffner et al., 2014). For example, SOM is the important sorbent in sandy soils followed by clay minerals (Weng et al., 2002; Weng et al., 2001). The role of iron hydroxides seems insignificant due to their low concentration in sandy soils (Weng et al., 2001). In clay soils, Acosta et al. (2011) and Appel and Ma (2002) found that adsorption of trace metals (Cu, Cd, Zn and Pb) depended more on clay mineralogy than organic matter content. In contrast, in temperate and tropical soils, several researchers reported that iron hydroxides along with SOM are important binding sites for Zn adsorption (Fan et al., 2005; Li et al., 2000; Saulnier and Mucci, 2000; Zoumis et al., 2001).

Zinc precipitation occurs when its concentration goes beyond the adsorption capacity of soil and the solubility product of Zn minerals (Bingham et al., 1964; Montalvo et al., 2016). Solubility calculations indicate that Zn precipitates as $ZnCO_3$ (smithsonite), $Zn(OH)_2$ (zinc hydroxide), ZnO (zincite), or Zn_2SiO_4 (willemite) when the soil pH is high (pH > 8) and concentration of free Zn is high ($> 10^4$ mol $^{L-1}$) (Lindsay, 1979; Montalvo et al., 2016). These specific conditions for Zn precipitation are typically found in heavily contaminated soils (Van Damme et al., 2010) and Zn fertilized soil bands (Kalbasi et al., 1978; Montalvo et al., 2016).

The identification of Zn precipitates and solid surfaces for Zn adsorption is complicated due to the heterogeneity of soils and different surface properties of soil (Hinz and Selim, 1994). Synchrotron techniques like EXAFS (Extended X-ray absorption fine structure) have demonstrated the presence of single mineral Zn precipitates as well as complex Zn species like Zn-LDH (layered double hydroxides), Zn-phyllosilicates, and Zn occupied metal (hydr)oxide and phyllosilicate minerals (Luxton et al., 2013; Montalvo et al., 2016).

Besides adsorption and precipitation, fixation of Zn within a mineral structure is another important mechanism to increase the nonlabile fraction of Zn (unavailable to plants). Zinc fixation in soils occurs by two possible mechanisms, i.e., solid-state diffusion into mineral lattices and precipitation (Buekers et al., 2007; Montalvo et al., 2016; Nachtegaal and Sparks, 2004). However, the fixation of Zn is not irreversible. If the conditions for Zn fixation are

changed, fixed Zn can become available. Buekers et al. (2007) reported that Zn fixation decreased from 75% to 56% when calcareous soils (pH > 7 and high $CaCO_3$ content) were acidified.

2.5 Zinc adsorption in soils: The role of solution and solid phases

The term Zn adsorption indicates the fraction of Zn that is adsorbed by the solid particles of soils. Soil factors controlling Zn adsorption in soil systems include soil pH, organic matter contents, calcite ($CaCO_3$), concentration of ions (cations and anions) in soil solution, concentration of other trace elements, soil moisture status, high available phosphorus status and microbial activity in the plant rhizosphere system (Alloway, 2009; Lindsay, 1979).

2.5.1 Effect of soil solution parameters

Several authors suggests that soil pH is the most important factor determining Zn adsorption capacity and its mobility and availability in soils (Fisher-Power et al., 2016; Mizutani et al., 2017; Montalvo et al., 2016; Weng et al., 2001). The high adsorption capacity of soil solid surfaces at elevated pH resulting from increased negative charge of soil solid surfaces is one of the main reasons for decreasing Zn availability in soils (Alloway, 2009). Soil pH is variable and depends on soil properties. It increases due to the presence of high concentration of $CaCO_3$, application of liming during the agricultural practices, high salt contents, and reducing conditions in soils (Kiekens, 1995). However, other authors reported that soil pH has less effect on Zn adsorption and mobility in soils, especially in tropical soils (de Matos et al., 2001; Gomes et al., 2001; Katyal and Sharma, 1991). In a study with Brazilian soil, Gomes et al. (2001) reported that the adsorption and mobility of Zn was not significantly correlated with soil pH. Similar results were observed by Katyal and Sharma (1991) studying 57 Indian soils. They reported that Zn adsorption and mobility was correlated with clay but not soil pH. de Matos et al. (2001) found that Zn adsorption and mobility was significantly positively correlated with CEC, soil Ca and sum of bases in Brazilian ultisols and oxisols but not with soil pH. They concluded that other soil properties can significantly affect Zn adsorption and mobility in low pH soil.

2.5.2 Effect of solid phases (carbonates, organic matter, Fe-oxides and clay minerals)

Calcareous soils have high concentration of $CaCO_3$ (> 15% weight percentage) and high pH value (pH > 8) (Wang and Harrell, 2005). The presence of high pH and $CaCO_3$ make calcareous soils retain Zn through adsorption and precipitation (Alloway, 2009; Kiekens, 1995; Zachara et al., 1991; Zachara et al., 1988). As a result, Zn availability and mobility are lower in

calcareous soils. Beside the high concentration of $CaCO_3$, an additional factor also influences Zn adsorption capacity in calcareous soils. For example, Fe oxides are often precipitated in calcareous soils and form a coating on the carbonate minerals. The presence of Fe oxides coatings on the calcite increased, for example, Zn bonding to 7-fold (Alloway, 2009; Uygur and Rimmer, 2000).

Soil organic matter (SOM) significantly influences Zn adsorption, mobility and availability. SOM includes the solid phase (linked with soil particles) and the dissolved phase (dissolved organic matter) (Fan et al., 2016). Generally, solid-phase organic matter is governed by humic acid, whereas dissolved organic matter is governed by fulvic acid (Baldock and Nelson, 2000). SOM has a high cation exchange capacity (CEC) (150 – 300 cmol kg^{-1}), a high specific surface area (800 – 900 m^2 g^{-1}) and functional groups such as carboxylates and phenolics (Fan et al., 2016; Sparks, 2003). Metal complexation with dissolved organic matter (DOM) increases the mobility and availability of metals, whereas solid-phase organic matter adsorbs metals, therefore reducing their mobility and availability (Kleber et al., 2015; Sparks, 2003). Several studies illustrated the influence of SOM on Zn adsorption and its mobility and availability in soils. Weng et al. (2002) demonstrated using the NICA-Donnan model calculation that Zn mobility in sandy soils is controlled by solid-phase organic matter. Fan et al. (2016) identified Zn species in soils by extended X-ray absorption fine structure spectroscopy and microfocus X-ray fluorescence, and reported that Zn binding to solid-phase organic matter is enhanced with increasing SOM content. Similary, Duffner et al. (2014) used a multi-surface modelling approach to predict free Zn ion concentration in low-zinc soils and found that it decreased with increasing SOM content. An increase of SOM content in soils reduced the proportion of nonspecific adsorbed Zn (Fan et al., 2016). Increasing SOM content in soils also increases Zn and DOM concentration in soils as Zn (80 mg kg^{-1}) would present in applied organic matter (OM) in soil and solid SOM turn into DOM.

A positive correlation is observed between Zn adsorption and total clay content in tropical and temperate soil, suggesting that clay fraction/minerals are important in Zn adsorption (Katyal and Sharma, 1991; Munkholm et al., 1993). The effect of clay minerals on Zn adsorption depends on the type of clay minerals (Uddin, 2017). In soils with 2:1 clay minerals such as montmorillonite, vermiculite, *etc*., generally have high cation exchange capacity (CEC); thus, Zn and other metals are adsorbed onto 2:1 clay minerals more strongly. In contrast, soils with 1:1 clay minerals such as kaolinite have low CEC (Appel and Ma, 2002; Rieuwerts, 2007). Numerous articles also present results that clay minerals do not adsorb more metals compared

with other constituents (SOM, Fe (hydr)oxides) (Duffner et al., 2014; Fisher-Power et al., 2016; Mizutani et al., 2017; Weng et al., 2001). The high concentration of cations in soil solution reduces metal adsorption by occupying the permanently negative charged sites.

Fe-(hydr)oxides have a high affinity for Zn (Chesne and Kim, 2014). Surface complexation modelling concluded that they are one of the major sorbents in soils (Duffner et al., 2014; Weng et al., 2001). Zn adsorption by Fe-(hydr)oxides is lower at low pH and higher at neutral to elevated pH, and around 85-95% of Zn adsorb at pH 7.0 (Chesne and Kim, 2014; Ponthieu et al., 2006). At pH > 8, Zn is fully adsorbed and precipitated/incorporated at Fe-(hydr)oxides surface (Chesne and Kim, 2014). Therefore, a low concentration of Fe-(hydr)oxides leads to low metal adsorption on soils (de Matos et al., 2001; Zachara et al., 1992).

2.6 Zn adsorption in soils: Adsorption mechanisms and surface complexes

In soils, Zn adsorbs by multiple processes, and a mechanistic understanding is required to manage Zn in agricultural fields and natural ecosystems effectively. This section provides an overview of Zn adsorption mechanisms and its surface complexes with the adsorption sites on soils.

Zn adsorption often describes two primary mechanisms: specific adsorption and non-specific adsorption. Specific adsorption of Zn is less reversible/irreversible, including inner-sphere complexes and more selective (McBride, 1994; Reed and Cline, 1994). The binding of Zn with SOM and variable charge minerals is one example of specific adsorption. It defines by surface complexation reactions between Zn and functional surface groups at the soil surface and edges. Functional surface groups involved for specific adsorption can be silanol groups (≡Si-OH), aluminol groups (≡Al-OH), inorganic hydroxyl groups (≡Fe-OH), or organic functional groups (-COOH). These functional groups are deprotonated at elevated pH, developing negatively charged surfaces that adsorb Zn by an inner-sphere mechanism (Bradl, 2004). The specific adsorption of Zn on soils therefore largely depends on soil pH and can be described as follows:

$$\equiv \mathrm{FeOH} + \mathrm{Zn^{2+}} + \mathrm{H_2O} \leftrightarrow \equiv \mathrm{FeOZnOH_2^{+}} + \mathrm{H^{+}} \quad (2.1)$$

Specific adsorption (inner-sphere complexes) can be monodentate and bidentate complexes (Chesne and Kim, 2014). In monodentate complexes, the complexes are formed with 1:1 stoichiometry (one surface functional group and one metal ion), whereas the complexes form with 2:1 stoichiometry (two surfaces functional group and one metal ion) in bidentate complexes (Palmqvist et al., 1997). An example of monodentate and bidentate complexes with the functional surface hydroxo groups (≡Fe-OH) of iron (hydr)oxides is present below:

$$\equiv FeOH + Zn^{2+} \leftrightarrow FeOZn^{+} + H^{+} \quad (2.2)$$

$$\equiv 2FeOH + Zn^{2+} \leftrightarrow (FeOH)_2Zn^{2+} \quad (2.3)$$

Both monodentate and bidentate complexes of Zn are reported in the literature for surface complexation models of Zn adsorption onto goethite and ferrihydrite (Dyer et al., 2004; Palmqvist et al., 1997; Palmqvist et al., 1999; Xu et al., 2006). Among the complexes, bidentate complexes are more dominant than monodentate. This result is supported by EXAFS analysis (Chesne and Kim, 2014). EXAFS analysis indicated that bidentate edge-shearing and bidentate corner-sharing complexes are the main mechanisms of Zn adsorption onto ferrihydrite and goethite (Chesne and Kim, 2014).

Non-specific adsorption is defined by surface complexation reactions between Zn and functional surface groups in the presence of water molecules. As water molecules present between Zn and functional surface groups, non-specific adsorption is called an outer-sphere complex. Generally, Zn forms outer-sphere complexes at the silanol (≡Si-OH) and aluminol site (≡Al-OH) of clay minerals (Ca-montmorillonite) (de Pablo et al., 2011; Stietiya and Hashem, 2010). Non-specific adsorption of Zn is less stable and reversible, and the adsorption reaction is controlled by diffusion and electrostatic interactions (Strawn, 2021). It is initially observed upon adsorption and conversion into specific adsorption (inner-sphere complexes) after a time interval is reported in several studies (Chesne and Kim, 2014; Lee et al., 2004). The non-specific adsorption of Zn can be described as follows:

$$\equiv FeOH + Zn(OH_2)^{2+} \leftrightarrow \equiv FeO(H_2O)Zn^{+} + H^{+} \quad (2.4)$$

In addition to the inner sphere and outer-sphere complexes, Zn can adsorb on the surface site of Fe-(hydr)oxides as ternary surface complexes (Chesne and Kim, 2014). Ternary surface complexes are defined by the co-adsorption of Zn and ligands (Cl, SO_4, PO_4, etc.) onto the same site of Fe-(hydr)oxides (Bradl, 2004; Strawn, 2021). Two different ways explain the formation of ternary surface complexes:

First, a metal that already adsorbs on the surface hydroxyl group attach ligands as follows:

$$\equiv FeOZn^{+} + L^{-} \leftrightarrow \equiv FeOZnL \quad (2.5)$$

Second, ligands that complex with a reactive surface by the replacement of the surface hydroxyl group formed a bridge between the surface and metal as follows:

$$\equiv FeOH + L^{-} + H^{+} \leftrightarrow \equiv FeL^{-} + H_2O \quad (2.6)$$

$$\equiv FeL^{-} + Zn^{2+} \leftrightarrow \equiv FeLZn^{+} \quad (2.7)$$

The second explanation of the ternary surface complex occurs preferably at low pH and characterizes by decreasing adsorption with increasing pH (Bradl, 2004).

Model and spectroscopic analysis examine metal adsorption onto Fe-(hydr)oxides as ternary surface complexes. Swedlund and Webster (2001) and Swedlund et al. (2009) reported that adsorption of Zn, Cu, Cd and Pb onto goethite and ferrihydrite is enhanced in the presence of sulfate because metals adsorb as ternary surface complexes (goethite-M^{2+}-SO_4^{2-}). Similarly, co-adsorption of Zn and PO_4 on the surface of ferrihydrite is reported by Liu et al. (2016). In NaCl solutions, Chesne and Kim (2014) examined that Zn adsorption onto goethite and ferrihydrite increased with increasing NaCl concentration by forming ternary surface complexes (Chesne and Kim, 2014).

2.7 Surface complexation models

Freundlich and the Langmuir isotherm models do not consider the chemistry of metals in soil solution and the electrostatic interactions between ions and a solid surfaces. Therefore, the description of metals adsorption onto particles by the adsorption isotherms cannot provide a realistic scenario of metal cycles in soil. To overcome these limitations, metal adsorption onto soil particles is described using surface complexation models, which account for the chemistry of metal and the reactions occurring between metal and surfaces of soil particles in soil solution. Models may differ in surface charge components, surface functional group, type and position of the adsorbed species, and the number and position of potential planes. The most widely used surface complexation models are the CCM (constant capacitance model), the DLM (diffuse layer model) and the TLM (triple layer model) (Fig. 2.3), which refer to the double layer by 2, 3, and 4 potential adsorption planes (Bradl, 2004; Goldberg, 1998). The adsorption of metals at solid-water interfaces is defined precisely at a macroscopic scale by surface complexation models with the advancement of the spectroscopic technique (Somasundaran, 2006).

2.7.1 CCM, DLM, and TLM model

The CCM is the simplest surface complexation model and is developed by Stumm et al. (1976) and by Schindler and Kamber (1968). The double layer of this model consists of two parallel planes where the surface charge σ_0 is connected to the one plane and the counter charge σ_1 is linked to the other plane (Fig. 2.3 A). The model is good selection for high ionic strength solution as the diffuse section of the double layer is compressed with increasing ionic strength. Metals are adsorbed through specific adsorption and all complexes are inner-sphere surface complexes.

The DLM model was introduced by Stumm et al. (1970) and developed by Dzombak and Morel (1990). The model has three different planes, namely plane 0, plane d and diffuse plane (Fig. 2.3 B). Ions are adsorbed in plane 0 as inner-sphere complexes, plane d represented the distance of closest approach of the counter ions and the surface potential is dropped zero after plane d. The model can describe metal adsorption as a function of different ionic strengths.

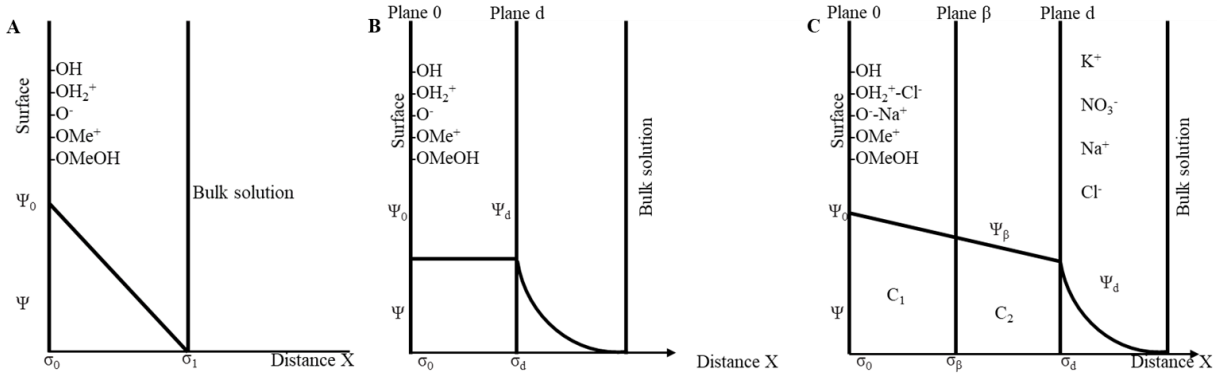


Figure 2.3 Schematic illustration of the constant capacitance model (A), double layer model (B), and triple layer model (C) adapted from (Bradl, 2004). The surface charge represents by σ whereas surface potential represents by Ψ. The relation between surface charge and surface potential is linear in the constant capacitance model. The summation of all specifically adsorbed ions represents by the surface charge σ_0 in constant capacitance and double layer model. In TLM, the metal ions adsorb at 0 plane or β plane. Therefore, the surface charge in TLM is equal to the net proton charge plus the charge from the 0 plane and β plane.

The triple layer model (TLM) is a version of the extended Stern model and comprises four planes (Fig. 2.3 C) (Davis et al., 1978; Yates et al., 1974). The TLM describes electrolyte and metal ions adsorption as inner and outer-sphere complexes depending on where ions are situated. The model can be applied to count ions adsorption in different range of ionic strengths. The TLM can provide more realistic picture of metal ions adsorption as metal adsorption can occur at the 0 plane (inner-sphere complex) or the β plane (outer-sphere complex) (Bradl, 2004; Hayes and Leckie, 1987). The TLM is more complex than the CCM and DLM. A brief explanations of surface complexation models assumptions as well as their mathematical equations are provided in the Appendix A.

2.7.2 Introducing the concept of multi-surface models

Surface complexation models involving a single mineral have mainly contributed understanding the fate of metals on iron (hydr)oxides, DOM, SOM, and clay in different environmental conditions (Dzombak and Morel, 1990; Gustafsson, 2001; Gustafsson et al., 2003; Kinniburgh et al., 1999; Milne et al., 2003; Singh and Mattigod, 1992). However, a single-phase surface complexation model cannot properly describe metal adsorption since soils

are a complex natural system with different sorbent components. To overcome this limitation, a combination of surface complexation models for the various reactive components into "multi-surface models" is a promising way to predict the metal cycle in soils (Dijkstra et al., 2004; Groenenberg and Lofts, 2014; Weng et al., 2001).

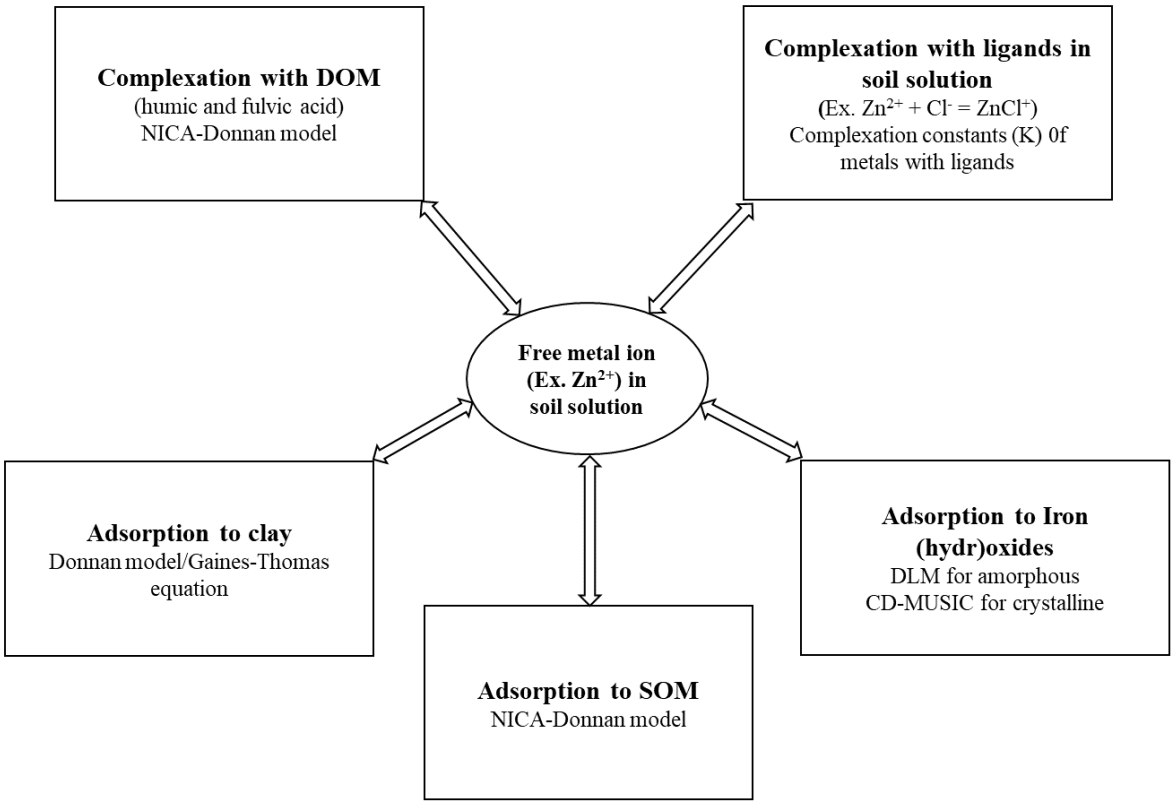


Figure 2.4 Multi-surface models to predict metals adsorption in soils (Weng et al., 2002).

Multi-surface models integrate of thermodynamic models for inorganic speciation and mineral equilibria, and models of reactive components, such as metal oxides, clay and organic matter (Fig. 2.4) (Groenenberg and Lofts, 2014). Thermodynamic principles are the basis of multi-surface models. Multi-surface models consider the competition among ions for binding. For these reasons, the models can implement in a wide range of environmental conditions, e.g., pH and ionic strengths (Groenenberg and Lofts, 2014). This advantage makes the models suitable to predict metal's cycle in soils beyond the parameterization range (Koopal et al., 2001). To obtain practical models, ion binding complexity to heterogenous complexants requires simplifications (Van Riemsdijk et al., 2006) and each reactive components model parameters (site densities and binding constants) need to be determined. Calculation of the total sorption in multi-surface models equals to the sum of sorption by each specific component. It assumed

that except for competition for ion binding, no interaction is between the models of each reactive component (Groenenberg and Lofts, 2014).

2.7.2.1 Binding to Iron/Aluminium (hydr)oxides

The DLM model recommended for specific binding of metals and anions on iron (hydr)oxides (FeO) and aluminium oxides (AlO) (Khai et al., 2008). FeO and AlO in soils determine by selective chemical extraction. The most common method is the oxalate extraction (Bonten et al., 2008; Lofts and Tipping, 1998; Weng et al., 2001). Some studies use ascorbate extraction (Khai et al., 2008). The amount of crystalline FeO calculates from the difference between dithionite-citrate-bicarbonate and oxalate extractions (Weng et al., 2002; Weng et al., 2001) or between Fe-dithionite and Fe-ascorbate (Khai et al., 2008). The mineral phases of amorphous FeO and crystalline FeO may modelled using by separate specific surface complexation model like the DLM for amorphous FeO and the CD-MUSIC for crystalline FeO or by combining crystalline phase in the amorphous phase after correcting the surface area (Groenenberg and Lofts, 2014; Khai et al., 2008). The recommended surface area of 600 m^2/g and 100 m^2/g generally use for amorphous FeO and AlO, and crystalline FeO to calculate the site concentration (Dijkstra et al., 2004; Dijkstra et al., 2009). For combining, the density of crystalline FeO needs to be divided by 6 to convert and combine crystalline FeO to amorphous FeO equivalents (Khai et al., 2008).

2.7.2.2 Binding to organic matter

The NICA-Donnan model is applied when describing the binding of metals to organic matter. It is a continuous distribution model (Milne et al., 2001). The model uses an isotherm incorporating humic heterogeneity and adsorbate (ion)–specific nonideality of binding to simulate specific binding of ions with organic matter (Groenenberg and Lofts, 2014). The model was developed by Koopal et al. (1994) using the Langmuir equation along with the distribution of binding affinities. Benedetti et al. (1995; 1996) then extended the NICA expression to describe the bimodal distribution of binding sites on humic substances (Benedetti et al., 1995; Benedetti et al., 1996). They added an electrostatic submodel to improve the model performance using an empirical electrostatic correction factor and by assuming charge neutrality "Donnan gel phase" with the humic molecules. The model assumed that the concentrations of accumulated ions within the gel phase are related to their concentrations in bulk solution.

Kinniburgh et al. (1999) developed a thermodynamically consistent model was by Kinniburgh and co-authors (Kinniburgh et al., 1999). This model accurately describes the competitive

binding nature of Ca^{2+}-Cd^{2+} and Ca^{2+}-Cu^{2+} to a peat HA over a range of pH values and ionic strength after calibration with single metal-binding datasets. Following that, Milne et al. (2001; 2003) derived the generic parameters of NICA-Donnan for binding of protons and 23 metals to HA and FA using the literature datasets. Gustafsson and Kleja (2005) extended the NICA-Donnan model to account for the ionic strength dependence of proton dissociation. Previously, it was presumed that humic substance electrostatic interactions in solid phase were similar to in solution. However, the assumption did not work correctly; therefore, a fixed Donnan volume of 1 L kg^{-1} for humic substance in the solid phase was introduced to improve model fits of proton and metal binding with the solid phase humic substance in different ionic strengths (Gustafsson and Kleja, 2005).

Natural organic matter comprises solid-state FA and HA, DOM, and low molecular weight organic molecules. The binding affinity of each fraction of natural organic matter for metals is different; therefore, measured SOM and DOM must be converted to a fraction of active/reactive organic matter with equivalent binding properties to HA or FA before input the concentration of DOM and SOM in the NICA-Donnan model (Groenenberg and Lofts, 2014; Weng et al., 2001).

The active fraction of DOM reported in the literature range from 31% to 100%. These fractions determine by specific measurements, acquired by model optimization, or selected based on average fractions reported in the literature (Groenenberg and Lofts, 2014). The fraction of 65% was used in several studies as an active fraction of DOM (Bryan et al., 2002). A fraction of 87% was also used in several studies (Khai et al., 2008; Linde et al., 2007), along with the assumption that the active DOM consisted of 50% HA and 50% FA (Weng et al., 2002).

The active fraction of SOM reported in the literature varies from 31% to 87% (Dijkstra et al., 2009; Groenenberg et al., 2012; Groenenberg and Lofts, 2014; Lumsdon, 2004). The active fraction of SOM can assess by determining the concentration of humic substances in soils, assuming that humic acid is solely responsible for metal, cation, and proton adsorption in soils (Dijkstra et al., 2009; Groenenberg et al., 2010; Lumsdon, 2004). Where direct measurement data of direct measurement are absent, the fraction of active SOM is estimated by model optimization (Gustafsson and van Schaik, 2003; Lofts et al., 2001). Tipping et al. (2003) and Groenenberg and Lofts (2014) obtained the fraction of active SOM in the range of 9% to 86% of total SOM by optimizing model VI in the PHREEQC. Gustafsson et al. (2003) and Groenenberg and Lofts (2014) reported this fraction in the range of 17% to 84% by optimizing the SHM (Stockholm humic model). Weng et al. (2001) and Groenenberg and Lofts (2014)

calculated the active fraction of SOM by subtracting the measured cation exchange capacity of SOM and clay fraction, and estimated the active fraction of SOM in sandy soil in the range 16% to 46% with an average of 36% relative to generic humic acid.

2.7.2.3 Binding to clay

Metals adsorption to phyllosilicate clay is controlled at lower pH by non-specific adsorption to the negatively charged clay particles and at higher pH by specific adsorption to the edge phases of the clay (Schindler et al., 1987; Weng et al., 2001). The ion exchange to phyllosilicate clays describes by the Donnan approach (Weng et al., 2001) or the Gaines-Thomas equation (Khai et al., 2008).

The density of phyllosilicate clay is estimated from the equation of van Reeuwijk after measuring the total organic carbon (TOC) and cation exchange capacity of the soil (van Reeuwijk, 1993).

$$\mathrm{CEC_{clay}} = \frac{100}{\%\ \mathrm{clay}}(\mathrm{CEC_{soil}} - 3.5 \times \mathrm{TOC}) \quad (2.8)$$

Where % clay is the clay content of soil, CEC_{soil} is the cation exchange capacity of soil (cmol Kg^{-1}), and TOC is the total organic carbon in percent.

In soil, high SOM in the top player (A horizon) might provide a biased estimation of clay density. Therefore, Khai et al. (2008) quantified the density of clay from the lower layer (C horizon) with minimum SOM using euation 2.8. They assumed the calculated clay density from the C horizon is valid for the A horizon. In addition, the density of the clay is estimated from a model calculation using the CEC of illite, assuming the CEC of clay is the same as the CEC of illite (0.1 to 0.4 mol kg^{-1}) (Weng et al., 2001).

2.8 Effect of NaCl and HCO_3 concentrations on the adsorption of Zn on goethite and soils

This thesis examines the effect of NaCl solution concentrations and HCO_3 ions on the adsorption of Zn on soils and goethite. This section presents an overview of the effect of changing carbonate and NaCl concentrations on the adsorption of Zn on soils and goethite. The knowledge gap concerning Zn adsorption on soils and goethite in different NaCl solution concentrations with and without carbonate effects is identified and discussed.

2.8.1 Effect of NaCl concentrations on the adsorption of Zn onto goethite

Increasing NaCl concentration should affect the adsorption of Zn onto goethite by the same mechanisms reported in section 2.9.1. The adsorption of Zn onto goethite is higher in NaCl solutions than $NaNO_3$ and $NaClO_4$ (Bolland et al., 1977; Forbes et al., 1976; Padmanabham, 1983). With increasing NaCl concentrations from 0.1 mol L^{-1} to 0.6 mol L^{-1}, Zn adsorption

onto goethite between pH 4 - 8 increases. The adsorption of Zn onto goethite as ternary surface complexes (Zn-Cl complexes) is a possible mechanism, as evidence from EXAFS spectroscopy suggests Chesne and Kim (2014). However, Balistrieri and Murray (1982) reported that Cl ion did not significantly influence Zn adsorption onto goethite even at a high NaCl concentration (0.53 mol L^{-1}). They reported that the adsorption of Zn onto goethite in 0.53 mol L^{-1} NaCl solution and in 0.1 mol L^{-1} $NaNO_3$ ionic solution was similar during experimental studies (Balistrieri and Murray, 1982). The above conflicting results of Zn adsorption in NaCl concentration are possibly due to the differences of initial Zn concentration and goethite concentration during the experimental processes. Initial Zn concentration was higher in Chesne and Kim studies (Zn = 0.5 mmol L^{-1}) than in Balistrieri and Murray studies (Zn = 0.003 mol L^{-1}), whereas goethite concentration was opposite (0.17 and 0.55 g L^{-1}). These experimental differences indicate that the effect of Cl^- ion on the adsorption of Zn mostly depends on the concentration of Zn and goethite. Studies on Zn adsorption onto goethite in different NaCl concentrations and with varying concentrations of Zn are missing.

2.8.2 Effect of NaCl concentrations on the adsorption of Zn on soils

Increasing NaCl concentrations in soil solution should affect Zn adsorption in soils by complexation of Cl anions with Zn and hence, altering the charge of the Zn^{2+} cation (Paalman et al., 1994) (Fig. 2.5). Competition between Na^+ cation and free Zn^{2+} ion for adsorption sites on the soil interfaces is also reported; however, the competition should not affect Zn adsorption notably because Na forms outer-sphere complexes whereas Zn forms inner-sphere complexes with mineral surfaces (Wang and Harrell, 2005).

Contradicting findings are reported on the effect of NaCl concentrations on the adsorption of Zn on soils. For example, Acosta et al. (2011) reported that an increase of NaCl concentration from 6 mmol L^{-1} to 0.3 mol L^{-1} did not significantly decrease Zn adsorption on calcareous soils (pH > 7.72). These results are in line with work by Shuman (1986), who reported that increasing the concentration of Na and anions (NO_3^-, Cl^- and SO_4^{2-}) did not influence on Zn adsorption in soils. In contrast, Wang and Harrell (2005) observed a significant decrease in Zn adsorption on calcareous and acidic soils with increasing Cl^- ion concentrations. Linde et al. (2007) reported that Zn adsorption on acid soils decreased with increasing NaCl concentration even at low NaCl concentration (50 mmol L^{-1}). Similarly, Chu et al. (2015) reported that Zn adsorption on the tropical estuary wetland soil decreased with increasing Cl^- ion concentration due to the formation of Zn-Cl complexes.

The previous results indicated that NaCl concentration decreased Zn adsorption on acid soils. However, contradicting findings were reported in calcareous soils. Previous studies have focused on determining Zn adsorption on soils in low NaCl concentrations (0.01 to 0.3 mol L^{-1}) with respect to a single soil pH. Therefore, much remains unknown about the pH dependent adsorption of Zn on soils in low to high NaCl concentrations (0.1 to 0.7 mol L^{-1}). For this, a more comprehensive investigation into Zn adsorption in different NaCl concentrations needs to see whether soil pH and increasing NaCl concentration due to seawater intrusion in agricultural fields have effect on Zn adsorption and its species. Accurate prediction of Zn adsorption on soils in different NaCl concentrations is important to predict Zn bioavailability to plants in different saline environments and manage Zn contamination in soils (D'Amore et al., 2005).

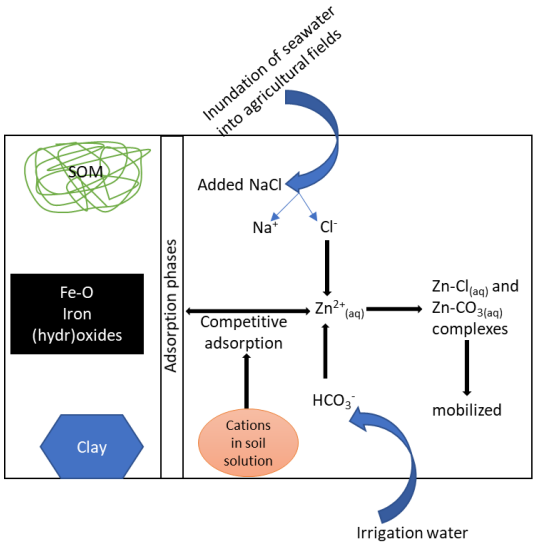


Figure 2.5 Effect of NaCl concentration and HCO_3^- ion on the adsorption of Zn on soil. NaCl and HCO_3 are added in the soil solution due to the inundation of seawater and by applying irrigation water into agricultural fields. Cl^- and HCO_3^- ion increases the mobility of Zn through the complexation. The cations in soil solution decrease Zn^{2+} adsorption due to the competition for adsorption sites on the soil interfaces.

2.8.3 Effect of carbonate on the adsorption of Zn on soils and goethite in NaCl solutions

Dissolved inorganic carbon is ubiquitous in natural aqueous environments and the concentrations typically vary from 0.1 mmol L^{-1} to 10 mmol L^{-1} (Mendez and Hiemstra, 2019; Villalobos and Leckie, 2000). Carbonate is adsorbed to goethite surface over a wide range of pH and directly competing with other anions for binding sites (Schulthess et al., 1998; Vangeen et al., 1994; Zachara et al., 1987). As a result, the presence and increasing concentration of Cl anions reduces carbonate adsorption on goethite (Villalobos and Leckie, 2000). The presence of carbonate also affects metals adsorption on goethite. Carbonate increases or decreases

adsorption by forming carbonat complexes of metals (Duff and Amrhein, 1996; Kohler et al., 1999; Mason et al., 1997; Villalobos et al., 2001). In addition, the high concentration of carbonate in solution can precipitated metal as metal-carbonate complex on the surface of goethite (Villalobos et al., 2001).

Groundwaters in the coastal area of South Asia typically have high concentrations of carbonate (Hug et al., 2008). This groundwater for irrigation increases carbonate concentration in soils (Shahabi et al., 2005). The high carbonate concentration and increased NaCl concentrations in soil solution will affect Zn mobility in the soil system as Zn forms complexes with Cl^- ion and dissolved carbonate (Fig. 2.5) (Powell et al., 2013). The Cl^- ion competes with carbonate (HCO_3^-) during complexation with Zn. The competitive adsorption of carbonate on goethite in the presence of different anions (Cl^-, NO_3^-, and PO_4^{3-}) and the effects of carbonate on the adsorption of Cr, U, Pb on goethite well reported in the literature (Vangeen et al., 1994; Villalobos and Leckie, 2001; Villalobos et al., 2001). However, the effect of carbonate on Zn adsorption on soils and goethite in different NaCl concentrations has not yet been achieved.

2.9 Application of surface complexation models on the adsorption of Zn and carbonate onto goethite and on soils in different NaCl concentrations.

This thesis aim to develop and apply existing surface complexation models (Gustafsson, 2019) to describe Zn adsorption in different NaCl concentration (0.1, 0.3 and 0.7 mol L^{-1}) in the presence of carbonate. This section presents an overview of what is currently known about the application of surface complexation models on the adsorption of Zn on soils and onto goethite in different NaCl concentrations. The previous work and the knowledge gap concerning surface complexation models of Zn in different NaCl concentrations are discussed and identified.

2.9.1 Application of CCM, DLM, and TLM on adsorption of Zn and carbonate onto goethite

CCM, DLM, and TLM successfully predict metal adsorption on goethite in single and competitive adsorbate systems as a function of pH, ionic solution (0.1 mol L^{-1} $NaNO_3$ and NaCl) and metal concentration (Kooner et al., 1995; Palmqvist et al., 1997; Palmqvist et al., 1999; Peacock and Sherman, 2004; Spathariotis and Kallianou, 2007; Swedlund and Webster, 2001; Swedlund et al., 2009; Villalobos et al., 2001; Xu et al., 2006). However, model adsorption constants derived from a single sorbate system cannot accurately predict metal adsorption onto goethite in multiple anion-rich solutions. For an accurate model, ternary surface complexes are introduced and the adsorption of the metals is then accurately modelled (Gao and Mucci, 2003; Peacock and Sherman, 2004; Swedlund and Webster, 2001; Swedlund

et al., 2009). Therefore, modifiying the models using spectroscopic evidence and surface characteristics is necessary to predict metal adsorption in a bi-solute system (Nomaan et al., 2021). The CCM applies in higher ionic solution ($I \geq 0.1$ mol l^{-1}) whereas the DLM works well in low ionic solution ($I \leq 0.1$ mol l^{-1}). In comparison, the TLM is applicable for a range of ionic strength solutions (Bradl, 2004). The DLM has a comprehensive set of model parameters for metal binding with iron (hydr)oxides (Dzombak and Morel, 1990) and has become a benchmark in surface complexation modelling.

The application of the CCM and DLM to describe Zn adsorption on goethite in seawater (≈ 0.7 mol L^{-1}) has not been reported. One study applied the TLM (Balistrieri and Murray, 1982). Studies of arsenic adsorption using the CCM and DLM model parameters showed that the models can describe arsenic adsorption onto goethite and HFO at seawater ionic solution if the activity co-efficient of ions do appropriately using the extended Debye-Huckel expression (Gao and Mucci, 2001; Gao and Mucci, 2003; Mercer and Tobiason, 2008). These results suggests that the CCM and the DLM model can also be used to describe Zn adsorption on goethite in high NaCl concentrations (0.7 mol L^{-1}).

Only a limited number of studies investigated carbonate adsorption onto goethite using the DLM. Vangeen et al. (1994) found that the DLM well predicted carbonate adsorption at pH > 5 but significantly overestimated carbonate adsorption at pH < 5. Like DLM, the TLM parameters describe successfully pH-dependent carbonate adsorption onto goethite in 0.1 mol L^{-1} NaCl and $NaNO_3$ solution (Villalobos and Leckie, 2001). Introducing a ternary surface complex [$\equiv FeOMeCO_3$], the model described the adsorption behaviour of trace species (Pb, Cr, U) in the presence of carbonate in 0.1 mol L^{-1} $NaNO_3$ ionic solution (Villalobos et al., 2001).

To date, to our knowledge, a surface complexation model for carbonate adsorption onto goethite at high NaCl concentration has not yet been established. This gap, however, is needed to assess the effect of salinisation on Zn adsorption in carbonate-rich water typically found in coastal areas.

2.9.2 Application of multi-surface models (MSMs) for soils

The application of MSMs to describe metal mobility in a wide range of soils is well reported in the literature (Bonten et al., 2008; Duffner et al., 2014; Groenenberg and Lofts, 2014; Khai et al., 2008; Ren et al., 2017; Weng et al., 2001). The accuracy of MSMs predictions for metal cations is generally good. The results suggest that MSMs with existing model parameters can

describe metal mobility in soils in different environmental conditions (Groenenberg and Lofts, 2014) and low Zn containing soils (Duffner et al., 2014). During batch adsorption experiments in 0.1 mol L^{-1} $NaNO_3$ ionic solution, Zn adsorption in soils was also assessed using MSMs (Fisher-Power et al., 2016; Mizutani et al., 2017).

MSMs models predicting Zn adsorption in soils were developed and validated for low ionic solution (0.01 mol L^{-1} to 0.02 mol L^{-1} $NaNO_3$) (Fisher-Power et al., 2016; Khai et al., 2008; Zhang et al., 2018a) but not for NaCl concentrations with a broader range, i.e., 0.1 mol L^{-1}, 0.3 mol L^{-1} and 0.7 mol L^{-1}, respectively or and in the presence of carbonate. At a high concentration of NaCl, the MSMs accuracy could be affected by two factors. First, model parameters adjusted for relatively low ionic solutions are not valid in higher ionic strength solutions (Duffner et al., 2014; Gustafsson and Kleja, 2005; Gustafsson et al., 2003). Second, the activity correction using the extended Debye-Huckel equation and/or Davies equation which are typically valid in solution up to I = 0.5 mol L^{-1} is not valid at 0.7 mol L^{-1}. In addition, the high concentration of carbonate in soil solution can precipitate metal which needs to be described precisely by surface complexation models. This thesis is the first comprehensive study examining the implementation of MSMs to describe the adsorption of Zn on soils in different NaCl concentrations in the presence of carbonate.

2.10 Activity correction

The application of the extended Debye–Hückel and Davis equation to determine the activity of metals in a saline solution like seawater is reviewed by several authors and it shows that they can successfully model the behaviour of ions at higher ionic strength (Baeza and RamisRamos, 1996; Bonito et al., 2018; Gao and Mucci, 2001; Gao and Mucci, 2003; Haynes, 2015-2016; Mercer and Tobiason, 2008). While the application of the specific ion interaction theory (SIT) to determine ion activity co-efficients at higher ionic strength (> 0.5 mol L^{-1}) is preferred (Powell et al., 2013), the lack of accurate ion interaction co-efficients ($\Delta\varepsilon$) and reaction enthalpies (ΔH) for many limits its application to soil solutions. Therefore, the application of the extended Debye–Hückel and Davis equation for aqueous solutions above 0.5 mol L^{-1} is validated (chapter 4) and subsequently used (chapter 5 and 6) in this work to determine ion activity co-efficients in different NaCl solutions during the model analysis.

2.11 Research aim and objectives

Coastal soils in tropic regions are increasingly affected by high NaCl and carbonate concentrations. This effect is due to an increase in the inundation of seawater into agricultural fields and the application of carbonate rich groundwater for irrigation. Predictive models that

allow these changes to affect the geochemical processes operating in these soils are urgently needed to better understand metal mobility in saline-carbonate-rich solutions. Adsorption is a vital process that needs to be understood as it controls metal mobility in soils and bioavailability for plants. Surface complexation models are well suited to predict adsorption in a changing chemical environment, but because of the complexity of chemical reactions occurring in saline and carbonate soil solutions, surface complexation models for Zn in these types of solutions have not been developed to date. Therefore, the thesis aims to develop accurate predictive surface complex models for Zn adsorption on soils and goethite in saline and carbonate rich solutions.

The three main research challenges addressed in this PhD thesis to better understand the adsorption of Zn on soils and goethite using surface complexation models are:

2.11.1 What is the role of changing speciation due to increased NaCl concentrations on Zn adsorption on tropical soil?

In chapter 4, I demonstrate the effect of increasing NaCl concentration on the formation of Zn species in bicarbonate-rich soil solutions and subsequently on the adsorption of Zn in coastal tropical soils using equilibrium speciation models and batch experiments. I hypothesize that Zn adsorption decreases with increasing NaCl and HCO_3^- concentration. To this end, I first use a geochemical speciation code to determine the distribution of aqueous Zn species in NaCl solutions with concentrations ranging between 0.1 and 0.7 moles L^{-1}. I then integrate bicarbonate anions into these codes with concentrations of 2 and 8 mmol L^{-1} to assess speciation in calcareous soils. I then identify the best activity correction model for high ion strength solutions by comparing predicted Zn speciation at $I \approx 0.67$ mol L^{-1} using the Davies equation and SIT method. Third, I determine the adsorption of Zn experimentally on two tropical soils at three different NaCl concentrations using batch adsorption and evaluate the application of MSMs in saline soil solutions. Finally, I use the MSMs to predict the effect of seawater intrusions on the adsorption of Zn in the coastal soils of Bangladesh.

2.11.2 Can multi-surface adsorption models accurately predict Zn adsorption on tropical soils?

In chapter 5, I use the model parameters optimized in chapter 4 to explore the accuracy of MMS to describe pH-dependent Zn adsorption on soils in saline solutions with varying Zn concentrations. To this end, the extent of Zn adsorption calculated using the MSM is validated against Zn adsorption determined using a batch adsorption experiment. Results show that the model is accurate for solutions with concentrations of NaCl ranging between 0.1 to 0.7 moles L^{-1} and carbonate range 8 mmol L^{-1} for the pH range between 6 and 10 but not for the range

between 4 and 6. I demonstrate that the poor fit in the lower pH range is because of the absence of ternary surface complexes of Zn with iron (hydr)oxides, i.e., of ≡FeO-Zn-chloride and ≡FeO-Zn-carbonate, in the default databases. I further show that the formation of Zn-carbonate complexes leads to enhanced precipitation of Zn from pH 6 at an initial Zn concentration of 50 ppm. The relative importance of soil reactive sites clay, SOM, and iron (hydr)oxides for Zn adsorption in different experimental systems are identified and modelled.

2.11.3 What is the role of ternary surface complexes in predicting accurately Zn adosprion on goethite?

Surface complexation model constants derived from Zn adsorption experiments in 0.1 mol L^{-1} $NaNO_3$/NaCl system are unable to predict Zn adsorption accurately in 0.7 mol L^{-1} NaCl solution. Recent experimental studies and the results of chapter 5 suggest that introducing ternary surface complexes could improve model performance. In chapter 6, I explore this hypothesis further using goethite as a model system. I first determine experimentally surface complexation model parameters for Zn and goethite in solutions with pH between 3 and 9 and NaCl concentrations between 0.1 and 0.7 mol l^{-1}. I incorporate ternary surface complexes and I can develop successfully accurate surface complexation models using the constant capacitance model.

3. Materials and Methods

The following section describes the experiments and model work used to describe Zn adsorption on soils and goethite. This section also highlights the instruments and chemicals used during adsorption experiments.

3.1 Chemicals and Solutions

Analytical grade chemicals and miliQ water were used for preparing solutions. Zinc stock solutions of 2500 mg L^{-1} (38.24 mmol L^{-1}) and 250 mg L^{-1} (3.82 mmol L^{-1}) were prepared using $ZnCl_2$. The stock solutions of Zn were acidified and stored in the refrigerator. A Stock solution of HCO_3 (400 mmol L^{-1}) was prepared from $NaHCO_3$. The stock solution of HCO_3 was always prepared freshly to minimize the possible contribution of CO_2 from the open atmosphere. In addition, stock solution of HCO_3 was degassed with N_2 to minimize the contribution of dissolved CO_2.

NaCl solutions (0.1 mol L^{-1}, 0.3 mol L^{-1}, and 0.7 mol L^{-1}) were prepared from NaCl salt. Solution of 0.43 mol L^{-1} HNO_3 and 2% (v/v) HNO_3 were prepared from 1 mol L^{-1} HNO_3 stock solution. Ammonium oxalate and oxalic acid (0.2 mol L^{-1}) were prepared from monohydrate ammonium oxalate and dihydrate oxalic acid, respectively. Different concentrations of Zn were prepared from a single element Zn standard (Merck, 1000 µg mL^{-1}) to obtain a calibration curve during the ICP-MS analysis. The product information of all chemicals and reagents is presented in table 3.1.

Table 3.1 Chemical reagents used in this work

Reagent	Name	Manufacture	Grade/purity	CAS
$ZnCl_2$	Zinc chloride	Sigma-Aldrich	Reagent grade, ≥ 98%	7646-85-7
$NaHCO_3$	Sodium bicarbonate	Sigma-Aldrich	ACS reagent, ≥ 99.7%	144-55-8
NaCl	Sodium chloride	Sigma-Aldrich	ACS reagent, ≥ 99.0%	7647-14-5
HNO_3	Nitric acid	Fisher scientific	NIST standard concentrate	7697-37-2
$(NH_4)_2C_2O_4.H_2O$	Ammonium oxalate monohydrate	VWR	Reagent grade, 99 – 100%	6009-70-7
$C_2H_2O_4.2H_2O$	Oxalic acid	VWR	Reagent grade, ≥ 99%	6153-56-6
	Zn standard (1000 µg mL^{-1})	MERCK	ICP-MS standard	

3.2 Instrumentation and Methods

3.2.1 Measurement of pH

pH was measured by the Metrohm pH meter (model - 826). The glass electrode of the pH meter was calibrated using buffer solution (Thermo Scientific) at pH of 4.00, 7.00 and 10.00 and applied in experimental system of diluted electrolyte solutions (< 0.1 mol L^{-1} NaCl). In concentrated electrolyte (0.1, 0.3, and 0.7 mol L^{-1} NaCl) solutions, the pH meter was calibrated using buffer solutions of concentred electrolytes. Buffer solutions of concentred electrolyte were prepared by adding NaCl salt in standard buffer solutions. The measurements indicate that voltage potential differences of buffer solution at pH of 4.00, 7.00 and 10.00 are shifted higher values with increasing electrolyte concentrations (Fig. 3.1). The correlation co-efficient (R^2) of the calibration curves was continually exceeding 0.99.

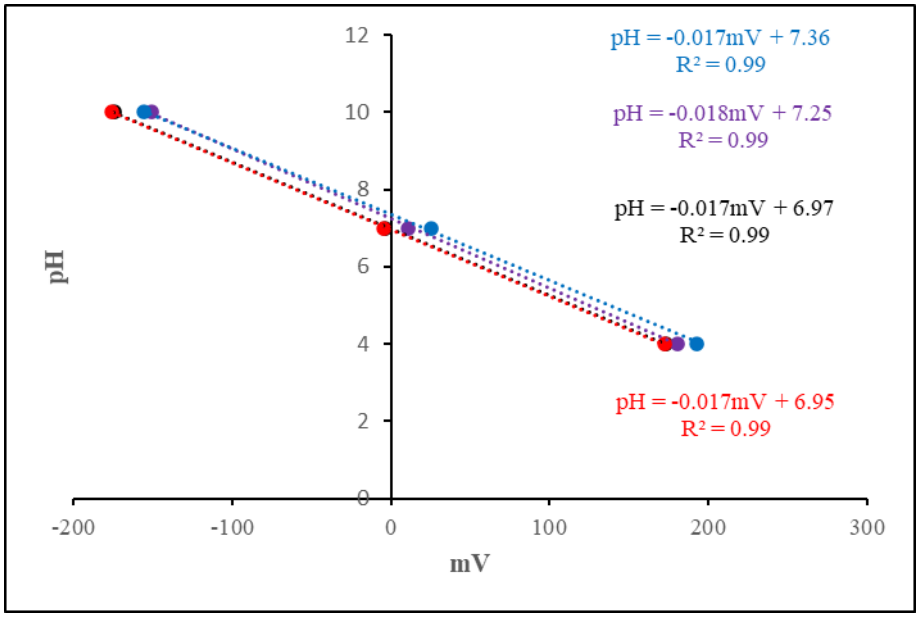


Figure 3.1 Calibration curves of pH meter at pH of 4.00, 7.00 and 10.00 in standard buffer solutions (red line) and in concentrated electrolytes [0.1 (black line), 0.3 (purple line), and 0.7 (blue line) mol L^{-1} NaCl].

3.2.2 Determination of Zn

Zinc was analysed using the Agilent 7900 quadrupole ICP-MS with a helium collision cell. Samples were acidified with 2% (v/v) HNO3 prior to ICP-MS analysis. At least five concentrations of Zn were prepared from a single element Zn standard to obtain a calibration curve (Merck, 1000 µg mL^{-1}). The detection limit was 0.001 µg/L. The correlation coefficient (R^2) of the calibration curve was always above 0.99 (Fig. 3.2) and the precision of this method was within ±5% based on multiple measurements of a single standard on the same day. Calibration and sample blank solutions were measured before the sample solutions. The elements In (Indium) was used as an internal standard solution to correct for changes in

sensitivity of the detector during analysis. Samples with a high concentration of total dissolved solids were diluted in 0.01 M prior to analysis.

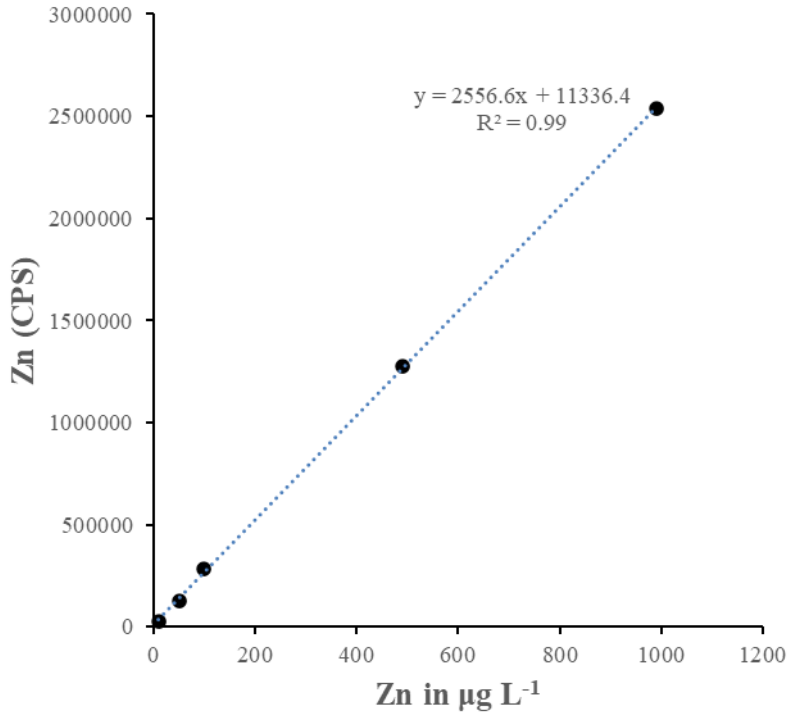


Figure 3.2 Calibration curve of Zn standard. Using LINEST, the standard error value for the regression line is 8729.00 µg L^{-1}.

3.3 Model calculation of Zn aqueous speciation in NaCl concentrations and examine the applicability of surface complexation models in seawater ionic concentration (0.7 mol L^{-1} NaCl)

The following section describes the model and experimental works used to (a) estimate the suitability of the Davis equation for activity correction at seawater ionic strength (0.7 mol L^{-1} NaCl), (b) calculate the aqueous speciation of Zn in different NaCl concentrations in the presence of carbonate (HCO_3) and dissolved organic carbon (DOC), (c) examine the effect of increasing NaCl concentrations and HCO_3 on the adsorption of Zn on tropical soils, and (d) examine the multi-surface models (MSMs) performance for predicting Zn adsorption on soils and predict the effect of increasing NaCl concentrations on Zn adsorption on coastal soils of Bangladesh. The results are presented and discussed in chapters 4 and 5.

3.3.1 Estimation of the suitability of the Davis equation for activity correction at seawater ionic strength (0.7 mol L^{-1} NaCl)

Generally, the activity correction by the Davies equation is limited up to 0.5 mol L^{-1} concentration. Therefore, the results obtained with the Davies equation were compared with those yielded by SIT method and reported by Powell et al. (2013). Visual Minteq ver. 3.1 (Gustafsson, 2019) with the database of '*thermo.vdb'* was used for comparing the speciation of Zn in seawater ionic solutions. The aqueous Zn species and its intrinsic equilibrium constants at I = 0 mol L^{-1} in the IUPAC technical report and Visual Minteq were presented in Table 3.2. As the database of Zn species in the Visual MINTEQ has important differences from that of the IUPAC technical report, the database of Zn species at the Visual Minteq was changed and made consistent with that of the IUPAC technical report before running the speciation model in Visual MINTEQ at I ≈ 0.67 mol L^{-1} for comparing the model results. The results showed that Zn speciation in seawater ionic strength (I ≈ 0.67 mol L^{-1} NaCl) can be adequately described by the activity correction approach (Davies equation) in Visual MINTEQ (discussed in Chapter 4).

Table 3.2 Zn species and their equilibrium constants in IUPAC technical report (Powell et al., 2013) and Visual Minteq database at I = 0 M. The IUPAC database was selected for model comparison at sea water concentration.

Reaction	IUPAC	Visual Minteq
$Zn^{2+} + H_2O = ZnOH^+ + H^+$	-8.96	-8.96
$Zn^{2+} + 2H_2O = Zn(OH)_2 + 2H^+$	-17.82	-16.9
$Zn^{2+} + Cl^- = ZnCl^+$	0.40	0.43
$Zn^{2+} + 2Cl^- = ZnCl_2$	0.69	0.45
$Zn^{2+} + 3Cl^- = ZnCl_3^-$	0.48	0.50
$Zn^{2+} + 4Cl^- = ZnCl_4^{2-}$	-	0.20
$Zn^{2+} + HCO_3^- = ZnHCO_3^+$	1.62	2.1
$Zn^{2+} + CO_3^{2-} = ZnCO_3$	4.75	5.30
$Zn^{2+} + 2CO_3^{2-} = Zn(CO_3)_2^{2-}$	5.4	9.63

3.3.2 The aqueous speciation of Zn

3.3.2.1 Solution compositions for speciation analysis

Coastal soil solutions are characterised by a variable concentration of salinity and bicarbonate alkalinity (HCO_3). The salinity range in the coastal soil solutions ranges between 4 dS m^{-1} and >15 dS m^{-1} (Dasgupta et al., 2015). As salinity is measured as Electric conductivity (EC), a simple linear relationship between ionic strength (I) and EC (I ≈ 0.016 × EC) proposed by Ponnamperuma et al. (1966) is used to convert salinity to concentration. The conversion indicated that the concentration range of coastal soil solution is 0.1 mol L^{-1} to > 0.3 mol L^{-1}.

In calcareous soils, the following reaction:

$$CaCO_3 + CO_2 + H_2O = Ca^{2+} + 2HCO_3^- \quad (3.1)$$

is responsible for the production of high concentrations of bicarbonate in soil solutions (Zuo et al., 2007). The bicarbonate range in coastal soil solutions ranges between 2 mmol L^{-1} to 8 mmol L^{-1} (Ahmed et al., 2020). Like salinity and bicarbonate, the concentration of dissolved organic matter is distinctive and ranges from 10 to 40 mg L^{-1} (Ayers et al., 2016).

Based on the chemical composition of coastal soil solutions, we have chosen three different concentrations of NaCl (0.1, 0.3, and 0.7 mol L^{-1} NaCl), two different concentrations of bicarbonate (2 mmol L^{-1} as low calcareous and 8 mmol L^{-1} as high calcareous solution) and one concentration of dissolved organic carbon (40 mg L^{-1}) in our speciation modelling analysis. As bicarbonate controls alkalinity in water, we referred to bicarbonate concentration as alkalinity in the speciation models. Zn concentration of 5 mg L^{-1} was used in the aqueous speciation models. The concentration of 5 mg L^{-1} in the soil solution is represented the maximum concentration of Zn present in soil solution due to fertilization or industrial processes (Payne et al., 1988).

3.3.2.2 Speciation model used

Visual Minteq ver. 3.1 with the database of '*thermo.vdb'* was used for modelling the speciation of Zn in aqueous solutions (Gustafsson, 2019). Visual Minteq uses the Davis equation for the activity correction as well as adequately describes the behaviour of ions in electrolyte systems (Bonito et al., 2018; Gustafsson, 2019). As the Davis equation works well up to seawater ionic concentration (0.7 mol L^{-1} NaCl), no parameters in Visual MINTEQ were fitted for the speciation analysis of Zn in NaCl and mixed NaCl-HCO_3 aqueous solutions.

To examine the effect of NaCl and HCO_3 on the species of Zn, two steps were used to calculate the species of Zn in soil solutions. In each step, the pH was varied from 4 to 10 at 25^{o} C using 1.0 pH increments. In the first step, the model analysis of Zn species was determined in saline system with the presence of dissolved organic carbon. The salinity is represented using NaCl concentrations (0.1 mol L^{-1}, 0.3 mol L^{-1} and 0.7 mol L^{-1}, respectively). The role of dissolved organic carbon (DOC) on Zn speciation in NaCl background solutions was evaluated and described by the NICA-Donnan model with the proposed generic parameters (Gustafsson and Kleja, 2005; Milne et al., 2003) and by assuming that 82.5% of DOM is composed of reactive fulvic acid (Table 3.3). In the second step, two different (2 mmol L^{-1} and 8 mmol L^{-1}) HCO_3 ion concentration was added, and the model analysis of Zn species was determined in mixed NaCl-HCO_3 systems with the presence of dissolved organic carbon.

Table 3.3 Parameter values for cation complexation to soil organic matter in the NICA-Donnan models (Gustafsson and Kleja, 2005; Milne et al., 2003)

Cation	Humic Acid				Fulvic Acid (solid phase and dissolved)			
	carboxylic type site*		phenolic type site**		carboxylic type site*		phenolic type site**	
	affinity log K_1	non-ideality n_1	affinity log K_2	non-ideality n_2	affinity log K_1	non-ideality n_1	affinity log K_2	non-ideality n_2
Ca^{2+}	-1.37	0.78	-0.43	0.75	-2.13	0.85	-3.0	0.80
Mg^{2+}	-0.6	0.77	0.6	0.59	-2.1	0.77	-2.4	0.59
Zn^{2+}	0.11	0.67	2.39	0.27	-3.84	0.67	-0.73	0.61
H^+	2.93	0.81	8.00	0.63	2.34	0.66	8.60	0.76

* = low affinity
** = high affinity

3.3.3 Examination of the effect of increasing NaCl concentrations and HCO_3 on the adsorption of Zn on tropical soils

3.3.3.1 Soils Characteristics

Soils for Zn adsorption were collected from rice fields in the Philippines due to their similarities with the coastal soils of Bangladesh. The soils were young, alluvial and perennially wet type. One soil was collected from Bay, Laguna, Philippines and the other soil was collected from Tiaong, Quezon, Philippines. The Bay soil has relatively low $CaCO_3$ whereas the Tiaong soil has relatively high $CaCO_3$. According to the US soil taxonomy, the Bay and Tiaong soil great group is Hydraquent and Tropaquept, respectively. After air-drying, the soils were sieved through a 2 mm sieve to remove plant debris and stored in a plastic jar. A description of soil collection processes is reported by Izquierdo et al. (2016). Soil chemical and physical properties were previously investigated and are presented in Table 3.4 (Izquierdo et al., 2016). To check the consistency of the results, soil pH and SOM were determined again, and the results are compared with previous results in Table 3.4. The comparison indicates that the new results are similar enough to the earlier studies. Soil properties like soil texture (% silt, % clay, % sand), soil carbonate, cation exchange capacity (CEC), *etc*. were relatively stable during the project time and did not change rapidly. Therefore, I believe that the previously investigated soil properties data are suitable for this study.

Table 3.4 Experimental soil properties (Izquierdo et al., 2006)

Soil Type	% Clay	% Silt	CEC (cmol kg^{-1})	Carbonate (g kg^{-1})	Soil pH*	Soil pH**	Organic C (g kg^{-1})	Organic C** (g kg^{-1})
Bajoa	49.9	43.3	10.6	1.6	7.3	7.26	54.3	52.5
Tiaong	42.2	39.2	9.0	95.9	8.5	8.55	72.8	71.0

* = soil and water ratio were 1:5 during the pH determination. ** = This study and average of three analysis

Besides the soil properties reported in Table 3.4, we furthermore determined total amorphous iron (hydr)oxides and the reactive major cation pool in soils (Table 3.5). Total amorphous iron (hydr)oxides was calculated from Fe extracted with ammonium oxalate solution. The reactive major cation pool (Ca. Mg and K) was calculated from the cations extracted with 0.43 mol L^{-1} HNO_3 (solid: liquid ratio = 1:10) for 2h of shaking (Duffner et al., 2014). The influence of extracted Fe and Al on Zn adsorption was ignored during our model analysis. Due to the relatively short time frame of the adsorption experiments (24 h), the dissolution of $Al(OH)_3$ and $Fe(OH)_3$ did not reach equilibrium (Fisher-Power et al., 2016; Shi et al., 2013; Shi et al., 2007); I assumed that Al and Fe have the minimal effect of Zn adsorption (Fisher-Power et al., 2016). The amount of Zn initially adsorbed to the soil is determined using 0.43 mol L^{-1} HNO_3 extraction (Duffner et al., 2014). The results show that little Zn is extracted from both soils. Bay soil has relatively higher extracted Zn (28.3 mg kg^{-1}) than Tiaong soil (8.5 mg kg^{-1}) ((Izquierdo et al., 2016). The concentration of Zn extracted with 0.43 mol L^{-1} HNO_3 is very low compared with our added concentration during the batch adsorption experiment. Therefore, we assume that the amount of Zn initially adsorbed to the soils has a minor influence during the batch adsorption experiment and the concentration does not account for calculating percent Zn adsorption and model prediction. XRD analysis showed that smectite, plagioclase and quartz dominated mineral phases. There was no obvious peaks of crystalline iron (hydr)oxides during XRD analysis (Fig. 5.1). Therefore, we assumed that the role of crystalline iron(hydr)oxides was minimal for binding and did not account for during the model analysis.

To predict the effect of increasing NaCl concentrations on Zn adsorption on coastal soils of Bangladesh by model analysis, soil properties, including major reactive cations pool (Ca, Mg, and K) were taken from the reconnaissance soil survey report of Bangladesh (Table 3.5) (Brammer, 1972; SRDI, 2010). The amount of amorphous iron hydroxide was taken from literature data (Islam and Lotse, 1986). Crystalline iron (hydr)oxides is generally absent in the coastal soils of Bangladesh (Islam and Lotse, 1986). The soils in the Ganges Tidal Floodplain region were classified as calcareous, non-calcareous and acidic according to the major soil types of Bangladesh (Huq and Shoaib, 2013). The concentration of HCO_3^- was assumed as 8 mM in calcareous soils and 2 mM in decalcified and acidic soils depending on the HCO_3 concentration in soil water content (Table 3.5) (Zuo et al., 2007).

3.3.3.2 Mineralogical and Elemental Features of Soils

Soils were characterized by XRD and XRF for their mineralogical and elemental features in the Natural History Museum, London. X-ray powder diffraction data were collected in Bragg-

Brentano geometry using a Panalytical X'Pert Pro MPD diffractometer equipped with an X'Celerator position-sensitive detector using Fe-filtered Cobalt Kα radiation (40KV and 40mA) in combination with primary and secondary Soller slits of 0.02 rad, a divergence slit of 0.25º and an anti-scatter slit of 0.5º. Bragg's law is written as:

$$n\lambda = 2d_{hkl}\sin\theta \quad (3.2)$$

where n is a positive integer, λ is the X-ray wavelength (Å), dhkl is the lattice spacing (Å), and θ is the angle of the diffracted X-rays (°)

For XRD, three grams of bulk soil samples were ground in an agate pestle and mortar for around 15-20 minutes. The resulting fine powder soil samples were loaded into a circular XRD holder (cavity dimensions: diameter 16 mm, depth 2.4 mm) and were quantified by full-pattern fitting. Scans were carried out in the angular range of 3-90º 2-theta, at 0.017º step size, and with 300 s counting time per step. The identification of minerals in soil samples was performed using the peak library within the Highscore software (MalvernPanalytical).

The Rietveld program BGMN-Profex (Bergmann et al., 1998; Doebelin and Kleeberg, 2015) was used to enhance the mineral proportions of soils. The databases, ICSD and BGMN were used for crystal structure data for the identified phases. The Rietveld procedure included the refinement of background, sample displacement, sample eccentricity, lattice parameters, peak profile function, and preferred orientation. A limited number of parameters were used to refine minor phases.

Soil clay samples were obtained by separating the <2 mm size fraction using timed sedimentation (Moore and Reynolds, 1997). Oriented mounts of the clay size fraction were prepared by pipetting a water-clay suspension onto a glass slide. The glass side was then left to dry at ~70ºC. The soil samples were solvated overnight using ethylene glycol in an oven at 60ºC and heat-treated at 400ºC for 2h to evaluate the presence of expandable clay minerals. XRD patterns of the oriented mounts were collected after air-drying, glycolation and 400ºC-heat treatment. The Panalytical X'Pert Pro MPD was used under the same conditions as described above, except that the angular range was 2.5-40º 2-theta and the counting time per step was 200 s.

The elemental compositions of soil samples were identified by XRF using the PANalytical Epsilon 3 XLE. The standard Omnian settings (PANalytical Omnian software) were used to carry out XRF analysis. XRF was standardized using synthetic goethite and the relative impurities of three analyses were below 1% of the total atomic weight.

Table 3.5 Selected soil properties of investigated and modelled soil samples

Soil Type	USDA Classification	Location coordinate	Reaction with 10% HCl	Soil pH	% Clay	CEC (cmol/kg)	SOC (%)	EC* (dS/m)	I (M)**	Total Fe-oxide (g/Kg)	0.43 M HNO_3-extractable (cmol/kg)			HCO_3^- (mM)****
											Ca	Mg	K	
Investigated Soils														
Bay	Tropaquept	NA	NA	7.30	49.9%	10.6	5.43	--	--	80	25	4.25	0.59	
Tiaong				8.50	42.2	9.0	7.28			60	48.5	3.58	0.46	
Modelled Soils														
Bajoa	Typic Endoaquepts	22.79722°N 89.44584°E	Calcareous	8.02	30.00	21.73	1.30	9.98	0.16	50***	20.4	6.01	0.44	8
Barisal	Typic Endoaquepts	22.64452°N 89.51864°E	Decalcified	6.52	44.00	28.69	1.60	14.57	0.23	50 ***	26.32	6.76	0.34	2
Kamalkathi	Typic Endoaquepts	22.26591°N 89.10258°E	No reaction	4.60	38.97	25.37	2.04	9.73	0.16	50***	6.76	5.08	0.46	2
Ramgati	Typic Endoaquepts	22.69375°N 89.52899°E	Calcareous	8.15	17.71	20.0	1.00	8.43	0.13	50***	12.28	3.32	0.37	8
Sara	Aeric Endoaquepts	22.93588°N 89.47106°E	Calcareous	7.70	24.02	6.06	1.35	8.93	0.14	50***	3.40	1.13	0.32	8

NA = Not applicable

* EC = Electrical conductivity

**Concentration is calculated by using the relationship between EC and I ($I \approx 0.016 \times EC$) proposed by (Ponnamperuma et al., 1966).

***Estimated considering 5% amorphous iron (hydr)oxides is present in soils of Bangladesh

****Estimated based on groundwater composition

3.3.3.3 Batch adsorption experiments

Adsorption of Zn on soils (Bay and Tiaong) at different pHs and NaCl concentrations (0.1 mol L^{-1}, 0.3 mol L^{-} and 0.7 mol L^{-1}) was conducted by three sets of batch adsorption experiments. In each set, 0.5 g soil with 49 mL solution of the desired concentrations was transferred to a 50 mL polypropylene Falcon centrifuge tube and capped and shaken on a VWR orbital shaker at 25°C with 300 rpm for 24 h to equilibrate at the desired concentrations. After 24 h, 1 mL of Zn stock solution (3.82 mmol L^{-1}) was added to each tube to reach the final volume of 50 mL so that the final concentration of Zn in each tube was 0.08 mmol L^{-1} (5 mg L^{-1}) and the solid-liquid ratio was 10 g L^{-1}. Simultaneously, the pH of each tube in each set was adjusted by adding small volumes of 1M HCl or NaOH solution. The pH range of the experiments was 3 – 10. The tubes were capped and shaken again for 24 h The kinetic study indicated that the equilibrium state of Zn is reached in 24 h during a batch adsorption experiment (Taylor et al., 2008). The blank samples were run side by side to evaluate the fraction of Zn coming from soils, MiliQ water and NaCl stock solutions. At the end of each experiment, tubes were centrifuged and immediately measured the pH of the supernatant. The pH of the supernatant was recorded and reported as the final pH of the experiment. The supernatant solutions were withdrawn with a syringe from each tube and filtered through 0.45 µm filters and filtrates were collected. The collected filtrates were acidified and analyzed for Zn using ICP-MS. The concentration of initial added Zn was also measured by the ICP-MS for calculating the adsorption of Zn on soils. The concentration of Zn adsorbed to the soil was calculated by the difference between the initial added Zn and Zn concentration remaining in the filtrate. All experiments included blank samples were conducted in triplicate.

To investigate the influence of carbonate (8 mmol L^{-1}0 on Zn adsorption on soils in NaCl concentrations (0.1 mol L^{-1}, 0.3 mol L^{-} and 0.7 mol L^{-1}), batch adsorption experiments in mixed NaCl-HCO_3 solution were also performed following the same procedure. A similar adsorption experimental set-up was also applied for the Zn adsorption on soils at Zn initial concentration of 0.8 mmol L^{-1} (50 mg L^{-1}) to make comparisons between Zn adsorption results and test the model performance at different concentrations.

The concentrations of Zn used in this study were approximately 20 and 200 times higher than the typical found in agricultural soils (Zn concentrations in soil solutions range from 4×10^{-7} to 4×10^{-3} mmol L^{-1}) (Montalvo et al., 2016). However, it is similar to Zn concentration in the solution of contaminated soils (Zn ranged from 1.68×10^{-4} to 0.34 mmol L^{-1}) (Stephan et al., 2008) and other studies on Zn adsorption (Fisher-Power et al., 2016; Mizutani et al., 2017;

Spathariotis and Kallianou, 2007). As the concentration of Zn in soil solution is continuously generated in toxic concentration due to by-products of industrial processes, the high concentration of Zn is used in this study to understand the mechanisms, adsorption pattern and model description of Zn adsorption on soils and goethite in different environmental conditions.

3.3.4 Examination of multi-surface models (MSMs) performance for predicting Zn adsorption on soils

Zn adsorption on soil was calculated using a MSMs adapted from (Khai et al., 2008) by assuming that three reactive surface sites in soils could adsorb Zn. The three reactive surface sites were phyllosilicate clay, soil organic matter and iron hydroxide. The model calculations were performed using the chemical equilibrium program Visual MINTEQ (v 3.1) which contains Zn solution complexation constants (Gustafsson, 2019).

3.3.4.1 Binding to phyllosilicate clay minerals

The Gaines-Thomas equation was used to simulate ion exchange to clays. The selectivity coefficient was set to unity for all cations. The cation exchange capacity of clay (CEC_{clay}) was assumed to be the same as the CEC of illite (0.1 – 0.4 mol/kg) (McBride, 1994). The experimental soil was rich in smectite minerals; therefore, the value of 0.4 mol/kg was assumed as a CEC of clay. Like experimental soils, the coastal soils of Bangladesh were rich in smectite minerals (Moslehuddin et al., 1999; Rahman et al., 2005). The CEC of clay was kept the same during the model analysis of Bangladesh soils.

3.3.4.2 Binding to iron (hydr)oxide

Zn adsorption and other cations and anions on amorphous iron (hydr)oxide were accounted for by the diffuse layer model (DLM) of hydrous ferric oxide (HFO) (Dzombak and Morel, 1990). The site concentrations for the amorphous iron (hydr)oxide were calculated by using the recommended surface area of 600 m^2/g (Dijkstra et al., 2004).

3.3.4.3 Binding to soil organic matter

The Non Ideal Competitive Adsorption Donnan model (NICA-Donnan) was used for binding Zn and other ions to soil organic matter (Milne et al., 2003) by assuming that 46% of SOM was active generic humic acid (Groenenberg and Lofts, 2014; Weng et al., 2001). The model is a combination of the description of binding to a heterogeneous material by the non-ideal competitive adsorption (NICA) isotherm, coupled with a Donnan electrostatic sub-model which describes the electrostatic interactions between ions and the humic material (Milne et al., 2003). The generic binding parameters of (Milne et al., 2003) and (Gustafsson and Kleja,

2005) were used in the NICA-Donnan model. The later consider a stronger salt effect for solid-phase humic and fulvic acid.

In addition to the surface charge information of clay, SOM and iron (hydr)oxides, the model also included other input parameters like total concentration of Zn, reactive major cations in soils (Ca, Mg and K), pH, released carbonate concentration from Tiaong soil due to acidification, the precipitation phase of Zn and the background NaCl concentration to simulate Zn adsorption on experimental soil in 3 different NaCl concentrations (0.1 mol L^{-1}, 0.3 mol L^{-1}, and 0.7 mol L^{-1}). The component additivity approach was used in the modelling with the assumption that all solutes have access to all sorbent surfaces and that the sorbents do not interact with each other (Zhang et al., 2018a). All the parameters were pre-defined in Visual MINTEQ, and no parameters were fitted in this study (Table 3.2, 3.3 and 3.6). The model performances in different NaCl concentrations were evaluated based on the root-mean-square error (RMSE) between model simulated and experimentally measured adsorption of Zn (equation 3.3).

$$\text{RMSE (\%adsorption vs. pH)} = \sqrt{\frac{1}{n_d - n_p}\sum\left(\frac{\%\text{ adsorbed experimental} - \%\text{ adsorbed model}}{100\%}\right)^2} \quad (3.3)$$

where n_d is the number of data points and

n_p is the number of adjustable parameters.

If the model prediction worked well, the MSMs were applied to determine the Zn adsorption in the coastal soils of Bangladesh and the changes due to seawater intrusion in agricultural fields. The concentration of NaCl concentrations in speciation models kept similar in adsorption models. The concentration of HCO_3^- was 8 mmol L^{-1} used in the adsorption model of calcareous soils whereas the concentration of HCO_3^- was 2 mmol L^{-1} used in non-calcareous and acidic soils. The concentration of DOC was kept at 40 mg L^{-1} in all the soils. The reactive major cations (Ca, Mg, and K) of soils were also added during the model analysis to predict Zn adsorption in a real soil environment.

Table 3.6 DDL model parameters of HFO in two surface sites (strong site and weak site). $logK^0$ is the equilibrium intrinsic constants of surface species. The surface area of HFO is considered as 600 m^2 g^{-1} (Dzombak and Morel, 1990).

Surface species (Strong site)	$logK^0$	Surface species (Weak site)	$logK^0$
≡Fe-OH	0	≡Fe-OH	0
≡Feh-OH_2^+	7.29	≡Fe-OH_2^+	7.29
≡Feh-O^-	-8.93	≡Fe-O^-	-8.93
≡Feh-$OHCa^{2+}$	4.97	≡Fe-OCa^+	-5.85
≡Feh-OZn^+	0.99	≡Fe-OZn^+	-1.99
≡Feh-OMg^+	nd*	≡Fe-OMg^+	-4.6
≡Feh-SO_4^-	7.78	≡Fe-SO4$^-$	7.78
≡Feh-$OHSO_4^{2-}$	0.79	≡Fe-$OHSO_4^{2-}$	0.79
≡Feh-CO_3^-	12.78	≡Fe-CO_3^-	12.78
≡Feh-CO_3H	20.37	≡Fe-CO_3H	20.37

nd* = not determined

3.4 Development of surface complexation model parameters for the accurate quantification of Zn on goethite

This section describes the experimental and model works used to (a) estimate the surface properties of goethite, and (b) develop surface complexation model parameters for accurate predicting Zn adsorption, especially in the highly saline environment (> 0.1 mol L^{-1} NaCl). The results are presented and discussed in chapter 6.

3.4.1 Surface properties of goethite

The surface properties of goethite are determined according to the following experiments.

3.4.1.1 Synthesis of goethite

Goethite was synthesized by mixing $Fe(NO_3)_3$ solution with KOH solution according to the method of Schwertmann and Cornell (2000). Briefly, a 100 ml of 1 M $Fe(NO_3)_3$ solution was mixed with 180 ml 5M KOH solution in a vessel and diluted to 2L with MiliQ water. A reddish-brown precipitate was initially formed. The diluted suspension was held in a closed polyethylene bottle and left in an oven at 70° C for 60 h. After 60 h, a yellowish precipitate was observed. The precipitate was then rinsed and washed several times with MiliQ water following centrifugation and decantation to remove excess K^+, NO_3^-, and OH^-. The goethite slurry was then dried in the oven at 40° C and then ground to pass through a 100 mesh sieve and stored in a plastic bottle for experimental analysis.

3.4.1.2 Mineralogical and elemental features of goethite

Goethite was characterized by XRD and XRF for their mineralogical and elemental features following the same procedure reported in section 3.3.3.2 in the Department of Materials,

Imperial College London. The crystalline shape of goethite was studied by transmission electron microscopy (TEM) using the JEOL JEM-2100F.

3.4.1.3 Surface area of Goethite

The BET (Brunauer, Emmett and Teller)-specific surface area of goethite was determined by the multipoint N_2-BET method in the region of P/P0=0.05-0.35. The Quantachrome Autosorb iQ was used to obtain N_2 adsorption-desorption isotherms after outgassing goethite at 100° C for 20 hours. The specific surface area of goethite is 40 m^2 g^{-1}.

3.4.1.4 Determination of Surface Charge

The acid-base properties of proton active sites at the goethite surface were determined by the potentiometric titration using previously determined protocols by Gao and Mucci (2001) and Lutzenkirchen et al. (2012). The titration was conducted using a Metrohm model 716 DMS Titrino auto titrator with standardized 0.1 mol L^{-1} NaOH and HCl. The strength of the titrant was calibrated against a standard solution of 1 mol L^{-1} HCl. A glass electrode related to the system was used to measure pH and voltage potential difference (mV). The glass electrode in the titration system was also calibrated using buffer solutions in each concentred electrolyte at pH of 4.00, 7.00, 10.00, and 13.00. 40 ml of goethite suspensions (8 g L^{-1}) in desired NaCl concentration (0.1 mol L^{-1}, 0.3 mol L^{-1} and 0.7 mol L^{-1}, respectively) was prepared and transferred into a vessel. The vessel was immersed in a water jacket and the temperature of the water jacket was maintained at 25° C. A propeller stirrer was used in the vessel to keep the suspensions homogeneous. Before titration, the suspensions were purged with N_2 gas for 24 h to remove carbon dioxide and equilibrate at the desired concentrations. The pH electrode was calibrated at pH 4, 7, 10 and 13 with the pH buffer solution, respectively, before titration. The pH of the goethite suspension was lowered incrementally to 4.0 with the addition of 0.1 mol L^{-1} HCl. The titration was then started with 0.1 mol L^{-1} NaOH to increase the pH of the goethite suspension incrementally to 11.0. A reverse titration from pH 11 to 4 was conducted with the addition of 0.1 mol L^{-1} HCl to check the hysteresis of titrations. To ensure equilibration at each titration point, a small volume of titrants (NaOH/HCl) was added to the suspension with the drift value of 0.5 mV/min. The vessel was always capped during the titration to avoid contamination with atmospheric CO_2 and an inert gas environment was maintained by purging the headspace of the vessel with N_2 gas. The N_2 gas was humified by bubbling through MiliQ water to minimize the evaporation of goethite suspension. The point of zero salt effect (pzse) was determined with the intersection of titration curves in 0.1, 0.3 and 0.7 mol L^{-1} NaCl. The

surface charge (Q) and the amount of adsorbed protons (H_{ads}) were determined by the following equation:

$$H_{ads} = Ca - Cb - [H^+] + [OH^-] \quad (3.4)$$

$$Q = F^*H_{ads}/(a^*S) \quad (3.5)$$

where C_a and C_b are the total mole concentration of acid and base added to the goethite suspension, a is the solid concentration in g L^{-1}, F is the Faraday constant (96,490 C mol^{-1}) and S is the specific surface area of goethite (m^2 g^{-1}).

3.4.2 Development of surface complexation model parameters for accurate predicting Zn in the highly saline environment

A method for the surface complexation of Zn on goethite using surface complexation models was developed, according to the following experiments.

3.4.2.1 Batch adsorption experiments

Carbonate free goethite slurry in NaCl solutions was used during the adsorption experiment on goethite. Batch adsorption experiments of Zn on goethite in NaCl concentrations (0.1 mol L^{-1}, 0.3 mol L^- and 0.7 mol L^{-1}) were performed following the same procedure reported in section 3.3.3.3. However, the solid-liquid ratio (1.6 g L^{-1}) in the goethite system was lower than in the soil system. Two initial concentrations (0.08 and 0.8 mmol L^{-1}) were used in the Zn adsorption experiment. The same experimental set-up was used for Zn adsorption experiments in NaCl solutions (0.1 mol L^{-1}, 0.3 mol L^- and 0.7 mol L^{-1}) in the presence of carbonate ($HCO_{3(init)}$ = 8 mmol L^{-1}).

3.4.2.2 Surface complexation model for goethite

The acid-base properties of goethite as well as the adsorption behaviour of Zn on goethite in different NaCl concentrations were processed using the CCM (constant capacitance model) (Hayes and Leckie, 1987) through the use of the computer program 'FITEQL' (version 2) (Westall, 1982). CCM is used due to its good performance in high ionic strength. FITEQL is used widely for the computation of chemical equilibrium constants in the adsorption studies of trace metals on goethite (Hayes et al., 1991; Peacock and Sherman, 2004; Robertson and Leckie, 1998). The quality of fits in FITEQL is stated by

$$V(Y) = (Y/S_Y)^2/(n_p{}^*n_{II} - n_u) \quad (3.6)$$

where Y is the actual error in the mass balance equation, S_Y is the estimated experimental error given by FITEQL and the reciprocal of the variance S_Y is the weighting factor. n_p is the number of data points, n_{II} is the number of chemical components with known total and free

concentrations, and n_u is the number of adjustable parameters. Values of V(Y) between 0.1 to 20 generally suggest a good fit (Westall, 1982).

Adsorption experiments are the key technique in all of my research chapters. Therefore, for better examination, a list of experimental setup, model works and the relevant methods used are presented in Table 3.7.

Table 3.7 List of experimental setup, model works and the relevant methods used in this thesis.

Title of the experiment/model work	Methods used	Instruments/software used	Results presented
Applicability of the Davis equation in 0.7 mol L^{-1} NaCl solution	Modelling	Visual MINTEQ	Chapter 4
Zn species in NaCl, NaCl-HCO_3 solutions	Modelling	Visual MINTEQ	Chapter 4
Soil characteristics	Full pattern scanning and fitting, and separating the < 2 mm size fraction	XRD, XRF and Rietveld program	Chapters 4 and 5
Effect of NaCl concentrations on the adsorption of Zn on soils at low concentration of Zn ($[Zn]_{init}$ = 0.08 mmol L^{-1})	Batch adsorption experiment	pH meter for pH measurement, ICP-MS for measuring Zn concentration in solutions.	Chapter 4
Reactive major cations poll and total amorphous iron (hydr)oxide	Extracted with 0.43 mol L^{-1} HNO_3 acid and ammonium oxalate solution	ICP-MS	Chapter 3 in Table 3.5
Multi-surface models (MSMs) for predicting Zn adsorption on soils at $[Zn]_{init}$ = 0.08 mmol L^{-1}	Modelling	Visual MINTEQ	Chapter 4
Effect of NaCl concentrations on Zn adsorption on two soils in low and high initial concentrations of Zn ($[Zn]_{init}$ = 0.08 and 0.8 mmol L^{-1})	Batch adsorption experiment	pH meter for pH measurement, ICP-MS for measuring Zn concentration in solutions.	Chapter 5
Effect of NaCl concentrations on Zn adsorption on two soils in the presence of HCO_3 in low and high initial concentrations of Zn ($[Zn]_{init}$ = 0.08 and 0.8 mmol L^{-1})	Batch adsorption experiment	pH meter for pH measurement, ICP-MS for measuring Zn concentration in solutions.	Chapter 5
Validity of multi-surface models parameterized in chapter 4 for predicting Zn adsorption on two soils in NaCl concentrations and the presence of HCO_3 in low and high initial concentrations of Zn ($[Zn]_{init}$ = 0.08 and 0.8 mmol L^{-1}).	Modelling	Visual MINTEQ	Chapter 5
Characteristics of goethite	Scanning	XRD, XRF, TEM and BET (Brunauer, Emmett and Teller)-specific surface area	Chapter 6 and appendix C
Surface charge of goethite	Potentiometric titration	Metrohm model 716 DMS Titrino auto titrator	Chapter 6
Zn adsorption on goethite in different NaCl concentrations in low and high initial concentrations of Zn ($[Zn]_{init}$ = 0.08 and 0.8 mmol L^{-1}).	Batch adsorption experiment	pH meter for pH measurement, ICP-MS for measuring Zn concentration in solutions.	Chapter 6
Surface complexation model	Modelling	FITEQL - 2	Chapter 6

3.5 Statistical analysis

All the adsorption experiments in each pH were repeated three times. The results were presented as the average value of three replicates if the final pH of each replicate did not change. If the final pH changed, the results were presented as a single value. The standard deviation was determined to see the variation or dispersion of values. The results of standard deviation show that the results are highly reproducible.

Chapter 4: Estimating and Predicting Zn adsorption in a tropical soil under NaCl salinization using Multi-Surface Thermodynamic Models (MSMs)

4.1 Introduction

Laboratory (Acosta et al., 2011; Lores and Pennock, 1998) and field experiment results (Hatje et al., 2003) indicate that increasing salinity decreases Zn adsorption in soils. Two major mechanisms control Zn adsorption in saline soil environments: (1) the complexation of Zn with chlorine and other anions, and (2) competition of adsorption sites with Na and other cations at the soil interfaces (Paalman et al., 1994). For example, Acosta et al. (2011) reported that Zn adsorption decreased significantly in $CaCl_2$, $MgCl_2$ or Na_2SO_4 solutions, but not in NaCl solutions. Their findings indicate that NaCl induced salinity does not lead to a significant decrease in Zn adsorption in the soil system. These findings are supported by work by Shuman (1986) reported that solutions with Na salts with NO_3^-, Cl^- and SO_4^{2-} had no influence on Zn adsorption in soils. In contrast, Linde et al. (2007) found a significant effect of NaCl solutions on Zn adsorption and reported that Zn adsorption in soils decreased with increasing NaCl concentration; similar results are reported by Chu et al. (2015). Accurate prediction of Zn adsorption in soils from solutions with different NaCl concentrations is important to predict Zn mobility and bioavailability in saline environments (D'Amore et al., 2005). To date, most studies (Acosta et al., 2011; Fisher-Power et al., 2016) investigating the effect of changing NaCl concentration on Zn species and adsorption in soils have been conducted at low NaCl concentrations (0.01 mol L^{-1} to 0.3 mol L^{-1}) and Zn adsorption in higher NaCl solutions typical for soils affected by seawater intrusions (≈ 0.7 mol L^{-1}) remains poorly understood.

The inundation of seawater due to climate change is one of the major threats to the coastal area of Bangladesh (Dasgupta et al., 2015). Due to the inundation of seawater, the distinctive features of coastal soil and aquifer solutions in Bangladesh are the presence of higher concentrations of Cl^-, HCO_3^- and SO_4^{2-} (Akter et al., 2020). As a result, the speciation analysis of Zn in the coastal soil solutions is extremely challenging due to the coexistence of NaCl, dissolved inorganic carbon (HCO_3) and dissolved organic matter (DOM) (Nolan et al., 2003; Ren et al., 2015; Tepavitcharova et al., 2011). Numerous analytical techniques like anodic stripping voltammetry (Palmqvist et al., 1997), ion-exchange resins (Alyuz and Veli, 2009) and the Donnan membrane technique (Nolan et al., 2003) have been used to determine Zn speciation in coastal soil solutions. However, a high concentration of dissolved organic matter

and inorganic ligands in coastal soil solutions has the potential to block the analytical signal, in which a portion of Zn species can be wrongly partitioned into other Zn species (Stephan et al., 2008). In addition, Zn speciation analysis in high saline solution is quite complex as sample pre-treatments are necessary to reduce the background and matrix effects (Regadio et al., 2017). Therefore, laboratory analysis of Zn speciation cannot adequately predict Zn species in the coastal saline environment. In lieu of direct analysis, an alternative approach to estimating metal speciation is using equilibrium speciation modelling programs (Pierrot and Millero, 2017). Speciation modelling programs which are thermodynamic modelling approaches, provide capabilities to analyse Zn species in different aqueous environments beyond the limits imposed by experimental study in the laboratory and provide a more sophisticated description of Zn species in aqueous solution (Long and Angino, 1977; Pierrot and Millero, 2017).

Thermodynamic surface complexation models for metals binding onto soil organic matter (Gustafsson, 2001; Van Riemsdijk et al., 2006), oxide minerals (Dzombak and Morel, 1990; Hiemstra and VanRiemsdijk, 1996; Tonkin et al., 2004) and clay minerals (Gu and Evans, 2007; Spathariotis and Kallianou, 2001) are also widely reported in the literature besides aqueous speciation models. A combination of these ion-binding and speciation models, widely called Multi-surface models (MSMs), has been used to predict metals adsorption in complex soil systems (Groenenberg and Lofts, 2014; Weng et al., 2001). The parameterization and development of thermodynamic models (speciation and surface complexation) to describe metal chemistry in solutions and at the solution-solid interface made considerable progress over the last two decades (Groenenberg and Lofts, 2014). Therefore, the accuracy of MSMs calculations for metal cations is usually good (Groenenberg and Lofts, 2014). For example, Bonten et al. (2011) applied MSMs (NICA-Donnan for complexation to organic matter, Donnan model for ion exchange on clay and the GTLM for complexation to FeO and AlO) to a forested site in Germany and successfully reproduced examined trends in porewater Cu, Zn, Cd, and Pb concentration from 1980 to 2004. The results suggested that MSMs can describe metal mobility in acidic soils. Similarly, other studies successfully applied MSMs to predict the dissolved concentration of Zn, Cu, Ni, Cd, Cr, Pb in a wide range of soils (Duffner et al., 2014; Groenenberg et al., 2017; Khai et al., 2008; Ren et al., 2017; Weng et al., 2001). Fisher-Power et al. (2016) showed that the predicted adsorption agreed well with the batch adsorption experimental results. In other studies, MSMs applied to predict free Zn^{2+} concentrations in soils with low Zn content agreed well with the experimental results (Duffner et al., 2014). The above results reported that MSMs is a powerful predictive tool that can provide a comprehensive

description of the Zn cycle in soils in different environmental systems (Duffner et al., 2014; Weng et al., 2001; Zhang et al., 2018a).

MSMs and equilibrium speciation models are independent of pH and ionic strength due to the thermodynamically based binding constants (Koopal and Avena, 2001) and are suitable for prediction outside the range of conditions used to fit the parameters (Zhang et al., 2018a). Recent studies which modelled Zn adsorption on soils by MSMs have primarily been done in the presence of low ionic strength (0.01 mol L^{-1} to 0.02 mol L^{-1}) (Fisher-Power et al., 2016; Khai et al., 2008; Zhang et al., 2018a). To our knowledge, MSMs have not been used before to predict Zn adsorption on soils with higher ionic strength, i.e., between 0.1 mol $L^{-1}$and 0.7 mol L^{-1}. The model parameters in multi-surface models have generally been adjusted/calibrated at comparatively low ionic strengths (Duffner et al., 2014; Gustafsson and Kleja, 2005; Gustafsson et al., 2003). The activity correction of equilibrium speciation models is mostly done using the Davies equation during the model analysis which in general works very well to ionic strength (I) = 0.5 mol L^{-1}, and it is uncertain if at high ionic strength (i.e. 0.7 mol L^{-1}), Zn speciation and adsorption can still be projected accurately with MSMs and speciation models calibrated at lower ionic strength.

Land use patterns of coastal areas in Bangladesh are changing, and agricultural land is being converted to industrial land (Ahmed et al., 2010), leading to increased discharge of metals into soils and higher toxicity levels. Therefore, it is necessary to have a model that accounts for a mechanistic description of Zn in coastal soils, where complex components like Cl, HCO_3 and DOM (dissolved organic matter) are ubiquitous and exert essential controls on Zn mobility in soils. In non-saline or slightly saline soils, soil organic matter (SOM) is the dominant sorbent for Zn at low to neutral pH whereas iron oxides are the dominant sorbent at pH > 7 (Duffner et al., 2014; Khai et al., 2008; Weng et al., 2001). In saline soils, a larger fraction of Zn forms complexes with inorganic anions (Powell et al., 2013) and may not be adsorbed onto SOM and Fe-(hydr)oxides. In addition, the availability of adsorption sites for Zn may be different in saline solutions with a higher concentration of cations and different binding surface compositions. I apply multi-surface and equilibrium speciation models to predict Zn speciation and adsorption on soils in solutions of different NaCl concentrations and test if equilibrium speciation and multi-surface models parametrized for lower ionic strength with the Davies equation predict accurately Zn species and adsorption on soils in seawater ionic strength ($I \approx$ 0.7 mol L^{-1}). To our knowledge, this is the first study quantifying Zn adsorption in soil solutions at seawater like ionic strength by multi-surface models. We compare predicted Zn species in

seawater ionic strength using Davies and SIT models (Powell et al., 2013) to test the suitability of Davies equation at seawater ionic strength. The models are applied to predict the Zn adsorption scenario with increasing salinity on the coastal soils of Bangladesh. Our objectives were as follows:

1. To test the suitability of the Davies equation at seawater ionic strength by comparing with the SIT method.
2. To identify the dominant Zn species in NaCl solutions representing saline soils and examine the effect of HCO_3 and DOC on Zn speciation in NaCl solutions by model analysis.
3. To examine the applicability of multi-surface models to predict Zn adsorption on soils in NaCl solutions using batch adsorption experiments and to explore the effects of soil clay, SOM and iron (hydr)oxide on Zn binding.
4. To apply the model so developed to predict the effect of increasing NaCl concentrations on Zn adsorption on coastal soils of Bangladesh.

4.2 Results

4.2.1 Comparison of Zn speciation computations at 0.67 mol L^{-1} NaCl solution using Davies and SIT activity correction models

As the Davies equation generally works very well to ionic strength (I) = 0.5 mol L^{-1}, here we examine the performance of Davies activity correction models at 0.67 mol L^{-1} NaCl solution by comparison with SIT activity correction models. Figure 4.1 shows a comparison between the Zn speciation in 0.67 mol L^{-1} NaCl results obtained using the Davies model for activity corrections during this study and those obtained using SIT model and reported previously (Powell et al., 2013). The distribution pattern uses the two models, with only slight differences. Using the Davies model, the percentage of Zn^{2+} (54%) between pH 6 and 8 is lower than predicted using the SIT model (61%). The difference for $ZnCl^+$ complexes (24% using Davies and 19% using SIT) and $ZnCl_2$ (13% using Davies and 8% using SIT) between pH 6 and 8 and for $ZnCO_3$ at pH 9 (59% using Davies and 69% using SIT). The per cent distribution of $ZnOH^+$, $Zn(OH)_2$, and $ZnCl_3^-$ by these two models are generally similar.

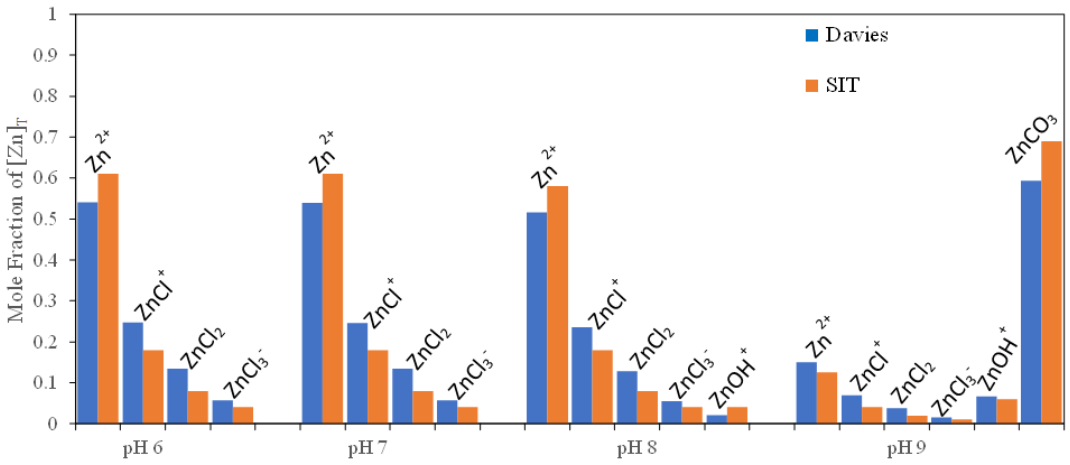


Figure 4.1 A comparison of Zn speciation model results at 0.67 mol L^{-1} NaCl ionic strength obtained with the Davies equation in Visual MINTEQ and those yielded by SIT method and reported by Powell et al. (2013) as IUPAC technical report. The equilibrium constants of Zn species at the Visual Minteq made consistent with that of the IUPAC technical report before running the speciation model in Visual MINTEQ.

4.2.2 Zn speciation model for NaCl solutions in the presence of dissolved organic carbon (DOC) and bicarbonate (HCO_3)

To examine the effect of NaCl concentrations on the speciation of Zn in aqueous solution, Zn species are calculated by speciation model in NaCl concentrations (0.1, 0.3, and 0.7 mol L^{-1}) in the presence of HCO_3 ion and dissolved organic carbon (DOC). The model results are presented in two sections, and it is assumed that section 4.2.2.1 represent Zn species in non-calcareous soil solution whereas section 4.2.2.2 represent Zn species in calcareous soil solution.

4.2.2.1 Speciation of Zn in NaCl solutions in the presence of DOC

The distribution of Zn species vs pH in 0.1, 0.3 and 0.7 mol L^{-1} NaCl concentration in the presence of dissolved organic carbon (DOC) is presented in Figure 4.2. There are three distinct distribution features over the pH range studied. The first feature in the pH range between 4 and 7 shows as major species free $Zn^{2+}_{(aq)}$ (87-79%), Zn-DOC (4-12%) and $ZnCl^+$ (≈ 8%) in 0.1 mol L^{-1} NaCl concentration. Increasing the NaCl concentration from 0.1 mol L^{-1} to 0.3 mol L^{-1} to 0.7 mol L^{-1}, the relative presence of free $Zn^{2+}_{(aq)}$ and Zn-DOC decreases whereas that of Zn-Cl complexes increases. Free $Zn^{2+}_{(aq)}$ decreases from 80% to 75% and 54%. Zn-DOC decreases from 12.5 % to 3.56% to 1.20% at pH 7. The monodentate Zn-Cl complex ($ZnCl^+$) is the only complex observed at 0.1 mol L^{-1} NaCl concentration. With increasing NaCl concentration, higher-order associations of Zn-Cl complexes become important and the formation of $ZnCl_3^-$ and $ZnCl_4^{2-}$ are reported at 0.7 mol L^{-1} NaCl concentration (Figure 4.2). Although, the formation of $ZnCl^+$ (17% and 27%, respectively), $ZnCl_2$ (2% and 6%, respectively), and $ZnCl_3^-$ (1% and 6%, respectively) is significant at 0.3 and 0.7 mol L^{-1} NaCl,

Zn^{2+} is still dominating (76 and 54%, respectively) at pH 4 - 7. The second feature of Zn species distribution is found at pH 8 where Zn-Carbonate and Zn-Hydroxide complexes are forming besides free Zn^{2+}, Zn-DOC and Zn-Cl complexes. At 0.1 mol L^{-1} and 0.7 mol L^{-1} NaCl, free Zn^{2+} is the dominant species with ≈ 60% and ≈ 50% of total Zn, a mixture of Zn-Cl complexes, Zn-Carbonate complexes and Zn-Hydroxide complexes making up the other 40% to 50%. The third feature of Zn species is seen between pH 9 and 10 where Zn-Carbonate complexes [$Zn(CO_3)_2^{2-}$, $Zn(CO_3)$] are predicted as a major species.

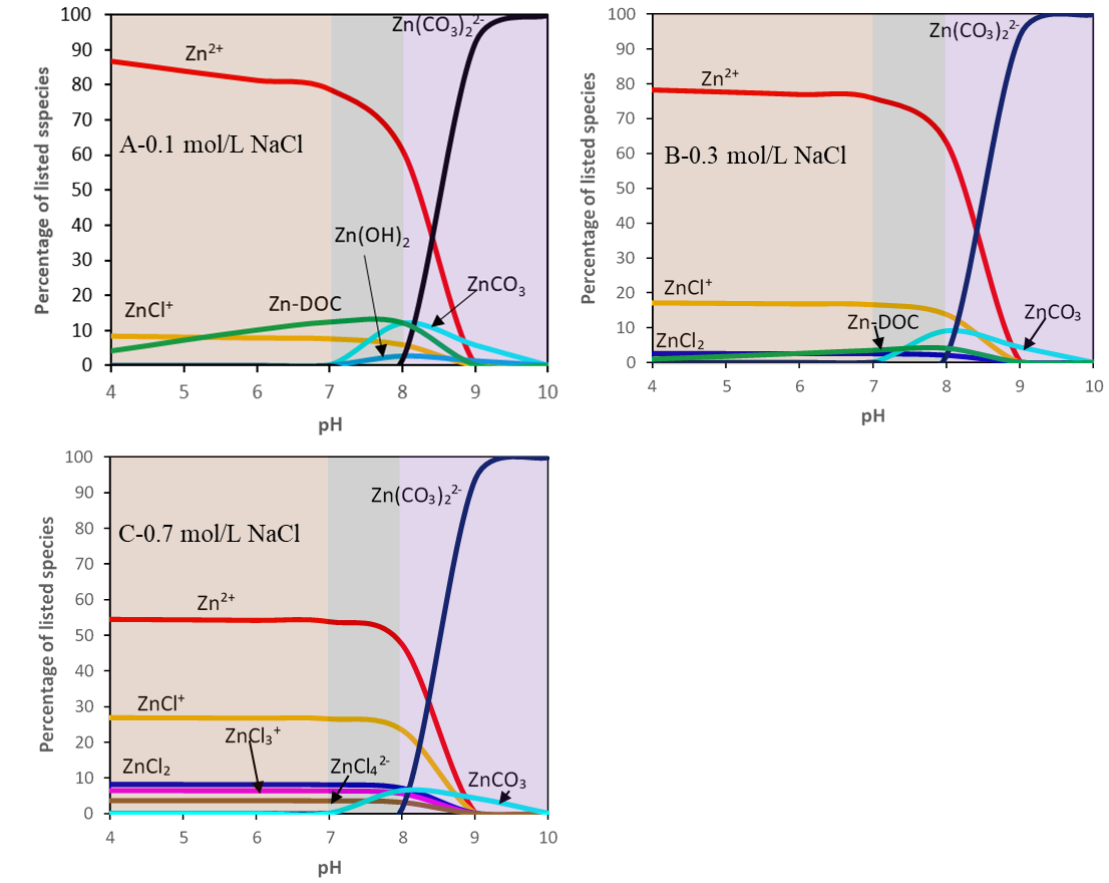


Figure 4.2 Visual MINTEQ Model results of Zn species in different NaCl concentrations, (A) Zn in 0.1 mol L^{-1} NaCl solution; (B) Zn in 0.3 mol L^{-1} NaCl solution, and (C) Zn in 0.7 mol L^{-1} NaCl solution. Zn species at pH 4-7; at pH 8; and at pH 9-10 are represented by orange shaded area, light grey shaded area and purple shaded area, respectively. The system was in equilibrium with partial pressure of CO_2 (3.8×10^{-4} atm). Zn complexation with DOC in NaCl solutions is represented by Zn-DOC.

4.2.2.2 Speciation of Zn in NaCl solutions in the presence of DOC and HCO_3

To assess the effect of calcareous soil solution, bicarbonate (HCO_3) was added to the Zn-NaCl-DOC system and the speciation analysis is presented in Figure 4.3. Figure 4.3A, 4.3C and 4.3E

represents speciation analysis of Zn in Zn-NaCl-DOC system with the presence of 2 mmol L^{-1} HCO_3 ion whereas Figure 4.3B, 4.3D and 4.3F represents Zn speciation analysis in 8 mmol L^{-1} HCO_3 ion in Zn-NaCl-DOC-HCO_3 system.

The Zn species between pH 4 and 7 show a presence of carbonate complexes ($ZnHCO_3^+$ and $ZnCO_3$). The relative distribution of Zn-Cl complexes between pH 4 and 7 is similar in the Zn-NaCl-DOC system and Zn-NaCl-DOC-HCO_3 with 2mmol L^{-1} HCO_3 system but different at 8mmol L^{-1} HCO_3 system. The HCO_3 in the Zn-NaCl-DOC systems is forming complexes with the free $Zn^{2+}_{(aq)}$ (Figure 4.3), therefore, the relative speciation of free Zn^{2+} in NaCl-DOC-HCO_3 system is lower than in NaCl-DOC system (Figs. 4.2 and 4.3). The decrease of Zn^{2+} due to addition of HCO_3 ion is higher in lower NaCl concentration and more prominent at pH 7 and in solution with higher HCO_3 concentration (8 mmol L^{-1}) (Figs. 4.2 and 4.3). In the NaCl-DOC system at 0.1 mol L^{-1} NaCl, free Zn^{2+} decreases around 5% and 18% following the addition of 2 mmol L^{-1} and 8mmol L^{-1} bicarbonate. This decrease changes from 4% and 13% at 0.3 mol L^{-1} NaCl and from 2% and 7% at 0.7 mol L^{-} (Figure 4.2 and 4.3). The relative concentration of the Zn-DOC complexes is slightly lower in the presence of HCO_3. The relative concentration of $ZnHCO_3^+$ increases with increasing HCO_3, however, decreases with increasing NaCl concentrations (Figure 4.3A, 4.3B, 4.3E and 4.3F). The relative concentration of $ZnHCO_3^+$ in the NaCl-DOC-HCO_3 system with 0.1 mol L^{-1} NaCl at 2mmol L^{-1} HCO_3 and at 8mmol L^{-1} HCO^3 change from about 6% to 20% at pH between 4 and 7. It decreased around 2% and 3% in HCO_3 concentration at 2 mmol L^{-1} and 5% and 10% in HCO_3 concentration at 8 mmol L^{-1} with changing NaCl from 0.3 mol L^{-1} to 0.7 mol L^{-1}, respectively (Figures 4.3A, 4.3B, 4.3C, 4.3D, 4.3E and 4.3F).

At pH 8, several Zn species are found. The precise of Zn carbonate complexes [$ZnCO_3$ and $Zn(CO_3)_2^{2-}$] is significantly higher and increases significantly at higher HCO_3 concentration, i.e., comparing 2 mmol L^{-1} and 8 mmol L^{-1} (Fig. 4.2 and 4.3). Due to the higher contribution of carbonate and Cl complexes, the activity of Zn^{2+} decreases significantly compared to the Zn-NaCl-DOC system. At pH between 9 and 10, the distribution pattern for Zn species consisted of Zn-carbonate complexes [$Zn(CO_3)_2^{2-}$, $Zn(CO_3)$] and $Zn(OH)_2$ species. Precipitation of Zn as $Zn(OH)_2$ is observed at pH 10 in NaCl-DOC-HCO_3 systems and higher at 0.7 mol L^{-1} NaCl concentration.

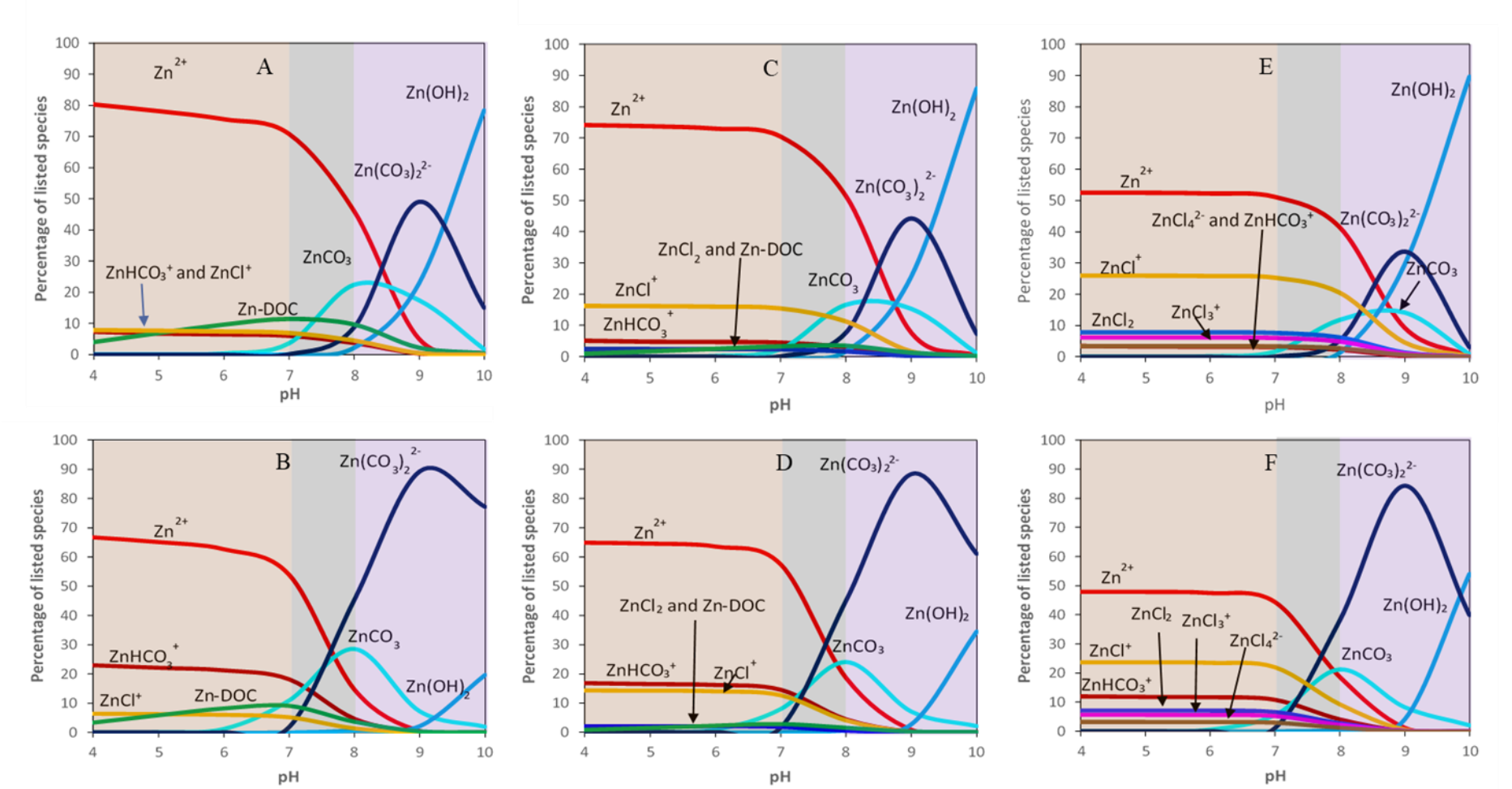


Figure 4.3 Visual MINTEQ model results of speciation diagram of Zn in NaCl-HCO_3- DOC system (calcareous solution) where A and B represents Zn in 0.1 mol L^{-1} NaCl – 2 mmol L^{-1} HCO_3 system and 0.1 mol L^{-1} NaCl – 8 mmol L^{-1} HCO_3 system, respectively; C and D represents Zn in 0.3 mol L^{-1} NaCl – 2 mmol L^{-1} HCO_3 system and 0.3 mol L^{-1} NaCl – 8 mmol L^{-1} HCO_3 system, respectively; and E and F represents Zn in 0.7 mol L^{-1} NaCl – 2 mmol L^{-1} HCO_3 system and 0.7 mol L^{1} NaCl – 8 mmol L^{-1} HCO_3 system, respectively. The system was in equilibrium with partial pressure of CO_2 (3.8×10^{-4} atm). Zn complexation with DOC in NaCl solutions is represented by Zn-DOC. Zn species at pH 4-7; at pH 8; and at pH 9-10 are represented by orange shaded area, light grey shaded area and purple shaded area, respectively.

4.2.3 Adsorption of Zn on Tropical Bay soil in NaCl solutions: Applicability of MSMs

4.2.3.1 pH adsorption edge in different NaCl concentration:

Batch adsorption results of Zn on a Bay (*Tropaquept*) soil in NaCl solutions at different pH are done to test the applicability of surface complexation models to predict Zn adsorption in different NaCl concentrations. The results show that the increase in NaCl concentration decreases the adsorption of Zn, between pH 3 and 7 (Fig. 4.4). Zn adsorption decreases sharply between pH 3 to 6 (Fig. 4.4). The adsorption of Zn decreased gradually then with pH from 6 to 7 and plateaued near 100% at pH 8. Zn adsorption decreases when the NaCl concentration increases from 0.1 mol L^{-1} to 0.3 mol L^{-1} but there is little difference in Zn adsorption between 0.3 mol L^{-1} to 0.7 mol L^{-1}.

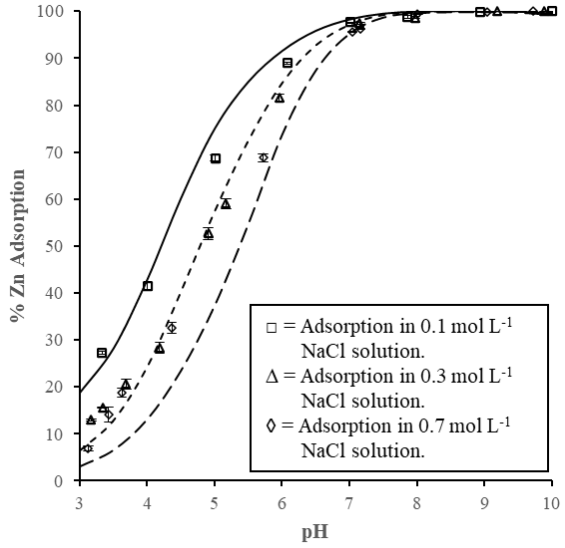


Figure 4.4 Percent adsorption of Zn on Bay soil (10 g/L) as a function of pH in 0.1 (□), 0.3 (Δ) and 0.7 (◊) mol L^{-1} NaCl concentration at Zn initial concentration = 0.08 mmol L^{-1}. The MSMs fits in 3 different NaCl solution are represented by the solid (0.1 mol L^{-1}), short-dashed (0.3 mol L^{-1}) and long-dashed lines (0.7 mol L^{-1}), respectively. The MSMs were performed with the inclusion of the major background cations. RMSEs between experimentally observed and model predicted Zn adsorption for each NaCl concentration are as follows: 0.1 mol L^{-1} NaCl – RMSE = 0.055%, 0.3 mol L^{-1} NaCl – 0.16%, 0.7 mol L^{-1} NaCl – 0.33%. All the experiments were repeated three times and the standard deviation shows that the results are highly reproducible.

The adsorption results of Zn on bay soil with increasing NaCl concentration from 0.3 mol L^{-1} to 0.7 mol L^{-1} indicated that although the percentage of Zn-Cl complexes is higher (Fig. 4.2C) when the chloride concentration is higher, the proportion of Zn susceptible to mobilization (decreased adsorption) through increasing NaCl concentration is smaller. Most likely, the fraction of Zn bound to the adsorption sites did not mobilize as Zn-Cl complexes with increasing NaCl concentration. Similarly, the fraction of Zn that can be mobilized through chloro-complexation with increasing NaCl concentration from 0.3 mol L^{-1} to 0.7 mol L^{-1} is not

stable enough to make an effect on Zn adsorption. This conclusion is on line with observation reporting that the non-significant pattern of Zn adsorption with increasing NaCl concentration was likely due to a lower stability of Zn-chloride complexes (Du Laing et al., 2008).

4.2.3.2 Comparison of multi surface model and experimental data

The experimental Zn adsorption results were compared and simulated by MSMs in Visual MINTEQ. Model and experimental data are presented in Figure. 4.4. The model predicted Zn adsorption at 0.1 and 0.3 mol L^{-1} NaCl concentration closely matches with the experimental data. The overall RMSE for Zn adsorption in 0.1 and 0.3 mol L^{-1} NaCl concentration is 0.055% and 0.16%, respectively. The model predicts Zn adsorption with experimental data in 0.7 mol L^{-1} NaCl concentration were good at pH higher than 6. The adsorption of Zn in 0.7 mol L^{-1} NaCl concentration was not satisfactory simulated when the pH is lower than 6. The overall RMSE for Zn adsorption in 0.7 mol L^{-1} NaCl concentration is 0.33%. According to Groenenberg and Lofts, the RMSE value of < 0.5% indicating a good model performance (Groenenberg and Lofts, 2014). Therefore, the model simulation results indicate that MSMs with the model parameters (Table 3.4, 3.5, and 3.6) adjusted at low ionic strength can be applied to predict Zn adsorption over a wide range of NaCl concentrations (up to 0.7 mol L^{-1}) without parameter adjustment.

The simulation results and RMSE in 0.1 mol L^{-1} NaCl concentration agree well with those found by Fisher-Power et al. (2016) and Mizutani et al. (2017). A comparison of RMSE for % adsorbed vs. pH data in 0.3 and 0.7 mol L^{-1} NaCl concentration is limited due to the unavailable data in the literature. The overestimation of Zn adsorption at pH < 5 during the experiment with 0.3 mol L^{-1} and 0.7 mol L^{-1} NaCl concentration increases error of model prediction. The predicted Zn adsorption is generally 5% lower at pH between 3 and 5 compared with measured adsorption in 0.3 mol L^{-1} NaCl solutions. For 0.7 mol L^{-1} NaCl solutions, the predicted Zn adsorption is 13% lower than measured adsorption for pH between 3-5.

4.2.3.3 Relative importance of soil reactive sites for Zn adsorption:

Models suggest that at very low pH (pH 3-4), Zn is highly mobile as free Zn^{2+} which was decreased with increasing NaCl concentration as free Zn^{2+} made complexation with chloride ions. At acidic pH, SOM is the dominant sorbent for Zn. At neutral and alkaline pH, SOM along with amorphous iron (hydr)oxide are the dominant sorbent for Zn (Fig. 4.5). Similar results were previously reported for Zn in low and high-Zn soil (Duffner et al., 2014), Zn in

sandy soil (Weng et al., 2001), Zn in natural sediment (Fisher-Power et al., 2016) and Zn in contaminated soils (Ren et al., 2017).

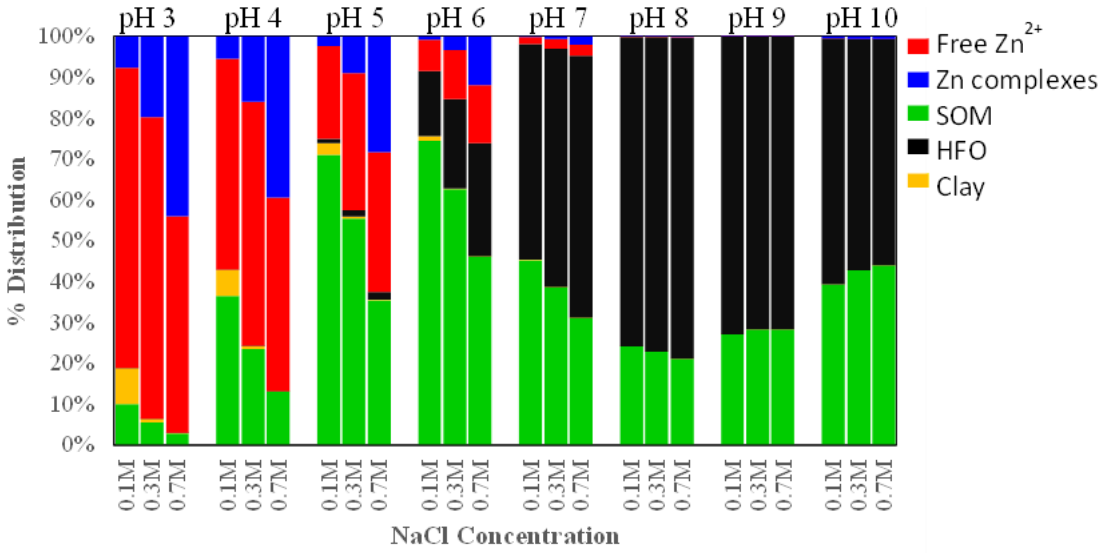


Figure 4.5 Contribution of soil components (clay, hydrous ferric oxides (HFO) and SOM) to Zn adsorption in the studied soils in 0.1, 0.3 and 0.7 mol L^{-1} NaCl concentration, as predicted by the MSMs with $[Zn]_{init}$ = 0.08 mmol L^{-1}. The calculations were performed with the inclusion of the major background cations. Zn complexes in in the distribution bar graph represented Zn-Cl complexes, $Zn(OH)_2$ and $ZnCO_3$.

The contribution of clay to Zn binding was very small. The presence of Na ion in NaCl solution and the Ca, Mg, K ions from the extractable soil solution reduced Zn adsorption by occupying clays permanently negative charged sites. Clay minerals are more important for adsorbing metal at low pH, at low organic matter content, and at low concentration of cations (Na, Ca) (Weng et al., 2001). The effect of NaCl concentration on Zn adsorption by model prediction indicated that increasing NaCl concentration decreased Zn binding by SOM whereas increased Zn binding by iron (hydr)oxide from pH 4 -7. With increasing NaCl concentration, the presence of chloride ion forms Zn-Cl complexes which reduced Zn binding by SOM (Lumsdon et al., 1995). Additionally, the cation Na ion due to increasing NaCl concentration might reduce Zn binding by SOM by competing with Zn for the sorption sites of SOM (Du Laing et al., 2009). As the adsorption constants for Na ion with SOM is not reported in the NICA-Donnan model, Na competition with Zn ion at SOM surfaces was not reported by the model calculation. Adsorption of Zn by iron (hydr)oxide increased with increasing NaCl concentration as the surface charge of iron (hydr)oxide increased. Model speciation predictions showed that the role of NaCl concentrations and the ions from extractable soil solution were affected Zn speciation (free Zn^{2+}, Zn-inorganic complexes and Zn adsorption) to pH 3 - 7. Zn was tightly bound by

SOM and iron (hydr)oxide at pH > 8, therefore, Zn speciation was not affected with increasing NaCl concentrations.

4.2.4 Application of multi surface model to predict the effect of NaCl salinity increase on Zn speciation and adsorption on coastal soils of Bangladesh

4.2.4.1 Effect of NaCl salinisation on Zn speciation

Following the successful prediction of Zn speciation on tropical bay soil by the MSMs in highly saline conditions, we used the model set up to predict Zn adsorption in soils [calcareous, non-calcareous (decalcified) and acidic] in the Ganges Tidal Floodplain region of Bangladesh using a solid/liquid ratio of 10 g/L and NaCl concentrations ranging between 0.1and 0.7 mol L^{-1}. The model results reveal a strong control of the soil pH and reactive surfaces of adsorbent (Fig. 4.6). The predicted ZnCl complexes in solutions with different NaCl concentrations agreed predicted speciation of Zn in NaCl concentrations. Zn-Cl complexes are dominant at low and neutral pH solutions and with increasing NaCl concentration, Zn-Cl complexes increase (Long and Angino, 1977). A higher relative contribution of ZnCl complexes is reported for acidic (Kamalkathi) and non-calcareous (Barisal) soils with increasing NaCl concentration. At alkaline pH, the activity of Zn-Cl complexes is minimum and the effect of increasing NaCl concentration on Zn is insignificant in alkaline calcareous soils such as those found in Bajoa, Ramgati, and Sara. The presence of HCO_3 ion does not increase Zn-carbonate complexes. Concerning the free Zn ion, the MSMs models predicted that concentrations slightly increase with increasing NaCl concentrations in alkaline calcareous soils of Bajoa, Ramgati, and Sara. In the non-calcareous Barisal and acidic Kamalkathi soil, the free Zn ion increases with increasing NaCl concentration between 0.1 mol L^{-1} to 0.3 mol L^{-1} and decreases at 0.7 mol L^{-1}. The initial increase of free Zn ion in near neutral non-calcareous and acidic soils is explained by Zn species and the effect of NaCl on these components. Zinc adsorbed by clay and SOM and complexed to DOM decreases with increasing salinity as the Na competes with Zn on clay and Cl complexation with Zn that did not adsorb by SOM and clay (Du Laing et al., 2009; Zhang et al., 2018a; Zhang et al., 2014). Therefore, an increasing trend of free Zn ion is expected with increasing NaCl concentrations from 0.1 mol L^{-1} to 0.3 mol L^{-1}. However, despite Zn desorption by SOM, clay and DOM due to the competitive and complexing effect of Na and Cl ion in 0.7 mol L^{-1} NaCl concentration, free Zn ion activity decreased as the Zn-inorganic complexes (mainly Zn-Cl complexes) increased in 0.7 mol L^{-1} NaCl concentration. Zn-Cl complexes increased around 15% and 34% with increasing NaCl ionic strength from 0.1

mol L^{-1} to 0.7 mol L^{-1} in non-calcareous soil and acidic soil, respectively which ultimately reduced the percentage of free Zn ion in acidic and non-calcareous soil.

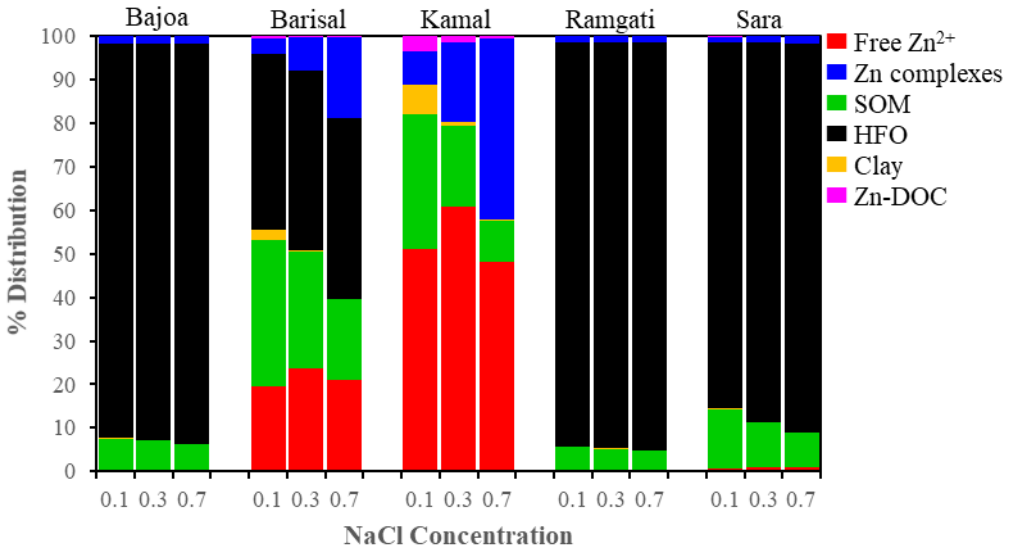


Figure 4.6 MSMs prediction of Zn adsorption and its distribution within soil components (clay, hydrous ferric oxides (HFO) and SOM) in some soils of the Ganges Tidal Floodplain in Bangladesh in different NaCl concentrations (0.1, 0.3 and 0.7 mol L^{-1}) at $[Zn]_{init}$ = 0.08 mmol L^{-1}. Kamalkathi soil series is acidic soil; Barisal soil series is non-calcareous soil; Bajoa, Ramgati and Sara soil series are calcareous alkaline soils. The calculations were performed with the inclusion of the major background cations. Zn complexes in in the distribution bar graph represented Zn-Cl complexes, $Zn(OH)_2$ and $ZnCO_3$.

4.2.4.2 Effect of NaCl salinity on Zn adsorption in soil

In acidic soils such as the Kamalkathi soil series (pH = 4.60), around 50% of Zn is present as a free Zn ion and SOM provides most binding sites for Zn. Adsorption by clay plays only a minor role (≈ 7%) in controlling Zn mobility at salinity. We find a higher complexation of Zn by DOM in low salty solutions. Zn adsorption by SOM and clay as well as the complexation of Zn with DOM decrease with increasing salinity. The mechanisms for decreasing Zn adsorption from SOM and clay and Zn complexation with DOM were similar to the batch adsorption results of tropical soil (Bay soil) and discussed previously.

In alkaline calcareous soils, including Bajoa, Ramgati and Sara soil series, free Zn ion is very low and iron oxides become more important for binding Zn. The effect of increasing salinity does not increase ZnCl complexes. Iron (hydr)oxides have a strong binding interaction with Zn and Chesne and Kim (2014) reported that Zn adsorption by iron (hydr)oxides increased with increasing NaCl concentration.

In non-calcareous acidic soil, i.e. the Barisal soil series, SOM and iron oxides are the main pool for Zn adsorption. Like in acidic soils, Zn binding by SOM decreases with increasing NaCl

concentration. Zn complexation with DOM is nearly absent in the non-calcareous Barisal soil series; although, the complexation of Zn-DOM was reported higher by aqueous speciation model analysis (Fig. 4.2 and 4.3) at pH 7 low salinity. This indicated that the role of DOM to complex Zn in solid-solution distribution is very low and Zn availability and mobility are largely determined by Zn binding to the solid phases. The model findings of the role of DOM is supported by Weng et al. (2002) who reported similar observation about Zn complexation with DOM in solid-solution distribution. Zinc adsorption on iron oxides in the Barisal soil series is rational as the adsorption of Zn onto iron oxides takes place at pH > 6 (Chesne and Kim, 2014). The point of zero charge (pH_{pzc}) of iron oxides is reported at pH 7 to pH 9.5 in the literature (Gao and Mucci, 2001). This indicated that at pH > 6, the surface charge of iron (hydr)oxides is neutral/negatively charged. Therefore, the interaction between negatively charged iron (hydr)oxides and free Zn ion is more favourable at higher pH.

4.3 Discussion:

4.3.1 Suitability of the Davies equation at seawater ionic strength

The empirical Davies model relates the charges on an ion to an activity coefficient at a specified ionic strength and does not consider the ion size parameter for activity correction. The SIT model, in contrast, is semi-empirical and interaction coefficients between the various ions present in the solution are taken into consideration. Therefore, the variation in Zn^{2+} and Zn-Cl complexes within the model's comparison could be due to the differences in the activity correction approach. This observation is in line with work that report that variation of metal speciation analysis using different geochemical codes due to different species equations, equilibrium constants, measurement of alkalinity, and the model to calculate activity co-efficient (Bonito et al., 2018). Tipping et al. (2016) and Unsworth et al. (2006) reported that a certain level of variation of model prediction of metal speciation in seawater ionic strength is accepted, without mentioning any specific details on the bias. Stockdale et al. (2015) reported a variation of ±16% for the free ion activities (Ni, Cu, Zn, Pb, Hg, and Cd) in coastal and estuaries areas within model results using the extended Debye-Hückel equation and mean salt method. However, they reported that these differences are small compared to the variation for experimentally determined speciation by competitive ligand and voltammetry methods. Consequently, they exclusively used the extended Debye-Hückel method for activity correction in marine systems. In my study, the variation of Zn^{2+}, $ZnCO_3$ and Zn-Cl complexes within the model results using Davies equation and those reported in the IUPAC technical

report using SIT is not more than 10%. As the differences are consistent with Stockdale et al. (2015), we used the default Visual MINTEQ approach: Davies equation for activity correction in different NaCl concentrations. This approach is consistent with other studies that have used Davies and extended Debye-Hückel method for activity correction and adequately described metal species in seawater ionic strength (Byrne et al., 1988; Derobertis et al., 1994; Majlesi et al., 2009; Tepavitcharova et al., 2014; Tepavitcharova et al., 2011; Tipping et al., 2016).

4.3.2 Effect of NaCl, HCO_3 and DOC on the speciation of Zn in aqueous solution

Chloride becomes an important ligand when increasing NaCl concentration from 0.1 to 0.7 mol L^{-1}. The Zn-Cl complexes in the aqueous solution are weak and it requires high concentration of Cl^- to form Zn-Cl complexes, high $[Cl^-]_T$:$[Zn^{2+}]_T$ ratios and high ionic strength solutions (Powell et al., 2013). Therefore, at low concentration of NaCl (0.1 mol L^{-1}), the $ZnCl^+$ complex is the only chloride complex reported by speciation models (Powell et al., 2013; Tepavitcharova et al., 2011). Although, four Zn-Cl complexes (i.e., $ZnCl^+$, $ZnCl_2$, $ZnCl_3^-$, $ZnCl_4^{2-}$) have been reported at pH between 4 and 8, the higher order association of Zn-Cl ($ZnCl_3^-$ and $ZnCl_4^{2-}$) complexes are only reported at higher NaCl concentrations (0.7 mol L^{-1}) and the relative importance of the Zn-Cl complexes in the NaCl solutions is $ZnCl^+ > ZnCl_2 > ZnCl_3^- > ZnCl_4^{2-}$.

The presence of DOC in the NaCl solution reduces free Zn^{2+}. The complexation of DOC with Zn is stronger than Zn complexation with Cl ion (($ZnCl^+$) between pH 6 and 8 in low NaCl concentration of (0.1 mol L^{-1}). The results are consistent with the experimental results of Boguta and Sokolowska (2020); Butler (2009); Christensen and Christensen (2000); Hyne et al. (2005) and Raspor et al. (1984) who determined higher complexation of Zn with 6 - 10 mg L^{-1} DOC at low concentration of NaCl (< 0.1 mol L^{-1}) and at pH 7. With the increasing NaCl concentration, the model findings indicate that the complexation of Zn-DOC significantly decreases likely due to the competitive effect of Cl ions. The modelling results are in line with findings by Raspor et al. (1984) who found that the presence of competing cations and anions in lake water and seawater reduced the percent complexation of Zn with DOC. In contrast, Bringolf et al. (2006) did not find any significant influence of NaCl concentration on Zn-DOC complexes during their laboratory tests. However, the concentration of ionic strength in their study was only 20 mmol L^{-1} NaCl which is a minimum fivefold lower and a maximum 35-fold lower than our background NaCl concentration.

The HCO_3 ion figures prominently in the speciation of Zn (Ferri et al., 1985; Pierrot and Millero, 2017; Ryan and Bauman, 1978; Stanley and Byrne, 1990). The relative decrease of

free Zn^{2+} following the addition of the HCO_3 ion in the Zn-NaCl-DOC system are consistent with model and experimental results conducted by different authors (Heijerick et al., 2002; Heijerick et al., 2003; Hyne et al., 2005). The $ZnHCO_3^+$ complex is dominated at acidic to neutral pH whereas $ZnCO_3$ is dominating at alkaline pH (8-10). The contribution of the $ZnCO_3$ complex is very low between pH 4 and 6 because the carbonate concentration at this pH is too low to affect the speciation (Ryan and Bauman, 1978). The relative concentration of $ZnHCO_3^+$ and $ZnCO_3$ is higher at 0.1 mol L^{-1} NaCl concentration. The decrease in relative concentration of $ZnHCO_3^+$ and $ZnCO_3$ with increasing NaCl concentration hints to the competitive nature of Cl and HCO_3 ions for the coordination with Zn. The relative concentration of ZnCl complexes is similar in the Zn-NaCl-DOC system and the Zn-NaCl-DOC-HCO_3 system. Therefore, the model results suggested that the Cl ion form stronger complexes with Zn than HCO_3 ion which is explained with the soft Lewis acidity of Zn. My calculations are in line with previous results (Millero and Hawke, 1992; Tepavitcharova et al., 2014; Tepavitcharova et al., 2011). My speciation model accurately reconstructs the anticipated behaviour of Cl and HCO_3 ions on Zn according to the mechanistic theory "hardness-softness" factor and the crystal field stabilization energy (CFSE). Zn-DOC complexes are relatively invariant with alkalinity (Figure 4.3). The results are consistent with findings that the Cu complexation with the organic matter did not change with increasing alkalinity (Sunda and Hanson, 1978).

4.3.3 Zn adsorption in NaCl concentrations

Decreasing Zn adsorption with increasing NaCl concentration from 0.1 mol L^{-1} to 0.3 mol L^{-1} can be explained by the complexation capacity of Zn with Cl ions. Chloride ions affect Zn mobility by decreasing its activity in the aqueous phase and by increasing desorption from sorption sites (Guevara-Riba et al., 2005). Figure 4.2 shows that the presence of chloride leads to an increase of Zn-Cl complexes and decrease of free Zn^{2+} activity. The major complexes are $ZnCl^+$ and $ZnCl_2$. The sorption sites of Zn between pH 3 and 7 are mainly clay minerals and SOM. For SOM surfaces, the presence of Zn-Cl complexes does not adsorb on SOM as ternary surface complex (Lumsdon et al., 1995). For clay minerals, the adsorption of Zn as a ternary surface complex is mostly reported with the presence of organic ligands (Stietiya and Hashem, 2010). Zn adsorption on the clay minerals as a ternary surface complex of Zn-Cl has not been reported in the literature. Thus, $ZnCl^+$ and $ZnCl_2$ do not adsorb on clay minerals and SOM, and decrease Zn adsorption. The adsorption results indicated that the adsorption of Zn on soils in different NaCl concentrations depends on soil pH and the complexation capacity of Zn with Cl ions. Chloro-complexation of Zn increases Zn desorption in soil with an acidic pH and does

not significantly decrease Zn adsorption in alkaline pH soil. These results suggest that NaCl salinity does not increase Zn mobility in alkaline pH soils. The effect of pH seen in my work agrees with Acosta et al. (2011) and Wang and Harrell (2005) studies. Beside chloro-complexation, the presence of Na^+ in soil solution could replace Zn from sorption sites (SOM and clay) and decrease Zn adsorption on soil. However, the competitive effect of Na^+ with Zn for decreasing Zn adsorption from clay surface could be less effective due to the less competitive nature of Na^+ with Zn for sorption sites (Jalali and Zinli, 2012; Wang and Harrell, 2005). Na forms only outer-sphere complexes with clay minerals. Therefore, it lies a greater distance from the surface and could not replace Zn from the sorption sites, even when the salinity increased 50 times (Acosta et al., 2011).

4.3.4 MSMs prediction and validation in different NaCl concentrations

The model predicted Zn adsorption at 0.1 and 0.3 mol L^{-1} NaCl concentration well matches the experimental data; however, the model discrepancy is observed at 0.7 mol L^{-1} NaCl concentration. The discrepancy between experimental measurements and MSMs predictions could be due to the lower estimation of clay charge and of active organic carbon or due to the model limitation to predict Zn adsorption at high ionic strength. Although a value of clay charge of 0.4 mol kg^{-1} and 46% of SOM as an active generic humic acid was used in our model simulations, a higher value for clay charge and SOM fraction could minimise the discrepancy between experimental quantifications and model predictions. The dominant clay mineral of the experimental soil is smectite which charge is higher than illite. The fraction of active SOM varies in the literature between 31% to 87% (Groenenberg and Lofts, 2014). Therefore, a low accounting of clay charge and SOM during model analysis might be responsible for the discrepancy between experimental measurements and MSMs predictions at 0.3 mol L^{-1} and 0.7 mol L^{-1} NaCl concentration. Another possibility for the model underestimation in 0.3 mol L^{-1} and 0.7 mol L^{-1} NaCl concentration at pH below 6 may be the uncertainty of the accuracy of the NICA-Donnan model at high NaCl concentration. Soil organic matter is the dominant phase to adsorb Zn at low pH. The parameters for the NICA-Donnan model are calibrated and adjusted at low ionic concentration (Duffner et al., 2014),. Although, the NICA-Donnan model satisfactorily describes proton dissociation of dead biomass from seaweeds (Rey-Castro et al., 2003) and Cu complexation with marine dissolved organic matter (Avendano et al., 2016), the application of the NICA-Donnan model as a part of MSMs to describe Zn adsorption by solid phase soil organic matter in ionic concentration above 0.01 mol L^{-1} is absent in the literature. Using MSMs to describe Zn adsorption on solid phase soil organic matter of soils in low ionic

solutions (0.01 mol L^{-1} $NaNO_3$) is reported by Fisher-Power et al. (2016) and Mizutani et al. (2017). The model underestimated Zn adsorption at acidic pH is also reported in their studies.

Another reason for the model discrepancy could be due to the absence of ternary surface complexes of Zn (≡FeOH-Zn-Cl) in the predefined databases. Zn adsorption as ternary surface complexes on the surface of iron (hydr)oxides at low pH in 0.6 mol L^{-1} NaCl solution is confirmed by spectroscopic analysis (Chesne and Kim, 2014). This absence might make the MSMs essentially impossible to produce exact predictions using the default parameters. The model description, therefore, might be improved by updating and calibrating the model parameters at sea water ionic strength.

My model results reveal that MSMs predict Zn adsorption on tropical bay soils at different soil pH and NaCl concentration. This suggests that MSMs can provide an advanced tool to estimate the impacts of soil management techniques on Zn adsorption, mobility and availability as a micro-nutrient fertilizer and as a heavy metal (Duffner et al., 2014). The batch adsorption experiment revealed that soils with pH 7 nearly adsorbed all the applied Zn which was equivalent to 900 kg ha^{-1} (Fig. 4.4 and 4.5). This results were well matched with Payne et al. (1988) and my model prediction. Therefore, by considering soil properties, MSMs will help to identify those soils where Zn was tightly held with soil components in different environmental systems. This insights by MSMs will help soil scientists to figure out whether excess application of Zn as a fertilizer or industrial by products has an environmental concern or not.

4.4. Conclusion

This study presents the first investigation into the suitability of chemical speciation and multi-surface adsorption models (MSMs) to predict Zn speciation and adsorption on soils in solutions with different NaCl concentrations. We find that,

1. Zn speciation in seawater ionic strength (≈ 0.67 mol L^{-1} NaCl) can be adequately described by the Davies equation and SIT model is not needed.
2. In the presence of NaCl, HCO_3 and DOC, the modelling shows that Zn species in the aqueous solution is controlled by the interactions with Cl, HCO_3 and DOC especially at pH 4-8. The complexation of Zn with Cl and HCO_3 ions increases with increasing NaCl and HCO_3 concentrations. In the NaCl-HCO_3 system, Zn chloride complexes increasingly dominate with increasing NaCl concentrations.

3. The complexation of Zn with DOC is higher in solution with lower NaCl concentration and decreases with increasing NaCl concentrations. In contrast, Zn-DOC complexation seems invariant to increasing HCO_3 concentration.
4. Zn adsorption experiments on soil in different NaCl concentrations (0.1 mol L^{-1}, 0.3 mol L^{-1} and 0.7 mol L^{-1}) indicate that increasing NaCl concentration decreased Zn adsorption. However, increasing NaCl concentration from 0.3 mol L^{-1} to 0.7 mol L^{-1} do not lead to a decrease in Zn adsorption. MSMs incorporating typical concentrations of major cations (Ca, Mg and K) and using generic surface complexation parameters optimized at low ionic strength predict Zn adsorption in different NaCl concentrations. The prediction is very good at 0.1 and 0.3 mol L^{-1} NaCl concentration and acceptable at 0.7 mol L^{-1} NaCl concentration. MSMs show that increasing Zn-Cl complexation with increasing NaCl concentration decreases Zn adsorption on the soil at pH between 3 and7. This effect is most pronounced at 0.7 mol L^{-1} NaCl concentration.
5. Iron (hydr)oxides is an important sorbent for Zn in alkaline pH soil whereas SOM is an important sorbent in near neutral and acidic pH. Clay is not an important sorbent for Zn in soils as the cations (Ca, Mg, K and Na) in soils solution competed with Zn and occupied most of the clay surface.
6. The model predicts that the effect of increasing NaCl concentration on Zn adsorption on coastal soils of Bangladesh is pH dependent. In calcareous alkaline soils (Bajoa, Ramgati and Sara) where the pH is > 7, Zn is predicted to be completely adsorbed by iron (hydr)oxides and SOM, and the effect of increasing NaCl concentration does not decrease Zn adsorption. In acidic (Kamalkathi) and near-neutral pH soils (Barisal), Zn adsorption decrease with increasing NaCl concentration. The influence of Cl ion to decrease Zn adsorption in Kamalkathi and Barisal soil series by complexing with Zn is dominated than DOC and HCO_3 ion. SOM is the main sorbent of Zn in acidic soils whereas SOM and iron (hydr)oxides are the main sorbents of Zn in near-neutral pH soils. As a result, Zn adsorption is higher in near-neutral pH soil (Barisal) than in acidic soils (Kamalkathi).

Chapter 5: Geochemical multi-surface modelling approach to predict Zn adsorption in tropical soils in NaCl saline solutions.

5.1 Introduction

Soils are the primary source of Zn and the availability of Zn in soils is deficient. Therefore, Zn deficiency is reported in millions of hectares of agricultural land (Alloway, 2009). To tackle Zn deficiency in soils, the application of Zn fertilizers is one of the strategies that has been successfully used. When Zn is applied in soils by fertilization or/and industrial processes, its availability and mobility in soils are primary regulated by its adsorption behaviour (Wang and Harrell, 2005). Soil constituents like clay, iron (hydr)oxide, soil organic matter (SOM), and carbonates control the adsorption capacity of Zn in soil. The cation exchange capacity of soils generally regulates Zn adsorption by soil clays. The contribution of clay minerals to adsorb Zn is small as the cations (Ca, Mg, K, Na) in soil solutions generally have a higher tendency to adsorb by the negative sites of clay minerals (Duffner et al., 2014; Fisher-Power et al., 2016; Weng et al., 2001). Therefore, the interaction between Zn with SOM and iron (hydr)oxide is the major Zn retention mechanism in soils (Duffner et al., 2014). The role of SOM and iron (hydr)oxide on Zn retention are pH-dependent. At acidic to neutral pH, SOM provides the primary binding sites for Zn, whereas iron (hydr)oxide becomes more dominant at alkaline pH (Mizutani et al., 2017; Weng et al., 2001). In calcareous soils, Zn adsorption by $CaCO_3$ and Zn precipitation as $Zn(OH)_2$ or $ZnCO_3$ also controls Zn availability in soils (Acosta et al., 2011; Jalali and Zinli, 2012). However, Duffner et al. (2014) and Trehan and Sekhon (1977) reported that the contribution of $CaCO_3$ in controlling Zn availability in calcareous soils is small due to the small surface area compared with SOM and iron (hydr)oxide.

The adsorption behaviour of Zn in soil generally depends on soil pH and the presence of ions in soil solutions. Na and Cl are the two most dominant ions in seawater. However, not much is yet known about the influence of NaCl concentrations on Zn adsorption on soils and the effect of different soil pH and reported effects are contradictory. Acosta et al. (2011) and Shuman (1986) reported that an increase in NaCl concentration from 0.006 mol L^{-1} to 0.3 mol L^{-1} did not significantly decrease Zn adsorption in their studied soils. Their findings indicated that Zn was not easily replaced by Na ion or complexed by Cl ion; therefore, NaCl solutions did not significantly increase Zn mobility in soil solutions. In contrast, Linde et al. (2007) reported that Zn mobility in soil solution was increased as Zn adsorption was decreased with NaCl solutions,

even at low concentrations (50 mmol L^{-1}). Similar results were also reported by Chu et al. (2015). The scare and contradicting information about Zn adsorption on soils in NaCl solutions indicated that further study is necessary to clarify Zn adsorption in NaCl solutions. Additionally, previous studies focused primarily on Zn adsorption in low concentrations of NaCl (up to 0.3 mol L^{-1}) and little effort was made to disclose Zn adsorption in seawater ionic strength (≈ 0.7 mol L^{-1} NaCl concentration) in different soil pH. Zn adsorption on soils in a high concentration of NaCl solution (≈ 0.7 mol L^{-1}) in different soil pH should be considered when evaluating the effects of increasing NaCl salinities in environmental risk assessments. Therefore, the study of Zn adsorption in NaCl concentrations will help to understand the impact of salinities due to climate change on Zn cycles (mobility, availability, and adsorption) in different soils.

Dissolution of solid calcium carbonate ($CaCO_3$) is an important soil forming process in the tropical coastal areas, and this, along with the application of alkaline groundwater for irrigation, provides a high concentration of bicarbonate (HCO_3) ion in soil solution (van den Berg and Loch, 2000; Zuo et al., 2007). HCO_3 ion sorbs to the surfaces of clay and iron (hydr)oxide minerals over a wide range of pH (Villalobos and Leckie, 2000) and may influence the adsorption behaviour of Zn in soil. Free Zn ion is known to form complexes with HCO_3 (Fig. 4.3) (Powell et al., 2013) and the complexes should have different adsorbing abilities. Zn may also precipitate as Zn-carbonate complexes with a high concentration of Zn and HCO_3 ion (Barakat, 2011; Kumari et al., 2016; Patterson et al., 1977). As both Cl and HCO_3 ions are present in relatively higher concentrations in coastal soil solutions due to seawater intrusion and dissolution of $CaCO_3$, they can compete with each other for complexing with Zn and for binding sites on iron(hydr)oxide (Villalobos and Leckie, 2000). Therefore, to describe the transport and fate of Zn in coastal soil systems, the effect of HCO_3 ion on Zn adsorption on soils should be considered. However, we do not find any available literature on Zn adsorption in the Cl-HCO_3 system.

Soils are complex natural systems and have different sorbent components. Multi-surface models (MSMs) where soil is considered as a set of individual sorption surfaces (SOM, iron hydroxides, CaCO3 and clay) are a promising way to predict metal cycle in soils (Dijkstra et al., 2004; Groenenberg and Lofts, 2014; Weng et al., 2001). Multi-surface models differentiate between electrostatic and ion-specific binding and consider the competition among ions for binding. The models can be implemented in a wide range of environmental conditions (e.g., pH, ionic strengths, etc.) (Groenenberg and Lofts, 2014). The models are extensively applied

to assessing metals bioavailability, mobility and adsorption (Zn, Cu, Cd, etc.) in soils (Duffner et al., 2014; Fisher-Power et al., 2016; Mizutani et al., 2017; Weng et al., 2001; Zhang et al., 2018a). However, MSMs have not been used before to predict Zn adsorption in low- and high-Zn concentrations in different NaCl concentrations with other ions. One of the limitations of MSMs is that the model parameters have generally been adjusted at a comparatively low ionic strength (Duffner et al., 2014; Gustafsson and Kleja, 2005; Gustafsson et al., 2003) and the activity correction of equilibrium speciation models is mainly done by extended Debye-Huckel equation and/or Davies equation which works very well too $I = 0.5$ mol L^{-1}. Although my model results in chapter 4 reported that MSMs and surface complexation models could successfully model the behaviour of ions in seawater ionic solution (Gao and Mucci, 2001; Gao and Mucci, 2003; Mercer and Tobiason, 2008), further research is needed to see the suitability of MSMs to predict metal adsorption in different initial concentration and high saline solution.

In soil with low Zn concentration, Zn may be bound with the high-affinity adsorption sites of soil components (Bonten et al., 2008). Compared to low Zn concentration, in soils with higher Zn concentration, a larger fraction of Zn may be precipitated as Zn-carbonate complexes (Degryse et al., 2011). Different methods have usually estimated model parameters used in MSMs. The concentration of amorphous and crystalline iron (hydr)oxides is determined experimentally. The charge of clay is assumed to be similar to the CEC of illite, which is in the range of 0.1 to 0.4 mol Kg^{-1} (Weng et al., 2001). The charge of clay can be estimated from the equation given by van Reeuwijk (Khai et al., 2008; van Reeuwijk, 1993). The site density of active SOM can be estimated by measuring the concentration of the humic substance and then optimizing with the cation exchange capacity of organic matter (Khai et al., 2008; Weng et al., 2001) or by assuming that the site density of active SOM varies between 31% to 87% of humic acid (Groenenberg and Lofts, 2014). In most of the literature, the concentration of clay and SOM used in MSMs were adjusted so that the root mean square error (RMSE) between experimentally measured and model simulated was minimum. However, it is uncertain if, under a natural soil environment where soil solution contains a high concentration of ions due to saline water intrusion, groundwater irrigation and fertilization, Zn adsorption can still be predicted with the density of clay, amorphous and crystalline iron (hydr)oxides and SOM that used and adjusted in a low concentration of Zn adsorption system.

Here, we test if a multi-surface model parameter (applied in Visual MINTEQ) that has been derived by modelling Zn adsorption in two tropical soils at $[Zn_{init}] = 0.08$ mmol L^{-1} predicts the pH-dependent Zn adsorption in a higher initial concentration of Zn and different NaCl

concentrations with the presence of other ions. The predicted Zn adsorptions are validated against the concentrations of Zn adsorption determined with the batch adsorption experiment. The effects of changing Zn concentration and adding HCO_3 on Zn adsorption in different NaCl concentrations are modelled with the multi-surface model to evaluate the validity of MSMs to describe Zn adsorption in different environmental systems. Therefore, the objectives of the chapter are:

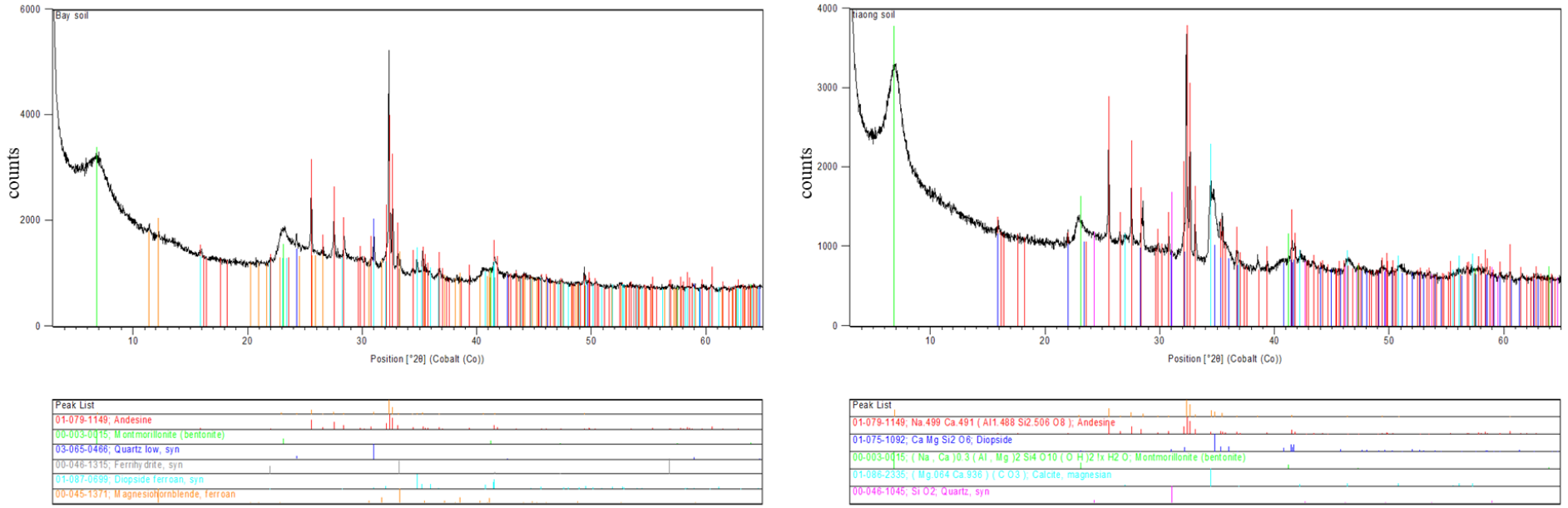
1. To determine pH-dependent Zn adsorption in NaCl and NaCl-HCO_3 solutions on two tropical soils by batch adsorption experiment.
2. To examine the accuracy of MSMs to predict Zn adsorption on Bay and Tiaong soil as a function of the different experimental systems (NaCl concentrations and mixed system of NaCl-HCO_3).
3. To determine the relative importance of soil components (i.e., clay, SOM, iron-oxides) for the binding of Zn at various initial concentrations of Zn and different NaCl concentrations with HCO_3.

5.2 Results:

5.2.1 Soils Properties

The physical and chemical properties of the studied soils (Bay and Tiaong) are taken from elsewhere (Izquierdo et al., 2016) and shown in Table 3.2. In the Bay soil (Tropaquept), the percentage of clay (49.9%) and silt (43.3%) is higher than in Tiaong soil (Hydraquent) (42.2% and 39.2%, respectively). Bay soil is slightly alkaline with pH = 7.3 and Tiaong soil is strongly alkaline with pH = 8.5. The organic carbon (72.8 g Kg^{-1}) and carbonate contents (95.9 g Kg^{-1}) are higher in Tiaong than in Bay soil (54.3 g Kg^{-1} and 1.6 g Kg^{-1}, respectively). Bay has a relatively high cation exchange capacity (10.6 cmol Kg^{-1}) than Tiaong soil (9.0 cmol Kg^{-1}). For model analysis, the reactive major cations pool and amorphous iron (hydr)oxides are determined experimentally and are presented in Table 3.3 of Chapter 3.

The full XRD patterns of bulk soils are presented in Figure 5.1. Mineral quantification by the Rietveld method indicated that minerals in substantial amounts are plagioclase (andesine) and smectite (montmorillonite) in both soils (Table 5.1). Smectite (montmorillonite) is more abundant in Bay soil than in Tiaong soils. Besides plagioclase and smectite, a substantial amount of calcite mineral is found in Tiaong soil. Smaller amounts of ferrihydrite, diopside ferroan (Calcium Magnesium Iron Silicate), and magnesium hornblende ferroan (Calcium Magnesium Iron Aluminum Silicate Hydroxide) are detected by XRD in Bay soil, whereas diopside (Calcium Magnesium Silicate) is found in Tiaong soil.



Bay soil Tiaong soil

Figure 5.1 XRD spectrum of minerals in the bulk soils. Mineral identification is performed using the PDF database within the Highscore software (Malvern Panalytical).

Table 5.1 Quantification of soil minerals by the Rietveld method

Soils	Mineralogical Analysis				
	Smectite**	Plagioclase	Calcite	Quartz	Diopside
Bay	75.6	20.5	--	1.9	<1
Tiaong	52.8	32.9	10.6	--	3.6

There is no apparent intense peak of ferrihydrite, hematite and goethite phase in the bulk mineralogical composition of both soils indicating that their phase proportions will be very low (< 1%) and are difficult to quantify by the Rietveld method.

The mineralogy of clay fractions in both soils is dominated by smectite minerals (Fig. 5.2). Smectite is identified by expanding the air-dried specimen peak from 1.4 nm to 1.7 nm after being saturated with glycerol. Generally, smectite mineral is dominated in alluvial and young soils (Wilson, 1999).

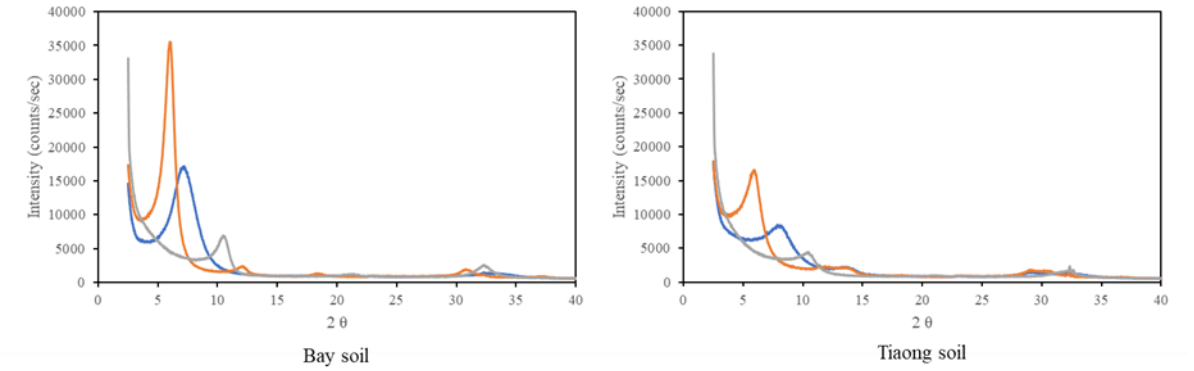


Figure 5.2 XRD spectrum of minerals in the clay fraction (< 2 µm). The blue, orange, and gray line are the XRD pattern of air dried, glycerol saturated, and heat treated (400ºC) soil specimen, respectively.

The elemental analysis of soil samples with XRF is presented in Table 5.2. Oxides of Al, Si, Ca, and Fe are mainly found in soil samples. Aluminosilicates and silica generally represent Al and Si in soils. The oxide of Ca and Fe are in the extraction residue closed in mineral structure (Baranowski et al., 2002). The mineralogical analysis and the information on soil classification indicated that both soils are young and less developed. The Rietveld profile of both soils is provided in Appendix B.

Table 5.2 Elemental analysis of soil samples by XRF

Soil	Element	Composition (%)	Soil	Element	Composition (%)
Bay	Na	0.14	Tiaong	Na	0.12
	Mg	0.33		Mg	0.96
	Al	8.97		Al	4.26
	Si	38.74		Si	23.75
	P	0.42		P	0.41
	S	0.34		S	0.41
	Cl	0.19		Cl	0.14
	K	1.63		K	0.77
	Ca	7.52		Ca	33.10
	Ti	2.20		Ti	1.29
	V	0.11		V	0.05
	Cr	0.02		Cr	0
	Mn	0.63		Mn	6.85
	Fe	37.62		Fe	27.51
	Cu	0.13		Cu	0.05
	Zn	0.11		Zn	0.06
	Ga	0.01		Ga	0.01
	As	0		As	0
	Br	0.01		Br	0.01
	Rb	0.03		Rb	0.01
	Sr	0.23		Sr	0

5.2.2 Batch Adsorption Results

5.2.2.1 Effect of NaCl solutions on Zn adsorption

Batch adsorption experiments were conducted to see the effect of increasing NaCl concentration on the adsorption of Zn on soils in two different initial concentrations. The effect of NaCl solutions (0.1, 0.3, and 0.7 mol L^{-1}) on Zn adsorption on Bay and Tiaong soil between pH 3 and 10 and with Zn initial concentration of 0.08 mmol L^{-1} and 0.8 mmol L^{-1} are shown in Figure 5.3. The upper figures represent Zn adsorption on Bay and Tiaong soils at Zn initial concentration of 0.08 mmol L^{-1}, whereas the lower figures represent Zn adsorption on Bay and Tiaong soils at Zn initial concentration of 0.8 mmol L^{-1}.

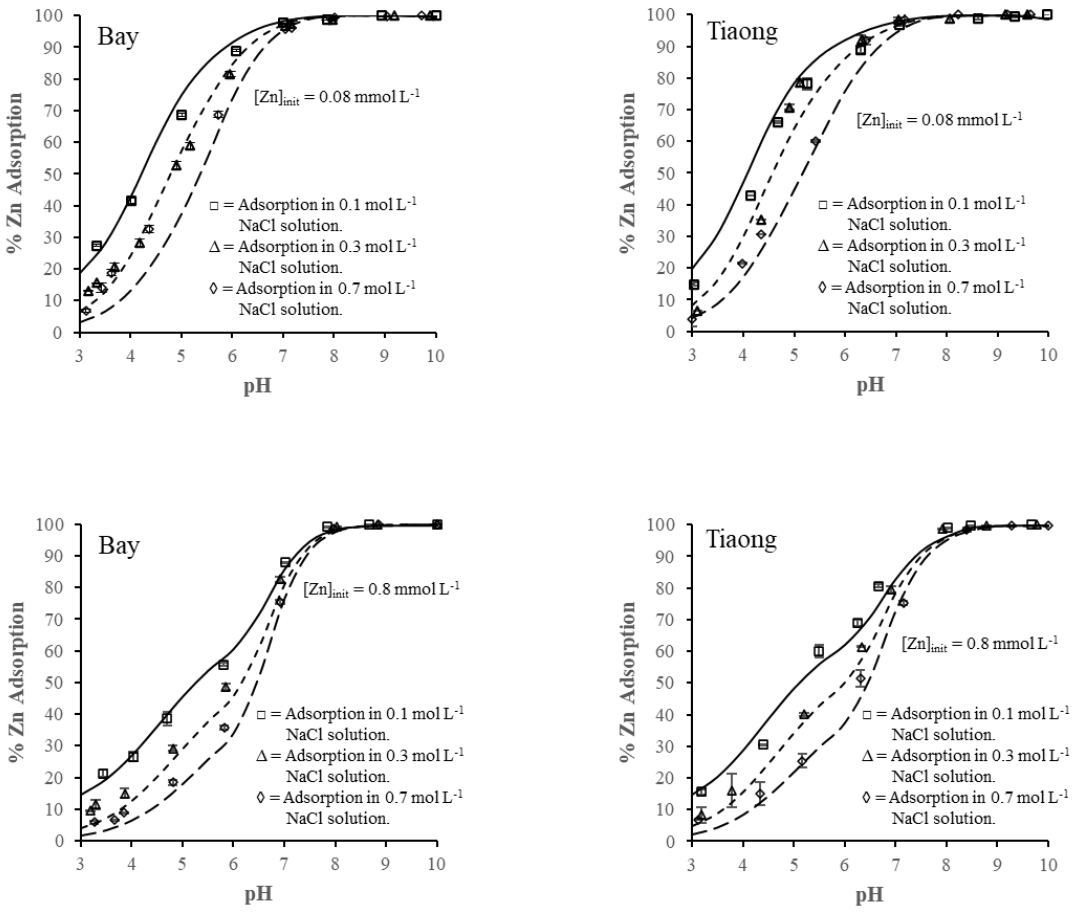


Figure 5.3 Percent adsorption of Zn on Bay and Tiaong soil (10 g L^{-1}) as a function of pH in 0.1 (□), 0.3 (Δ) and 0.7 (◊) mol L^{-1} NaCl solution at two different initial concentration: 0.08 mmol L^{-1} and 0.8 mmol L^{-1}. The MSMs fits in 3 different NaCl concentration are represented by the solid (0.1 mol L^{-1}), short-dashed (0.3 mol L^{-1}) and long-dashed lines (0.7 mol L^{-1}), respectively. All the experiments have three replications, and the standard deviation shows that the results are highly reproducible.

The adsorption isotherm shows that the effect of increasing NaCl concentration on Zn adsorption on soils is pH dependent (Fig. 5.3). In the range between pH 3 and 7, the adsorption of Zn on soils is increased with increasing soil pH. Zn is nearly entirely adsorbed on the soil surface between pH 8 and 10. Zn adsorption decreases from pH 3 and 7 in both soils and in both initial concentrations of Zn with increasing NaCl concentration from 0.1 mol L^{-1} to 0.3 mol L^{-1} (Fig. 5.3). Zn adsorption onto Bay and Tiaong soil decreases around 10-12% at Zn initial concentration of 0.08 mmol L^{-1} and around 8-10% at Zn initial concentration of 0.8 mmol L^{-1}. The increase of NaCl concentration from 0.3 mol L^{-1} to 0.7 mol L^{-1} does not seem to influence Zn adsorption on the Bay and Tiaong soil at Zn initial concentration of 0.08 mmol L^{-1}. However, the effects are pronounced at Zn initial concentration of 0.8 mmol L^{-1} and Zn adsorption decreases around 6-10% from pH 3 – 6 in both soil with increasing NaCl concentration from 0.3 mol L^{-1} to 0.7 mol L^{-1}.

Considering the pH effect, the adsorption curves of Zn on the Bay and Tiaong soil in different NaCl concentrations at Zn initial concentration of 0.08 mmol L^{-1} indicate that Zn adsorption on soils is increased sharply by increasing the pH from 3.0 to 6.0 (Fig. 5.3). The adsorption of Zn increases gradually with pH from 6 to 7 and plateaus near 100% at pH 8. Similar trends are observed for both soils at Zn initial concentration of 0.8 mmol L^{-1}; however, the adsorption curve moves to higher pH values (Fig. 5.3). For soils with Zn initial concentration of 0.8 mmol L^{-1}, an adsorption edge occurs at pH 4-7; adsorption gradually increases with pH from 7 to 8 and plateaus near 100% at pH 8. The shifting pattern of the adsorption curve to higher pH due to the differences in Zn initial concentration is attributed to the expansion of the adsorbate/adsorbent ratio. Therefore, for the equal number of available sites at a particular pH, less percentage of Zn is adsorbed at a higher initial concentration of Zn. The results of Zn adsorption on the Bay and Tiaong soil in different soil pH and the shifting nature of the adsorption curve towards higher pH value at higher concentration of Zn (0.8 mmol L^{-1}) are consistent with previous results reported by Fisher-Power et al. (2016), Mizutani et al. (2017) and Spathariotis and Kallianou (2001).

5.2.2.2 Effect of NaCl and HCO_3 on Zn adsorption

To determine the effect of HCO_3 on the adsorption of Zn on soils in NaCl concentrations, HCO_3 is added during the batch adsorption experiments. The fraction of Zn adsorption on the Bay and Tiaong soil at the initial concentration of Zn of 0.08 mmol L^{-1} in the presence of 8 mmol L^{-1} carbonate (HCO_3) in 0.1, 0.3, and 0.7 mol L^{-1} NaCl concentration is shown in Figure 5.4 and 5.5. For comparison purposes, the adsorption results and models fit of Zn adsorption in 0.1, 0.3 and 0.7 mol L^{-1} NaCl concentration in the absence of carbonate are reproduced from sections 5.2.2.1 in Fig. 5.4 and 5.5. In Bay soil, Zn adsorptions in 0.1 and 0.3 mol L^{-1} NaCl solution are unaffected upon adding 8 mmol L^{-1} carbonate (HCO_3) (Fig. 5.4a and 5.4b). In 0.7 mol L^{-1} NaCl concentration, Zn adsorption on Bay soil decreases a bit at pH 3-5 after adding 8 mmol L^{-1} carbonate (HCO_3) but is decreased around 5-7% from pH > 6 (Fig. 5.4c). In Tiaong soil, Zn adsorption is unaffected in 0.1 mol L^{-1} NaCl concentration after adding 8 mmol L^{-1} carbonate (Fig. 5.5a). A slight decrease of Zn adsorption on Tiaong soil is observed at pH 4 – 7 in 0.3 mol L^{-1} NaCl concentration and at pH 5 - 9 in 0.7 mol L^{-1} NaCl concentration following the addition of 8 mmol L^{-1} carbonate (HCO_3) (Fig. 5.5b and 5.5c).

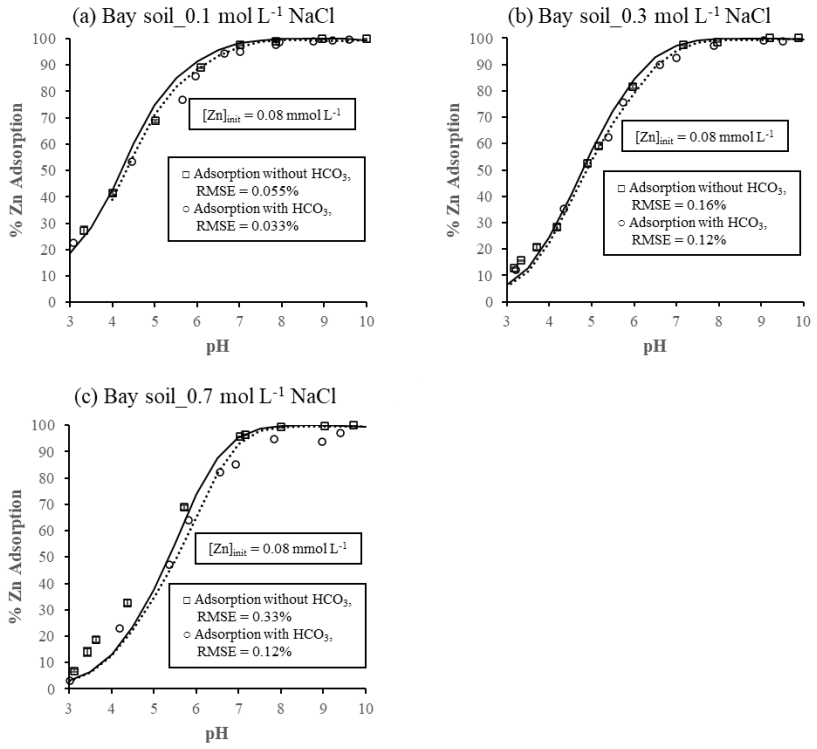


Figure 5.4 Percent adsorption of Zn on Bay soil as a function of pH in 0.1 (A), 0.3 (B) and 0.7 (C) mol L^{-1} NaCl concentration, respectively at $[Zn]_{init}$ = 0.08 mmol L^{-1} in the presence of carbonate: ○: 8 mmol L^{-1}. For comparison, the experimental results and model fits of Zn adsorption in the absence of carbonate is reproduced and represented by □ and a line, respectively. The MSMs predictions for Zn adsorption in the presence of carbonate is presented by round dot line.

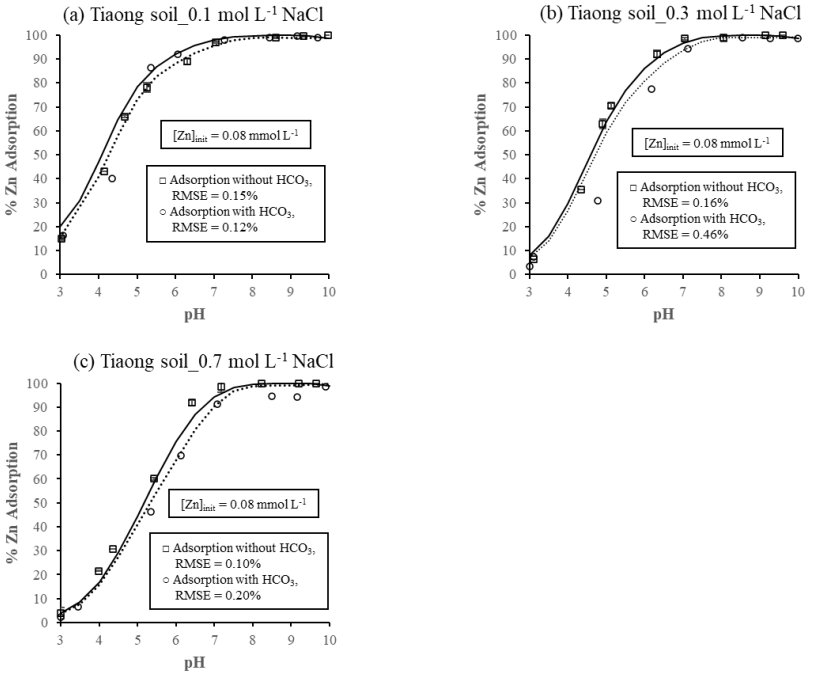


Figure 5.5 Percent adsorption of Zn on Tiaong soil as a function of pH in 0.1, 0.3 and 0.7 mol L^{-1} NaCl concentration, respectively at $[Zn]_{init}$ = 0.08 mmol L^{-1} in the presence of carbonate: ○: 8 mmol L^{-1}. For comparison, the experimental results and model fits of Zn adsorption in the absence of carbonate is reproduced and represented by □ and a line, respectively. The MSMs predictions for Zn adsorption in the presence of carbonate is presented by round dot lines.

The fractions of Zn adsorption on the Bay and Tiaong soil in the presence of 8 mmol L^{-1} carbonate at the initial concentration of Zn of 0.8 mmol L^{-1} are presented in Figures 5.6 and 5.7. In comparison with Zn adsorption in NaCl concentrations (0.1, 0.3 and 0.7 mol L^{-1}, respectively) in the absence of carbonate, the percent Zn adsorption at pH 6 to 7.5 is moved towards higher adsorption values in both soils after adding 8 mmol L^{-1} carbonate in 0.1, 0.3, and 0.7 mol L^{-1} NaCl concentration (Figure 5.6 and 5.7). The movement of Zn adsorption towards higher values is higher in 0.1 mol L^{-1} NaCl concentration than in 0.3 and 0.7 mol L^{-1} NaCl concentration. At alkaline pH (8 – 10), Zn adsorption on Bay and Tiaong soil is unaltered after adding 8 mmol L^{-1} carbonate in 0.1, 0.3 and 0.7 mol L^{-1} NaCl concentration. At acidic pH (3 - 5), Zn adsorption on Bay soil does not change after the addition of 8 mmol L^{-1} carbonate in 0.1 and 0.3 mol L^{-1} NaCl concentration (Fig. 5.6a and 5.6b), whereas a slight increase of Zn adsorption is observed in 0.7 mol L^{-1} NaCl concentration (Fig. 5.6C). In Tiaong soil, Zn adsorption increases slightly under acidic pH (3-5) after adding 8 mmol L^{-1} carbonate in 0.3 and 0.7 mol L^{-1} NaCl concentration (Fig. 5.7b and 5.7c). However, Zn adsorption is not affected following the addition of 8 mmol L^{-1} carbonate in 0.1 mol L^{-1} NaCl concentration (5.7a).

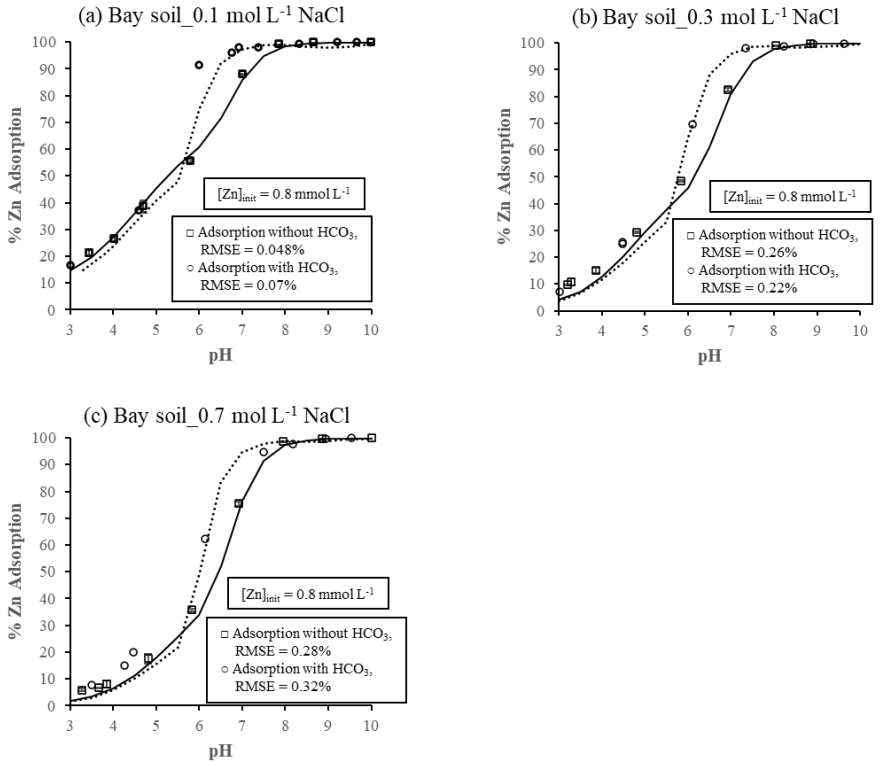


Figure 5.6 Percent adsorption of Zn on Bay soil as a function of pH in 0.1, 0.3 and 0.7 mol L^{-1} NaCl concentration, respectively at $[Zn]_{init}$ = 0.8 mmol L^{-1} in the presence of carbonate: ○: 8 mmol L^{-1}. For comparison, the experimental results and model fits of Zn adsorption in the absence of carbonate is reproduced and represented by □ and a line, respectively. The MSMs prediction for Zn adsorption in the presence of carbonate are presented by round dot lines.

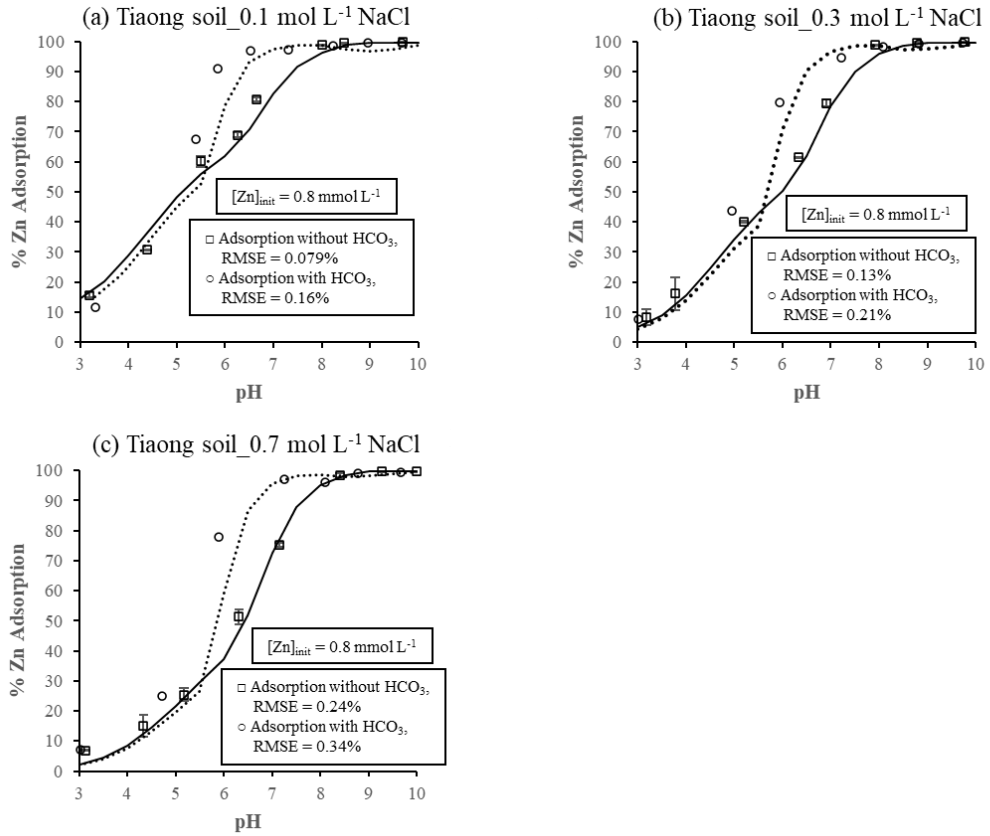


Figure 5.7 Adsorption of Zn on Tiaong soil (in percentage) as a function of pH in 0.1, 0.3 and 0.7 mol L^{-1} NaCl concentration, respectively at $[Zn]_{init}$ = 0.8 mmol L^{-1} in the presence of carbonate: ○: 8 mmol L^{-1}. For comparison, the experimental results and model fits of Zn adsorption in the absence of carbonate is reproduced and represented by □ and a line, respectively. The MSMs prediction for Zn adsorption in the presence of carbonate are presented by round dot lines.

5.2.3 Testing the validity of multi-surface models to predict Zn adsorption on Bay and Tiaong soil

5.2.3.1 Application of MSMs to predict Zn adsorption in NaCl concentrations

MSMs approach is used to predict the adsorption of Zn onto Bay and Tiaong soils in different NaCl concentrations with different initial concentrations of Zn. The prediction of Zn adsorption as a function of the NaCl and initial concentration of Zn is evaluated based on the RMSE between the predicted and measured values. The fits with the MSMs models for the Bay and Tiaong soil are shown in Figures 5.3. The model results in different NaCl concentrations at the initial concentration of Zn of 0.08 mmol L^{-1} and 0.8 mmol L^{-1}, respectively are presented by the solid lines (0.1 mol L^{-1}), short-dashed lines (0.3 mol L^{-1}) and long-dashed lines (0.7 mol L^{-1}), respectively.

The model fits are very good for Bay soil at the initial concentration of Zn of 0.08 mmol L^{-1} and 0.8 mmol L^{-1} respectively in 0.1 mol L^{-1} NaCl concentration. The overall RMSE values are 0.055% and 0.048%, respectively. The model simulations for Zn adsorption in 0.3 mol L^{-1}

NaCl concentration at the initial concentration of Zn of 0.08 mmol L^{-1} and 0.8 mmol L^{-1}, respectively agree well with the observations. The overall RMSE values are 0.16% and 0.26%, respectively. For Zn adsorption in 0.7 mol L^{-1} NaCl concentration at the initial concentration of Zn of 0.08 mmol L^{-1} and 0.8 mmol L^{-1} respectively, the simulation in most cases corresponds rather well with measured data (Fig 5.3). The model fits for Zn adsorption in 0.7 mol L^{-1} NaCl concentration are good when the pH is higher than 6. The models prediction underestimated Zn adsorption when the pH is lower below 6. The overall RMSE values are 0.33% and 0.28%, respectively.

For Tiaong soils, the model fits for Zn adsorption in 0.1 mol L^{-1} NaCl concentration are good at a concentration of Zn of 0.08 mmol L^{-1} and very good at a concentration of Zn of 0.8 mmol L^{-1}. The overall RMSE values are 0.15% and 0.079%, respectively. The model predicted value of Zn adsorption in 0.3 mol L^{-1} NaCl concentration agrees well with the observed total adsorption of Zn. The overall RMSE values at the initial concentration of Zn of 0.08 mmol L^{-1} and 0.8 mmol L^{-1} are 0.16% and 0.13%, respectively. For Zn adsorption in 0.7 mol L^{-1} NaCl concentration and at Zn initial concentration of 0.08 mmol L^{-1}, the model predictions agree well with the measured total adsorption of Zn whereas, at Zn initial concentration of 0.8 mmol L^{-1}, the model predictions in most cases corresponds well with measured data. Like Bay soil, the models underestimate Zn adsorption at pH < 6 in 0.3 mol L^{-1} and 0.7 mol L^{-1} NaCl concentration. The overall RMSE values are 0.10% and 0.24%, respectively (Fig. 5.3).

5.2.3.2 Application of MSMs to predict Zn adsorption in NaCl – HCO_3 system

During the modelling of Zn adsorption in 8 mmol L^{-1} carbonate in NaCl concentrations on the Bay and Tiaong soils, model parameters in MSMs are fixed at values used for the model fits in the absence of carbonate. Results of the predicted Zn adsorption on the Bay and Tiaong soil by MSMs in two different initial concentrations of Zn (0.08 mmol L^{-1} and 0.8 mmol L^{-1}) and in 0.1, 0.3 and 0.7 mol L^{-1} NaCl concentration after adding 8 mmol L^{-1} carbonate are shown in Figure 5.4, 5.5, 5.6 and 5.7, respectively. The overall RMSEs are within the range of 0.033% to 0.12% (0.033%, 0.12%, and 0.12%) and 0.12% to 0.46% (0.12%, 0.46%, and 0.20%) in 0.1, 0.3 and 0.7 mol L^{-1} NaCl concentration for the adsorption experiment of Zn on Bay and Tiaong soil at initial concentration of 0.08 mmol L^{-1}. For the adsorption experiment of Zn on the Bay and Tiaong soil at the initial concentration of 0.8 mmol L^{-1}, the overall RMSEs are within the range of 0.07% to 0.32% (0.07%, 0.22%, and 0.32%) and 0.16% to 0.34% (0.16%, 0.21%, and 0.34%) in 0.1, 0.3 and 0.7 mol L^{-1} NaCl concentration.

The overall RMSE results are less than 0.5%, which indicate that the model fits for Zn adsorption in the presence of carbonate at Zn initial concentration of 0.08 and 0.8 mmol L^{-1} and in both soils (Bay and Tiaong) are good in NaCl concentrations (0.1, 0.3, and 0.3 mol L^{-1}) (Groenenberg and Lofts, 2014). However, the specific pH-dependent model fits are variable within the pH range. The MSMs fails to accurately reproduce the percent adsorption in acidic pH in all NaCl concentration, especially in Tiaong soil at Zn initial concentration of 0.8 mmol L^{-1}. The model results for adsorption at Zn initial concentration of 0.08 mmol L^{-1} and 0.8 mmol L^{-1} in both soils, and all NaCl concentrations are generally good at pH higher than 6 (Fig. 5.4, 5.5, 5.6, and 5.7).

5.2.4 Contribution of soil components on Zn adsorption based on model

Model speciation predictions at Zn initial concentration of 0.08 mmol L^{-1} show that SOM is the dominant sorbent for Zn at acidic pH. At neutral and alkaline pH, SOM and amorphous iron (hydr)oxide are the dominant sorbents for Zn (Fig. 5.8A). My results are consistent with those previously reported for Zn in low and high-Zn soil (Duffner et al., 2014), Zn in sandy soil (Weng et al., 2001), Zn in natural sediment (Fisher-Power et al., 2016) and Zn in contaminated soils (Ren et al., 2017). The contribution of clay to Zn binding is very small in the adsorption process. The presence of Na in the background electrolyte of NaCl and the Ca, Mg, K from the extractable soil solution reduce Zn adsorption by occupying clays permanently negative charged sites. Metal adsorption to clay minerals is more important at low pH, low organic matter content, and low concentration of cations (Na, Ca) (Weng et al., 2001). Model predictions of decreasing Zn binding by SOM with increasing NaCl concentrations suggest that the ternary surface complexes are not formed in the Zn-Cl-SOM system (Lumsdon et al., 1995). Additionally, the Na ion might reduce Zn binding by SOM by competing with free Zn ion for the sorption sites of SOM (Du Laing et al., 2009). Adsorption of Zn by iron (hydr)oxide increases with increasing pH and NaCl concentrations as the negative surface charge of iron (hydr)oxide increases (Chesne and Kim, 2014; Gao and Mucci, 2001). Model speciation predictions show that the effect of increasing NaCl concentration on the adsorption of Zn and Zn aqueous species is generally noticeable at pH 3 – 7. The effects are unnoticeable at pH> 8 because Zn is entirely bound by SOM and iron (hydr)oxide.

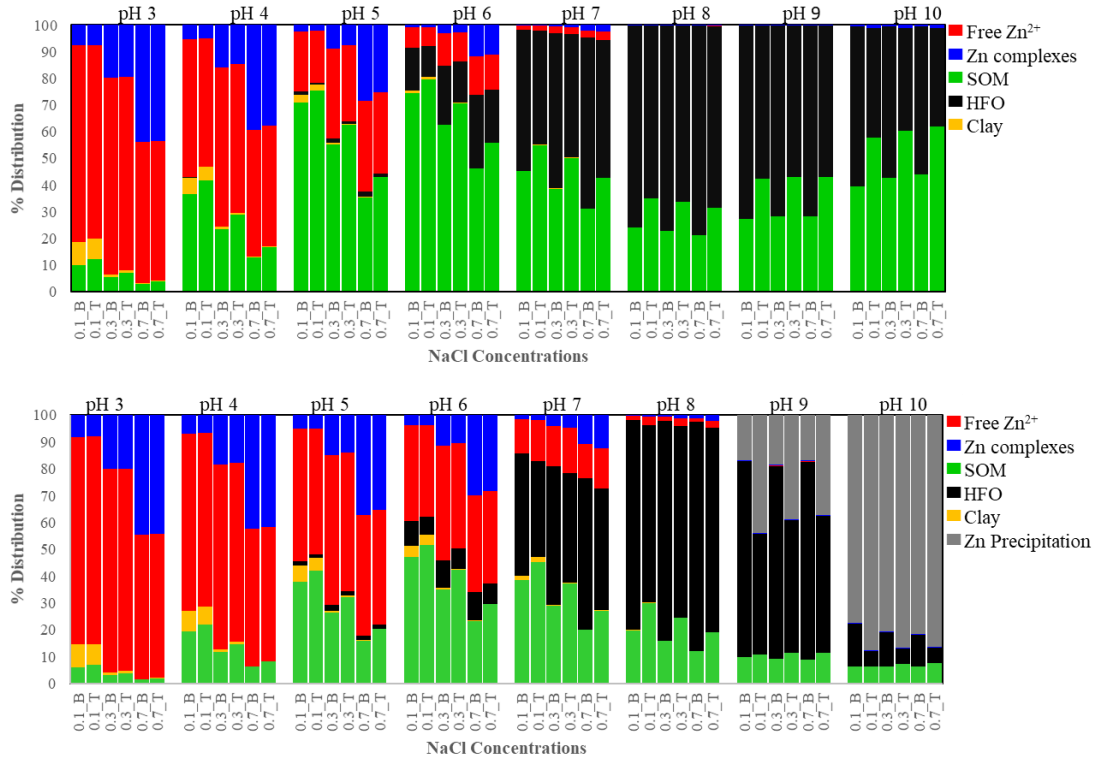


Figure 5.8 Contribution of soil components (clay, hydrous ferric oxides (HFO) and SOM) to Zn adsorption in the studied soils in different NaCl concentrations, as predicted by the MSMs: A) $[Zn]_{initial}$ = 0.08 mmol L^{-1}; B) $[Zn]_{initial}$ = 0.8 mmol L^{-1}. The model prediction of Zn adsorption data in Bay soil in 0.1, 0.3, and 0.7 mol L^{-1} NaCl solutions is represented by 0.1_B, 0.3_B, and 0.7_B, respectively whereas Zn adsorption in Tiaong soil is represented by 0.1_T, 0.3_T, 0.7_T, respectively. The calculations are performed with the inclusion of the major background cations. Zn complexes in in the distribution bar graph represented Zn-Cl complexes, $Zn(OH)_2$ and $ZnCO_3$, respectively.

The model calculations at Zn initial concentration of 0.8 mmol L^{-1} indicate that the relative contribution of SOM and iron (hydr)oxides to adsorb Zn are lower compared to Zn initial concentration of 0.08 mmol L^{-1} (Fig. 5.8B). These results are in line with batch adsorption results where we observe a shift of adsorption towards higher pH values due to the high adsorbate/adsorbent ratio. Zn precipitations play a major role in controlling Zn mobility at higher Zn concentrations in both soils at pH > 8. Our model analysis shows that the saturation index of Zn minerals i.e. ZnO, $Zn(OH)_2$ and $Zn_5(OH)_8Cl_2$(s) are positive from pH 8.5 in Tiaong soil and from pH 9 in Bay soil (Table 5.3). Reports suggest that Zn precipitates at pH values above 7 and at high concentrations (> 10 mg L^{-1}), where it exceeds the maximum adsorption capacity of the soil. Zn precipitates also occur where the solubility product of Zn is surpassed in the soil solution (Brummer et al., 1983; Lindsay, 1979). In contrast, Brummer et al. (1983) reported that soil surfaces with sufficient adsorption capacity at pH values above 7 lower the equilibrium concentration of Zn species and reduce Zn precipitation. Their observation is

supported by model analysis, where no Zn precipitation is predicted at the initial concentration of 0.08 mmol L^{-1} (Fig. 5.8A). The model predicts that Zn precipitation is higher in Tiaong soil than in Bay soil. These differences are due to the concentration of amorphous iron (hydr)oxides present in both soils. Iron (hydr)oxides are the main adsorbent component in soils with alkaline pH. As the concentration of amorphous iron (hydr)oxides are lower in Tiaong soil, the adsorption sites for Zn are smaller in Tiaong soil than in Bay soil.

Table 5.3 Saturation index values of various Zn mineral phases in Bay and Tiaong soil at $[Zn]_{initial}$ = 0.8 mM by model analysis.

Minerals	Saturation index							
	pH 8.5		pH 9.0		pH 9.5		pH 10	
	Bay	Tiaong	Bay	Tiaong	Bay	Tiaong	Bay	Tiaong
Zincite	-0.21	0.35	0.29	0.95	0.91	1.51	1.54	1.97
$Zn(OH)_2$ (am)	-1.45	-0.90	-0.95	-0.3	-0.34	0.27	0.30	0.72
$Zn(OH)_2$ (beta)	-0.73	-0.18	-0.23	0.42	0.38	0.99	1.02	1.44
$Zn(OH)_2$ (delta)	-0.82	-0.27	-0.32	0.33	0.29	0.90	0.93	1.35
$Zn(OH)_2$ (epsilon)	-0.51	0.05	-0.01	0.64	0.60	1.21	1.24	1.66
$Zn(OH)_2$ (gamma)	-0.71	-0.16	-0.21	0.44	0.40	1.01	1.04	1.46
$Zn_5(OH)_8Cl_2$(s)	-2.62	0.16	-1.13	2.14	0.94	3.97	3.11	5.25

The model prediction shows that the presence of HCO_3 in NaCl solutions at Zn initial concentration of 0.08 mmol L^{-1} increases Zn aqueous complexes at pH 4 - 6 as free Zn^{2+} makes complexes with HCO_3. The relative distribution of Zn adsorption by SOM, clay and iron (hydr)oxides at pH 4 – 5 and pH 8 – 10 are similar to the distribution in NaCl solutions. At pH 6 – 7, the adsorption of Zn by iron (hydr)oxides is decreased than the distribution in NaCl solutions (Fig. 5.9). This decrease is due to the competitive effect of HCO_3 and Zn for the adsorption sites on iron (hydr)oxides because the maximum adsorption of HCO_3 on iron (hydr)oxides occurs at pH 6 – 7 (Villalobos and Leckie, 2000). At $[Zn]_{init}$ = 0.8 mmol L^{-1}, the model predict Zn precipitation is started in both soils from pH 6 (Fig. 5.10, Table 5.4). The model prediction is also supported by experimental results where the increased adsorption of Zn in both soils is observed at pH 6 – 7.5 after adding 8 mmol L^{-1} carbonate (Fig. 5.5 and 5.7).

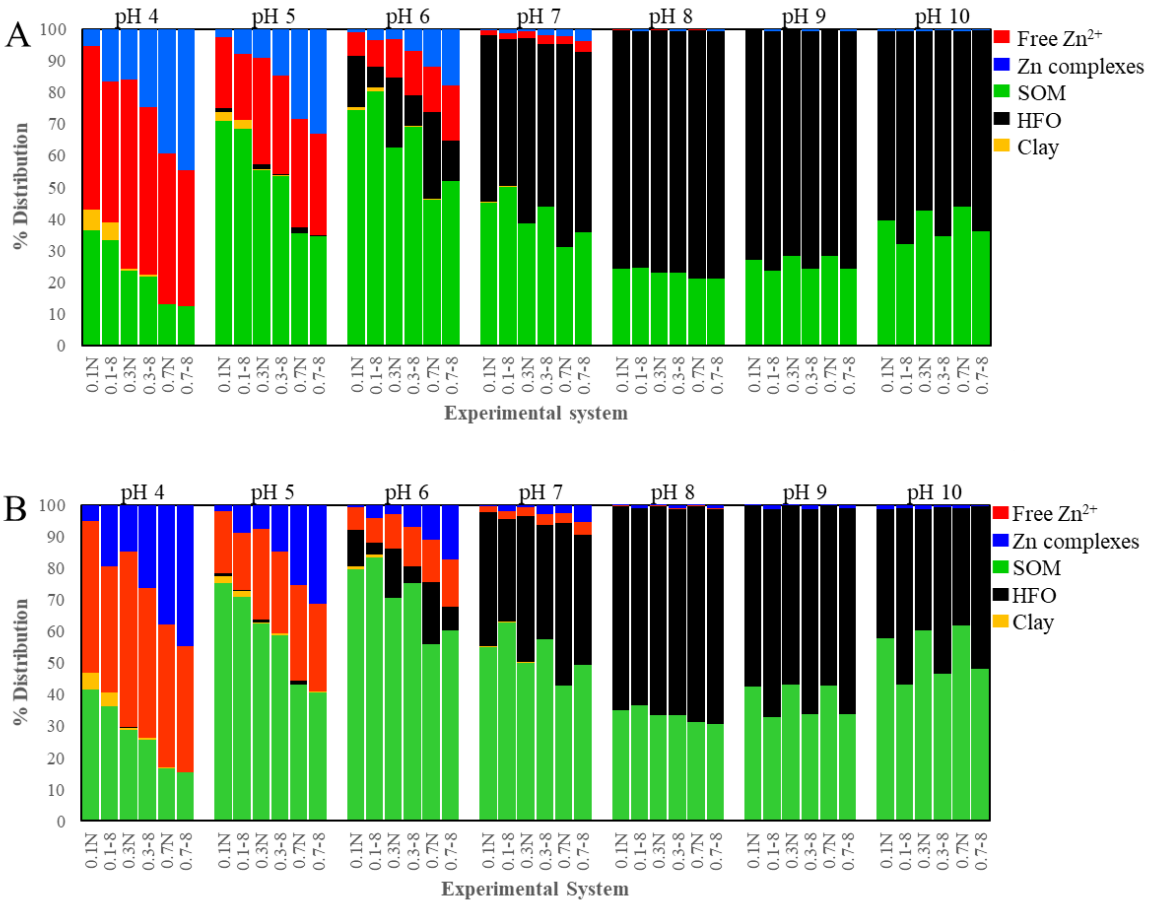


Figure 5.9 Contribution of soil components (clay, hydrous ferric oxides (HFO) and SOM) to Zn adsorption in the studied soils in different NaCl concentration at $[Zn]_{initial}$ = 0.08 mmol L^{-1} in the presence of 8 mmol L^{-1} HCO_3, as predicted by the MSMs: A) Bay soil; B) Tiaong soil. For comparison, the model calculation datas of Zn adsorption in different NaCl concentrations in the absence of HCO_3 are reproduced and represented by 0.1N, 0.3N and 0.7N. The model calculations of Zn adsorption in the presence of HCO_3 in 0.1, 0.3, and 0.7 mol L^{-1} NaCl concentrations are represenetd by 0.1-8, 0.3-8, and 0.7-8, respectively. The calculations are performed with the inclusion of the major background cations. Zn complexes in in the distribution bar graph represented Zn-Cl complexes, $Zn(OH)_2$ and $ZnCO_3$, respectively.

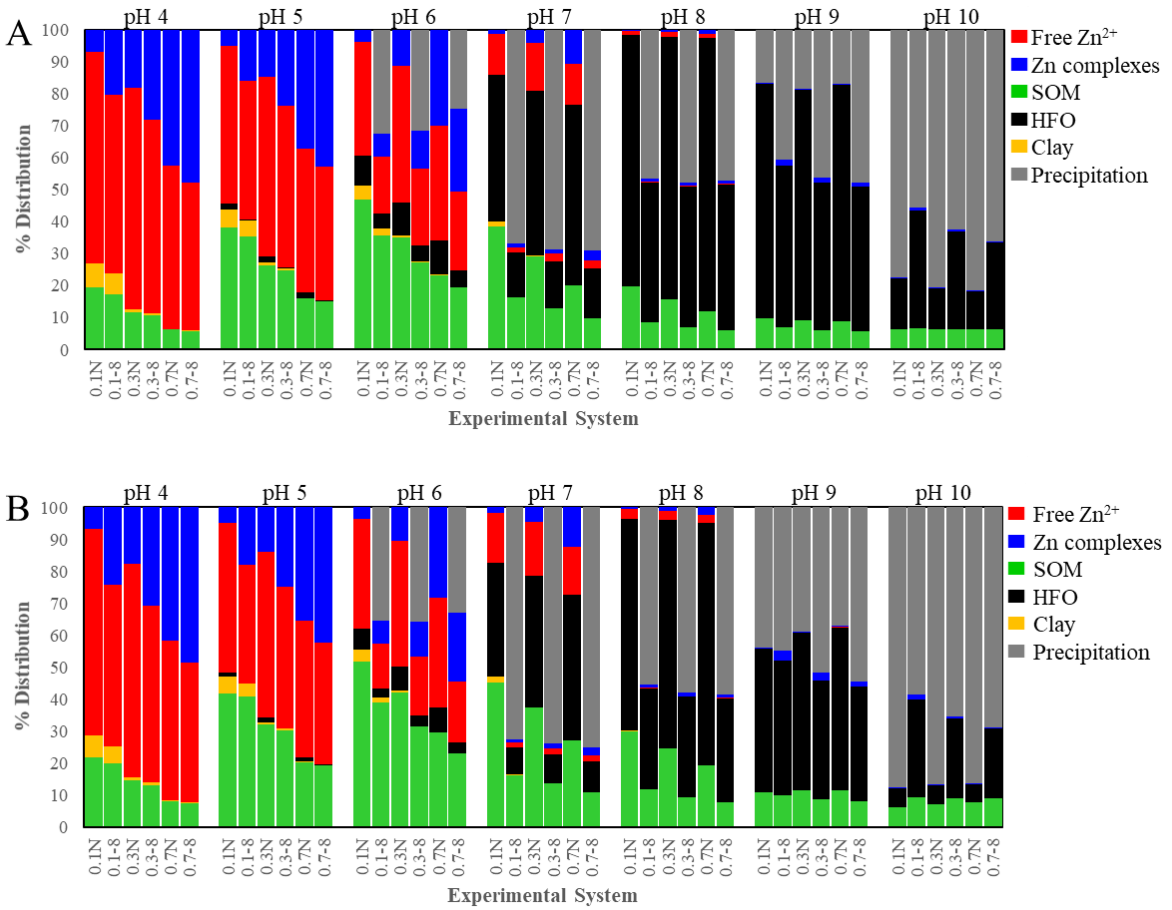


Figure 5.10 Contribution of soil components (clay, hydrous ferric oxides (HFO) and SOM) to Zn adsorption in the studied soils in different NaCl concentration at $[Zn]_{initial}$ = 0.8 mmol L^{-1} in the presence of 8 mmol L^{-1} HCO_3, as predicted by the MSMs: A) Bay soil; B) Tiaong soil. For comparison, the model calculation datas of Zn adsorption at $[Zn]_{initial}$ = 0.8 mmol L^{-1} in different NaCl concentrations in the absence of HCO_3 are reproduced and represented by 0.1N, 0.3N and 0.7N. The model calculations of Zn adsorption in the presence of HCO_3 in 0.1, 0.3, and 0.7 mol L^{-1} NaCl concentrations are represenetd by 0.1-8, 0.3-8, and 0.7-8, respectively. The calculations are performed with the inclusion of the major background cations. Zn complexes in in the distribution bar graph represented Zn-Cl complexes, $Zn(OH)_2$ and $ZnCO_3$, respectively.

Table 5.4 Saturation index values of various Zn mineral phases in Bay and Tiaong soil at $[Zn]_{initial}$ = 0.8 mM in the presence of 8 mmol L^{-1} HCO_3 by model analysis.

	Saturation index									
Minerals	pH 6		pH 7		pH 8		pH 9		pH 10	
	Bay	Tiaong	Bay	Tiaong	Bay	Tiaong	Bay	Tiaong	Bay	Tiaong
Smithsonite	0.21	0.36	0.81	1.05	0.63	1.10	0.44	0.79	0.16	0.45
ZnCO3(s)	0.11	0.26	0.71	0.95	0.53	0.99	0.34	0.69	0.06	0.35
ZnCO3:1H2O(s)	-0.43	--	0.16	0.41	-0.01	0.46	-0.20	0.15	-0.48	-0.19
Hydrozincite	--	--	--	0.50	1.79	3.74	4.14	5.59	7.25	8.47
Zincite	--	--	--	--	--	--	0.02	0.28	1.25	1.46
Zn(OH)2 (am)	--	--	--	--	--	--	--	--	0.001	0.22
Zn(OH)2 (beta)	--	--	--	--	--	--	--	--	0.72	0.94
Zn(OH)2 (delta)	--	--	--	--	--	--	--	--	0.63	0.85
Zn(OH)2 (epsilon)	--	--	--	--	--	--	--	--	0.94	1.16
Zn(OH)2 (gamma)	--	--	--	--	--	--	--	--	0.74	0.96
Zn5(OH)8Cl2(s)	--	--	--	--	--	--	--	--	1.64	2.71

5.3 Discussion

5.3.1 How does NaCl salinity affect Zn adsorption in soils?

Generally, the adsorption of Zn on soil is regulated by SOM, iron (hydr)oxides and clay. The decreasing Zn adsorption with increasing NaCl concentrations from pH 3 - 7 is likely explained by the complexation capacity of Zn with Cl ions and the competitive effect of Na for adsorption sites. Zn is adsorbed mainly by SOM at acidic to neutral pH (3 – 7). Soil clay minerals also have the capacity to adsorb Zn at this pH range, however, the role of clay minerals to adsorb Zn is lower compared with SOM (Duffner et al., 2014; Weng et al., 2001). The presence of chloride and its increasing concentration leads to an increase of Zn-Cl aqueous complexes and a decrease in free Zn^{2+} activity in soil solution (Fig. 4.2). For SOM surfaces, which do not form a ternary surface complex of Zn, the presence of Zn-Cl complexes does not adsorb by SOM. Therefore, Zn absorption should always decrease with increasing NaCl concentrations (Lumsdon et al., 1995). For clay minerals, the adsorption of Zn as a ternary surface complex is mostly reported with the presence of organic ligands (Stietiya and Hashem, 2010) and Zn adsorption on the clay minerals as a ternary surface complex of Zn-Cl is not reported in the literature. Therefore, the predominance of Zn-Cl complexes in NaCl solutions can explain the desorption behaviour of Zn on the Bay and Tiaong soil with increasing NaCl concentrations. However, the unnoticeable effect of increasing NaCl concentration from 0.3 mmol L^{-1} to 0.7 mmol L^{-1} on the adsorption of Zn on both soils at Zn initial concentration of 0.08 mmol L^{-1} can explain by the lower stability of Zn-chloride complexes. The low stability of metal-Cl complexes was reported by Du Laing et al. (2008) who concluded that Cu mobility did not significantly affect by increasing NaCl concentrations due to the lower stability of metal-Cl complexes.

Besides chloro-complexation, the presence of Na ion in soil solution can replace Zn from the sorption sites of clay by a competitive effect and decrease Zn adsorption on the soil. However, the competitive effect of Na ion with Zn for clay surfaces could be lower due to the less competitive nature of Na with Zn for sorption sites (Jalali and Zinli, 2012; Wang and Harrell, 2005). Na ion forms only outer-sphere complexes with clay minerals (Jalali and Zinli, 2012). Therefore, it lies at a greater distance from the surface and could replace Zn from the sorption sites to a lesser extent, even when the salinity increased 50 times (Acosta et al., 2011). The competition of Na ion with Zn at SOM surfaces was not accounted for in the explanations due to the lack of adsorption data for Na ion on organic matter. Zhang et al. (2018a) reported that metal adsorption results on soils with the background solution of $NaNO_3$ were similar to those

of distilled water only. This indicates that the presence of Na ion did not significantly influence metal adsorption on soils. Therefore, the lack of adsorption constants for Na ion with SOM seems not a big problem for model prediction or describing metal adsorption on soils. Considering the complexation nature of Na with soil sorbents, we can conclude that the complexation of Zn with Cl ions is the main mechanism to decrease Zn adsorption on soils with increasing NaCl solutions.

The inhibitory effect of Cl ion on Zn adsorption has been previously reported for temperate soils in the USA and sub-tropical soils in Iran (Jalali and Zinli, 2012; Wang and Harrell, 2005) with a background concentration of 50 and 10 mmol L^{-1}, respectively. Opposite results are also reported for sub-tropical soils in Spain by Acosta et al. (2011) with the conclusion that Zn was not easily complex by Cl ion due to its lower affinity to Cl even at 300 mmol L^{-1} NaCl background concentration. Clearly, contradicting evidence exists in the literature and we found that the reason behind this contradiction will be due to the differences in soil pH in the studied soils. The soils of Acosta's studies were alkaline (pH > 7.5) in nature whereas the soils of Wang's studies had acidic and alkaline pH (Acosta et al., 2011; Wang and Harrell, 2005). Wang and Harrell (2005) reported that the effect of Cl ion on the lability of adsorbed Zn was higher in acidic pH soils and less in alkaline pH soils. Therefore, the non-significant effect of increasing NaCl concentrations on Zn adsorption in Acosta studies was mainly due to the high pH of studied soils (Acosta et al., 2011). During the batch adsorption experiments, the unnoticeable effect of increasing NaCl concentrations on the adsorption of Zn is observed at pH > 7 in both soils and both initial concentrations of Zn (Fig. 5.3). The findings of Zn adsorption on alkaline soils (pH > 7.5) in Acosta et al. (2011) and Wang and Harrell (2005) studies are similar to our pH dependent adsorption results. Therefore, we can conclude that soil pH is the most important factor to determine the effect of increasing NaCl concentrations on Zn adsorption in soils. Alongside soil pH, the difference in SOM concentration between the soils may another factor that affected Zn adsorption in different NaCl concentrations. The inhibitory effect of Cl ion on Zn adsorption is higher on soils with low pH and high SOM than on soils with low pH and low SOM (Wang and Harrell, 2005).

5.3.2 Effect of carbonate on Zn adsorption in NaCl solutions

The presence of carbonate in solutions influences metal binding by two main mechanisms. The first one relates carbonate competitiveness with other anions for surface sites, whereas the second one relates to the formation of aqueous metal-carbonate complexes and their competitiveness for binding on surface sites (Villalobos et al., 2001). The addition of 8 mmol

L^{-1} carbonate during the adsorption experiment at the initial concentration of Zn of 0.08 mmol L^{-1} and 0.8 mmol L^{-1}, respectively in 0.1, 0.3 and 0.7 mol L^{-1} NaCl concentration, correspond to a condition where the presence of carbonate produces Zn-carbonate complexes. Zn Adsorption at the initial concentration of 0.08 mmol L^{-1} is not affected after the addition of 8 mmol L^{-1} carbonate for the Bay soil in 0.1 (Fig. 5.4a) and 0.3 mol L^{-1} (Fig. 5.4b) NaCl concentration and on the Tiaong soil in 0.1 mol L^{-1} NaCl concentration (Fig. 5.5a) due to high affinity of free Zn for the surface sites than Zn-carbonate complexes. These results agreed well with the Pb adsorption experiment on goethite with the presence of CO_2 where total Pb adsorption did not affect after equilibration with up to 1% $CO_{2(g)}$ (Villalobos et al., 2001).

The decrease of Zn adsorption at $[Zn]_{initial}$ = 0.08 mmol L^{-1} on the Tiaong soil in 0.3 (Fig. 5.5b) and in 0.7 mol L^{-1} NaCl concentration (Fig. 5.5c) and on the Bay soil in 0.7 mol L^{-1} NaCl concentration (Fig. 5.4c) upon addition of 8 mmol L^{-1} carbonate is in line with ions abundances and surface affinity ratios. The ratio is higher in 0.7 mol L^{-1} NaCl concentration and in Tiaong soils than in Bay soil in 0.3 mol L^{-1} NaCl concentration (the total concentration of dissolved carbonate was 10.5 mmol L^{-1} in Tiaong soil compared with 8 mmol L^{-1} carbonate in Bay soil). Therefore, the outcompeting effects of carbonate, Cl and Na on Zn for complexation and surface sites are higher in 0.3 and 0.7 mol L^{-1} NaCl concentration than in 0.1 mol L^{-1} NaCl concentration. Carbonate adsorbs on the surface of iron (hydr)oxides from pH 3.5 to 8 (Villalobos and Leckie, 2000), and the presence of a high concentration of carbonate can reduce Zn adsorption on the surface of iron (hydr)oxides. This observation is well agreed by Laflamme and Murray (1987) who reported that thorium adsorption on goethite was decreased as a function of carbonate alkalinity. Besides the carbonated effect, a combined effect of Cl, Na and carbonate was also plausible for reducing Zn adsorption on the Bay and Tiaong soil in 0.7 mol L^{-1} NaCl concentration. Adsorption of Na by clay and iron (hydr)oxides (Nanzyo and Watanabe, 1982; Schulthess and Ndu, 2017) and Cl by iron (hydr)oxides (Schulthess and Ndu, 2017) are also reported in the literature and can decrease Zn adsorption. In addition, the presence of Cl ion increase carbonate adsorption and decrease Zn adsorption by anion-anion enhancement interactions (Schulthess and Ndu, 2017). Wijnja and Schulthess (2002) reported that the presence of CO_3 enhanced SeO_4 adsorption on goethite even at higher concentrations of CO_3. They proposed that the proton on the surface sites was stabilized initially by the co-adsorption of H ions with CO_3. With the presence of a competing anion (SeO_4) which also involved the co-adsorption of H ions, the adsorption of SeO_4 will be increased as the goethite surface is previously pre-protonated (Schulthess and Ndu, 2017). Enhanced adsorption was

also observed with CO_3 on SO_4; CH_3COO on SeO_4, CH_3COO on SO_4 (Wijnja and Schulthess, 2002) and Cl on phthalate (Schulthess and Ndu, 2017). Therefore, we propose that a high concentration of Cl ion during the batch adsorption experiment in 0.3 and 0.7 mol L^{-1} NaCl solution could be enhanced carbonate adsorption and decrease Zn adsorption.

At the initial concentration of Zn of 0.8 mmol L^{-1}, more Zn is available for complexation with carbonate upon the addition of 8 mmol L^{-1} carbonate and increased Zn adsorption on the Bay soil in 0.7 mol L^{-1} NaCl solution (Fig. 5.6c) and the Tiaong soil in 0.3 and 0.7 mol L^{-1} NaCl concentration (Fig. 5.7b and 5.7c) at acidic pH (3-5). The increased Zn adsorption at acidic pH indicated that Zn could adsorb as aqueous carbonate complexes ($ZnHCO_3^+$) on the soil surfaces. Adsorption of Zn oxyhydroxo complexes is reported for clay surfaces (Bradl, 2004) and of Pb-carbonate complexes on goethite (Villalobos et al., 2001). At pH 6 – 7.5, the increased adsorption of Zn in both soils and all NaCl concentrations indicated that Zn could be precipitated from pH 6. Metals precipitation in soils at acidic pH is reported by McLean and Bledsoe (1992), Zhang et al. (2018b). With the presence of a high concentration of Zn and carbonate in soil solutions during the batch adsorption experiment, I propose that the solubility product of Zn minerals is exceeded at pH 6. My observation was supported by the model analysis (Fig. 5.10) and by several authors (Alloway, 1990; Bradl, 2004; Lindsay, 1979).

5.3.3 Model performance and the reasons for model underestimation

The model underestimation in 0.3 mol L^{-1} and 0.7 mol L^{-1} NaCl concentration at pH below 6 may be the uncertainty of the MSMs application, especially the NICA-Donnan model application in high NaCl concentration. Alternatively, the poor efficiency of the NICA-Donnan model to describe Zn adsorption by solid-phase organic matter in high NaCl concentration is likely due to the poor effectiveness of the model to account for the ionic strength dependence of proton dissociation. Soil organic matter is the dominant phase to adsorb Zn at low pH. The model parameters in the NICA-Donnan model are calibrated and adjusted at a low ionic concentration (Duffner et al., 2014), therefore, there is an uncertainty to use the NICA-Donnan model at a high ionic concentration. Although the NICA-Donnan model satisfactorily describes the proton dissociation of dead biomass from seaweeds (Rey-Castro et al., 2003) and Cu complexation with marine dissolved organic matter (Avendano et al., 2016), the application of the NICA-Donnan model as a part of MSMs to describe Zn adsorption by solid-phase soil organic matter in high ionic concentration (> 0.01 mol L^{-1}) is the absence in the literature. A MSMs approach of Zn adsorption on soils by solid-phase soil organic matter in low ionic concentration (0.01 mol L^{-1} $NaNO_3$) is reported by Fisher-Power et al (2016) and Mizutani et

al. (2017). The model underestimated Zn adsorption at acidic pH is also reported in their studies. The lower estimation of the fraction of the active organic carbon at low pH could be another factor. The fraction of active SOM varies between 31% to 87% in the literature (Groenenberg and Lofts, 2014). Although a fraction of 46% active SOM is used in all our model simulations, a higher fraction of active SOM may involve in adsorbing Zn at low pH.

Another reason for the model discrepancy in both soils at low pH could be the absence of ternary surface complexes of Zn (≡FeOH-Zn-Cl) in the predefined databases. Zn adsorption as ternary surface complexes on the surface of iron (hydr)oxides at low pH in 0.6 mol L^{-1} NaCl solution is confirmed by spectroscopic analysis (Chesne and Kim, 2014). Therefore, the incorporation of ternary surface complexes in the MSMs databases might improve model performance at low pH in high NaCl concentration.

Furthermore, the models underestimated Zn adsorption in Tiaong soil could be due to the absence of calcite ($CaCO_3$) surfaces in our model analysis. The presence of calcite is an important characteristic of both soils. Tiaong soil has a relatively higher concentration (9.59 %) of calcite than Bay soil (0.16 %). The importance of calcite surface to Zn adsorption has been highlighted before (Mesquita and Silva, 1996). However, in my case, we do not include calcite surface in the model analysis because the contribution of calcite surface for Zn adsorption is small due to the small specific surface area of calcite (Duffner et al., 2014; Trehan and Sekhon, 1977). Dong et al. (2001) also reported that calcite has an influence on Zn adsorption when the soil pH is > 8 and calcite contents of > 10%. The investigated soils in our experiment are not in the above category as the calcite contents of < 10%.

A Smaller RMSE value indicates a better prediction. Groenenberg and Lofts (2014) reported that the RMSE value of < 0.5% indicates a good model performance. The RMSE values of Zn adsorption in 0.1 mol L^{-1} NaCl concentration in both soils and both initial concentrations of Zn (0.08 mmol L^{-1} and 0.8 mmol L^{-1}) agreed well with previous (Fisher-Power et al., 2016). The overall RMSE between the modelled and measured values of Zn adsorption in 0.3 mol L^{-1} and 0.7 mol L^{-1} NaCl concentration in both soils is lower than 0.5%. My results reported that the Zn adsorption predicted by the MSMs agreed well with observed Zn adsorption over a wide range of NaCl concentrations (0.1 mol L^{-1} to 0.7 mol L^{-1}) without any parameter adjustment. These results indicate that the MSMs can be applied to gain a quantitative understanding of Zn speciation in highly saline soils.

One more reason for the poor fit in the NaCl-HCO_3 system is the absence of ternary surface complexation constants of Zn (≡FeO-Zn-chloride and ≡FeO-Zn-carbonate) and surface complexations constants of anion-anion (Cl – HCO_3) enhancement interactions in the chosen databases of MSMs. At high initial concentration, Zn and metal adsorption on goethite and sediments in acidic pH as a ternary surface complexes (Zn-chloro adsorption complexes and Zn-carbonate adsorption complexes) are supported by EXAFS analysis (Bargar et al., 1998; Chesne and Kim, 2014; Grafe and Sparks, 2005; Webb and Gaillard, 2015). However, I did not include those surface complexation constants in the model due to their unavailability in the literature. As the literature data indicate that metal-chloride, metal-carbonate complexes and anion-anion enhancement interactions are present on the surfaces of minerals during the adsorption, a more complex parameterization may require to accurately describe Zn adsorption in complex environmental conditions.

5.4 Conclusions

This chapter aimed to test the validity of MSMs derived by modelling Zn adsorption in two tropical soils at $[Zn_{init}]$ = 0.08 mmol L^{-1} for predicting Zn adsorption at higher initial concentrations in different NaCl solutions and carbonate-rich NaCl solutions. We find that,

1. Zinc adsorption experiments on both soils in different NaCl concentrations (0.1 mol L^{-1}, 0.3 mol L^{-1} and 0.7 mol L^{-1}) indicate that increasing NaCl concentration decrease Zn adsorption between pH 3 and 6 in both initial concentrations at pH 3 - 7. However, increasing NaCl concentration from 0.3 mol L^{-1} to 0.7 mol L^{-1} at $[Zn]_{init}$ = 0.08 mmol L^{-1} does not lead to a decrease in Zn adsorption. Zinc is fully adsorbed at pH > 7.
2. Compare with Zn adsorption in NaCl concentrations (0.1, 0.3 and 0.7 mol L^{-1}, respectively) in the absence of carbonate, the presence of carbonate in 0.1 and 0.3 mol L^{-1} NaCl solutions do not change Zn adsorption on both soils at $[Zn]_{init}$ = 0.08 mmol L^{-1} but a slight decreased (3 - 4%) is observed at pH > 6 in 0.7 mol L^{-1} NaCl solution. At $[Zn]_{init}$ = 0.8 mmol L^{-1}, the adsorption of Zn in NaCl solutions at pH 6 – 7.5 is increased (30 – 35 %) in the presence of HCO_3. A slight increase (2 – 4%) is also observed at acidic pHs (3 – 5) in 0.7 mol L^{-1} NaCl solution.
3. Multi-surface model parameters derived by modelling Zn adsorption at $[Zn_{init}]$ = 0.08 mmol L^{-1} in two tropical soils are found to be useful to predict Zn adsorption in higher initial concentration and carbonate-rich NaCl solutions. This prediction indicates that MSMs with calculated parameters can be applied to predict Zn adsorption in different experimental systems. The model prediction is good at 0.1 and 0.3 mol L^{-1} NaCl

concentration and acceptable at 0.7 mol L^{-1} NaCl concentration. Model uncertainties at low pH (3 – 5) in 0.7 mol L^{-1} NaCl solution and different initial concentrations indicate the need for the improvement of present databases with ternary surface complexes.

4. Iron hydroxides are important sorbents for Zn in alkaline pH soil, whereas SOM is an important sorbent in near neutral and acidic pH. Clay is not an important sorbent for Zn in soils as the cations (Ca, Mg, K and Na) in soils solution competed with Zn and occupied most of the clay surface. At $[Zn_{init}]$ = 0.8 mmol L^{-1}, the relative contribution of SOM and iron hydroxides to adsorb Zn are lower compared to Zn initial concentration of 0.08 mmol L^{-1} due to the high adsorbate/adsorbent ratio. Zinc precipitations play a major role in controlling Zn mobility at higher Zn concentrations in both soils at pH > 8 in the absence of carbonate. In the presence of carbonate, Zinc precipitations play a major role at pH > 6.

Chapter 6: Interface processes of Zn and goethite in saline solutions: parameterisation of accurate surface complexation model

6.1 Introduction:

The surface complexation models analysis in chapters 4 and 5 highlighted that the predefined model databases are unable to predict Zn adsorption accurately in a higher concentration of NaCl. In a coastal aqueous system where Cl^- ions tend to form strong complexes with Zn, it is expected that Zn can adsorb on the surface of goethite as ternary surface complexes. The adsorption of Zn as a ternary surface complex is mostly reported on the surface of iron (hydr)oxides (Chesne and Kim, 2014). However, despite this attention, the ternary surface complexation constants of Zn with iron (hydr)oxides are limited in the literature. Therefore, in this chapter, I attempted to determine ternary surface complexation reactions of Zn and their constants in NaCl solutions by surface complexation models.

Soils are the primary source of Zn and the determination of the Zn as a nutrient or contaminant metal is largely dependent upon the total concentration of Zn in soil solution and its adsorption and desorption behaviour with soil mineral surfaces (Acosta et al., 2011; Ponthieu et al., 2006). Concerning the Zn adsorption capacity, goethite, one of the most reactive iron (hydr)oxides minerals in soils, is extensively researched due to its large surface area and surface-active sites (Liu et al., 2014). Goethite (α-FeOOH) is a very common mineral in soils and sediment and thermodynamically one of the most stable iron oxide minerals (Cornell and Schwertmann, 2003). Adsorption of Zn on goethite is governed by the initial concentration of Zn and the chemical composition of the aqueous solution, including pH, salt content (ionic strength) and inorganic and organic ions present in soil solution. pH is the most important variable that influences Zn adsorption onto goethite. Zn adsorption onto goethite is lower at acidic pH and higher at neutral to high pH (Chesne and Kim, 2014; Ponthieu et al., 2006). Around 85-95% of Zn is adsorbed onto the goethite surface at pH 7 (Chesne and Kim, 2014). Zinc is quantitatively adsorbed or precipitated on the goethite surface at pH > 8. The presence of ions influences the Zn adsorption on goethite as the complexation of anions with Zn and the competition for sorption sites play an important role (Paalman et al., 1994).

Zinc forms aqueous complexes with Cl (Powell et al., 2013). The variable charge of the goethite surface exhibits a strong dependence on the NaCl concentration in solution as the surface charge increases with the increasing concentration of NaCl (Gao and Mucci, 2001). The

investigation of the effect of NaCl concentration on Zn adsorption onto goethite led to contradicting findings. For example, Bolland et al. (1977), Chesne and Kim (2014), Forbes et al. (1976), Gunton (2007) and Padmanabham (1983) reported increased Zn adsorption onto goethite with increasing NaCl concentration from 0.1 to 1 mol L^{-1} at pH below 8. Spectroscopic analysis using EXAFS indicated that the adsorption of Zn as Zn-Cl complexes on goethite surfaces is the reason for increasing adsorption with increasing NaCl concentrations (Chesne and Kim, 2014). In contrast, Balistrieri and Murray (1982) found no significantly increased adsorption of Zn at higher NaCl concentrations. The conflicting results in the previous experiments are possibly due to different initial Zn concentrations and goethite concentrations during the experimental processes. In the Chesne and Kim (2014) study, the initial Zn concentration was higher (Zn = 0.5 mmol L^{-1} vs Zn = 0.003 mmol L^{-1}) and the goethite concentration was lower (0.17 vs 0.55 g L^{-1}) than Balistrieri and Murray (1982) study. The adsorption of Zn onto goethite is expected to be controlled by different solid-liquid ratios, initial Zn concentration, and various concentrations of NaCl. However, despite this observation, the effect of increasing Cl concentration on pH dependent Zn adsorption onto goethite at various initial concentrations of Zn is not well reported in the literature. For describing Zn mobility in the coastal aqueous system, the role of NaCl on Zn adsorption needs to be understood and a model describing Zn adsorption onto goethite in NaCl solutions is greatly needed.

At the solid-solution interaction, surface complexation models have described the adsorption phenomena of metals and anions onto goethite (Gao and Mucci, 2001). Zinc adsorption on goethite in 0.1 mol L^{-1} NaCl and $NaNO_3$ solutions predict successfully with the constant capacitance model (CCM) (Palmqvist et al., 1997; Palmqvist et al., 1999; Spathariotis and Kallianou, 2007), the triple-layer model (TLM) (Kooner et al., 1995; Xu et al., 2006), and the CD-MUSIC model (Komarek et al., 2018; Ponthieu et al., 2006). However, the application of the CCM and diffuse layer model (DLM) for predicting Zn adsorption on goethite in NaCl solutions with seawater concentration (≈ 0.7 mol L^{-1}) has not been tested with experimental results yet. The CCM and DLM accurately predicted the adsorption of arsenic onto goethite and HFO at 0.7 mol L^{-1} NaCl solution (Gao and Mucci, 2001; Gao and Mucci, 2003; Mercer and Tobiason, 2008) suggest that these models can be used to describe Zn adsorption on goethite in high NaCl concentration (0.7 mol L^{-1}).

Surface complexation models use experimentally determined parameters that allow the prediction of metal adsorption on mineral surfaces under varying environmental conditions

(Gao and Mucci, 2001). However, the models developed from the experimental system with lower metal and low NaCl concentrations do not account for the adsorption phenomenon of as metal-Cl complexes. Therefore, model parameters derived from a single metal sorbate system at low NaCl concentration led to an inaccurate prediction of metal adsorption onto goethite at a high ionic concentration of NaCl (> 0.1 mol L^{-1}) as observed for Cu, Zn, Cd, and Pb. The inclusion of ternary surface complexes improved significantly model fits (Chesne and Kim, 2014; Gao and Mucci, 2001; Gao and Mucci, 2003; Swedlund et al., 2009). In a coastal aqueous system where Cl ions tend to form strong complexes with Zn, it is expected that surface complexation constants derived from Zn adsorption onto goethite in low NaCl concentration cannot predict Zn adsorption accurately in high NaCl concentration. However, to date, to our knowledge, a surface complexation model for Zn adsorption onto goethite in seawater concentration of NaCl aqueous system has not yet been established.

The availability of relevant thermodynamic data is the prerequisite for describing Zn adsorption onto goethite by SCM in different NaCl concentrations. Therefore, this chapter aims to examine the effect of NaCl concentrations on the adsorption of Zn onto goethite and to parameterise the surface complexation model. The specific objectives were:

1. To determine the acid-base properties of goethite ($K_{1\text{-int}}$ and $K_{2\text{-int}}$) in different NaCl concentrations (0.1, 0.3, and 0.7 mol L^{-1}) using electric double layer models.
2. To determine the surface complexation constants for the adsorption reaction of Zn onto goethite in NaCl concentrations (0.1, 0.3, and 0.7 mol L^{-}) using pH adsorption edges.
3. To validate SCM based on surface complexation reactions and constants derived during steps 1 and 2 and improve model accuracy over the NaCl concentrations and pH range by introducing ternary surface complexation reactions.

6.2 Results

6.2.1 Goethite Characterization

The synthesis of goethite was characterized by X-ray diffraction analysis. The peaks at 21.22, 36.68, 33.24 2θ confirmed its mineralogy (Figure 6.1). In addition, the uniform acicular crystals and elemental composition of goethite are confirmed by Transmission Electron Microscopy (TEM) and XRF analysis (Annex C). The specific surface area of goethite was 40 m^2/g as measured by the single point N_2-BET method.

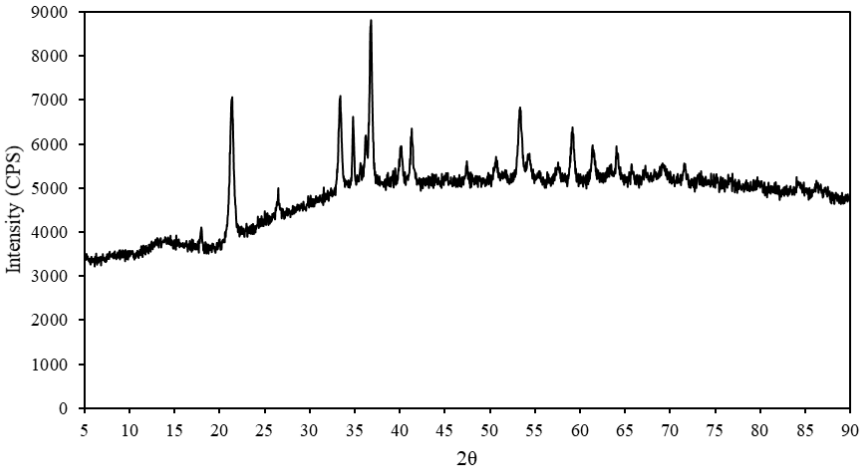


Figure 6.1 X-ray diffraction analysis of synthesis goethite.

6.2.2 Acid-Base Properties of Goethite

6.2.2.1 Potentiometric titration of goethite in 0.1, 0.3 and 0.7 mol L^{-1} NaCl solutions

The potentiometric titration curves of goethite from pH 4 to 9.5 at three NaCl concentrations are presented in Figure 6.2. No hysteresis is observed between the titration of acid and base legs, and the results of base titration are presented here. The titrations are carried out in an inert gas environment (CO_2 free) by continuous purging nitrogen gas into the titration vessel. Therefore, the contribution of protons deriving from atmospheric CO_2 adsorption onto goethite is negligible. The titration curves at three NaCl concentrations display an analogous shape. The number of protons adsorbed on the surface of goethite decreases with increasing pH. At any given pH, the surface charge of goethite increases with increasing NaCl concentration. These observations are similar to the observation reported by Gao and Mucci (2001), Dzombak and Morel (1990), and Balistrieri and Murray (1981). The point of zero charges (pH_{PZC}) is determined from the point where the three titrations intersect, and the surface charge is equal to zero. In this study, the pH_{PZC} is 8.5 which is similar with the result of Gao and Mucci (2001), Hayes et al. (1991), and Plamqvist et al. (1997 and 1999). The values of pH_{PZC} are variable in the literature and reported between 8.5 and 9.5 (Gao and Mucci, 2001; Peacock and Sherman, 2004; Swedlund et al., 2009).

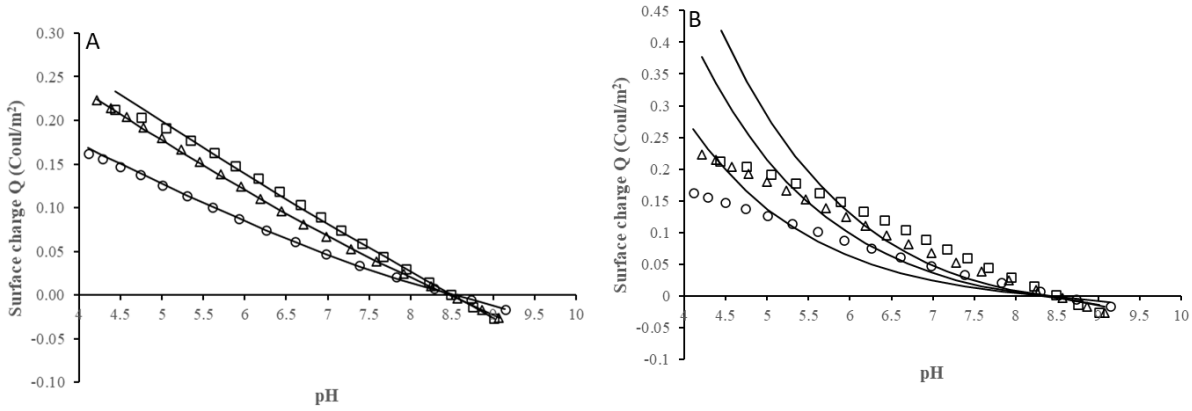


Figure 6.2 Potentiometric titration of goethite (40 ml of 8 g L^{-}) at 0.1 (○), 0.3 (Δ), and 0.7 (□) mol L^{-1} NaCl concentration and 25°C, shown as surface charge (Q) in Coul m^{-2}. Model fits of potentiometric data using the CCM (A) and DLM (B) are presented by solid lines.

6.2.2.2 Acid-base properties of goethite: surface complexation modelling using CCM

The acid-base properties of the goethite surface are modelled using the 2-pK model. Two pK models are based on the protonation and dissociation of a reactive surface functional group, SOH, and are described by the following two reactions (Goldberg, 2013).

$$\equiv Fe\text{-}OH + H^{+} = \equiv Fe\text{-}OH_2^{+} \ldots\ldots\ldots\ldots\ldots K_{1\,int.} \quad (6.1)$$

$$\equiv Fe\text{-}OH = \equiv Fe\text{-}O^{-} + H^{+} \ldots\ldots\ldots\ldots\ldots\ldots K_{2\,int.} \quad (6.2)$$

In this model, the surface of goethite is assumed to be homogeneous with one active surface functional group during the model analysis (Gao and Mucci, 2001; Peacock and Sherman, 2004). Several 2-pK models like constant the capacitance model (CCM), diffuse layer model (DLM), triple layer model (TLM) and basic stern model (BSM) have been developed to describe the surface properties of goethite. In the present study, the surface acidity constants of goethite are described by the CCM and DLM (Fig. 6.2). The surface area of goethite is determined by BET analysis. The total number of reactive surface functional groups (S_T) of goethite is determined using the equation 6.3 (Goldberg, 2013).

$$S_T = \frac{Sa10^{18}}{N_A} N_S \ldots\ldots\ldots\ldots (6.3)$$

In equation 6.3, S is the surface area, a is the particle concentration, N_A is Avogadro's number and N_s is site density (observing maximum adsorption densities of Zn onto goethite). The surface site density of goethite is controlled by morphologies, surface roughness, and specific surface area of the crystals (Livi et al., 2017) and can vary by an order of magnitude depending on analysis methods. Crystallographic calculations provide the lowest value of surface site density, whereas tritium exchange provides the highest (Goldberg, 2013). Reported surface site

density of goethite range from 2 to 20 sites nm^{-2} (Hayes et al., 1991). The surface site density in my study is fixed at 8 sites/nm^2. This value is consistent with site densities of 6 – 10 sites/nm^2 reported by several authors (Hayes and Leckie, 1987; Hayes et al., 1991; Hiemstra and VanRiemsdijk, 1996; Peacock and Sherman, 2004; Xu et al., 2006).

In the CCM, background electrolyte ions do not form surface complexes. The constant capacitance model (CCM) has four adjustable model parameters: two surface acidity constants ($K_{1\ int.}$ and $K_{2\ int.}$), surface site density (N_s), and the specific capacitance (C_1). The surface acidity constants are obtained by fitting the potentiometric titration data with the selected site density. The specific capacitance (C_1) is obtained by adjusting its value with the best fit of potentiometric data.

In the DLM, three model parameters are required to be adjusted: surface site density and two acidity constants. The surface site density is the same as used in the CCM and the TLM, and the surface acidity constants are determined by fitting the potentiometric titration data with the selected site density.

The potentiometric data at three different NaCl concentrations fit well with the CCM. The DLM shows a poor fit with all three different NaCl concentrations (Fig. 6.2). This is due to the high ionic concentration of NaCl and high surface site densities (8 sites/nm^2) during the model analysis (Peacock and Sherman, 2004; Swedlund et al., 2009). In the DLM, the electrolyte ions are considered as point charges and at high surface densities, the electrolyte ions are involved in extrapolating to site saturation and providing unrealistic surface potentials (Swedlund et al., 2009). Therefore, the DLM is well appropriate to model the surface titration data at low values of surface densities (1 – 2 sites/nm^2) and low concentration of NaCl (< 0.1 mol L^{-1}) (Hayes et al., 1991; Peacock and Sherman, 2004; Swedlund et al., 2009).

Acidity constants (K_1 and K_2) and other model parameters acquired using the CCM and DLM at three different NaCl concentrations are presented in Table 6.1. The pH_{PZC} derived from CCM and TLM is 8.5 ± 0.04 which is similar to the experimental results. In the CCM, the acidity constants and specific surface capacitance (C_1) increase with increasing NaCl. Since the CCM is calibrated at each NaCl, increasing protolysis constants is the only way to compensate for the increasing H^+ or OH^- release due to increasing NaCl concentration (Hayes et al., 1991).

Table 6.1 Acid-base properties of goethite in different NaCl concentration (0.1 mol L^{-1}, 0.3 mol L^{-1}, and 0.7 mol L^{-1}, respectively) using CCM and DLM (goethite surface area[d]: 40 m^2 g^{-1}, site density[e]: 8 sites nm^{-2}, goethite concentration: 8.0-8.83 g L^{-1}). [a] Determined from potentiometric titration data (this study), [b] Determined from FITEQL simulation of potentiometric titration data (this study), [c] From Hayes et al. (1991) (Hayes et al., 1991), [d] Determined from BET analysis (this study), [e] Determined from maximum adsorption densities of Zn onto goethite.

Parameters	CCM			DLM		
	NaCl concentration (mol L^{-1})					
	0.1	0.3	0.7	0.1	0.3	0.7
pH_{PZC}[a]	8.5	8.5	8.5	8.40	8.31	8.38
log K_1[b] int.	6.45	6.74	7.10	5.84	5.91	6.00
log K_2[b] int.	-10.63	-10.21	-9.92	-10.96	-10.70	-10.76
log K_{an}[b]						
log K_{cat}[b]						
C_1 (F m^{-2})[b]	0.90	1.20	1.20			
C_2 (F m^{-2})[c]						
V (Y)	2.74	0.60	6.98	474	541	747

6.2.3 Zn Adsorption onto Goethite and Development of Surface Complexation Constants

6.2.3.1 Effect of Increasing NaCl concentration on Zn adsorption onto goethite

Batch adsorption isotherm experiments are conducted between pH 3 and 10 in NaCl solutions with three different concentrations (0.1, 0.3, and 0.7 mol L^{-1}) and with Zn initial concentration of 0.08 mmol L^{-1} and 0.8 mmol L^{-1}. The results are shown in Figure 6.3. Figure 6.3A represent µmol Zn adsorption m^{-2} on goethite at Zn initial concentration of 0.08 mmol L^{-1} whereas figure 6.3B represents µmol Zn adsorption m^{-2} at Zn initial concentration of 0.8 mmol L^{-1}.

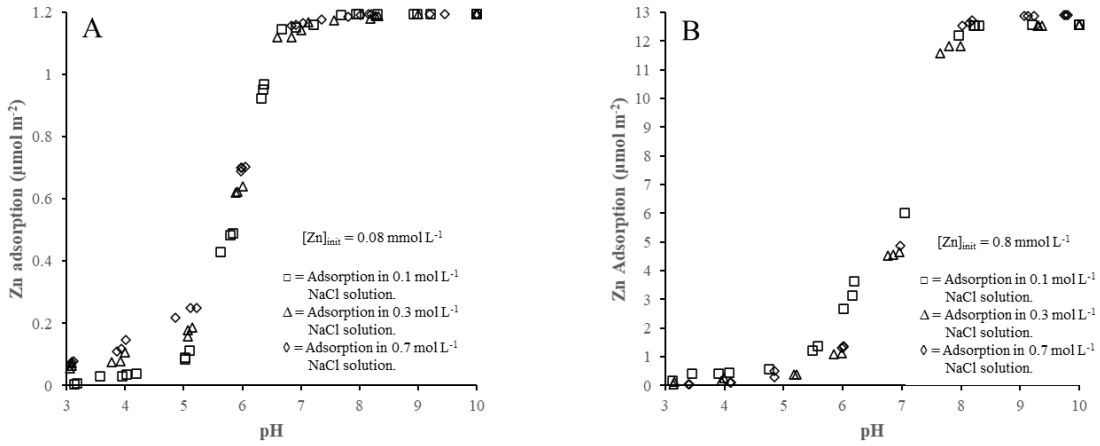


Figure 6.3 Zn adsorption on goethite (1.6 g L^{-1}) as a function of pH in 0.1 (□), 0.3 (Δ) and 0.7 (◊) mol L^{-1} NaCl solution at two different initial concentration: 0.08 mmol L^{-1} (A) and 0.8 mmol L^{-1} (B). Each experiment has three distinct replications, and the results of all replications are presented in the figure.

The adsorption isotherm shows for all experiments (changing NaCl and initial Zn concentration) a strong pH dependency between pH 3 and 7. Adsorption of Zn at $[Zn]_{init}$ of 0.08 mmol L^{-1} increases sharply between pH 3.0 and 7.0 (Fig. 6.3A), gradually after pH 7 to 8 and plateaus near 100% at pH > 8. Similar trends are observed at $[Zn]_{init}$ of 0.8 mmol L^{-1}; however, the adsorption curve moves to higher pH values (Fig. 6.3B). The adsorption edge occurs between pH 3 and 8; adsorption gradually increases between pH 8 and 9 and plateaus near 100% at pH > 9. Zinc (Zn) is nearly entirely adsorbed on the surface of goethite between pH 8 and 10 with $[Zn]_{init}$ at 0.08 and 0.8 mmol L^{-1} (Fig. 6.3). The shift of the adsorption curve to higher pH is attributed to the changes in the adsorbate/adsorbent ratio. Therefore, for the equal number of available sites at a particular pH, relative less Zn is adsorbed at higher $[Zn]_{init}$. The observations are consistent with previous results reported by Xu et al. (2006) and Spathariotis and Kallianou (2007).

At $[Zn]_{init}$ of 0.08 mmol L^{-1}, the adsorption onto goethite increases between 5 and 7% between pH 3 and 6 with [NaCl] increasing from 0.1 to 0.7 mol L^{-1} (Fig. 6.3A). In contrast, the adsorption experiment with $[Zn]_{init}$ of 0.8 mmol L^{-1} show a decrease in Zn adsorption with increasing NaCl concentration. With increasing [NaCl] from 0.1 to 0.3 mol L^{-1}, the decrease is smaller between pH 3 and 5 (between 2 and 3%) than at pH 6 (around 10%). The increase of [NaCl] from 0.3 mol L^{-1} to 0.7 mol L^{-1} does not affect Zn adsorption on goethite at Zn initial concentration of 0.8 mmol L^{-1} (Fig. 6.3B).

6.2.3.2 Surface Complexations Constants of Zn in 0.1, 0.3, and 0.7 mol L^{-1} NaCl Solutions

6.2.3.2.1 Equilibria in solution

The intrinsic thermodynamic complexation constants (at I = 0 M, $\log K^{int}$) for Zn with inorganic ligands (Cl^-, OH^-, HCO_3^-, CO_3^{2-}) present in the solution are presented in Table 6.2. The values are taken from Powell et al. (2013) and were calculated for I = 0.1 mol L^{-1}, 0.3 mol L^{-1}, and 0.7 mol L^{-1} using the SIT equation. The SIT equation is applied due to its reliability in a high ionic strength solution (≥ 0.5 mol L^{-1}). The calculated constants using the SIT equation and the SIT reaction co-efficient (Δε) in high ionic solution (I = 0.67 mol L^{-1}) agree well with the reported values in IUPAC technical report. For reactions where SIT reaction co-efficient (Δε) was not available, the Davies equation with a 0.2I term was used (Davies, 1938). The Davies equation is applied because the calculated constants of Zn-Cl complexes using the Davies equation agree well (± 0.04 variation) with those calculated using SIT equation (Annex D). The suitability of

the Davies equation to estimate complexation constants in high ionic strength solutions is reviewed by Millero and Schreiber (1982) and Gao and Mucci (2001).

Table 6.2 Aqueous complexation constants of Zn and carbonate used to model Zn and carbonate adsorption on goethite in 0.1, 0.3 and 0.7 mol L^{-1} NaCl solution.

Reactions	log K			
	I = 0 mol L^{-1}	I = 0.1 mol L^{-1}	I = 0.3 mol L^{-1}	I = 0.7 mol L^{-1}
$Zn^{2+} + H_2O = ZnOH^+ + H^+$	-8.96	-9.18	-9.28	-9.36
$Zn^{2+} + 2H_2O = Zn(OH)_2 + 2H^+$	-17.82	-18.06	-18.18	-18.32
$Zn^{2+} + 3H_2O = Zn(OH)_3^- + 3H^+$	-28.05	-28.07	-28.11	-28.18
$Zn^{2+} + Cl^- = ZnC^+$	0.40	-0.02	-0.17	-0.26
$Zn^{2+} + 2Cl^- = ZnCl_2$	0.69	0.05	-0.17	-0.30
$Zn^{2+} + 3Cl^- = ZnCl_3^-$	0.48	-0.15	-0.36	-0.46
$Zn^{2+} + CO_3^{2-} = ZnCO_3$ *	4.75	3.85	3.55	3.47
$Zn^{2+} + 2CO_3^{2-} = Zn(CO_3)_2^{2-}$ *	5.4	4.50	4.20	4.12
$Zn^{2+} + HCO_3^- = ZnHCO_3^-$	1.62	1.20	1.05	0.96

* Using Davies

6.2.3.2.2 Modelling Zn adsorption in NaCl solutions

Zinc adsorption on goethite at $[Zn]_{init}$ = 0.08 mmol L^{-1} in 0.1, 0.3 and 0.7 mol L^{-1} NaCl solutions was modelled (Fig. 6.4) using the CCM and the optimized acid-base parameters of goethite (Table 6.1) and the thermodynamic Zn equilibrium reactions in solution (Table 6.2). Surface species 1 - 3 are initially considered in our modelling in the effort to model the observed Zn adsorption in different NaCl concentrations (Table 6.3). Since the CCM need a distinct set of model constants at different NaCl ionic concentrations, the model constants at each NaCl ionic concentration are variable and only valid at specific NaCl ionic concentration. The complexation constants of Zn in different NaCl solutions are presented in Table 6.3.

The best fit to the observed Zn adsorption data in 0.1 mol L^{-1} NaCl solution is obtained comprising monodentate ($\equiv FeOZn^+$), bidentate [$(\equiv FeOH)_2Zn^{2+}$], and surface precipitate complexes [$\equiv FeOZn(OH)_2^-$] (Fig. 6.4 A). $\equiv FeOZn^+$ and $(\equiv FeOH)_2Zn^{2+}$ are the dominant surface complexes at pH < 6, $\equiv FeOZn^+$, $(\equiv FeOH)_2Zn^{2+}$, and $\equiv FeOZn(OH)_2^-$ are predominate between pH 6 and 8, whereas $\equiv FeOZn(OH)_2^-$ is the most abundant surface species at pH > 8.

The model fit to the Zn adsorption in 0.3 mol L^{-1} NaCl solution is shown in Figure 6.4 B. Initially, using $(\equiv FeOH)_2Zn^{2+}$ and $\equiv FeOZn(OH)_2^-$ only, a good fit to the examined Zn adsorption data is found [V(Y) = 6.93]. $(\equiv FeOH)_2Zn^{2+}$ is the dominant surface complexes at pH < 7 whereas $\equiv FeOZn(OH)_2^-$ is predominant surface species at pH > 7. However, the fit is poor at low pH between 3 and 4.

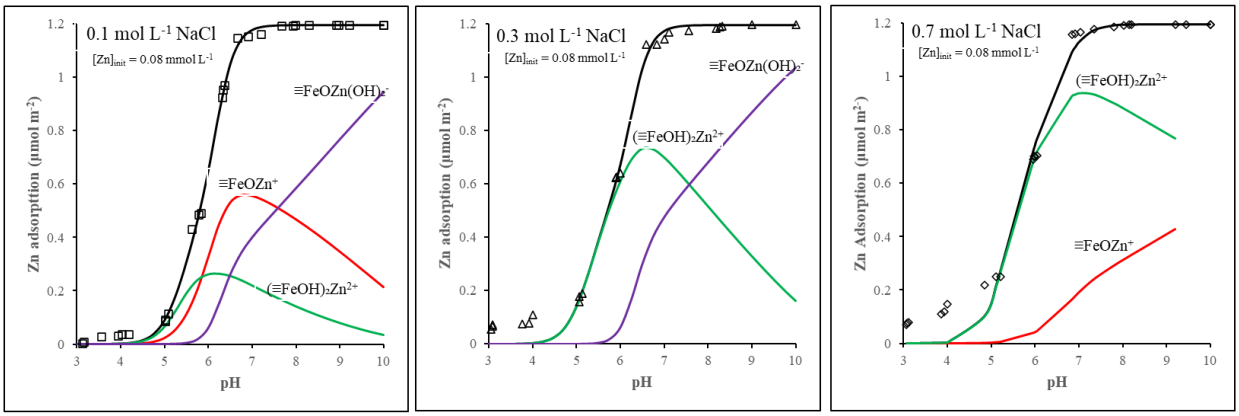


Figure 6.4 Model predicted Zn Adsorption onto goethite as a function of pH in 0.1, 0.3 and 0.7 mol L^{-1} NaCl solutions. Symbols are data points, lines are CCM fits showing total and individual surface species. Initial Zn and goethite concentration were $[Zn]_{init}$ = 0.08 mmol L^{-1} and 1.6 g L^{-1}, respectively. For comparison, Figure 6.3A is reproduced and Zn adsorption on goethite in 0.1, 0.3 and 0.7 mol L^{-1} NaCl solution are represented by □, Δ and ◊, respectively.

The model fit of Zn adsorption data in 0.7 mol L^{-1} NaCl solution is shown in Figure 6.4 C. The bidentate surface complex, $(\equiv FeOH)_2Zn^{2+}$ and $\equiv FeOZn^+$ (monodentate) surface complex provides a good fit [V(Y) = 14.52], however, the predicted adsorption is lower in the pH ranges between 3 and 5. Model results indicate that the monodentate surface complex ($\equiv FeOZn^+$) reduces as NaCl concentration increases whereas the bidentate surface complex increase (Fig, 6.4).

Table 6.3 Surface complexation reactions and constants describing Zn adsorption onto goethite in 0.1, 0.3, and 0.7 mol L^{-1} NaCl solutions.

Reactions	log K (0.1)*	log K*****	log K (0.3)*	log K (0.3)**	log K (0.7)*	log K (0.7)***	log K (0.7)****
	E						
1) $\equiv FeOH + Zn^{2+} = \equiv FeOZn^{+} + H^{+}$	2.74	-2.0	N.A.	N.A.	1.96	N.A.	N.A.
2) $2 \equiv FeOH + Zn^{2+} = (\equiv FeOH)_2Zn^{2+}$	13.75	10.67	14.10	N.A.	14.69	14.11	N.A.
3) $\equiv FeOH + Zn^{2+} + 2H_2O = \equiv FeOZn(OH)_2^{-} + 3H^{+}$	-13.98	-18.20	-14.36	-13.53	N.A.	N.A.	N.A.
4) $\equiv FeOH + Zn^{2+} + Cl^{-} = \equiv FeOHZnCl^{+}$	N.A.	N.A.	N.A.	8.96	N.A.	8.93	9.00
5) $2 \equiv FeOH + Zn^{2+} + Cl^{-} = \equiv (FeO)_2ZnCl^{-} + 2H^{+}$	N.A.	N.A.	N.A.	N.A.	N.A.	N.A.	1.65
V(Y)	1.21	--	6.93	5.26	14.52	12.04	8.04

* Model fit without ternary surface complex
** Model fit of Zn adsorption in 0.3 mol L^{-1} NaCl concentration with one ternary surface complex ($\equiv FeOHZnCl^{+}$)
*** Model fit of Zn adsorption in 0.7 mol L^{-1} NaCl concentration with one ternary surface complex ($\equiv FeOHZnCl^{+}$)
**** Model fit of Zn adsorption in 0.7 mol L^{-1} NaCl concentration with two ternary surface complexs ($\equiv FeOHZnCl^{+}$ and $\equiv (FeO)_2ZnCl^{-}$)
***** from Plamqvist et al. (1997)
V(Y) = Model error

6.2.4 Models Improvement by Introducing Ternary Surface Species and their Validation

6.2.4.1 Ternary Surface Species

To improve the model fit of Zn adsorption at low pH in 0.3 and 0.7 mol L^{-1} NaCl solutions, ternary surface complex ($\equiv FeOHZnCl^{+}$) is considered in conjunction with $(\equiv FeOH)_2Zn^{2+}$ and $\equiv FeOZn(OH)_2^{-}$. The adsorption of Zn as ternary surface complexes, i.e. Zn-Cl complexes, is in line with evidence from EXAFS spectroscopy (Chesne and Kim, 2014). Including this complex provides a better fit to the examined Zn adsorption data in 0.3 mol L^{-1} NaCl solutions [V(Y) = 5.26] than the model fit without ternary surface complex [V(Y) = 6.93], however, the adsorption is still lower predicted at low pH (Fig. 6.5 A).

The model fit of Zn adsorption data with ternary surface complex in 0.7 mol L^{-1} NaCl solution is shown in Figure 6.5. Initially, the bidentate surface complex, $(\equiv FeOH)_2Zn^{2+}$ and ternary surface complex, $\equiv FeOHZnCl^{+}$ provide a good fit [V(Y) = 12.04] than the model fit without ternary surface species [V(Y) = 14.52], however, the predicted adsorption is lower in the pH ranges between 3 and 4 and 6 and 7 (Fig. 6.5 B). As Zn-Cl complexes are more present in 0.7 mol L^{-1} NaCl solution (Fig. 4.2), the inclusion of ternary surface complex, $(\equiv FeO_2)ZnCl^{-}$ should improve the fit [V(Y) = 8.04] (Fig. 6.5 C). However, like at 0.3 mol L^{-1} NaCl solution, the predicted adsorption is yet lower by the model at low pH. The constants ternary surface species of Zn are presented in Table 6.3.

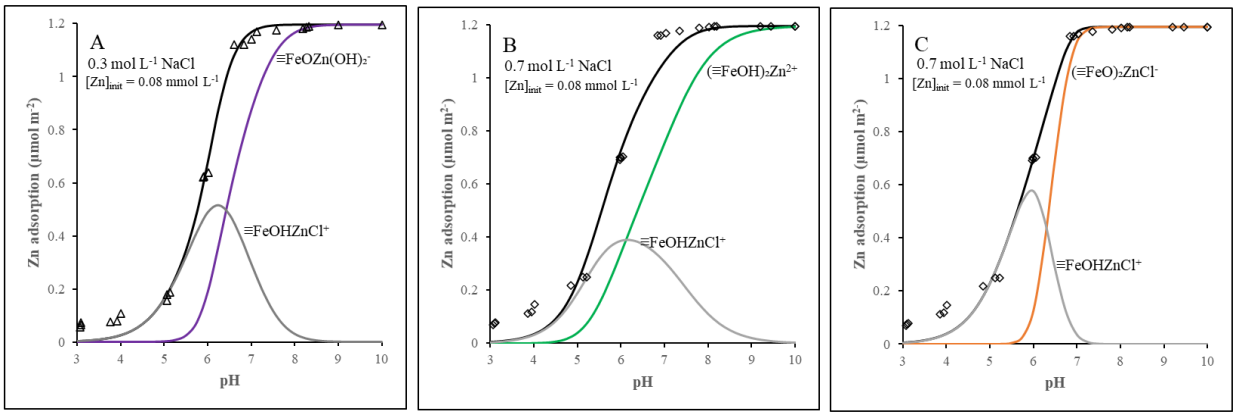


Figure 6.5 Model fit of Zn Adsorption onto goethite in 0.3 and 0.7 mol L^{-1} NaCl solution in the presence of the ternary surface complex. A: model fit in 0.3 mol L^{-1} NaCl solution; B: model fit in 0.7 mol L^{-1} NaCl solution with one ternary surface complex, C: model fit in 0.7 mol L^{-1} NaCl solution with two ternary surface complexes. Symbols are data points, lines are CCM fits showing total and individual surface species. Initial Zn and goethite concentration were $[Zn]_{init}$ = 0.08 mmol L^{-1} and 1.6 g L^{-1}, respectively. Figure 6.3A is reproduced and Zn adsorption on goethite in 0.3 and 0.7 mol L^{-1} NaCl solution is represented by Δ and ◊.

6.2.4.2 Model Validation

To test the model performance at $[Zn]_{init}$ = 0.8 mmol L^{-1}, the CCM model derived from Zn adsorption on goethite at $[Zn]_{init}$ = 0.08 mmol L^{-1} is run with corresponding surface species in NaCl concentrations (0.1, 0.3, and 0.7 mol L^{-1}) and the model results are compared with experimental results. Surface species, 1 – 3 with their corresponding equilibrium constants are considered in 0.1 mol L^{-1} NaCl solution. The model predicts the adsorption of Zn in 0.1 mol L^{-1} NaCl solution reasonably well, however, it overpredicts adsorption at pH 7 (Fig. 6.6 A). In 0.3 mol L^{-1} NaCl solution, the model with the surface species 2 and 3 and their corresponding equilibrium constants predict a good fit at pH between 3 and 4 and between 8 and 10, however, overpredict Zn adsorption at pH 5 – 7 (Fig. 6.6 B – solid line). The model with ternary surface complex (surface species 3 and 4) and their corresponding equilibrium constants underpredict Zn adsorption at pH > 6 in 0.3 mol L^{-1} NaCl solution (Fig 6.6 B – dash line). In 0.7 mol L^{-1} NaCl solution, all the models underpredict Zn adsorption at pH > 6 (Fig. 6.6 C)

The reason for the lower prediction in 0.7 mol L^{-1} NaCl solution at $[Zn]_{init}$ = 0.8 mmol L^{-1} is the absence of surface precipitate complex in the model. A surface precipitation reaction occurs at high pH and high initial concentration of metal (Katz and Hayes, 1995b; Palmqvist et al., 1997). Therefore, to extend the model prediction at a higher initial concentration of Zn, the surface precipitates complex is needed in the model.

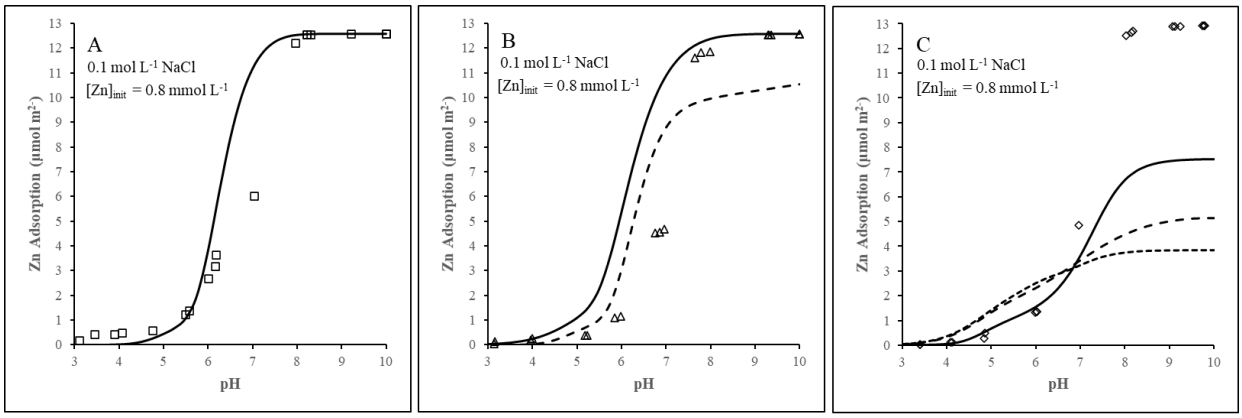


Figure 6.6 Model prediction of Zn adsorption at $[Zn]_{init}$ = 0.8 mmol L^{-1} in 0.1 (A), 0.3 (B), and 0.7 (C) mol L^{-1} NaCl solutions using surface complexation reactions and constants in Table 6.3. Symbols are data points, lines are CCM fits. Goethite concentration was1.6 g L^{-1}. Solid, dash and square dot lines represent model fit by considering different surface species and their corresponding equilibrium constants in Table 6.3. For comparison, Figure 6.3B is reproduced and Zn adsorption on goethite in 0.1, 0.3 and 0.7 mol L^{-1} NaCl solution are represented by □, Δ and ◊, respectively.

To improve the model performance in 0.7 mol L^{-1} NaCl solution, the surface precipitate complex ($\equiv FeOZn(OH)_2^-$ = -13.98) is added to the model in conjunction with surface species 1 and 2. The model results are shown in Figure 6.7. However, like at 0.1 and 0.3 mol L^{-1} NaCl solution, the predicted adsorption is yet higher by the model at pH 6 and 7.

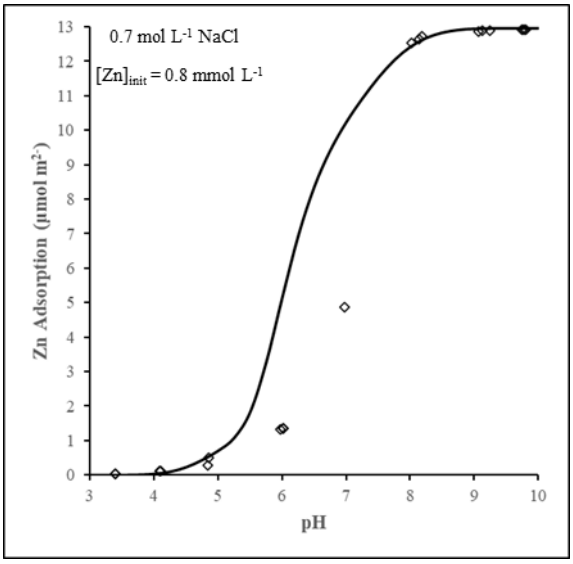


Figure 6.7 Model prediction of Zn adsorption at $[Zn]_{init}$ = 0.8 mmol L^{-1} in 0.7 mol L^{-1} NaCl solution with the complex of surface precipitation. Model is predicted with surface species 1 and 2 and their corresponding equilibrium constants in 0.7 mol L^{-1} NaCl solution in Table 6.3. The equilibrium constant of the surface precipitate complex ($\equiv FeOZn(OH)_2^-$ = -13.98) is added to the model to improve model fit. Symbols are data points, lines are CCM fits. Goethite concentration was1.6 g L^{-1}. For comparison, Zn adsorption on goethite in 0.7 mol L^{-1} NaCl solution is reproduced from Figure 6.3B and represented by ◊.

6.2.4.3 Modelling Zn Adsorption at Higher Initial Concentration

As the surface species and their corresponding equilibrium constants are unable to predict Zn adsorption accurately at $[Zn]_{init}$ = 0.8 mmol L^{-1}, a new set of model parameters is developed using the CCM to predict Zn adsorption in different NaCl concentrations. Modelling strategy at higher initial concentration needs to increase surface sites and incorporate surface precipitation reaction in the model (Katz and Hayes, 1995b; Mercer and Tobiason, 2008). Therefore, surface precipitation reaction is added to my model. However, the surface sites are not changed because of the maximum surface site number (8 sites/nm^2) I used in my model.

The model prediction results with the surface complexation reactions and constants in Table 6.4 are presented in Figure 6.8. The modelling approach at the high initial concentration of Zn (Zn_{init} = 0.8 mmol L^{-1}) accurately predicts Zn adsorption in different NaCl concentrations. Monodentate ($\equiv FeOZn^+$) and surface precipitate complex [$\equiv FeOZn(OH)_2^-$] are observed in 0.1 and 0.3 mol L^{-1} NaCl solution by the model prediction whereas bidentate [$(\equiv FeOH)_2Zn^{2+}$] and surface precipitate [$\equiv FeOZn(OH)_2^-$] are observed in 0.7 mol L^{-1} NaCl solution. The surface

species and their corresponding equilibrium constants in different NaCl concentrations are presented in Table 6.4.

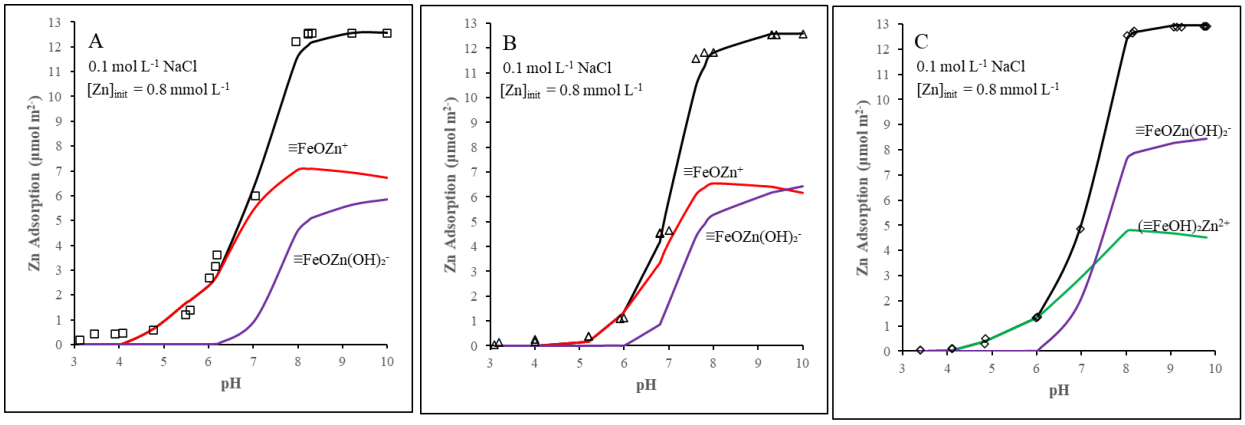


Figure 6.8 Modelling approach of Zn adsorption at $[Zn]_{init}$ = 0.8 mmol L^{-1}. Model prediction at $[Zn]_{init}$ = 0.8 mmol L^{-1} in 0.1 (A), 0.3 (B), and 0.7 (C) mol L^{-1} NaCl solutions is done using surface complexation reactions and constants in Table 6.4. Symbols are data points, lines are CCM fits showing total and individual surface species. Initial Zn and goethite concentration were $[Zn]_{init}$ = 0.8 mmol L^{-1} and 1.6 g L^{-1}, respectively. For comparison, Figure 6.3B is reproduced and Zn adsorption on goethite in 0.1, 0.3 and 0.7 mol L^{-1} NaCl solution are represented by □, Δ and ◊, respectively.

Table 6.4 Surface complexation reactions and constants describing Zn adsorption onto goethite in 0.1, 0.3, and 0.7 mol L^{-1} NaCl solutions at $[Zn]_{init}$ = 0.8 mmol L^{-1}. V(Y) = model error, N.A. = not determined

Reactions	Surface equilibrium constants		
	log K (0.1)	log K (0.3)	log K (0.7)
$\equiv FeOH + Zn^{2+} = \equiv FeOZn^{+} + H^{+}$	3.75	2.00	N.A.
$2 \equiv FeOH + Zn^{2+} = (\equiv FeOH)_2Zn^{2+}$	N.A.	N.A.	13.85
$\equiv FeOH + Zn^{2+} + 2H_2O = \equiv FeOZn(OH)_2^{-} + 3H^{+}$	-17.87	-16.94	-17.42
V(Y)	10.57	10.70	5.95

6.3 Discussion

6.3.1 Zn adsorption on goethite

Goethite is a variable charge mineral, and the surface properties are pH dependent. The surface of goethite is positively charged at low pH and negatively charged at high pH (Liu et al., 2014). Therefore, the adsorption of positive charge divalent trace elements (Zn^{2+}, Cu^{2+}, Pb^{2+}, etc.) is low at acidic pH. The increase in Zn adsorption with increasing [NaCl] between pH 3 and 6 with $[Zn]_0$ of 0.08 mmol L^{-1} (Fig. 6.3 A) is likely explained by metal-chloride surface complexes. Increasing $[Cl^-]$ leads to increased formation of Zn-Cl aqueous complexes (Fig. 4.2) and Zn is adsorbed on the surface of goethite as a ternary surface complex (≡Feh-O-Zn-Cl) as reported by Chesne and Kim (2014), Gunton (2007) and Gunton et al. (2006). Recent EXAFS studies showed further evidence of adsorption of Zn and Pb onto goethite as ternary surface complexes at pH < 6 in NaCl saline solution (Bargar et al., 1998; Chesne and Kim, 2014).

At the higher initial concentration of Zn, the adsorption of Zn on goethite is decreased with increasing NaCl concentration from 0.1 to 0.3 mol L^{-1} due to the weak bonding interaction between Zn and goethite surface. Zn adsorption on iron oxides including goethite and ferrihydrite is relatively weak at higher $[Zn]_{init}$ (> 0.2 mmol L^{-1}) as studied by Liu et al. (2016) and Grafe and Sparks (2205). Therefore, the initial Zn desorption at $[Zn]_{init}$ = 0.8 mmol L^{-1} after increasing NaCl concentration from 0.1 mol L^{-1} to 0.3 mol L^{-1} suggests that the weakly bound Zn may release and form stable aqueous Zn-Cl complexes (Fig. 6.3 B). However, the opposite result is reported during the adsorption experiment with increasing NaCl concentration from 0.3 to 0.7 mol L^{-1}. This indicates that as the NaCl concentration increases from 0.3 mol L^{-1} to 0.7 mol L^{-1}, Zn complexes with more chloride available and adsorbs on the surface of goethite through inner-sphere mechanisms (Chesne and Kim, 2014). Therefore, there is little increase in pH dependent Zn adsorption on goethite with increasing ionic strength from 0.3 mol L^{-1} to 0.7 mol L^{-1}.

6.3.2 Modelling approach and its development

My initial model (Fig. 6.4) including three surface complexes (monodentate, bidentate, surface precipitate) in 0.1 mol L^{-1} NaCl solution at $[Zn]_{init}$ = 0.08 mmol L^{-1} is consistent with the surface complexation model information reported by Palmqvist et al. (1997). However, their reported surface complexation constants are not easily assessed with the results of this study because they are defined in concentrated solutions and the acid-base properties of goethite surface are described by a different model. Variation in model complexation constants in different experimental sets up is well reported in the literature (Gao and Mucci, 2001). In addition, some models only include monodentate surface complex to describe Zn adsorption data on goethite (Spathariotis and Kallianou, 2007). However, this approach does not improve the model fit to my data and this finding is not in keeping with spectroscopic analysis because both monodentate and bidentate surface complexation of Zn is identified by spectroscopic analysis. Therefore, multispecies surface complexation of Zn on goethite is needed to explain Zn adsorption on goethite (Katz and Hayes, 1995a; Peacock and Sherman, 2004).

The model results of Zn adsorption at $[Zn]_{init}$ = 0.08 mmol L^{-1} in 0.1 and 0.7 mol L^{-1} NaCl solutions (Fig. 6.4) and experimental results from the EXAFS spectroscopic studies support that bidentate and ternary surface complexation increases with increasing NaCl ionic concentration from 0.1 mol L^{-1} to 0.7 mol L^{-1} (Chesne and Kim, 2014). The formation of tridentate surface complexation at 0.6 mol L^{-1} NaCl solution is also reported by Chesne and Kim (2014). However, I did not consider the tridentate surface complex further because of the

good fit [V(Y) < 20] to my data with monodentate, bidentate and ternary surface complexes. At low pH (3 – 5), my model provides a lower model fit which likely reflects the absence of ternary surface complexes in my model analysis. Including ternary surface complexes provide a better fit to the examined Zn adsorption data in 0.3 and 0.7 mol L^{-1} NaCl solutions, however, the adsorption is still lower predicted at low pH (Fig. 6.5). The lower prediction by model analysis after inclusion of ternary surface complexes might be due to surface site heterogeneity of goethite. The electric double layer model assumes a homogeneous surface with only one surface functional group (Gao and Mucci, 2001). However, heterogeneity of goethite surface has been reported by several authors (Hiemstra and VanRiemsdijk, 1996; Ponthieu et al., 2006). Therefore, a homogeneous surface of goethite with only one surface functional group cannot provide a good model estimation of Zn adsorption in 0.3 and 0.7 mol L^{-1} NaCl solutions.

Model performance at $[Zn]_{init}$ = 0.8 mmol L^{-1} indicated that the CCM model derived from Zn adsorption on goethite at $[Zn]_{init}$ = 0.08 mmol L^{-1} and the corresponding surface species (Table 6.3) in NaCl concentrations (0.1, 0.3, and 0.7 mol L^{-1}) is not capable to describe Zn adsorption on goethite at $[Zn]_{init}$ = 0.8 mmol L^{-1}. One reason for low model performance is the absence of a surface precipitate complex. Adding surface precipitate complex ($\equiv FeOZn(OH)_2^-$) in conjunction with other surface species improve the model fit in 0.7 mol L^{-1} NaCl solution (Fig. 6.7). However, the predicted adsorption is yet higher by the model at pH 6 and 7. The overprediction of Zn adsorption at $[Zn]_{init}$ = 0.8 mmol L^{-1} and at pH 6 – 7 in 0.1, 0.3 and 0.7 mol L^{-1} NaCl solution is difficult to explain. The model prediction does not follow the effect of changes in the adsorbate/adsorbent ratio on the adsorption where the adsorption curve is shifted to higher pH. The underprediction or overprediction of surface complexation models with corresponding surface species at a different initial concentration of ions is reported by several authors (Balistrieri and Chao, 1990; Gao and Mucci, 2001). Therefore, another CCM modelling approach with the inclusion of surface precipitation reaction of Zn on goethite surface is applied for describing Zn adsorption at $[Zn]_{init}$ = 0.8 mmol L^{-1}. This approach successfully predicted Zn adsorption on goethite in different NaCl concentrations at $[Zn]_{init}$ = 0.8 mmol L^{-1} (Fig. 6.8) and indicated that the formation of ternary surface complexes might not be important in the adsorption experiment at high solid-liquid ratio. The CCM model results suggest that different surface complexation reactions and constants are needed to describe Zn adsorption on goethite at different initial concentrations.

6.4 Conclusions

This chapter aimed to develop a surface complexation model to address ternary surface complexes of Zn in high concentrations of NaCl and determine intrinsic equilibrium constants for Zn surface complexation with goethite in NaCl solutions. We find that

1. The potentiometric data at different NaCl concentrations (0.1, 0.3 and 0.7 mol L^{-1}) fit well with the CCM. The DLM shows a poor fit with all three different NaCl concentrations.
2. Zinc adsorption onto goethite with $[Zn]_{init}$ = 0.08 mmol L^{-1} increases between 5 and 7% from pH 3 and 6 with increasing NaCl concentration from 0.1 to 0.7 mol L^{-1}. In contrast, the Zn adsorption experiment with $[Zn]_{init}$ = 0.8 mmol L^{-1} decreases with increasing NaCl concentrations from 0.1 mol L^{-1} to 0.3 mol L^{-1}. An increase of NaCl concentration from 0.3 mol L^{-1} to 0.7 mol L^{-1} does not affect Zn adsorption on goethite.
3. Zinc complexation on goethite with $[Zn]_{init}$ = 0.08 mmol L^{-1} in 0.1 mol L^{-1} NaCl solution is accurately described using the CCM consisting of monodentate, bidentate, and surface precipitate complexes. The CCM model prediction, however, underestimates Zn adsorption in 0.3 and 0.7 mol L^{-1} NaCl solutions. The inclusion of ternary surface complexes [($\equiv FeOHZnCl^{+}$) and ($\equiv FeO_2$)$ZnCl^{-}$] into the CCM model improves the accuracy of Zn adsorption in 0.3 and 0.7 mol L^{-1} NaCl solutions which indicated that increasing Zn adsorption at $[Zn]_{init}$ = 0.08 mmol L^{-1} with increasing NaCl concentration is due to adsorption of Zn as ternary surface complex [($\equiv FeOHZnCl^{+}$) and ($\equiv FeO_2$)$ZnCl^{-}$].
4. The CCM model parameters derived from Zn adsorption at $[Zn]_{init}$ = 0.08 mmol L^{-1} successfully simulate Zn adsorption also with $[Zn]_{init}$ = 0.8 mmol L^{-1} in 0.1 and 0.3 mol L^{-1} NaCl solutions at pH between 3 and 6 and between 8 and 10, however, overpredicted at pH between 6 and 7. In 0.7 mol L^{-1} NaCl solution, the model underpredicted Zn adsorption at pH > 6. This indicated that the CCM models with the corresponding surface species in NaCl concentrations (0.1, 0.3, and 0.7 mol L^{-1}) derived from Zn adsorption on goethite at $[Zn]_{init}$ = 0.08 mmol L^{-1} are not capable to describe Zn adsorption on goethite at $[Zn]_{init}$ = 0.8 mmol L^{-1}.
5. At a higher initial concentration of Zn, the model identifies that precipitation is an important Zn removal mechanism. The inclusion of the surface precipitation reaction of Zn on the goethite improves the model performance at $[Zn]_{init}$ = 0.8 mmol L^{-1}.

Therefore, two model protocols are established for predicting Zn adsorption in different initial concentrations.

6. Ternary surface complexes are only reported at the low initial concentration of Zn (Zn_{init} = 0.08 mmol L^{-1}) by model prediction. At the higher initial concentration of Zn (Zn_{init} = 0.8 mmol L^{-1}), the model successfully simulates Zn adsorption without the inclusion of ternary surface complexation parameters. The model prediction thus shows that the effect of ternary surface complexes on the adsorption of Zn may depend on the initial concentration of Zn, NaCl concentrations and solid-liquid ratios.

Chapter 7: Conclusion and Future Research

7.1 Summary and Conclusions

This thesis investigated the effect of increasing salinity and hence NaCl concentrations on the geochemistry of zinc in tropical soils. The focus was to improve our understanding of Zn aqueous speciation in NaCl solutions and surface processes of Zn using experimental laboratory studies with *Tropaquept* (Bay) and *Hydraquent* (Tiaong) soils and with goethite and, combining these with geochemical modelling. The central focus was on evaluating the accuracy of the geochemical model with predefined databases for predicting Zn adsorption and aqueous speciation in seawater ionic strength (= 0.7 mol L^{-1} NaCl solution) and developing a geochemical model with surface complexation constants for describing the adsorption mechanisms of Zn accurately in 0.7 mol L^{-1} NaCl solution.

The analysis of Zn aqueous speciation in seawater ionic strength (≈ 0.7 mol L^{-1} NaCl) using the Davis equation in the geochemical program "Visual MINTEQ" highlighted that activity corrections using the Davis equation allow for the accurate determination of aqueous Zn species in solutions up to 0.7 mol L^{-1} NaCl. Modelling of the Zn speciation in saline soil solutions shows that Zn speciation is increasingly controlled by interactions with chloride (Cl) and carbonate ions (HCO_3) and dissolved organic carbon (DOC), especially in the pH range between 4 and 8. The competitive nature of Cl, DOC and HCO3 ions for the coordination with Zn was observed during the model analysis and Zn-Cl complexes were more dominant than Zn-CO3 complexes in the Zn-NaCl-HCO3 system. The domination of Zn-Cl complexes was explained by the soft Lewis acidity of Zn, the mechanistic theory of hardness-softness factor and the crystal field stabilization energy.

The adsorption of Zn on *Tropaquept* (Bay) and *Hydraquent* (Tiaong) soils at $[Zn]_{init}$ = 0.08 and 0.8 mmol L^{-1}, respectively was decreased with increasing NaCl concentrations from 0.1 to 0.3 and 0.7 mol L^{-1} in the pH range between 3 and 7. This was primarily due to the increasing Zn-Cl complexes with increasing NaCl concentrations. It was found that Zn is adsorbed mainly by SOM and clay at acidic to neutral pH (3 – 7) and the presence of Zn-Cl complexes does not adsorb by SOM and clay. Compared with the Zn adsorption curve in NaCl solutions, the presence of carbonate in NaCl solutions does not change Zn adsorption in both soils at $[Zn]_{init}$ = 0.08 mmol L^{-1}. However, the shape of the Zn adsorption curve was moved to 30-35% higher at pH 6 to 7.5 in the presence of carbonate in NaCl solutions at $[Zn]_{init}$ = 0.8 mmol L^{-1}. Model results suggested that the increased shape of the Zn adsorption between pH 6 and 7.5 was due

to precipitation in the presence of HCO_3. Zn was entirely adsorbed on soils at pH > 7 due to the high affinity of iron (hydr)oxides surfaces and the adsorption did not change with increasing NaCl concentrations, and with the presence of carbonate.

Multi-surface models (MSMs) with experimentally determined model parameters (an active fraction of SOM, iron (hydr)oxides and the surface charge of clay) and predefined generic surface complexation parameters optimized at low ionic strength were used to predict Zn adsorption and dominant sorbent phases in soils in different NaCl concentrations and NaCl-HCO_3 system. The study found that the MSMs accurately predict Zn adsorption in 0.1 and 0.3 mol L^{-1} NaCl concentrations and in the presence of carbonate. However, zinc adsorption is underpredicted in the low pH range (3-5) in 0.7 mol L^{-1} NaCl, likely due to the absence of ternary surface complexation constants (≡FeOH-Zn-Cl and ≡FeOH-Zn-HCO_3) in the model databases. Modelling results revealed that the dominant sorbent phase was SOM in near neutral and acidic pH soil and iron (hydr)oxides in alkaline pH soil. Clay is not an important sorbent for Zn in soils as the cations (Ca, Mg, K and Na) in soil solution compete with Zn and occupy most of the clay surface. MSMs prediction also indicated that Zn precipitation is an important surface process to remove Zn from solutions at $[Zn_{init}]$ = 0.8 mmol L^{-1}. Modelling results of Bangladesh soils with MSM's verify experimental observation. This observation suggests that the MSMs can apply to a wide range of soils for predicting metal adsorption in different environmental conditions.

A central theme of this thesis was the identification of multi-surface models (MSMs) performance for predicting Zn adsorption on soils at seawater ionic strength. The model uncertainty in the 0.7 mol L^{-1} NaCl solution highlighted the need for improving the model database of iron (hydr)oxides by introducing ternary surface complexation constants. Therefore, the constant capacitance model (CCM) was used to assess Zn adsorption on goethite in two initial concentrations of Zn and to develop surface complexation model parameters of Zn on goethite. Experimental results revealed that the increased concentration of NaCl from 0.1 to 0.7 mol L^{-1} increased the adsorption of Zn on goethite at $[Zn]_{init}$ = 0.08 mmol L^{-1} whereas Zn adsorption decreased at $[Zn]_{init}$ = 0.8 mmol L^{-1}. The CCM with monodentate and bidentate surface complexes of Zn gave an accurate prediction in the adsorption of Zn in 0.1 mol L^{-1} NaCl solution. The CCM accuracy to predict Zn adsorption on goethite at $[Zn]_{init}$ = 0.08 mmol L^{-1} in 0.3 and 0.7 mol L^{-1} NaCl solutions were improved when ternary surface complexations were introduced. Prediction of Zn adsorption at $[Zn]_{init}$ = 0.8 mmol L^{-1} was inaccurate, due to the influence of Zn precipitation. Precipitation is an important Zn removal mechanism at a high

initial concentration of Zn. Therefore, the surface complexation constants for Zn adsorption obtained from the adsorption experiment at $[Zn]_{init}$ = 0.08 mmol L^{-1} were not valid for predicting Zn adsorption at a high initial concentration of Zn. The CCM offers two model protocols that can be used to predict Zn adsorption in different initial concentrations.

7.2 New Concepts Emerging from this Work

This thesis proposes new concepts and innovations. Firstly, this work benchmarks for the first time the applicability of multi surface models (MSMs) with pre-defined databases to study the effect of salinity on Zn surface processes in tropical soils. The models accurately predict Zn surface processes in saline solutions up to 0.7 mol L^{-1} NaCl and at neutral to alkaline pH. Model uncertainty is observed at low pH and NaCl concentration above 0.3 mol L^{-1}. This suggests that the MSMs can be applied accurately in soils with pH > 7 to evaluate the effect of salinity increase due to climate change and/or management options on the mobility and bioavailability of Zn. Secondly, this work improves our understanding of the effect of NaCl concentration/salinity on Zn surface processes in tropical soils with different initial Zn concentrations. The effect of NaCl is generally most distinct in acidic conditions. The MSMs also identifies the major adsorption species of Zn in soils in different pHs. Thirdly, surface complexation modelling confirms the presence of ternary complexes in NaCl concentration above 0.1 mol L^{-1} that were previously reported by spectroscopic analysis. Improved parameterisation reproduce the adsorption of Zn at low pH in high NaCl solution. Determining complexation constants of ternary surfaces with other iron (hydr)oxides by the CCM, DLM and TLM and incorporating in existing databases of MSMs will be allowing MSMs to accurately predict Zn adsorption in soils. Finally. this work indicates that the application of a high concentration of Zn in soils with pH > 7 might not be detrimental to crop production and human health. Our experimental and model analysis indicated that large Zn applications (≈ 900 kg/ha) are fully adsorbed at pH > 7 and increasing NaCl concentration does not decrease Zn adsorption significantly.

7.3 Future Research

I suggest the following areas of future research.

1. Clay models are underrepresented in MSMs. Illite is generally considered a representative clay mineral with a surface charge of 0.1 to 0.4 mol kg^{-1}. This approach significantly underrepresents clays because smectite, vermiculite, and other clay minerals are also present in soil systems with a higher surface charge. Therefore, the

concept of the clay model needs to be extended to more realistic and natural systems by counting sub-models of different clay minerals. This extension will help to develop generic model parameters for clay minerals as well as improve and further broaden the applicability of MSMs.

2. The active fraction of SOM needs to be determined by a systematic evaluation of selective methods for providing a recommended fraction for model analysis. The active fraction of SOM reported in the literature range from 31% to 87% (Groenenberg and Lofts, 2014). Because of this variation, it is difficult to provide a recommended fraction for model analysis. A higher fraction of SOM during a model analysis generally overestimates model prediction whereas a lower fraction of SOM underestimates model prediction. Therefore, a systematic evaluation of selective methods for determining the active fraction of SOM is required with a set of tropical and temperate soils representing a different amounts of organic matter for providing a general guideline for determining the active fraction of soil organic matter. In addition, model parameters of humic acid need to be updated with recent experimental data and calibrated in higher NaCl concentrations.
3. The role Zn-Cl complexes on Zn adsorption at a different initial concentration of Zn needs further analysis in different solid-liquid ratios to confirm whether and increasing Zn-Cl complexes increase Zn adsorption by ternary surface complexes or whether increasing Zn-Cl complexes decrease Zn adsorption by increasing Zn mobility. This could be achieved by conducting combined laboratory adsorption experiments and spectroscopic analysis. The advantage of spectroscopic analysis like EXAFS analysis is that it will provide binding pieces of information of Zn with adsorption surfaces. This information will help to develop a surface complexation modelling approach of Zn at a different initial concentration in different NaCl solutions.
4. Surface complexation constants of metal ternary surface complexes are not updated, cross-checked and included in the model databases. To improve the model performance in wider environmental conditions, a set of generic model parameters of metal ternary surface complexes is needed. Conducting experiments with different concentrations of inorganic ligands (Cl, SO_4, PO_4, etc) in different liquid to solid ratios (different initial concentrations of metal), spectroscopic analysis, and various surface complexation modelling approaches (CCM, DLM, TLM, and CD-MUSIC) will be a good way to build a set of generic model parameters of metal ternary surface complexes.

5. MSMs are a very promising technique for predicting Zn and metal mobility on soils if the model parameters are determined correctly. The next challenge is to introduce MSMs for predicting metal uptake by plants and other organisms in soil-plant interactions. Plants rhizosphere areas are different from than soil environment. In the rhizosphere, plant roots release a variety of light organic acids which make complexes with metal and increase metal uptake by plants. A variety of microorganisms present in the rhizosphere also influence metal mobility. Incorporating experimental data on metal with root induced organic acid and microorganisms in MSMs will improve the predicting capability of metal in soil-plant interactions as well as in the response to soil management options.

References

Acosta, J.A., Jansen, B., Kalbitz, K., Faz, A., Martinez-Martinez, S., 2011. Salinity increases mobility of heavy metals in soils. Chemosphere 85(8), 1318-1324. https://doi.org/10.1016/j.chemosphere.2011.07.046

Ahmed, A., Ghosh, P.K., Hasan, M., Rahman, A., 2020. Surface and groundwater quality assessment and identification of hydrochemical characteristics of a south-western coastal area of Bangladesh. Environmental Monitoring and Assessment 192(4), 258. https://doi.org/10.1007/s10661-020-8227-0

Ahmed, F., Khanam, A., Haider, M.Z., Rahman, M.S., 2010. Land use pattern and socio-economic condition of the Sundarbans adjacent coastal area of Bangladesh. Khulna University Studies 2010, 57-72.

Akter, S., Ahmed, K.R., Marandi, A., Schuth, C., 2020. Possible factors for increasing water salinity in an embanked coastal island in the southwest Bengal Delta of Bangladesh. Science of the Total Environment 713, 136668. https://doi.org/10.1016/j.scitotenv.2020.136668

Alessi, D.S., Fein, J.B., 2010. Cadmium adsorption to mixtures of soil components: Testing the component additivity approach. Chemical Geology 270(1-4), 186-195. https://doi.org/10.1016/j.chemgeo.2009.11.016

Alloway, B.J., 1990. Soil processes and the behaviour of metals. In: B.J. Alloway (Ed.), Heavy metals in soils. pp. 7-28.

Alloway, B.J., 2008. Zinc in soils and crop nutrition. International Zinc Association (IZA) and International Fertilizer Industry Association (IFA), Belgium and France.

Alloway, B.J., 2009. Soil factors associated with zinc deficiency in crops and humans. Environmental Geochemistry and Health 31(5), 537-548. https://doi.org/10.1007/s10653-009-9255-4

Alyuz, B., Veli, S., 2009. Kinetics and equilibrium studies for the removal of nickel and zinc from aqueous solutions by ion exchange resins. Journal of Hazardous Materials 167(1-3), 482-488. https://doi.org/10.1016/j.jhazmat.2009.01.006

Appel, C., Ma, L., 2002. Concentration, pH, and surface charge effects on cadmium and lead sorption in three tropical soils. Journal of Environmental Quality 31(2), 581-589. https://doi.org/10.2134/jeq2002.5810

Avendano, L., Gledhill, M., Achterberg, E.P., Rerolle, V.M.C., Schlosser, C., 2016. Influence of ocean acidification on the organic complexation of iron and copper in northwest European shelf seas; a combined observational and model study. Frontiers in Marine Science 3. https://doi.org/10.3389/fmars.2016.00058

Ayers, J.C., Goodbred, S., George, G., Fry, D., Benneyworth, L., Hornberger, G., Roy, K., Karim, M.R., Akter, F., 2016. Sources of salinity and arsenic in groundwater in southwest Bangladesh. Geochemical Transactions 17 (4). https://doi.org/10.1186/s12932-016-0036-6

Baeza, J.J.B., RamisRamos, G., 1996. A series expansion of the extended Debye-Huckel equation and application to linear prediction of stability constants. Talanta 43(9), 1579-1587. https://doi.org/10.1016/0039-9140(96)01942-X

Baldock, J.A., Nelson, P.N., 2000. Soil organic matter. In: M.E. Sumner (Ed.), Handbook of Soil Science. CRC Press, USA, pp. B25 - B84.

Balistrieri, L.S., Chao, T.T., 1990. Adsorption of selenium by amorphous iron oxyhydroxide and manganese-dioxide. Geochimica Et Cosmochimica Acta 54(3), 739-751. https://doi.org/10.1016/0016-7037(90)90369-V

Balistrieri, L.S., Murray, J.W., 1981. The surface-chemistry of goethite (α-FeOOH) in major ion seawater. American Journal of Science 281(6), 788-806. https://doi.org/10.2475/ajs.281.6.788

Balistrieri, L.S., Murray, J.W., 1982. The adsorption of Cu, Pb, Zn, and Cd on goethite from major ion sea-water. Geochimica Et Cosmochimica Acta 46(7), 1253-1265. https://doi.org/10.1016/0016-7037(82)90010-2

Barakat, M.A., 2011. New trends in removing heavy metals from industrial wastewater. Arabian Journal of Chemistry 4(4), 361-377. https://doi.org/10.1016/j.arabjc.2010.07.019

Baranowski, R., Rybak, A., Baranowska, I., 2002. Speciation analysis of elements in soil samples by XRF. Polish Journal of Environmental Studies 11(5), 473-482.

Bargar, J.R., Brown, G.E., Parks, G.A., 1998. Surface complexation of Pb(II) at oxide-water interfaces: III. XAFS determination of Pb(II) and Pb(II)-chloro adsorption complexes on goethite and alumina. Geochimica Et Cosmochimica Acta 62(2), 193-207. https://doi.org/10.1016/S0016-7037(97)00334-7

Benedetti, M.F., Milne, C.J., Kinniburgh, D.G., Vanriemsdijk, W.H., Koopal, L.K., 1995. Metal-ion binding to humic substances - application of the nonideal competitive adsorption model. Environmental Science & Technology 29(2), 446-457. https://doi.org/10.1021/es00002a022

Benedetti, M.F., vanRiemsdik, W.H., Koopal, L.K., 1996. Humic substances considered as a heterogeneous donnan gel phase. Environmental Science & Technology 30(6), 1805-1813. https://doi.org/10.1021/es950012y

Bergmann, J., Friedel, P., Kleeberg, R., 1998. BGMN - a new fundamental parameters based Rietveld program for laboratory X-ray sources, it's use in quantitative analysis and structure investigations CPD Newsletter. Commission of Powder Diffraction, International Union of Crystallography, pp. 5-8.

Bingham, F.T., Page, A.L., Sims, J.R., 1964. Retention of Cu and Zn by H-Montmorillonite. Soil Science Society of America Journal 28(3), 351-354. https://doi.org/10.2136/sssaj1964.03615995002800030015x

Boguta, P., Sokolowska, Z., 2020. Zinc Binding to fulvic acids: assessing the impact of pH, metal concentrations and chemical properties of fulvic acids on the mechanism and stability of formed soluble complexes. Molecules 25(6), 1297. https://doi.org/10.3390/molecules25061297

Bolland, M.D.A., Posner, A.M., Quirk, J.P., 1977. Zinc adsorption by goethite in absence and presence of phosphate. Australian Journal of Soil Research 15(3), 279-286. https://doi.org/10.1071/SR9770279

Bonito, M.D., Lofts, S., Groenenberg, J.E., 2018. Models of Geochemical Speciation: Structure and Applications. In: B.D. Vivo, H.E. Belkin, A. Lima (Eds.), Environmental Geochemistry. Elsevier, pp. 237-305.

Bonten, L.T.C., Groenenberg, J.E., Meesenburg, H., de Vries, W., 2011. Using advanced surface complexation models for modelling soil chemistry under forests: Solling forest, Germany. Environmental Pollution 159(10), 2831-2839. https://doi.org/10.1016/j.envpol.2011.05.002

Bonten, L.T.C., Groenenberg, J.E., Weng, L., van Riemsdijk, W.H., 2008. Use of speciation and complexation models to estimate heavy metal sorption in soils. Geoderma 146(1-2), 303-310. https://doi.org/10.1016/j.geoderma.2008.06.005

Bradl, H.B., 2004. Adsorption of heavy metal ions on soils and soils constituents. Journal of Colloid and Interface Science 277(1), 1-18. https://doi.org/10.1016/j.jcis.2004.04.005

Brammer, H., 1972. Reconnaissance soil survey of Bangladesh. Soil Resource Development Institute, Dhaka, Bangladesh.

Brecht, H., Dasgupta, S., Laplante, B., Murray, S., Wheeler, D., 2012. Sea-level rise and storm surges: high stakes for a small number of developing countries. Journal of Environment & Development 21(1), 120-138. https://doi.org/10.1177/1070496511433601

Briffa, J., Sinagra, E., Blundell, R., 2020. Heavy metal pollution in the environment and their toxicological effects on humans. Heliyon 6(9). https://doi.org/10.1016/j.heliyon.2020.e04691

Bringolf, R.B., Morris, B.A., Boese, C.J., Santore, R.C., Allen, H.E., Meyer, J.S., 2006. Influence of dissolved organic matter on acute toxicity of zinc to larval fathead minnows (Pimephales promelas). Archives of Environmental Contamination and Toxicology 51(3), 438-444. https://doi.org/10.1007/s00244-005-0088-6

Broadley, M., Brown, P., Chkmak, I., Rengel, J., Zhao, F., 2012. Functions of nutrients: micronutrients. In: P. Marschner (Ed.), Mineral Nutrition of Higher Plants. Academic press, USA, pp. 191-248.

Brown, K.H., Peerson, J.M., Rivera, J., Allen, L.H., 2002. Effect of supplemental zinc on the growth and serum zinc concentrations of prepubertal children: a meta-analysis of randomized controlled trials. American Journal of Clinical Nutrition 75(6), 1062-1071. https://doi.org/10.1093/ajcn/75.6.1062

Brummer, G., Tiller, K.G., Herms, U., Clayton, P.M., 1983. Adsorption desorption and/or precipitation - dissolution processes of zinc in soils. Geoderma 31(4), 337-354. https://doi.org/10.1016/0016-7061(83)90045-9

Bryan, S.E., Tipping, E., Hamilton-Taylor, J., 2002. Comparison of measured and modelled copper binding by natural organic matter in freshwaters. Comparative Biochemistry and Physiology C-Toxicology & Pharmacology 133(1-2), 37-49. https://doi.org/10.1016/S1532-0456(02)00083-2

Buekers, J., Van Laer, L., Amery, F., Van Buggenhout, S., Maes, A., Smolders, E., 2007. Role of soil constituents in fixation of soluble Zn, Cu, Ni and Cd added to soils. European Journal of Soil Science 58(6), 1514-1524. https://doi.org/10.1111/j.1365-2389.2007.00958.x

Butler, B.A., 2009. Effect of pH, ionic strength, dissolved organic carbon, time, and particle size on metals release from mine drainage impacted streambed sediments. Water Research 43(5), 1392-1402. https://doi.org/10.1016/j.watres.2008.12.009

Byrne, R.H., Kump, L.R., Cantrell, K.J., 1988. The influence of temperature and pH on trace-metal speciation in seawater. Marine Chemistry 25(2), 163-181. https://doi.org/10.1016/0304-4203(88)90062-X

Chesne, R.B., Kim, C.S., 2014. Zn(II) and Cu(II) adsorption and retention onto iron oxyhydroxide nanoparticles: effects of particle aggregation and salinity. Geochemical Transactions 15, 6. https://doi.org/10.1186/1467-4866-15-6

Christensen, J.B., Christensen, T.H., 2000. The effect of pH on the complexation of Cd, Ni and Zn by dissolved organic carbon from leachate-polluted groundwater. Water Research 34(15), 3743-3754. https://doi.org/10.1016/S0043-1354(00)00127-5

Chu, B., Chen, X.J., Li, Q.S., Yang, Y.F., Mei, X.Q., He, B.Y., Li, H., Tan, L., 2015. Effects of salinity on the transformation of heavy metals in tropical estuary wetland soil. Chemistry and Ecology 31(2), 186-198. https://doi.org/10.1080/02757540.2014.917174

Cornell, R.M., Schwertmann, U., 2003. The iron oxides: structure, properties, reactions, occurrences and uses (Ed. 2). Wiley press Ltd.

Corwin, D.L., 2021. Climate change impacts on soil salinity in agricultural areas. European Journal of Soil Science 72(2), 842-862. https://doi.org/10.1111/ejss.13010

D'Amore, J.J., Al-Abed, S.R., Scheckel, K.G., Ryan, J.A., 2005. Methods for speciation of metals in soils: A review. Journal of Environmental Quality 34(5), 1707-1745. https://doi.org/10.2134/jeq2004.0014

Dasgupta, S., Hossain, M.M., Huq, M., Wheeler, D., 2015. Climate change and soil salinity: The case of coastal Bangladesh. Ambio 44(8), 815-826. https://doi.org/10.1007/s13280-015-0681-5

Dasgupta, S., Kamal, F.A., Khan, Z.H., Choudhury, S., Nishat, A., 2014. River salinity and climate change: evidence from coastal Bangladesh. Policy Research Working Paper - World Bank (6817), 44 pp.

Davies, C.W., 1938. 397. The extent of dissociation of salts in water. Part VIII. An equation for the mean ionic activity coefficient of an electrolyte in water, and a revision of the dissociation constants of some sulphates. Journal of the Chemical Society (Resumed) (0), 2093-2098. https://doi.org/10.1039/JR9380002093

Davis, J.A., James, R.O., Leckie, J.O., 1978. Surface ionization and complexation at the oxide/water interface: I. Computation of electrical double layer properties in simple electrolytes. Journal of Colloid and Interface Science 63(3), 480-499. https://doi.org/10.1016/S0021-9797(78)80009-5

de Matos, A.T., Fontes, M.P.F., da Costa, L.M., Martinez, M.A., 2001. Mobility of heavy metals as related to soil chemical and mineralogical characteristics of Brazilian soils. Environmental Pollution 111(3), 429-435. https://doi.org/10.1016/S0269-7491(00)00088-9

de Pablo, L., Chavez, M.L., Abatal, M., 2011. Adsorption of heavy metals in acid to alkaline environments by montmorillonite and Ca-montmorillonite. Chemical Engineering Journal 171(3), 1276-1286. https://doi.org/10.1016/j.cej.2011.05.055

Degryse, F., Smolders, E., Parker, D.R., 2009. Partitioning of metals (Cd, Co, Cu, Ni, Pb, Zn) in soils: concepts, methodologies, prediction and applications - a review. European Journal of Soil Science 60(4), 590-612. https://doi.org/10.1111/j.1365-2389.2009.01142.x

Degryse, F., Voegelin, A., Jacquat, O., Kretzschmar, R., Smolders, E., 2011. Characterization of zinc in contaminated soils: complementary insights from isotopic exchange, batch extractions and

XAFS spectroscopy. European Journal of Soil Science 62(2), 318-330. https://doi.org/10.1111/j.1365-2389.2010.01332.x

Derobertis, A., Destefano, C., Sammartano, S., Gianguzza, A., 1994. Equilibrium studies in natural fluids - a chemical speciation model for the major constituents of seawater. Chemical Speciation and Bioavailability 6(2-3), 65-84. https://doi.org/10.1080/09542299.1994.11083225

Dijkstra, J.J., Meeussen, J.C.L., Comans, R.N.J., 2004. Leaching of heavy metals from contaminated soils: An experimental and modeling study. Environmental Science & Technology 38(16), 4390-4395. https://doi.org/10.1021/es049885v

Dijkstra, J.J., Meeussen, J.C.L., Comans, R.N.J., 2009. Evaluation of a generic multisurface sorption model for inorganic soil contaminants. Environmental Science & Technology 43(16), 6196-6201. https://doi.org/10.1021/es900555g

Doebelin, N., Kleeberg, R., 2015. Profex: a graphical user interface for the Rietveld refinement program BGMN. Journal of Applied Crystallography 48, 1573-1580. https://doi.org/10.1107/S1600576715014685

Dong, W.M., Guo, Z.J., Du, J.Z., Zheng, L.Y., Tao, Z.Y., 2001. Sorption characteristics of zinc(II) by calcareous soil-radiotracer study. Applied Radiation and Isotopes 54(3), 371-375. https://doi.org/10.1016/S0969-8043(99)00263-8

Du Laing, G., De Vos, R., Vandecasteele, B., Lesage, E., Tack, F.M.G., Verloo, M.G., 2008. Effect of salinity on heavy metal mobility and availability in intertidal sediments of the Scheldt estuary. Estuarine Coastal and Shelf Science 77(4), 589-602. https://doi.org/10.1016/j.ecss.2007.10.017

Du Laing, G., Rinklebe, J., Vandecasteele, B., Meers, E., Tack, F.M.G., 2009. Trace metal behaviour in estuarine and riverine floodplain soils and sediments: A review. Science of the Total Environment 407(13), 3972-3985. https://doi.org/10.1016/j.scitotenv.2008.07.025

Duff, M.C., Amrhein, C., 1996. Uranium(VI) adsorption on goethite and soil in carbonate solutions. Soil Science Society of America Journal 60(5), 1393-1400. https://doi.org/10.2136/sssaj1996.03615995006000050014x

Duffner, A., Weng, L., Hoffland, E., van der Zee, S.E.A.T.M., 2014. Multi-surface modeling to predict free zinc ion concentrations in low-zinc soils. Environmental Science & Technology 48(10), 5700-5708. https://doi.org/10.1021/es500257e

Dyer, J.A., Trivedi, P., Scrivner, N.C., Sparks, D.L., 2004. Surface complexation modeling of zinc sorption onto ferrihydrite. Journal of Colloid and Interface Science 270(1), 56-65 https://doi.org/10.1016/S0021-9797(03)00618-0.

Dzombak, D.A., Morel, F.M.M., 1990. Surface Complexation Modeling: Hydrous Ferric Oxide. John Wiley & Sons, New York.

Fan, M., Boonfueng, T., Xu, Y., Axe, L., Tyson, T.A., 2005. Modeling Pb sorption to microporous amorphous oxides as discrete particles and coatings. Journal of Colloid and Interface Science 281(1), 39-48. https://doi.org/10.1016/j.jcis.2004.08.050

Fan, T.T., Wang, Y.J., Li, C.B., He, J.Z., Gao, J., Zhou, D.M., Friedman, S.P., Sparks, D.L., 2016. Effect of organic matter on sorption of Zn on soil: elucidation by wien effect measurements and EXAFS spectroscopy. Environmental Science & Technology 50(6), 2931-2937. https://doi.org/10.1021/acs.est.5b05281

Fang, J., Lau, C.K.M., Lu, Z., Wu, W., Zhu, L., 2019. Natural disasters, climate change, and their impact on inclusive wealth in G20 countries. Environmental Science and Pollution Research 26(2), 1455-1463. https://doi.org/10.1007/s11356-018-3634-2

Ferri, D., Grenthe, I., Hietanen, S., Neherneumann, E., Salvatore, F., 1985. Studies on metal carbonate equilibria.12. Zinc(II) carbonate complexes in acid solutions. Acta Chemica Scandinavica Series a-Physical and Inorganic Chemistry 39(5), 347-353. https://doi.org/10.3891/acta.chem.scand.39a-0347

Fisher-Power, L.M., Cheng, T., Rastghalam, Z.S., 2016. Cu and Zn adsorption to a heterogeneous natural sediment: Influence of leached cations and natural organic matter. Chemosphere 144, 1973-1979. https://doi.org/10.1016/j.chemosphere.2015.10.109

Forbes, E.A., Posner, A.M., Quirk, J.P., 1976. Specific adsorption of divalent Cd, Co, Cu, Pb, and Zn on goethite. Journal of Soil Science 27(2), 154-166. https://doi.org/10.1111/j.1365-2389.1976.tb01986.x

Gao, Y., Mucci, A., 2001. Acid base reactions, phosphate and arsenate complexation, and their competitive adsorption at the surface of goethite in 0.7 M NaCl solution. Geochimica Et Cosmochimica Acta 65(14), 2361-2378. https://doi.org/10.1016/S0016-7037(01)00589-0

Gao, Y., Mucci, A., 2003. Individual and competitive adsorption of phosphate and arsenate on goethite in artificial seawater. Chemical Geology 199(1-2), 91-109. https://doi.org/10.1016/S0009-2541(03)00119-0

Goldberg, S., 1998. Ion Adsorption at the Soil Particle-Solution Interface: Modeling and Mechanisms. In: P.M. Huang, N. Senesi, J. Buffle (Eds.), Structure and Surface Reactions of Soil Particles. Wiley, New YorK, pp. 377.

Goldberg, S., 2013. Surface Complexation Modeling. In: S.A. Elias (Ed.), Reference Module in Earth Systems and Environmental Sciences. Elsevier.

Gomes, P.C., Fontes, M.P.F., da Silva, A.G., Mendonca, E.D., Netto, A.R., 2001. Selectivity sequence and competitive adsorption of heavy metals by Brazilian soils. Soil Science Society of America Journal 65(4), 1115-1121. https://doi.org/10.2136/sssaj2001.6541115x

Grafe, M., Sparks, D.L., 2005. Kinetics of zinc and arsenate co-sorption at the goethite-water interface. Geochimica Et Cosmochimica Acta 69(19), 4573-4595. https://doi.org/10.1016/j.gca.2005.04.016

GRID-Arendal, 2009. Impact of sea level rise in Bangladesh, pp. https://www.grida.no/resources/5648

Groenenberg, J.E., Dijkstra, J.J., Bonten, L.T.C., de Vries, W., Comans, R.N.J., 2012. Evaluation of the performance and limitations of empirical partition-relations and process based multisurface models to predict trace element solubility in soils. Environmental Pollution 166, 98-107. https://doi.org/10.1016/j.envpol.2012.03.011

Groenenberg, J.E., Koopmans, G.F., Comans, R.N.J., 2010. Uncertainty analysis of the nonideal competitive adsorption-donnan model: effects of dissolved organic matter variability on predicted metal speciation in soil solution. Environmental Science & Technology 44(4), 1340-1346. https://doi.org/10.1021/es902615w

Groenenberg, J.E., Lofts, S., 2014. The use of assemblage models to describe trace element partitioning, speciation, and fate: a review. Environmental Toxicology and Chemistry 33(10), 2181-2196. https://doi.org/10.1002/etc.2642

Groenenberg, J.E., Romkens, P.F.A.M., Van Zomeren, A., Rodrigues, S.M., Comans, R.N.J., 2017. Evaluation of the single dilute (0.43 M) nitric acid extraction to determine geochemically reactive elements in soil. Environmental Science & Technology 51(4), 2246-2253. https://doi.org/10.1021/acs.est.6b05151

Gu, Q., Lin, R.-L., 2010. Heavy metals zinc, cadmium, and copper stimulate pulmonary sensory neurons via direct activation of TRPA1. Journal of Applied Physiology 108(4), 891-897. https://doi.org/10.1152/japplphysiol.01371.2009

Gu, X.Y., Evans, L.J., 2007. Modelling the adsorption of Cd(II), Cu(II), Ni(II), Pb(II), and Zn(II) onto Fithian illite. Journal of Colloid and Interface Science 307(2), 317-325. https://doi.org/10.1016/j.jcis.2006.11.022

Guevara-Riba, A., Sahuquillo, A., Rubio, R., Rauret, G., 2005. Effect of chloride on heavy metal mobility of harbour sediments. Analytical and Bioanalytical Chemistry 382(2), 353-359. https://doi.org/10.1007/s00216-005-3103-x

Gunton, C.G., 2007. An experimental study of the effect of NaCl and Na_2SO_4 on Cu and Zn adsorption onto synthetic goethite, PhD Thesis. The Australian National University, Australia.

Gunton, C.G., McPhail, D.C., Christy, A.G., 2006. The influence of chloride and sulfate on Cu and Zn adsorption on goethite. Geochimica Et Cosmochimica Acta 70(18), A220-A220. https://doi.org/10.1016/j.gca.2006.06.442

Gupta, A., Sharma, V., Sharma, K., Kumar, V., Choudhary, S., Mankotia, P., Kumar, B., Mishra, H., Moulick, A., Ekielski, A., Mishra, P.K., 2021. A review of adsorbents for heavy metal decontamination: growing approach to wastewater treatment. Materials 14(16). https://doi.org/10.3390/ma14164702

Gustafsson, J.P., 2001. Modeling the acid-base properties and metal complexation of humic substances with the Stockholm Humic Model. Journal of Colloid and Interface Science 244(1), 102-112. https://doi.org/10.1006/jcis.2001.7871

Gustafsson, J.P., 2019. Visual MINTEQ. KTH Royal Institute of Technology, Stockholm, Sweden.

Gustafsson, J.P., Kleja, D.B., 2005. Modeling salt-dependent proton binding by organic soils with the MICA-Donnan and Stockholm Humic models. Environmental Science & Technology 39(14), 5372-5377. https://doi.org/10.1021/es0503332

Gustafsson, J.P., Pechova, P., Berggren, D., 2003. Modeling metal binding to soils: The role of natural organic matter. Environmental Science & Technology 37(12), 2767-2774. https://doi.org/10.1021/es026249t

Gustafsson, J.P., van Schaik, J.W.J., 2003. Cation binding in a mor layer: batch experiments and modelling. European Journal of Soil Science 54(2), 295-310. https://doi.org/10.1046/j.1365-2389.2003.00526.x

Haque, S.A., 2006. Salinity problems and crop production in coastal regions of Bangladesh. Pakistan Journal of Botany 38(5), 1359-1365.

Hatje, V., Payne, T.E., Hill, D.M., McOrist, G., Birch, G.F., Szymczak, R., 2003. Kinetics of trace element uptake and release by particles in estuarine waters: effects of pH, salinity, and particle loading. Environment International 29(5), 619-629. https://doi.org/10.1016/S0160-4120(03)00049-7

Hayes, K.F., Leckie, J.O., 1987. Modeling ionic-strength effects on cation adsorption at hydrous oxide-solution interfaces. Journal of Colloid and Interface Science 115(2), 564-572. https://doi.org/10.1016/0021-9797(87)90078-6

Hayes, K.F., Redden, G., Ela, W., Leckie, J.O., 1991. Surface complexation models - an evaluation of model parameter estimation using FITEQL and oxide mineral titration data. Journal of Colloid and Interface Science 142(2), 448-469. https://doi.org/10.1016/0021-9797(91)90075-J

Haynes, W.M., 2015-2016. CRC Handbook of Chemistry and Physics. 96th ed. Taylor and Francis, Florida, USA.

Heijerick, D.G., De Schamphelaere, K.A.C., Janssen, C.R., 2002. Predicting acute zinc toxicity for Daphnia magna as a function of key water chemistry characteristics: Development and validation of a biotic ligand model. Environmental Toxicology and Chemistry 21(6), 1309-1315. https://doi.org/10.1002/etc.5620210628

Heijerick, D.G., Janssen, C.R., De Coen, W.M., 2003. The combined effects of hardness, pH, and dissolved organic carbon on the chronic toxicity of Zn to D-magna: Development of a surface response model. Archives of Environmental Contamination and Toxicology 44(2), 210-217. https://doi.org/10.1007/s00244-002-2010-9

Hiemstra, T., VanRiemsdijk, W.H., 1996. A surface structural approach to ion adsorption: The charge distribution (CD) model. Journal of Colloid and Interface Science 179(2), 488-508. https://doi.org/10.1006/jcis.1996.0242

Hinz, C., Selim, H.M., 1994. Transport of zinc and cadmium in soils - experimental evidence and modeling approaches. Soil Science Society of America Journal 58(5), 1316-1327. https://doi.org/10.2136/sssaj1994.03615995005800050006x

Hohl, H., Stumm, W., 1976. Interaction of Pb^{2+} with hydrous γ-Al_2O_3. Journal of Colloid And Interface Science 55(2), 281-288. https://doi.org/10.1016/0021-9797(76)90035-7

Hug, S.J., Leupin, O.X., Berg, M., 2008. Bangladesh and Vietnam: Different groundwater compositions require different approaches to arsenic mitigation. Environmental Science & Technology 42(17), 6318-6323. https://doi.org/10.1021/es7028284

Huq, S.M.I., Shoaib, J.U.M., 2013. The soils of Bangladesh. Springer publication Ltd. pp.-165. https://doi.org/10.1007/978-94-007-1128-0

Hyne, R.V., Pablo, F., Julli, M., Markich, S.J., 2005. Influence of water chemistry on the acute toxicity of copper and zinc to the cladoceran Ceriodaphnia cf dubia. Environmental Toxicology and Chemistry 24(7), 1667-1675. https://doi.org/10.1897/04-497R.1

Impa, S.M., Johnson-Beebout, S.E., 2012. Mitigating zinc deficiency and achieving high grain Zn in rice through integration of soil chemistry and plant physiology research. Plant and Soil 361(1-2), 3-41. https://doi.org/10.1007/s11104-012-1315-3

Islam, A., Lotse, E.G., 1986. Quantitative mineralogical analysis of some Bangladesh soils with X-ray, ion-exchange and selective dissolution techniques. Clay Minerals 21(1), 31-42. https://doi.org/10.1180/claymin.1986.021.1.03

Islam, M.M., Karim, M.R., Zheng, X., Li, X., 2018. Heavy metal and metalloid pollution of soil, water and foods in Bangladesh: A critical review. International Journal of Environmental Research and Public Health 15(12), 2825. https://doi.org/10.3390/ijerph15122825

Izquierdo, M., Impa, S.M., Johnson-Beebout, S.E., Weiss, D.J., Kirk, G.J.D., 2016. Measurement of isotopically-exchangeable Zn in Zn-deficient paddy soil. European Journal of Soil Science 67(1), 51-59. https://doi.org/10.1111/ejss.12303

Jalali, M., Zinli, N.A.M., 2012. Effects of common ions on Zn sorption in some calcareous soils of Western Iran. Pedosphere 22(2), 190-200. https://doi.org/10.1016/S1002-0160(12)60005-8

Jeffery, J.J., Uren, N.C., 1983. Copper and zinc species in the soil solution and the effects of soil pH. Australian Journal of Soil Research 21(4), 479-488. https://doi.org/10.1071/SR9830479

Johnson-Beebout, S.E., Lauren, J.G., Duxbury, J.M., 2009. Immobilization of zinc fertilizer in flooded soils monitored by adapted DTPA soil test. Communications in Soil Science and Plant Analysis 40(11-12), 1842-1861. https://doi.org/10.1080/00103620902896738

Kalbasi, M., Racz, G.J., Lewenrudgers, L.A., 1978. Reaction products and solubility of applied zinc compounds in some manitoba soils. Soil Science 125(1), 55-64.

Katyal, J.C., Sharma, B.D., 1991. DTPA-extractable and total Zn, Cu, Mn, and Fe in Indian soils and their association with some soil properties. Geoderma 49(1-2), 165-179. https://doi.org/10.1016/0016-7061(91)90099-F

Katz, L.E., Hayes, K.F., 1995a. Surface complexation modeling: 1. strategy for modeling monomer complex formation at moderate surface coverage. Journal of Colloid and Interface Science 170(2), 477-490. https://doi.org/10.1006/jcis.1995.1127

Katz, L.E., Hayes, K.F., 1995b. Surface complexation modeling: 1. strategy for modeling polymer and precipitation reactions at high surface coverage. Journal of Colloid and Interface Science 170(2), 491-501. https://doi.org/10.1006/jcis.1995.1128

Khai, N.M., Oborn, I., Hillier, S., Gustafsson, J.P., 2008. Modeling of metal binding in tropical Fluvisols and Acrisols treated with biosolids and wastewater. Chemosphere 70(8), 1338-1346. https://doi.org/10.1016/j.chemosphere.2007.09.046

Kiekens, L., 1995. Zinc. In: B.J. Alloway (Ed.), Heavy Metals in Soils. Blackie Academic and Professional, London, pp. 284-305.

Kinniburgh, D.G., van Riemsdijk, W.H., Koopal, L.K., Borkovec, M., Benedetti, M.F., Avena, M.J., 1999. Ion binding to natural organic matter: competition, heterogeneity, stoichiometry and thermodynamic consistency. Colloids and Surfaces a-Physicochemical and Engineering Aspects 151(1-2), 147-166. https://doi.org/10.1016/S0927-7757(98)00637-2

Kleber, M., Eusterhues, K., Keiluweit, M., Mikutta, C., Mikutta, R., Nico, P.S., 2015. Mineral-organic associations: formation, properties, and relevance in soil environments. Advances in Agronomy, Vol 130 130, 1-140. https://doi.org/10.1016/bs.agron.2014.10.005

Kohler, M., Honeyman, B.D., Leckie, J.O., 1999. Neptunium(V) sorption on hematite (α-Fe_2O_3) in aqueous suspension: the effect of CO_2. Radiochimica Acta 85(1-2), 33-48. https://doi.org/10.1524/ract.1999.85.12.33

Komarek, M., Antelo, J., Kralova, M., Veselska, V., Cihalova, S., Chrastny, V., Ettler, V., Filip, J., Yu, Q., Fein, J.B., Koretsky, C.M., 2018. Revisiting models of Cd, Cu, Pb and Zn adsorption onto Fe(III) oxides. Chemical Geology 493, 189-198. https://doi.org/10.1016/j.chemgeo.2018.05.036

Kooner, Z.S., Cox, C.D., Smoot, J.L., 1995. Prediction of adsorption of divalent heavy metals at the goethite/water interface by surface complexation modeling. Environmental Toxicology and Chemistry 14(12), 2077-2083. https://doi.org/10.1002/etc.5620141210

Koopal, L.K., Avena, M.J., 2001. A simple model for adsorption kinetics at charged solid-liquid interfaces. Colloids and Surfaces a-Physicochemical and Engineering Aspects 192(1-3), 93-107. https://doi.org/10.1016/S0927-7757(01)00719-1

Koopal, L.K., van Riemsdijk, W.H., Kinniburgh, D.G., 2001. Humic matter and contaminants. General aspects and modeling metal ion binding. Pure and Applied Chemistry 73(12), 2005-2016. https://doi.org/10.1351/pac200173122005

Koopal, L.K., Vanriemsdijk, W.H., Dewit, J.C.M., Benedetti, M.F., 1994. Analytical isotherm equations for multicomponent adsorption to heterogeneous surfaces. Journal of Colloid and Interface Science 166(1), 51-60. https://doi.org/10.1006/jcis.1994.1270

Koretsky, C., 2000. The significance of surface complexation reactions in hydrologic systems: a geochemist's perspective. Journal of Hydrology 230(3-4), 127-171. https://doi.org/10.1016/S0022-1694(00)00215-8

Kumari, D., Qian, X.-Y., Pan, X., Achal, V., Li, Q., Gadd, G.M., 2016. Microbially-induced carbonate precipitation for immobilization of toxic metals. Advances in Applied Microbiology, Vol 94 94, 79-108. https://doi.org/10.1016/bs.aambs.2015.12.002

Laflamme, B.D., Murray, J.W., 1987. Solid-solution interaction: the effect of carbonate alkalinity on adsorbed thorium. Geochimica Et Cosmochimica Acta 51(2), 243-250. https://doi.org/10.1016/0016-7037(87)90235-3

Lee, S., Anderson, P.R., Bunker, G.B., Karanfil, C., 2004. EXAFS study of Zn sorption mechanisms on montmorillonite. Environmental Science & Technology 38(20), 5426-5432. https://doi.org/10.1021/es0350076

Li, X.D., Wai, O.W.H., Li, Y.S., Coles, B.J., Ramsey, M.H., Thornton, I., 2000. Heavy metal distribution in sediment profiles of the Pearl River estuary, South China. Applied Geochemistry 15(5), 567-581. https://doi.org/10.1016/S0883-2927(99)00072-4

Linde, M., Oborn, I., Gustafsson, J.P., 2007. Effects of changed soil conditions on the mobility of trace metals in moderately contaminated urban soils. Water Air and Soil Pollution 183(1-4), 69-83. https://doi.org/10.1007/s11270-007-9357-5

Lindsay, W.L., 1979. Chemical equilibria in soils. The blackburn press, pp.-449.

Liu, H.B., Chen, T.H., Frost, R.L., 2014. An overview of the role of goethite surfaces in the environment. Chemosphere 103, 1-11. https://doi.org/10.1016/j.chemosphere.2013.11.065

Liu, J., Zhu, R.L., Xu, T.Y., Xu, Y., Ge, F., Xi, Y.F., Zhu, J.X., He, H.P., 2016. Co-adsorption of phosphate and zinc(II) on the surface of ferrihydrite. Chemosphere 144, 1148-1155. https://doi.org/10.1016/j.chemosphere.2015.09.083

Livi, K.J.T., Villalobos, M., Leary, R., Varela, M., Barnard, J., Villacis-Garcia, M., Zanella, R., Goodridge, A., Midgley, P., 2017. Crystal face distributions and surface site densities of two synthetic goethites: implications for adsorption capacities as a function of particle size. Langmuir 33(36), 8924-8932. https://doi.org/10.1021/acs.langmuir.7b01814

Lofts, S., Tipping, E., 1998. An assemblage model for cation binding by natural particulate matter. Geochimica Et Cosmochimica Acta 62(15), 2609-2625. https://doi.org/10.1016/S0016-7037(98)00183-5

Lofts, S., Woof, C., Tipping, E., Clarke, N., Mulder, J., 2001. Modelling pH buffering and aluminium solubility in European forest soils. European Journal of Soil Science 52(2), 189-204. https://doi.org/10.1046/j.1365-2389.2001.00358.x

Long, D.T., Angino, E.E., 1977. Chemical speciation of Cd, Cu, Pb, and Zn in mixed freshwater, seawater, and brine solutions. Geochimica Et Cosmochimica Acta 41(9), 1183-1191. https://doi.org/10.1016/0016-7037(77)90064-3

Lores, E.M., Pennock, J.R., 1998. The effect of salinity on binding of Cd, Cr, Cu and Zn to dissolved organic matter. Chemosphere 37(5), 861-874. https://doi.org/10.1016/S0045-6535(98)00090-3

Lumsdon, D.G., 2004. Partitioning of organic carbon, aluminium and cadmium between solid and solution in soils: application of a mineral-humic particle additivity model. European Journal of Soil Science 55(2), 271-285. https://doi.org/10.1111/j.1365-2389.2004.00599.x

Lumsdon, D.G., Evans, L.J., Bolton, K.A., 1995. The influence of pH and chloride on the retention of cadmium, lead, mercury, and zinc by soils. Journal of Soil Contamination 4(2), 137-150. https://doi.org/10.1080/15320389509383488

Lutzenkirchen, J., Preocanin, T., Kovacevic, D., Tomisic, V., Lovgren, L., Kallay, N., 2012. Potentiometric titrations as a tool for surface charge determination. Croatica Chemica Acta 85(4), 391-417. https://doi.org/10.5562/cca2062

Luxton, T.P., Miller, B.W., Scheckel, K.G., 2013. Zinc speciation studies in soil, sediment and environmental samples. In: S. Bakirdere (Ed.), Speciation studies in soil, sediment and environmental samples. CRC press, New York, pp. 433-477.

Majlesi, K., Zare, K., Rezaienejad, S., Nemati, F., 2009. Comparison of the application of Debye-Huckel and specific ion interaction theories for the complexation of tungsten(VI) with ethylenediaminediacetic acid. Russian Journal of Inorganic Chemistry 54(5), 803-807. https://doi.org/10.1134/S0036023609050209

Martin, R., 2015. Climate change: why the tropical poor will suffer most, MIT Technology Review.
Mason, C.F.V., Turney, W., Thomson, B.M., Lu, N., Longmire, P.A., ChisholmBrause, C.J., 1997. Carbonate leaching of uranium from contaminated soils. Environmental Science & Technology 31(10), 2707-2711. https://doi.org/10.1021/es960843j
McBride, M.B., 1994. Environmental chemistry of soils. OUP, USA. pp. 406.
McLean, J.E., Bledsoe, B.E., 1992. Behavior of metals in soils, U.S. Environmental Protection Agency, Washington D.C.
Mendez, J.C., Hiemstra, T., 2019. Carbonate adsorption to ferrihydrite: competitive interaction with phosphate for use in soil systems. Acs Earth and Space Chemistry 3(1), 129-141. https://doi.org/10.1021/acsearthspacechem.8b00160
Mercer, K.L., Tobiason, J.E., 2008. Removal of arsenic from high ionic strength solutions: Effects of ionic strength, pH, and preformed versus in situ formed HFO. Environmental Science & Technology 42(10), 3797-3802. https://doi.org/10.1021/es702946s
Mesquita, M., Silva, J., 1996. Zinc adsorption by a calcareous soil. Copper interaction. Geoderma 69(1-2), 137-146. https://doi.org/10.1016/0016-7061(95)00058-5
Millero, F.J., Hawke, D.J., 1992. Ionic interactions of divalent metals in natural waters. Marine Chemistry 40(1-2), 19-48. https://doi.org/10.1016/0304-4203(92)90046-D
Millero, F.J., Schreiber, D.R., 1982. Use of the ion pairing model to estimate activity coefficients of the ionic components of natural waters. American Journal of Science 282(9), 1508-1540. https://doi.org/10.2475/ajs.282.9.1508
Milne, C.J., Kinniburgh, D.G., Tipping, E., 2001. Generic NICA-Donnan model parameters for proton binding by humic substances. Environmental Science & Technology 35(10), 2049-2059. https://doi.org/10.1021/es000123j
Milne, C.J., Kinniburgh, D.G., Van Riemsdijk, W.H., Tipping, E., 2003. Generic NICA-Donnan model parameters for metal-ion binding by humic substances. Environmental Science & Technology 37(5), 958-971. https://doi.org/10.1021/es0258879
Mishra, B., McDonald, L.M., Roy, M., Lanzirotti, A., Myneni, S.C.B., 2020. Uptake and speciation of zinc in edible plants grown in smelter contaminated soils. Plos One 15(4), e0226180. https://doi.org/10.1371/journal.pone.0226180
Mizutani, K., Fisher-Power, L.M., Shi, Z., Cheng, T., 2017. Cu and Zn adsorption to a terrestrial sediment: Influence of solid-to-solution ratio. Chemosphere 175, 341-349. https://doi.org/10.1016/j.chemosphere.2017.02.069
Montalvo, D., Degryse, F., da Silva, R.C., Baird, R., McLaughlin, M.J., 2016. Agronomic effectiveness of zinc sources as micronutrient fertilizer. In: D.L. Sparks (Ed.), Advances in agronomy. Academic press, pp. 215-267. https://doi.org/10.1016/bs.agron.2016.05.004
Moore, D.M., Reynolds, R.C.J., 1997. X-ray Diffraction and the Identification and Analysis of Clay minerals. 2nd ed. Oxford University Press, UK.
Moslehuddin, A.Z.M., Hussain, M.S., Saheed, S.M., Egashira, K., 1999. Clay mineral distribution in correspondence with agroecological regions of Bangladesh soils. Clay Science 11(1), 83-94.
Munkholm, L.J., Esu, I., Moberg, J.P., 1993. Trace elements in some northern nigerian soils. Communications in Soil Science and Plant Analysis 24(7-8), 657-672. https://doi.org/10.1080/00103629309368831
Nachtegaal, M., Sparks, D.L., 2004. Effect of iron oxide coatings on zinc sorption mechanisms at the clay-mineral/water interface. Journal of Colloid and Interface Science 276(1), 13-23. https://doi.org/10.1016/j.jcis.2004.03.031
Nagajyoti, P.C., Lee, K.D., Sreekanth, T.V.M., 2010. Heavy metals, occurrence and toxicity for plants: a review. Environmental Chemistry Letters 8(3), 199-216. https://doi.org/10.1007/s10311-010-0297-8
Nanzyo, M., Watanabe, Y., 1982. Diffuse reflectance infrared spectra and ion adsorption properties of the phosphate surface complex on goethite. Soil Science and Plant Nutrition 28(3), 359-368. https://doi.org/10.1080/00380768.1982.10433651
Nolan, A.L., McLaughlin, M.J., Mason, S.D., 2003. Chemical speciation of Zn, Cd, Cu, and Pb in pore waters of agricultural and contaminated soils using Donnan dialysis. Environmental Science & Technology 37(1), 90-98. https://doi.org/10.1021/es025966k

Nomaan, S.M., Stokes, S.N., Han, J., Katz, L.E., 2021. Application of spectroscopic evidence to diffuse layer model (DLM) parameter estimation for cation adsorption onto ferrihydrite in single- and bi-solute systems. Chemical Geology 573. https://doi.org/10.1016/j.chemgeo.2021.120199

Oppenheimer, M., Glavovic, B.C., Hinkel, J., Van De Wal, R., Magnan, A.K., Abd-Elgawad, A., Cai, R., Cifuentes-Jara, M., DeConto, R.M., Ghosh, T., Hay, J., Isla, F., Marzeion, B., Meyssignac, B., Sebesvari, Z., 2019. Sea level rise and implications for low-lying islands, coasts and communities. In: H.-O. Pörtner, D.C. Roberts, V. Masson-Delmotte, P. Zhai, M. Tignor, E. Poloczanska, K. Mintenbeck, A. Alegría, M. Nicolai, A. Okem, J. Petzold, B. Rama, N.M. Weyer (Eds.), IPCC special report on the ocean and cryosphere in a changing climate. Cambridge university press, Cambridge, UK. https://doi.org/10.1017/9781009157964.006

Paalman, M.A.A., Vanderweijden, C.H., Loch, J.P.G., 1994. Sorption of cadmium on suspended matter under estuarine conditions; competition and complexation with major seawater ions. Water Air and Soil Pollution 73(1-4), 49-60. https://doi.org/10.1007/BF00477975

Padmanabham, M., 1983. Comparative study of the adsorption-desorption behavior of copper(II), zinc(II), cobalt(II) and lead(II) at the goethite solution interface. Australian Journal of Soil Research 21(4), 515-525. https://doi.org/10.1071/SR9830515

Palmqvist, U., Ahlberg, E., Lovgren, L., Sjoberg, S., 1997. In situ voltammetric determinations of metal ions in goethite suspensions: Single metal ion systems. Journal of Colloid and Interface Science 196(2), 254-266. https://doi.org/10.1006/jcis.1997.5189

Palmqvist, U., Ahlberg, E., Lovgren, L., Sjoberg, S., 1999. Competitive metal ion adsorption in goethite systems using in situ voltammetric methods and potentiometry. Journal of Colloid and Interface Science 218(2), 388-396. https://doi.org/10.1006/jcis.1999.6446

Patterson, J.W., Allen, H.E., Scala, J.J., 1977. Carbonate precipitation for heavy metals pollutants. Journal Water Pollution Control Federation 49(12), 2397-2410. https://www.jstor.org/stable/25039473

Payne, G.G., Martens, D.C., Winarko, C., Perera, N.F., 1988. Form and availability of copper and zinc following long-term copper sulfate and zinc sulfate applications. Journal of Environmental Quality 17(4), 707-711. https://doi.org/10.2134/jeq1988.00472425001700040031x

Peacock, C.L., Sherman, D.M., 2004. Copper(II) sorption onto goethite, hematite and lepidocrocite: A surface complexation model based on ab initio molecular geometries and EXAFS spectroscopy. GeochimicaEtCosmochimicaActa68(12),2623-2637.https://doi.org/10.1016/j.gca.2003.11.030

Pierrot, D., Millero, F.J., 2017. The speciation of metals in natural waters. Aquatic Geochemistry 23(1), 1-20. https://doi.org/10.1007/s10498-016-9292-4

Ponnamperuma, F.N., Tianco, E.M., Loy, T.A., 1966. Ionic strengths of the solutions of flooded soils and other natural aqueous solutions from specific conductance. Soil Science 102(6), 408-413.

Ponthieu, M., Juillot, F., Hiemstra, T., van Riemsdijk, W.H., Benedetti, M.F., 2006. Metal ion binding to iron oxides. Geochimica Et Cosmochimica Acta 70(11), 2679-2698. https://doi.org/10.1016/j.gca.2006.02.021

Powell, K.J., Brown, P.L., Byrne, R.H., Gajda, T., Hefter, G., Leuz, A.K., Sjoberg, S., Wanner, H., 2013. Chemical speciation of environmentally significant metals with inorganic ligands. Part 5: The Zn^{2+} + OH^-, Cl^-, CO_3^{2-}, SO_4^{2-}, and PO_4^{3-}systems (IUPAC Technical Report). Pure and Applied Chemistry 85(12), 2249-2311. https://doi.org/10.1351/pac-rep-13-06-03

Rahman, M.H., Moslehuddin, A.Z.M., Saha, D.K., Ahmed, I.U., Egashira, K., 2005. Mineralogy of soils from different Agroecological Regions of Bangladesh: Region 12 - Low Ganges River Floodplain. Clay Science 12(6), 321-326.https://doi.org/10.11362/jcssjclayscience1960.12.321

Ramanathan, V., Feng, Y., 2009. Air pollution, greenhouse gases and climate change: Global and regional perspectives. Atmospheric Environment 43(1), 37-50. https://doi.org/10.1016/j.atmosenv.2008.09.063

Raspor, B., Nurnberg, H.W., Valenta, P., Branica, M., 1984. Studies in seawater and lake water on interactions of trace metals with humic substances isolated from marine and estuarine sediments: II. voltammetric investigations on trace metal complex formation in the dissolved phase. Marine Chemistry 15(3), 231-249. https://doi.org/10.1016/0304-4203(84)90020-3

Reed, B.E., Cline, S.R., 1994. Retention and release of lead by a very find sandy loam .1. isotherm modeling. Separation Science and Technology 29(12), 1529-1551. https://doi.org/10.1080/01496399408007372

Regadio, M., Riano, S., Binnemans, K., Vander Hoogerstraete, T., 2017. Direct analysis of metal ions in solutions with high salt concentrations by total reflection X-ray fluorescence. Analytical Chemistry 89(8), 4595-4603. https://doi.org/10.1021/acs.analchem.7b00097

Ren, Z.-L., Tella, M., Bravin, M.N., Comans, R.N.J., Dai, J., Garnier, J.-M., Sivry, Y., Doelsch, E., Straathof, A., Benedetti, M.F., 2015. Effect of dissolved organic matter composition on metal speciation in soil solutions. Chemical Geology 398, 61-69. https://doi.org/10.1016/j.chemgeo.2015.01.020

Ren, Z.L., Sivry, Y., Tharaud, M., Cordier, L., Li, Y.T., Dai, J., Benedetti, M.F., 2017. Speciation and reactivity of lead and zinc in heavily and poorly contaminated soils: Stable isotope dilution, chemical extraction and model views. Environmental Pollution 225, 654-662. https://doi.org/10.1016/j.envpol.2017.03.051

Rengel, Z., 1999. Mineral Nutrition of Crops: Fundamental mechanisms and implications. Haworth press, New York, USA.

Rey-Castro, C., Lodeiro, P., Herrero, R., De Vicente, M.E.S., 2003. Acid-base properties of brown seaweed biomass considered as a Donnan gel. A model reflecting electrostatic effects and chemical heterogeneity. Environmental Science & Technology 37(22), 5159-5167. https://doi.org/10.1021/es0343353

Rieuwerts, J.S., 2007. The mobility and bioavailability of trace metals in tropical soils: a review. Chemical Speciation and Bioavailability 19(2), 75-85. https://doi.org/10.3184/095422907X211918

Robertson, A.P., Leckie, J.O., 1998. Acid/base, copper binding, and Cu^{2+}/H^{+} exchange properties of goethite, an experimental and modeling study. Environmental Science & Technology 32(17), 2519-2530. https://doi.org/10.1021/es9709942

Ryan, M.P., Bauman, J.E., 1978. Thermodynamics of the zinc bicarbonate ion pair. Inorganic Chemistry 17(12), 3329-3331. https://doi.org/10.1021/ic50190a004

Saulnier, I., Mucci, A., 2000. Trace metal remobilization following the resuspension of estuarine sediments: Saguenay Fjord, Canada. Applied Geochemistry 15(2), 191-210. https://doi.org/10.1016/S0883-2927(99)00034-7

Sauve, S., Hendershot, W., Allen, H.E., 2000. Solid-solution partitioning of metals in contaminated soils: Dependence on pH, total metal burden, and organic matter. Environmental Science & Technology 34(7), 1125-1131. https://doi.org/10.1021/es9907764

Schindler, P., Kamber, H.R., 1968. Die Acidität von Silanolgruppen. Vorläufige Mitteillung. Helvetica Chimica Acta 51(7), 1781-1786. https://doi.org/10.1002/hlca.19680510738

Schindler, P.W., Liechti, P., Westall, J.C., 1987. Adsorption of copper, cadmium and lead from aqueous solution to the kaolinite/water interface. Netherlands Journal of Agricultural Science 35(3), 219-230. https://doi.org/10.18174/njas.v35i3.16720

Schulthess, C.P., Ndu, U., 2017. Modeling the adsorption of hydrogen, sodium, chloride and phthalate on goethite using a strict charge-neutral ion-exchange theory. Plos One 12(5), e0176743. https://doi.org/10.1371/journal.pone.0176743

Schulthess, C.P., Swanson, K., Wijnja, H., 1998. Proton adsorption on an aluminum oxide in the presence of bicarbonate. Soil Science Society of America Journal 62(1), 136-141. https://doi.org/10.2136/sssaj1998.03615995006200010018x

Schwertmann, U., Cornell, R.M., 2000. Iron oxides in the laboratory: preparation and characterization (Ed.2). Wiley press Ltd., pp.-188. https://doi.org/10.1002/9783527613229

Shahabi, A., Malakouti, M.J., Fallahi, E., 2005. Effects of bicarbonate content of irrigation water on nutritional disorders of some apple varieties. Journal of Plant Nutrition 28(9), 1663-1678. https://doi.org/10.1080/01904160500203630

Shahid, S.A., Zaman, M., Heng, L., 2018. Soil Salinity: Historical Perspectives and a World Overview of the Problem. In: S.A. Shahid, M. Zaman, L. Heng (Eds.), Guideline for Salinity Assessment, Mitigation and Adaptation Using Nuclear and Related Techniques. https://doi.org/10.1007/978-3-319-96190-3_2

Shi, Z.Q., Allen, H.E., Di Toro, D.M., Lee, S.Z., Harsh, J.B., 2013. Predicting Pb-II adsorption on soils: the roles of soil organic matter, cation competition and iron (hydr)oxides. Environmental Chemistry 10(6), 465-474. https://doi.org/10.1071/EN13153

Shi, Z.Q., Allen, H.E., Di Toro, D.M., Lee, S.Z., Meza, D.M.F., Lofts, S., 2007. Predicting cadmium adsorption on soils using WHAM VI. Chemosphere 69(4), 605-612. https://doi.org/10.1016/j.chemosphere.2007.03.001

Shuman, L.M., 1986. Effect of ionic strength and anions on zinc adsorption by two soils. Soil Science Society of America Journal 50(6), 1438-1442. https://doi.org/10.2136/sssaj1986.03615995005000060012x

Singh, S., Parihar, P., Singh, R., Singh, V.P., Prasad, S.M., 2016. Heavy Metal tolerance in plants: role of transcriptomics, proteomics, metabolomics, and ionomics. Frontiers in Plant Science 6, 1143. https://doi.org/10.3389/fpls.2015.01143

Singh, S.P.N., Mattigod, S.V., 1992. Modeling boron adsorption on kaolinite. Clays and Clay Minerals 40(2), 192-205. https://doi.org/10.1346/CCMN.1992.0400209

Somasundaran, P., 2006. Encyclopedia of surface and colloid science (8 volume set) (Ed.2). CRC press. pp.-8034.

Sparks, D.L., 2003. Environmental Soil Chemistry. Academic Press, USA. https://doi.org/10.1016/B978-0-12-656446-4.X5000-2

Spathariotis, E., Kallianou, C., 2001. Adsorption of copper, zinc, and cadmium on clay fraction of two acid soils: Surface complexation modeling. Communications in Soil Science and Plant Analysis 32(19-20), 3185-3205. https://doi.org/10.1081/CSS-120001115

Spathariotis, E., Kallianou, C., 2007. Adsorption of copper, zinc, and cadmium on goethite, aluminum-substituted goethite, and a system of kaolinite-goethite: Surface complexation modeling. Communications in Soil Science and Plant Analysis 38(5-6), 611-635. https://doi.org/10.1080/00103620701216005

Sposito, G., 1984. The Surface Chemistry of Soils. Oxford University Press, New York.

SRDI, 2010. Saline Soils of Bangladesh, Soil Resource Development Institute, Dhaka, Bangladesh.

Stanley, J.K., Byrne, R.H., 1990. Inorganic complexation of zinc(II) in seawater. Geochimica Et Cosmochimica Acta 54(3), 753-760. https://doi.org/10.1016/0016-7037(90)90370-Z

Stephan, C.H., Courchesne, F., Hendershot, W.H., McGrath, S.P., Chaudri, A.M., Sappin-Didier, V., Sauve, S., 2008. Speciation of zinc in contaminated soils. Environmental Pollution 155(2), 208-216. https://doi.org/10.1016/j.envpol.2007.12.006

Stietiya, Hashem, M., 2010. Sorption mechanisms of zinc in different clay minerals and soil systems as influenced by various natural ligands. PhD thesis, Louisiana State University, United States.

Stockdale, A., Tipping, E., Lofts, S., 2015. Dissolved trace metal speciation in estuarine and coastal waters: comparison of WHAM/MODEL VII predictions with analytical results. Environmental Toxicology and Chemistry 34(1), 53-63. https://doi.org/10.1002/etc.2789

Strawn, D.G., 2021. Sorption mechanisms of chemicals in soils. Soil Systems 5(1), 13. https://doi.org/10.3390/soilsystems5010013

Stumm, W., Huang, C.P., Jenkins, S.R., 1970. Specific chemical interaction affecting the stability of dispersed systems. Croatica Chemica Acta 42(2), 223-245. https://hrcak.srce.hr/197549

Sun, Y.B., Li, Y., 2021. Application of surface complexation modeling on adsorption of uranium at water-solid interface: A review. Environmental Pollution 278. https://doi.org/10.1016/j.envpol.2021.116861

Sunda, W.G., Hanson, P.J., 1978. Chemical speciation of copper in river water - effect of total copper, pH, carbonate and dissolved organic matter. Abstracts of Papers of the American Chemical Society 176(SEP), 39-39. https://doi.org/10.1021/bk-1979-0093.ch008

Swedlund, P.J., Webster, J.G., 2001. Cu and Zn ternary surface complex formation with SO_4 on ferrihydrite and schwertmannite. Applied Geochemistry 16(5), 503-511. https://doi.org/10.1016/S0883-2927(00)00044-5

Swedlund, P.J., Webster, J.G., Miskelly, G.M., 2009. Goethite adsorption of Cu(II), Pb(II), Cd(II), and Zn(II) in the presence of sulfate: Properties of the ternary complex. Geochimica Et Cosmochimica Acta 73(6), 1548-1562. https://doi.org/10.1016/j.gca.2008.12.007

Taylor, R.W., Hassan, K., Mehadi, A.A., Shuford, J.W., 2008. Kinetics of zinc sorption by soils. Communications in Soil Science and Plant Analysis 26 (11-12), 1761-1771. https://doi.org/10.1080/00103629509369407

Tepavitcharova, S., Rabadjieva, D., Todorov, T., Kovacheva, A., Dassenakis, M., Paraskevopoulou, V., 2014. Chemical speciation in fresh, saline and hyper-saline waters. Pure and Applied Chemistry 86(7), 1097-1104. https://doi.org/10.1515/pac-2014-0107

Tepavitcharova, S., Todorov, T., Rabadjieva, D., Dassenakis, M., Paraskevopoulou, V., 2011. Chemical speciation in natural and brine sea waters. Environmental Monitoring and Assessment 180(1-4), 217-227. https://doi.org/10.1007/s10661-010-1783-y

Thies-Weesie, D.M.E., de Hoog, J.P., Mendiola, M.H.H., Petukhov, A.V., Vroege, G.J., 2007. Synthesis of goethite as a model colloid for mineral liquid crystals. Chemistry of Materials 19(23), 5538-5546. https://doi.org/10.1021/cm071229h

Tipping, E., Lofts, S., Stockdale, A., 2016. Metal speciation from stream to open ocean: modelling v. measurement. Environmental Chemistry 13(3), 464-477. https://doi.org/10.1071/EN15111

Tipping, E., Rieuwerts, J., Pan, G., Ashmore, M.R., Lofts, S., Hill, M.T.R., Farago, M.E., Thornton, I., 2003. The solid-solution partitioning of heavy metals (Cu, Zn, Cd, Pb) in upland soils of England and Wales. Environmental Pollution 125(2), 213-225. https://doi.org/10.1016/S0269-7491(03)00058-7

Tonkin, J.W., Balistrieri, L.S., Murray, J.W., 2004. Modeling sorption of divalent metal cations on hydrous manganese oxide using the diffuse double layer model. Applied Geochemistry 19(1), 29-53. https://doi.org/10.1016/S0883-2927(03)00115-X

Trehan, S.P., Sekhon, G.S., 1977. Effect of clay, organic matter and $CaCO_3$ content on zinc adsorption by soils. Plant and Soil 46(2), 329-336. https://doi.org/10.1007/BF00010089

Uddin, M.K., 2017. A review on the adsorption of heavy metals by clay minerals, with special focus on the past decade. Chemical Engineering Journal 308, 438-462. https://doi.org/10.1016/j.cej.2016.09.029

Unsworth, E.R., Warnken, K.W., Zhang, H., Davison, W., Black, F., Buffle, J., Cao, J., Cleven, R., Galceran, J., Gunkel, P., Kalis, E., Kistler, D., Van Leeuwen, H.P., Martin, M., Noel, S., Nur, Y., Odzak, N., Puy, J., Van Riemsdijk, W., Sigg, L., Temminghoff, E., Tercier-Waeber, M.L., Toepperwien, S., Town, R.M., Weng, L.P., Xue, H.B., 2006. Model predictions of metal speciation in freshwaters compared to measurements by in situ techniques. Environmental Science & Technology 40(6), 1942-1949. https://doi.org/10.1021/es051246c

Uygur, V., Rimmer, D.L., 2000. Reactions of zinc with iron-oxide coated calcite surfaces at alkaline pH. European Journal of Soil Science 51(3), 511-516. https://doi.org/10.1046/j.1365-2389.2000.00318.x

Van Damme, A., Degryse, F., Smolders, E., Sarret, G., Dewit, J., Swennen, R., Manceau, A., 2010. Zinc speciation in mining and smelter contaminated overbank sediments by EXAFS spectroscopy. Geochimica Et Cosmochimica Acta 74(13), 3707-3720. https://doi.org/10.1016/j.gca.2010.03.032

van den Berg, G.A., Loch, J.P.G., 2000. Decalcification of soils subject to periodic waterlogging. European Journal of Soil Science 51(1), 27-33. https://doi.org/10.1046/j.1365-2389.2000.00279.x

van Reeuwijk, L.P., 1993. Procedures for soil analysis. International Soil Reference and Information Centre (ISRIC), Wageningen, The Netherlands.

Van Riemsdijk, W.H., Koopal, L.K., Kinniburgh, D.G., Benedetti, M.F., Weng, L., 2006. Modeling the interactions between humics, ions, and mineral surfaces. Environmental Science & Technology 40(24), 7473-7480. https://doi.org/10.1021/es0607786

Vangeen, A., Robertson, A.P., Leckie, J.O., 1994. Complexation of carbonate species at the goethite surface: implications for adsorption of metal ions in natural waters. Geochimica Et Cosmochimica Acta 58(9), 2073-2086. https://doi.org/10.1016/0016-7037(94)90286-0

Villalobos, M., Leckie, J.O., 2000. Carbonate adsorption on goethite under closed and open CO2 conditions. Geochimica Et Cosmochimica Acta 64(22), 3787-3802. https://doi.org/10.1016/S0016-7037(00)00465-8

Villalobos, M., Leckie, J.O., 2001. Surface complexation modeling and FTIR study of carbonate adsorption to goethite. Journal of Colloid and Interface Science 235(1), 15-32. https://doi.org/10.1006/jcis.2000.7341

Villalobos, M., Trotz, M.A., Leckie, J.O., 2001. Surface complexation modeling of carbonate effects on the adsorption of Cr(VI), Pb(II), and U(VI) on goethite. Environmental Science & Technology 35(19), 3849-3856. https://doi.org/10.1021/es001748k

Villalobos, M., Trotz, M.A., Leckie, J.O., 2003. Variability in goethite surface site density: evidence from proton and carbonate sorption. Journal of Colloid and Interface Science 268(2), 273-287. https://doi.org/10.1016/j.jcis.2003.07.044

Wang, J.J., Harrell, D.L., 2005. Effect of ammonium, potassium, and sodium cations and phosphate, nitrate, and chloride anions on zinc sorption and lability in selected acid and calcareous soils. Soil Science Society of America Journal 69(4), 1036-1046. https://doi.org/10.2136/sssaj2004.0148

Webb, S.M., Gaillard, J.F., 2015. Zinc speciation in contaminated sediments: Quantitative determination of zinc coordination by X-ray absorption spectroscopy. Aquatic Geochemistry 21(2-4), 295-312. https://doi.org/10.1007/s10498-014-9243-x

Weng, L.P., Temminghoff, E.J.M., Lofts, S., Tipping, E., Van Riemsdijk, W.H., 2002. Complexation with dissolved organic matter and solubility control of heavy metals in a sandy soil. Environmental Science & Technology 36(22), 4804-4810. https://doi.org/10.1021/es0200084

Weng, L.P., Temminghoff, E.J.M., van Riemsdijk, W.H., 2001. Contribution of individual sorhents to the control of heavy metal activity in sandy soil. Environmental Science & Technology 35(22), 4436-4443. https://doi.org/10.1021/es010085j

Westall, J.C., 1982. FITEQL - 2: A computer program for determination of chemical equilibrium constants from experimental data. Department of chemistry, Oregon State University, Corvallis, USA.

Wheeler, D., 2011. Quantifying vulnerability to climate change: Implications for adaptation assistance. Center for Global Development Working Paper No. 240. https://doi.org/10.2139/ssrn.1824611

Wijnja, H., Schulthess, C.P., 2002. Effect of carbonate on the adsorption of selenate and sulfate on goethite. Soil Science Society of America Journal 66(4), 1190-1197. https://doi.org/10.2136/sssaj2002.1190

Wilson, M.J., 1999. The origin and formation of clay minerals in soils: past, present and future perspectives. Clay Minerals 34(1), 7-25. https://doi.org/10.1180/000985599545957

Xu, Y., Axe, L., Yee, N., Dyer, J.A., 2006. Bidentate complexation modeling of heavy metal adsorption and competition on goethite. Environmental Science & Technology 40(7), 2213-2218. https://doi.org/10.1021/es051916e

Yates, D.E., Levine, S., Healy, T.W., 1974. Site-binding model of electrical double layer at oxide/water interface. Journal of the Chemical Society-Faraday Transactions I 70, 1807-1818. https://doi.org/10.1039/F19747001807

Yoon, J., Cao, X.D., Zhou, Q.X., Ma, L.Q., 2006. Accumulation of Pb, Cu, and Zn in native plants growing on a contaminated Florida site. Science of the Total Environment 368(2-3), 456-464. https://doi.org/10.1016/j.scitotenv.2006.01.016

Zachara, J.M., Cowan, C.E., Resch, C.T., 1991. Sorption of divalent metals on calcite. Geochimica Et Cosmochimica Acta 55(6), 1549-1562. https://doi.org/10.1016/0016-7037(91)90127-Q

Zachara, J.M., Girvin, D.C., Schmidt, R.L., Resch, C.T., 1987. Chromate adsorption on amorphous iron oxyhydroxide in the presence of major groundwater ions. Environmental Science & Technology 21(6), 589-594. https://doi.org/10.1021/es00160a010

Zachara, J.M., Kittrick, J.A., Harsh, J.B., 1988. The mechanism of Zn^{2+} adsorption on calcite. Geochimica Et Cosmochimica Acta 52(9), 2281-2291. https://doi.org/10.1016/0016-7037(88)90130-5.

Zachara, J.M., Smith, S.C., Resch, C.T., Cowan, C.E., 1992. Cadmium sorption to soil separates containing layer silicates and iron and aluminum oxides. Soil Science Society of America Journal 56(4), 1074-1084. https://doi.org/10.2136/sssaj1992.03615995005600040012x

Zaman, M., Heng, L., Shahid, S.A., 2018. Guideline for salinity assessment, mitigation and adaptation using nuclear and related techniques. Springer publication Ltd., pp.162. https://doi.org/10.1007/978-3-319-96190-3

Zhang, C., Gu, X., Gu, C., Evans, L.J., 2018a. Multi-surface modeling of Ni(II) and Cd(II) partitioning in soils: Effects of salts and solid/liquid ratios. Science of the Total Environment 635, 859-866. https://doi.org/10.1016/j.scitotenv.2018.04.191

Zhang, C., Yu, Z.G., Zeng, G.M., Jiang, M., Yang, Z.Z., Cui, F., Zhu, M.Y., Shen, L.Q., Hu, L., 2014. Effects of sediment geochemical properties on heavy metal bioavailability. Environment International 73, 270-281. https://doi.org/10.1016/j.envint.2014.08.010

Zhang, X.W., Yang, L.S., Li, Y.H., Li, H.R., Wang, W.Y., Ye, B.X., 2012. Impacts of lead/zinc mining and smelting on the environment and human health in China. Environmental Monitoring and Assessment 184(4), 2261-2273. https://doi.org/10.1007/s10661-011-2115-6

Zhang, Y., Zhang, H., Zhang, Z., Liu, C., Sun, C., Zhang, W., Marhaba, T., 2018b. pH effect on heavy metal release from a polluted sediment. Journal of Chemistry 2018, 7597640-Article ID 7597640. https://doi.org/10.1155/2018/7597640

Zoumis, T., Schmidt, A., Grigorova, L., Calmano, W., 2001. Contaminants in sediments: remobilisation and demobilisation. Science of the Total Environment 266(1-3), 195-202. https://doi.org/10.1016/S0048-9697(00)00740-3

Zuo, Y., Ren, L., Zhang, F., Jiang, R.F., 2007. Bicarbonate concentration as affected by soil water content controls iron nutrition of peanut plants in a calcareous soil. Plant Physiology and Biochemistry 45(5), 357-364. https://doi.org/10.1016/j.plaphy.2007.03.017

Appendices

Appendix A:

The CCM model have the following assumptions (Bradl, 2004):

1. Metals are adsorbed through specific adsorption and all complexes are inner-sphere surface complexes,
2. The activity coefficients of the aqueous species in the equilibrium condition are determined by the constant ionic medium reference state and the background electrolyte does not form any complexes with ions,
3. The development of surface complexes occurs in a chargeless environment in the standard state, and
4. Surface charge decreases linearly with increasing distance X from the surface. It is proportional to the surface potential, Ψ through a constant capacitance, G and written as follows:

$$\sigma_0 = G\,\Psi$$

where σ_0 is the surface charge (mol L^{-1}), Ψ is the surface potential (V). The summation of all specifically adsorbed ions is represented as the surface charge, σ_0. Non-specifically adsorbed ions are excluded from plane 0 and do not consider for calculating the surface charge.

The DLM have the following assumptions (Bradl, 2004):

1. Metals are adsorbed through specific adsorption and all complexes are inner-sphere surface complexes and ions are not formed in any surface complexes with the background electrolyte.
2. The reference state of infinite dilution is used for the solution and the zero charge reference state is used for the surface.

Like CCM, the summation of all specifically adsorbed ions is represented as the surface charge, σ_0. Yet the Gouy–Chapman theory is used to calculate the capacitance G and the ionic strength is considered. For a z:z electrolyte the relation of the surface charge and the surface potential [$\sigma_0 = f(\Psi)$] can be calculated as:

$$\sigma_0 = \sigma_d = \sqrt{8\,\epsilon\epsilon_0 RTI10^3}\,\sinh\left(\frac{zF\Psi_0}{2RT}\right)$$

where σ_d is the diffuse layer charge (C m^{-2}), ε is the dielectric constant, ε_0 is the permittivity of free space, R is the molar gas constant (J mol^{-1} K^{-1}), T is the absolute temperature (K), F is the Faraday constant (C mol^{-1}), Ψ is the surface potential (V) and I the medium ionic strength (mol L^{-1}).

The TLM model:

As an additional plane β is introduced in the TLM, the adsorption of ions on the plane β produces an additional charge σ_β (Bradl, 2004). Therefore, the electroneutrality of the TLM can be expressed as:

$$\sigma_0 + \sigma_\beta + \sigma_d = 0$$

where σ_0, σ_β and σ_d are the surface charge (C m^{-2}) in the 0, β and d planes, respectively (C m^{-2}). Considering the capacitance G_1 and G_2 between the planes 0 and *β* and between *β* and d, respectively, the relation between charge and potential is written as:

$$\Psi_0 - \Psi_\beta = \frac{\sigma_0}{G_1}$$

and

$$\Psi_\beta - \Psi_d = \frac{\sigma_0 + \sigma_d}{G_2} = -\frac{\sigma_d}{G_2}$$

where Ψ_0, Ψ_β and Ψ_d are the surface potential (V) in the 0, β and d planes, respectively. The Gouy–Chapman theory can be used to calculate the relation between charge and potential on the diffuse plane d:

$$\sigma_d = \sqrt{8\,\epsilon\epsilon_0 RTI10^3}\,\sinh\left(\frac{zF\Psi_d}{2RT}\right)$$

where σ_d is the diffuse layer charge (mol L^{-1}), ε is the dielectric constant, ε_0 is the permittivity of free space, R is the molar gas constant (J mol^{-1} K^{-1}), T is the absolute temperature (K), F is the Faraday constant (C mol^{-1}), Ψ is the surface potential (V) and I the medium ionic strength (mol L^{-1}).

Appendix B: Rietveld profile of soils

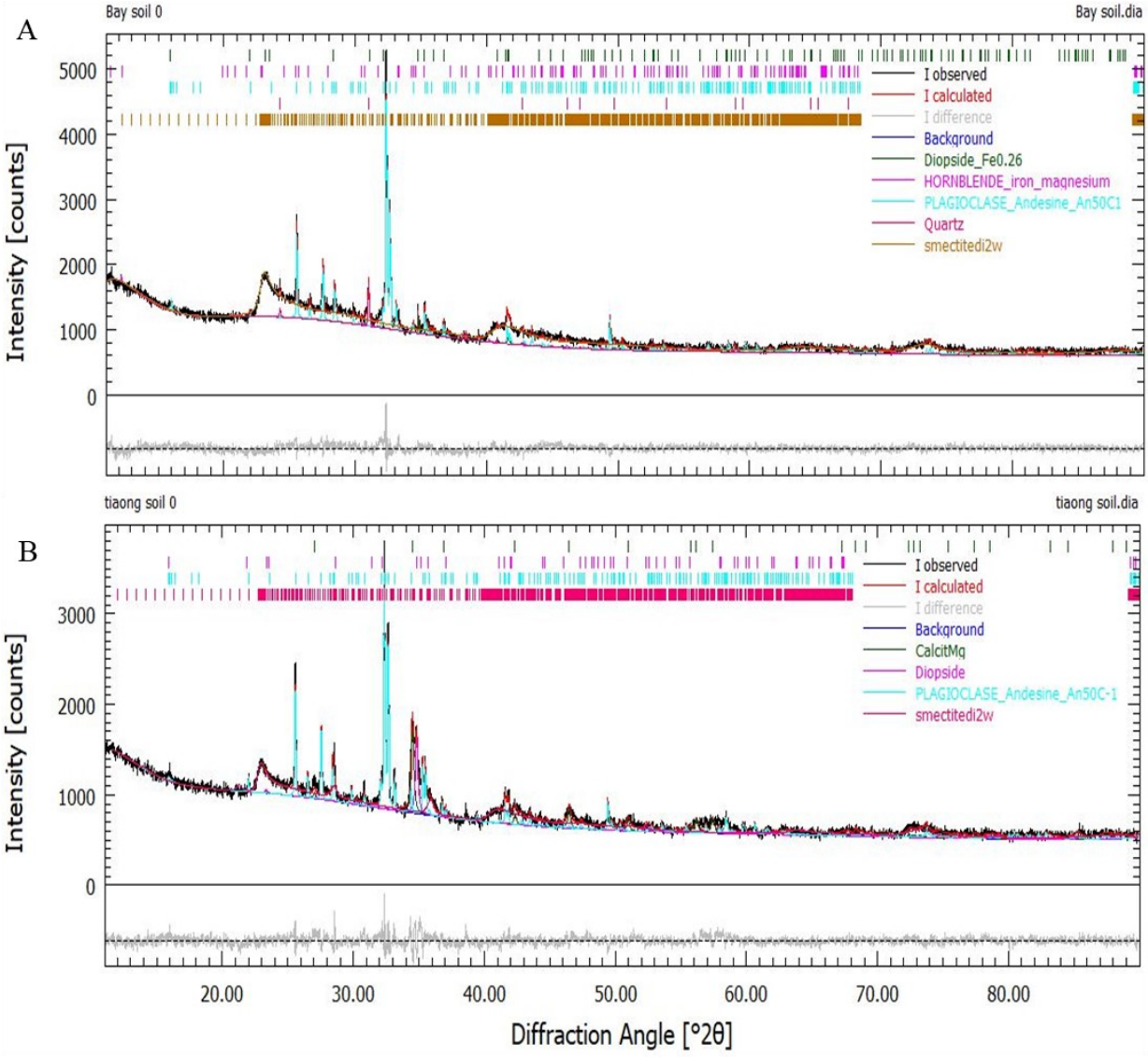
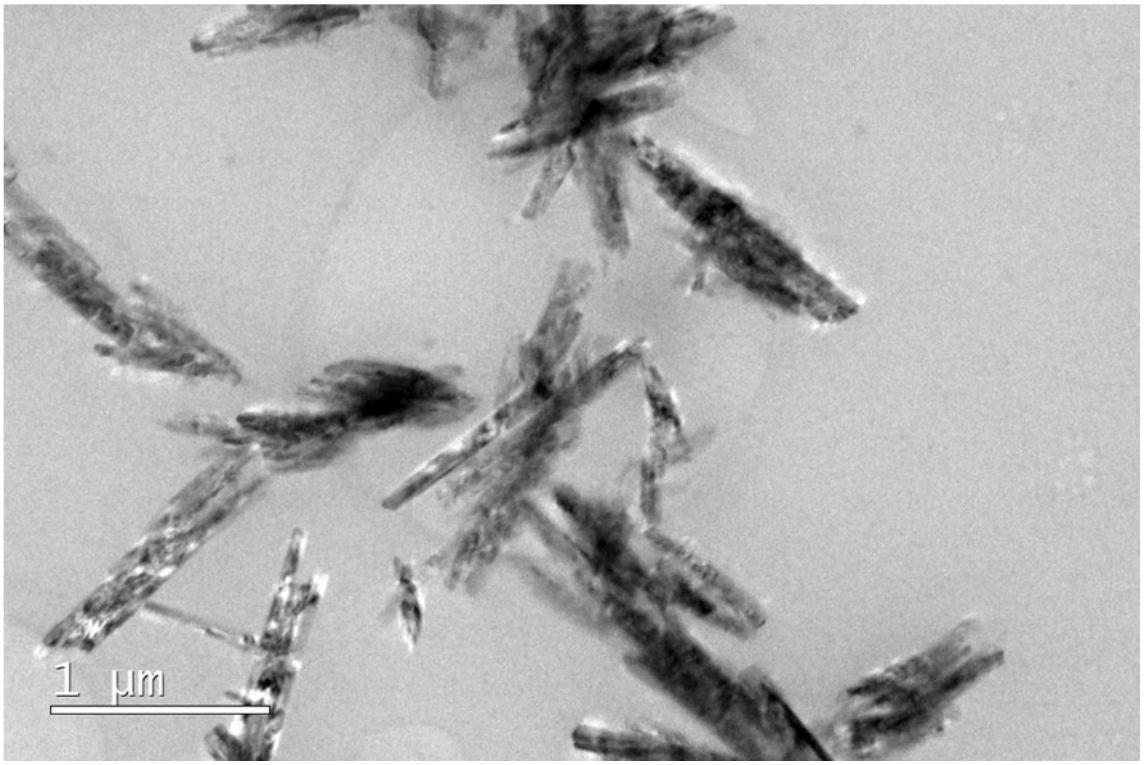


Figure A.1 Rietveld profile of Bay (A) and Tiaong (B) soils

Appendix C: A. Elemental composition of goethite by XRF analysis

Element	%
MgO	0.00
SiO_2	0.05
P_2O_5	0.09
Cl	0.03
K_2O	0.19
CaO	0.06
Cr_2O_5	0.05
Fe_2O_3	99.41
SnO_2	0.01
La_2O_3	0.03
Ta_2O_5	0.08
PtO_2	0.00

B. TEM image of goethite:



The Synthesis of goethite is further characterized by TEM. The TEM image indicated that the nanocrystals particle are typical lathlike and polydisperse (Thies-Weesie et al., 2007)

Appendix D: Calculated constants of Zn-Cl complexes using the Davies and SIT equation

Equation	SIT			Davies		
	I = 0.1 mol/L	I = 0.3 mol/L	I = 0.7 mol/L	I = 0.1 mol/L	I = 0.3 mol/L	I = 0.7 mol/L
$Zn^{2+} + Cl^- = ZnC^+$	-0.02	-0.17	-0.26	-0.05	-0.20	-0.24
$Zn^{2+} + 2Cl^- = ZnCl_2$	0.05	-0.17	-0.30	0.02	-0.21	-0.27
$Zn^{2+} + 3Cl^- = ZnCl_3^-$	-0.15	-0.36	-0.46	-0.19	-0.42	-0.48

Appendix E: FITEQL code for surface complexation modelling

Example 1: Input file of Potentiometric Titration of Goethite in 0.1 mol L^{-1} NaCl solution

```
1
1
1
1
1
50
```

Five output routines are to be invoked. The optimization procedure will be limited to 50 interactions.

```
    2     1     0     1     0
```

Group components

```
00160  -1.00  0.00E00   PSI
00001  -2.33  4.69E-3   SOH
00010  0.00   0.00      H+
```

PSI is an electrostatic component, SOH is the total concentration of goethite in mol L^{-1} and its log value and H^+ is the value for free hydrogen ion concentration.

```
00010  0.00    10  1
00100  -13.95  10 -1
00001  0.00     1  1
00011  7.47     1  1  10  1 160 1
00012  -9.51    1  1  10 -1 160 -1
```

Protonation and deprotonation constants of goethite from the literature

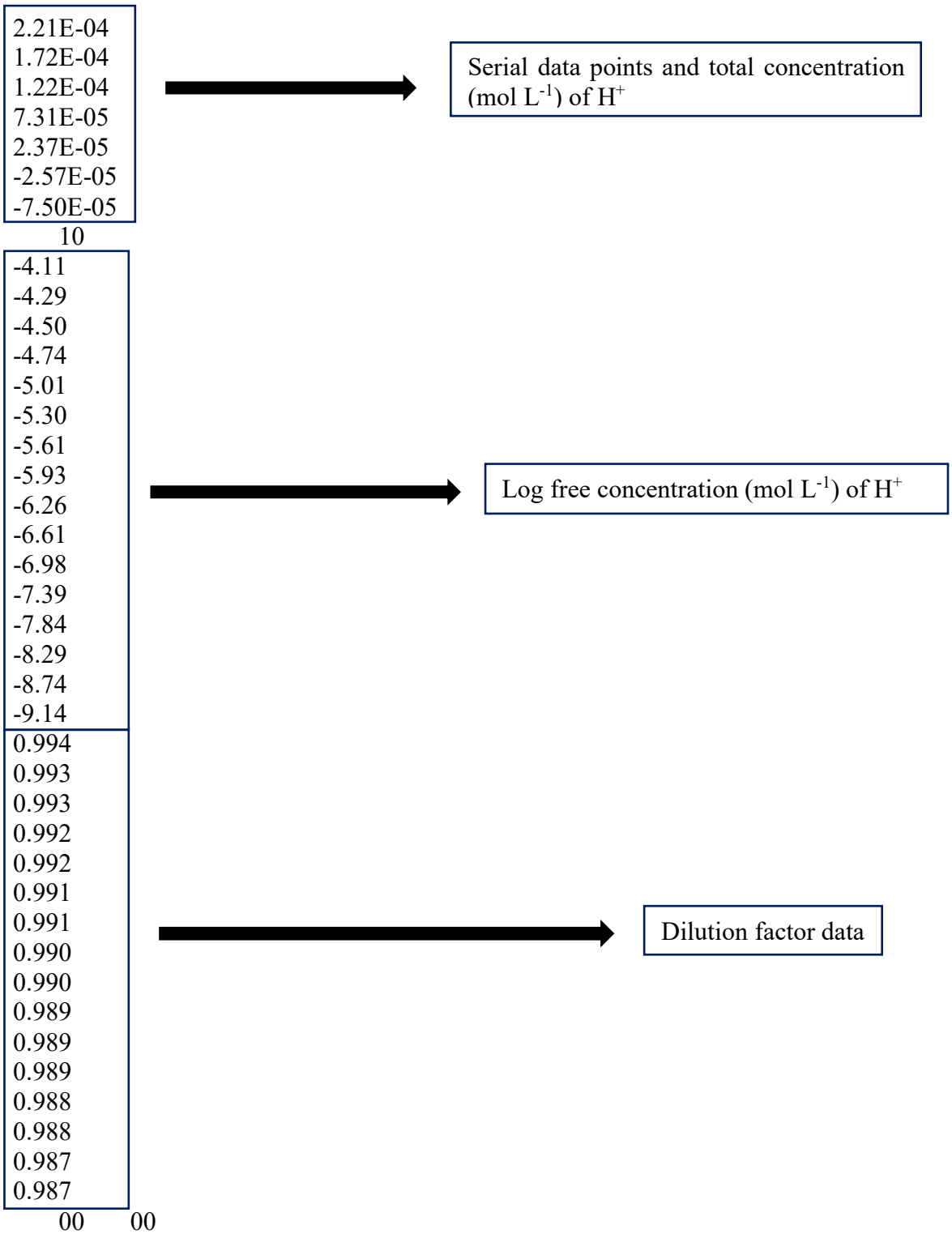
```
00001    40.0   8.83    0.90
0.10   1.0
```

Surface characteristics of goethite

```
    2        0
    11
    12
    16       1        1        1
    10
```

Adjustable parameters

```
6.69E-04
6.19E-04
5.70E-04
5.20E-04
4.70E-04
4.20E-04
3.70E-04
3.21E-04
2.71E-04
```


2.21E-04
1.72E-04
1.22E-04
7.31E-05
2.37E-05
-2.57E-05
-7.50E-05
10
Serial data points and total concentration (mol L-1) of H+
-4.11
-4.29
-4.50
-4.74
-5.01
-5.30
-5.61
-5.93
-6.26
-6.61
-6.98
-7.39
-7.84
-8.29
-8.74
-9.14
Log free concentration (mol L-1) of H+
0.994
0.993
0.993
0.992
0.992
0.991
0.991
0.990
0.990
0.989
0.989
0.989
0.988
0.988
0.987
0.987
00
00
Dilution factor data

Example 2: Input file of pH dependent Zn adsorption on goethite at $[Zn]_{init}$ = 0.08 mmol L^{-1} in 0.1 mol L^{-1} NaCl solution

```
       1
       1
       1
       1
       1
      50
       5       1       2       1       1
00160  -1.00  0.00E00  PSI
00001  -3.07  8.50E-4  SOH
00090  -4.12  7.65E-5  Zn
00020  -1.00  1.00E-1  Na
00030  -1.00  1.00E-1  Cl
00099   0.00  0.00     Zn Ads
00170   0.00  1.00E-1  ACT
00010   0.00  0.00     H+

00010  0.00    10  1
00100  -13.95  10 -1
00001  0.00     1  1
00011  6.45     1  1  10  1 160 1
00012  -10.63   1  1  10 -1 160 -1
00090  0.00    90  1
00091  -9.18   90  1   10 -1
00092  -18.06  90  1   10 -2
00093  -28.07  90  1   10 -3
00095  -0.02   90  1   30  1
00096  0.05    90  1   30  2
00097  -0.15   90  1   30  3
00098  3.85    90  1
00900  2.74     1  1   90 1  10 -1  160  1  99  1
00901  13.75    1  2   90 1  160 2  99  1
00902  -13.98   1  1   90 1  10 -3  160 -1  99  1
00020  0.00    20  1
00030  0.00    30  1
00170  0.00   170  1

00170        170 00
00010        170 0.5
00100        170 0.5
00020        170 0.5
00030        170 0.5
00090        170 2.0
00091        170 0.5
00092        170 00
00093        170 0.5
00095        170 0.5
00096        170 00
```

Aqueous complexation of Zn with chloride (Cl) and carbonate (HCO_3).

Reported equilibrium constants of Zn Surface complexation with goethite.

```
00097        170 0.5
00098        170 00
00001        170 00
00011        170 00
00012        170 00
00900        170 0.5
00901        170 2.0
00902        170 0.5

00001    40.00   1.6     0.90
0.1     1.0
      0         0
      29        0         1         0
      10
-3.00
-3.25
-3.50
-3.75
-4.00
-4.25
-4.50
-4.75
-5.00
-5.25
-5.50
-5.75
-6.00
-6.25
-6.50
-6.75
-7.00
-7.25
-7.50
-7.75
-8.00
-8.25
-8.50
-8.75
-9.00
-9.25
-9.50
-9.75
-10.0
      00       00
```

Example 3: Input file of pH dependent Zn adsorption on goethite with ternary surface complexes at $[Zn]_{init}$ = 0.08 mmol L^{-1} in 0.7 mol L^{-1} NaCl solution

```
       1
       1
       1
       1
       1
      50
       5       1       2       1       1
00160  -1.00  0.00E00  PSI
00001  -3.07  8.50E-4  SOH
00090  -4.12  7.65E-5  Zn
00020  -0.15  7.00E-1  Na
00030  -0.15  7.00E-1  Cl
00099   0.00  0.00     Zn Ads
00170   0.00  7.00E-1  ACT
00010   0.00  0.00     H+

00010  0.00    10  1
00100  -13.95  10 -1
00001  0.00     1  1
00011  7.10     1  1  10  1 160 1
00012  -9.92    1  1  10 -1 160 -1
00090  0.00    90  1
00091  -9.36   90  1   10 -1
00092  -18.32  90  1   10 -2
00093  -28.18  90  1   10 -3
00095  -0.26   90  1   30  1
00096  -0.30   90  1   30  2
00097  -0.46   90  1   30  3
00098  3.47    90  1
00901  1.65     1  2   90 1  160 2  99  1  30  1  10 -2
00902  9.00     1  1   90 1  160 1  99  1  30  1
00020  0.00    20  1
00030  0.00    30  1
00170  0.00   170  1

00170        170 00
00010        170 0.5
00100        170 0.5
00020        170 0.5
00030        170 0.5
00090        170 2.0
00091        170 0.5
00092        170 00
00093        170 0.5
00095        170 0.5
00096        170 00
00097        170 0.5
```

```
00098         170 00
00001         170 00
00011         170 0.5
00012         170 0.5
00901         170 0.5
00902         170 0.5

00001    40.00   1.6     1.20
0.7     1.0
      0         0
      29        0         1         0
      10
-3.00
-3.25
-3.50
-3.75
-4.00
-4.25
-4.50
-4.75
-5.00
-5.25
-5.50
-5.75
-6.00
-6.25
-6.50
-6.75
-7.00
-7.25
-7.50
-7.75
-8.00
-8.25
-8.50
-8.75
-9.00
-9.25
-9.50
-9.75
-10.0
      00       00
```

Example 4: Input file pH dependent Zn adsorption on goethite at $[Zn]_{init}$ = 0.8 mmol L^{-1} in 0.1 mol L^{-1} NaCl solution for optimization

```
       1
       1
       1
       1
       1
      50
       5       1       2       1       1
00160  -1.00  0.00E00  PSI
00001  -3.07  8.50E-4  SOH
00090  -3.09  8.05E-4  Zn
00020  -1.00  1.00E-1  Na
00030  -1.00  1.00E-1  Cl
00099   0.00  0.00     Zn Ads
00170   0.00  1.00E-1  ACT
00010   0.00  0.00     H+

00010  0.00    10  1
00100  -13.95  10 -1
00001  0.00     1  1
00011  6.45     1  1  10  1 160 1
00012  -10.63   1  1  10 -1 160 -1
00090  0.00    90  1
00091  -9.18   90  1   10 -1
00092  -18.06  90  1   10 -2
00093  -28.07  90  1   10 -3
00095  -0.02   90  1   30  1
00096  0.05    90  1   30  2
00097  -0.15   90  1   30  3
00098  3.85    90  1
00900  -2.0     1  1   90 1  10 -1  160  1  99  1
00902  -18.2    1  1   90 1  10 -3  160 -1  99  1
00020  0.00    20  1
00030  0.00    30  1
00170  0.00   170  1

00170        170 00
00010        170 0.5
00100        170 0.5
00020        170 0.5
00030        170 0.5
00090        170 2.0
00091        170 0.5
00092        170 00
00093        170 0.5
00095        170 0.5
00096        170 00
00097        170 0.5
```

```
00098        170 00
00001        170 00
00011        170 00
00012        170 00
00900        170 0.5
00902        170 0.5

00001    40.00   1.6     0.90
0.1     1.0
      2         0
      900
      902
      17        1         1         0
      99
1.12E-05
2.66E-05
2.71E-05
2.94E-05
3.66E-05
7.76E-05
8.86E-05
1.71E-04
2.02E-04
2.32E-04
3.84E-04
7.81E-04
8.02E-04
8.03E-04
8.03E-04
8.04E-04
8.04E-04
     10
-3.12
-3.45
-3.90
-4.08
-4.76
-5.49
-5.58
-6.01
-6.16
-6.19
-7.04
-7.96
-8.22
-8.23
-8.31
-9.21
-10.00
      00       00
```